LA-13993-MS

Approved for public release; distribution is unlimited.

Characterization Well MCOBT-4.4 and Borehole MCOBT-8.5 Completion Report

Los Alamos NATIONAL LABORATORY

Los Alamos National Laboratory is operated by the University of California for the United States Department of Energy under contract W-7405-ENG-36.

Produced by the Risk Reduction and Environmental Stewardship Division

Cover photo shows a modified Foremost DR-24 dual-rotary drill rig. The DR-24 is one of several drill-rig types being used for drilling, well installation, and well development in support of the Los Alamos National Laboratory Hydrogeologic Workplan. The Hydrogeologic Workplan is jointly funded by the Environmental Restoration Project and Defense Programs to characterize groundwater flow beneath the 43-square-mile area of the Laboratory and to assess the impact of Laboratory activities on groundwater quality. The centerpiece of the Hydrogeologic Workplan is the installation of up to 32 deep wells in the regional aquifer.

LA-13993-MS
Issued: December 2002

Characterization Well MCOBT-4.4 and Borehole MCOBT-8.5 Completion Report

David Broxton
David Vaniman
Patrick Longmire
Brent Newman
William Stone
*Andy Crowder**
*Paula Schuh***
*Rick Lawrence***
*Eric Tow***
*Mark Everett****
Richard Warren
*Ned Clayton*****
Dale Counce
Emily Kluk
*Deborah Bergfeld******

**PMC Technologies, Exton, PA*
***Tetra-Tech EMI, Albuquerque, NM*
****Kleinfelders, Inc., Albuquerque, NM*
*****SchlumbergerSema Utilities, Denver, CO*
******US Geological Survey, Menlo Park, CA*

Los Alamos
NATIONAL LABORATORY

Table of Contents

Appendices

List of Figures

List of Tables

LIST OF ACRONYMS AND ABBREVIATIONS

ASTM	American Society for Testing and Materials
bgs	below ground surface
CMR	combinable magnetic resonance
CVAA	cold vapor atomic absorption
DL	detection limit
DOC	dissolved organic carbon
DR	dual rotation
EES	Earth and Environmental Sciences
Eh	decreasing oxidation-reduction potential
EPA	Environmental Protection Agency
ER	Environmental Restoration (Project)
ESH	Environmental, Safety, and Health
FIP	field implementation plan
FMU	Facility Management Unit
FSF	Field Support Facility (part of the Environmental Restoration Project)
GEL	General Engineering Laboratories
gpm	gallons per minute
HSA	hollow-stem auger
IC	ion chromatography
ICPMS	inductively coupled (argon) plasma mass spectrometry
ICPOES	inductively coupled (argon) plasma optical emission spectroscopy
I.D.	inner diameter
IRMS	isotope ratio mass spectrometry
ISE	ion selective electrode
LANL	Los Alamos National Laboratory
MDL	method detection limit
NMED	New Mexico Environment Department
NMWQCC	New Mexico Water Quality Control Commission
NTU	nephelometric turbidity unit
O.D.	outer diameter
QXRD	quantitative X-ray diffraction
RC	reverse circulation
RCRA	Resource Conservation and Recovery Act
RL	reporting limits
RLWRF	radioactive liquid waste treatment facility
RRES-WQH	Risk Reduction and Environmental Stewardship–Water Quality and Hydrology
SBDC	Stewart Brothers Drilling Company
SI	saturation index
SSHASP	Site-Specific Health and Safety Plan
TA	technical area
TD	total depth

TDS	total dissolved solids
3-D	three-dimensional
TKN	total Kjeldahl nitrogen
TW	test well
TOC	total organic carbon
UR-DTH	under-reaming down-the-hole-hammer bit
WCSF	waste characterization strategy form
WGII	Washington Group International, Inc.
XRF	X-ray fluorescence
XRD	X-ray diffraction

Metric to US Customary Unit Conversions

Multiply SI (Metric) Unit	By	To Obtain US Customary Unit
kilometers (km)	0.622	miles (mi)
kilometers (km)	3281	feet (ft)
meters (m)	3.281	feet (ft)
meters (m)	39.37	inches (in.)
centimeters (cm)	0.03281	feet (ft)
centimeters (cm)	0.394	inches (in.)
millimeters (mm)	0.0394	inches (in.)
micrometers or microns (µm)	0.0000394	inches (in.)
square kilometers (km^2)	0.3861	square miles (mi^2)
hectares (ha)	2.5	acres
square meters (m^2)	10.764	square feet (ft^2)
cubic meters (m^3)	35.31	cubic feet (ft^3)
kilograms (kg)	2.2046	pounds (lb)
grams (g)	0.0353	ounces (oz)
grams per cubic centimeter (g/cm^3)	62.422	pounds per cubic foot (lb/ft^3)
milligrams per kilogram (mg/kg)	1	parts per million (ppm)
micrograms per gram (µg/g)	1	parts per million (ppm)
liters (L)	0.26	gallons (gal.)
milligrams per liter (mg/L)	1	parts per million (ppm)
degrees Celsius (°C)	9/5 + 32	degrees Fahrenheit (°F)

ABSTRACT

Characterization well MCOBT-4.4 and borehole MCOBT-8.5 were installed in June 2001 by the Environmental Restoration Project as part of the Mortandad Canyon Work Plan. MCOBT-4.4 is located at the confluence of Mortandad and Ten Site Canyons, about 1000 ft west of characterization well R-15. MCOBT-8.5 is located about 3000 ft east of R-15. Mortandad Canyon received effluent discharged from the Los Alamos National Laboratory's former wastewater treatment plant at TA-35 from 1951 to 1963 and from the radioactive liquid waste treatment facility at TA-50 from 1963 to present. Potential contaminants of concern include tritium, nitrate, perchlorate, fluoride, total dissolved solids, cesium-137, strontium-90, americium-241, and uranium and plutonium isotopes. The primary purpose of this investigation is to determine contaminant and moisture distributions in the upper part of the vadose zone and to provide information on location, extent, and water-quality and water-level data for intermediate perched groundwater. These data will be used to improve the hydrogeologic conceptual model for Mortandad Canyon, evaluate groundwater monitoring needs, and constrain numerical models addressing contaminant migration through the vadose zone to the regional aquifer.

Drilling occurred at MCOBT-4.4 and MCOBT-8.5 in two phases. During Phase I, a hollow-stem auger with a wireline core retrieval system was used to collect core samples for moisture and anion profiles in the upper 310 ft of MCOBT-4.4 and upper 350 ft of MCOBT-8.5. During Phase II, MCOBT-4.4 and MCOBT-8.5 were drilled to depths of 767 ft and 740 ft, respectively, using fluid-assisted, air-rotary techniques. Borehole video and geophysical surveys were made in both boreholes, and sidewall core samples were collected from selected locations in the deeper geologic units. MCOBT-4.4 was completed as a 4.5-in. (inside diameter) stainless-steel single-screen well with the screen interval spanning 482.1 ft to 524 ft. No water was detected in MCOBT-8.5, and it was plugged and abandoned.

MCOBT-4.4 and MCOBT-8.5 provide new geologic control for stratigraphic units in Mortandad Canyon. In descending order, geologic units penetrated include alluvium, tephras and volcaniclastic sediments of the Cerro Toledo interval (MCOBT-4.4 only), Otowi Member of the Bandelier Tuff, upper Puye Formation, Cerros del Rio basalt, and lower Puye Formation. Delineation of geologic units was based on examination of core, cuttings, borehole video and geophysical logs, and laboratory analyses of borehole materials.

At MCOBT-4.4, an intermediate-depth perched zone was encountered at a depth of 493 ft. This perched system occurs in the upper Puye Formation and may extend down into the top of the underlying Cerros del Rio basalt. The location of this perched system is higher than expected based on an earlier investigation at R-15 that found perched water in the lower part of the Cerros del Rio basalt.

Perched water was also considered possible at MCOBT-8.5, but no saturation was detected during drilling of the borehole. Comparison of groundwater occurrences at MCOBT-4.4, R-15, and MCOBT-8.5 suggests that perched water zones beneath Mortandad Canyon are likely to be local features of limited extent and that perching horizons can occur above a variety of perching layers because of stratigraphic variations.

Vadose zone characterization at MCOBT-4.4 and MCOBT-8.5 included analysis of pore water for bromide, chloride, fluoride, nitrate, perchlorate, phosphate, oxalate, and stable isotopes. Pore water was leached from core collected by hollow-stem auger and by sidewall coring. The anion and stable isotope results indicate that contaminants such as nitrate and perchlorate have migrated to depths of at least 500 ft beneath the canyon floor.

Groundwater samples were collected from MCOBT-4.4 after well development and were analyzed for radionuclides, anions, metals and trace elements, volatile organic compounds, and stable isotopes of

hydrogen, nitrogen, and oxygen. Groundwater in the perched zone is characterized by a mixed (calcium-sodium-nitrate-sulfate-bicarbonate) ionic composition. Based on this initial sampling, contaminants in this perched groundwater zone include tritium (12797 ± 1368 pCi/L; 3 sigma error), uranium (0.00028 mg/L), nitrate plus nitrite (as N) (13.2 mg/L), and perchlorate (0.142 mg/L). Concentrations of nitrate and perchlorate exceed the US Environmental Protection Agency primary standard for nitrate (10 mg/L) and the draft provisional risk-based level for perchlorate (0.001 mg/L, 1μg/L).

This investigation supports earlier Laboratory studies that show contamination from Laboratory discharges is present both in unsaturated rocks of the vadose zone and in perched groundwater beneath Mortandad Canyon. Surface flow of treated effluent in Mortandad Canyon has probably infiltrated the thick alluvial deposits on the canyon floor. Moisture in these alluvial deposits, including zones of shallow perched alluvial groundwater, probably act as a source of recharge to the underlying vadose zone. Vertical transport rates in Mortandad Canyon range between 8.2 and 30. 8 ft/yr based on the subsurface distribution of a unique isotopically light nitrate effluent released to the canyon from 1986 to 1989.

1.0 INTRODUCTION

This report describes drilling, well installation, and testing activities and provides a preliminary interpretation of the data for characterization well MCOBT-4.4 and borehole MCOBT-8.5. MCOBT-4.4 is located at the confluence of Mortandad and Ten Site Canyons, approximately 1000 ft west of characterization well R-15 at the Los Alamos National Laboratory (LANL or the Laboratory) (Figure 1.0-1). MCOBT-8.5 is located in Mortandad Canyon approximately 3000 ft east of well R-15.

MCOBT-4.4 and MCOBT-8.5 were installed by the Environmental Restoration (ER) Project as part of the implementation of the Mortandad Canyon Work Plan (LANL 1997, 56835). These drilling activities also provide data for the "Hydrogeologic Workplan" (LANL 1998, 59599) in support of the Laboratory's "Groundwater Protection Management Program Plan" (LANL 1996, 70215). The primary purpose of this investigation is to determine contaminant and moisture distributions in the upper part of the vadose zone and to provide information on location, extent, and water-quality and water-level data for intermediate perched groundwater. The data on contaminant distributions and perched groundwater are being used with similar data from the existing well R-15 to improve the conceptual model for hydrogeology, evaluate groundwater needs, and provide constraints on numerical models addressing contaminant migration through the vadose zone to the regional aquifer.

Data collection activities at MCOBT-4.4 and MCOBT-8.5 are described in the Mortandad Canyon Work Plan (LANL, 1997, 59599). The data quality objectives for this investigation were reviewed and modified to incorporate new data about the occurrence of perched groundwater in characterization well R-15 which was drilled during the summer of 1999. Revisions to original target depths and characterization activities were incorporated into the Field Implementation Plan (FIP) for MCOBT-4.4 and MCOBT-8.5 (LANL 2001, 70928). Appendix A compares work planned in the Mortandad Canyon Work Plan and FIP to work performed.

MCOBT-4.4 and MCOBT-8.5 are downstream from active and inactive outfalls at Technical Area (TA)-5, TA-35, TA-48, TA-50, TA-52, TA-55, and TA-60. From a groundwater perspective, the sources of most concern are the former wastewater treatment plant at TA-35 and the present-day wastewater treatment plant at TA-50 (Figure 1.0-1).

The Laboratory's wastewater treatment plant at TA-35 was operated from 1951 to 1963. Routine and accidental discharges from the wastewater treatment plant resulted in release of contaminants to Ten Site Canyon (Figure 1.0-1). Contaminants of potential concern associated with the TA-35 wastewater plant include ^{140}La, ^{140}Ba, ^{89}Sr and ^{90}Sr, ^{90}Y, ^{137}Cs, ^{106}Ru, ^{238}Pu, $^{239,240}Pu$, caustic, acid, sodium carbonate, strontium nitrate, iron sulfate, and dielectric oil (LANL 1997, 56835). By the early 1960s, the wastewater treatment plant at TA-35 reached its capacity to handle the increasing volume of liquid radioactive wastes associated with expanding Laboratory operations. In 1963, TA-35 wastewater operations were transferred to a new radioactive liquid waste treatment facility (RLWTF) at TA-50.

The Laboratory's RLWTF at TA-50 discharges treated wastewater to Mortandad Canyon via Effluent Canyon through an outfall that is currently permitted as NPDES outfall 051. From 1963 through 1995, a total of 342 million gal. (1,294,500 m^3) of treated wastewater were discharged (LANL 1997, 56835). Laboratory surveillance data collected in Mortandad Canyon show elevated concentrations or activities of fluoride, total dissolved solids (TDS), ClO_4, NO_3, ^3H, ^{90}Sr, ^{137}Cs, $^{239,240}Pu$, ^{241}Am, and $^{234,235,238}U$ in surface water and in alluvial groundwater.

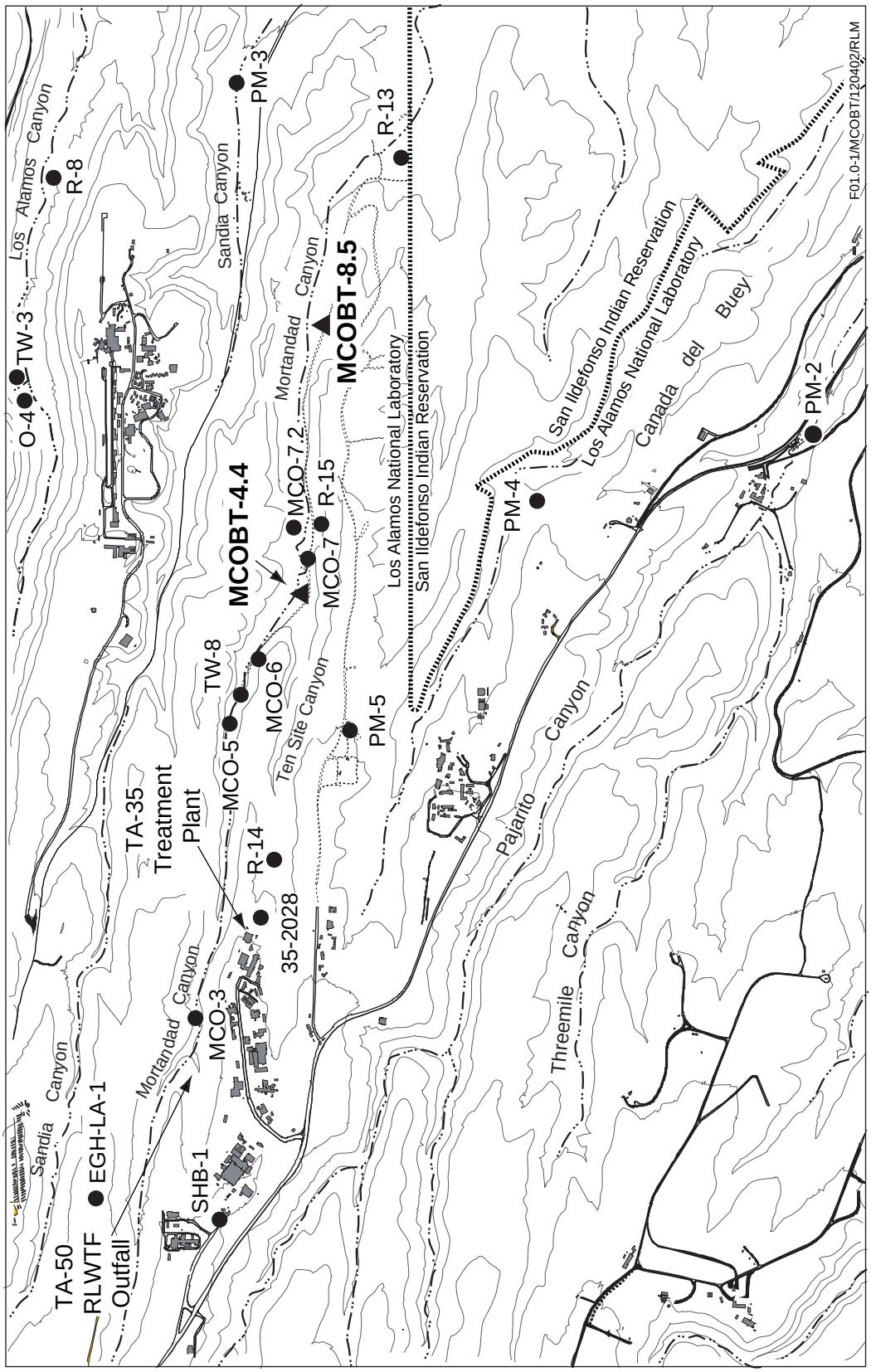

Figure 1.0-1. Locations of MCOBT-4.4 and MCOBT-8.5 in Mortandad Canyon

Drilling activities at MCOBT-4.4 resulted in the completion of a single-screen well to sample a perched water zone found in the upper part of the Puye Formation. No intermediate-depth perched water was found at MCOBT-8.5, and the borehole was plugged and abandoned.

This report consists of two parts. Part I is a chronological presentation of preparatory, drilling, well construction, well development, testing, and completion activities. Part II summarizes initial interpretations of the geologic, geophysical, hydrologic, and geochemical data collected during and immediately following the activities described in Part I. A more thorough treatment of the data collected awaits supporting data that will be obtained through other hydrogeologic characterization wells and related field studies.

PART I: SITE ACTIVITIES

2.0 PRELIMINARY ACTIVITIES

2.1 Administrative Preparation

Washington Group International, Inc. (WGII) received contractual authorization to start administrative preparation tasks on April 2, 2001. As part of this preparation, WGII developed a modification to the existing Site-Specific Health and Safety Plan (SSHASP #273) to include well MCOBT-4.4 and borehole MCOBT-8.5. WGII also prepared the MCOBT-4.4 and -8.5 Waste Characterization Strategy Form (WCSF). The Laboratory prepared the FIP, which outlined drilling and sampling plans for MCOBT-4.4 and MCOBT-8.5, to guide field personnel in the execution of field activities. The host facility, Facility Management Unit (FMU)-80, signed a Facility Tenant Agreement to provide access and security control for the MCOBT-4.4 and -8.5 activities.

All administrative documents, permits, agreements, and plans were completed prior to an ER Readiness Review Meeting on May 15, 2001. The Groundwater Investigations Focus Area project leader authorized Phase I on May 21, 2001, to begin fieldwork. The Readiness Review Checklist for Phase II was signed on May 31, 2001.

2.2 Site Preparation

Site preparation work began on May 21, 2001, at the MCOBT-8.5 site and on June 1, 2001, at the MCOBT-4.4 site. SG Western Construction prepared the drilling sites. Initially, the sites were cleared using a bulldozer. A pit for the drill cuttings was then excavated and lined with plastic. Each site was graded and leveled; base-course gravel was spread over the area and compacted. The site was fenced for access control.

3.0 SUMMARY OF DRILLING ACTIVITIES

Drilling activities at MCOBT-4.4 and MCOBT-8.5 were completed in two phases. Phase I drilling and core sampling was performed by Stewart Brothers Drilling Company (SBDC) using 4 1/4-in. inside diameter (I.D.), 9-in. outside diameter (O.D.) Truspin™ hollow-stem augers (HSA) with a Moss™ wireline core retrieval system. The primary goal of Phase I drilling at both locations was to collect continuous core samples from the surface to the base of the Bandelier Tuff to determine the moisture content and the anion, stable isotope, and tritium distributions in the upper part of the vadose zone. Planned total depths (TD) for Phase I drilling were approximately 484 ft in MCOBT-4.4 and 342 ft in MCOBT-8.5.

Phase II deep drilling activities were conducted at both locations by Dynatec Drilling Company, Inc. (Dynatec) using an air-rotary, reverse-circulation (RC) system. Phase II drilling objectives were to produce samples of encountered geologic formations, collect water samples from perched zones, if present, and provide a borehole for well installation if intermediate-perched water zones were encountered.

The ER Project's Field Support Facility (FSF) provided drill casings, drilling bits, a small front-end loader, the dust suppression system, field support trailers (including logging and sampling trailers), water containment tanks, a Hermit data logger and pressure transducers, a depth-to-water meter, water sampling bailers, a diesel-powered electric generator, and water sample testing and filtering apparatus. The Laboratory's geology and geochemistry group (formerly Earth and Environmental Sciences [EES]-1, now EES-6) provided a core-logging microscope. The former ESH-18 (now Risk Reduction and Environmental Stewardship-Water Quality and Hydrology [RRES-WQH]) provided a geophysical logging trailer.

The following sections discuss site preparation, Phase I drilling activities, and Phase II drilling activities, respectively. Drilling and well activity shift information for MCOBT-4.4 is summarized in Table 3.1-1. Similar information is provided in Table 3.1-2 for MCOBT-8.5. The chronology of drilling and site preparation activities is shown graphically in Appendix B.

3.1 Site Preparation for Drilling

Site preparation for Phase I and II drilling at both sites was conducted by SG Western Construction Company from May 21 through June 6, 2001. Activities included site clearing, access road modification and improvement, drill pad leveling and construction, and construction of a lined cuttings pit. Site preparation was completed over four day shifts at MCOBT-4.4 (Table 3.1-1) and eight day shifts at MCOBT-8.5 (Table 3.1-2).

Table 3.1-1
Well MCOBT-4.4 Drilling Shift Information

Activity	Dates	Number of Shifts[a]
Site preparation	May 21–May 25, 2001	4
Phase I drilling/rig mobilization	June 1–June 8, 2001	8
Phase II drilling	June 9–June 14, 2001	9
Geophysics/well design	June 14–June 29, 2001	17
Well Installation/annular backfilling	June 29–July 1, 2001	6
Well development/hydrologic testing	July 9, 2001–February 13, 2002	18 [b]
Dedicated pump installation	February 5–February 8, 2002	4
Well completion tasks	September 5–September 28, 2001	10
Demobilization	July 13–July 16, 2001	4
Total Shifts	May 21–February 8, 2002	80

[a] Shifts are defined as 12 hr in duration. Work performed for any portion of a shift is recorded as one shift in this table.

[b] Well development activities were performed during four discrete time periods: July 9–12, 2001 (8 shifts), July 17, 2001 (1 shift), November 12–21, 2001 (8 shifts), and February 13, 2002 (1 shift).

Table 3.1-2
Well MCOBT-8.5 Drilling Shift Information

Activity	Dates	Number of Shifts[a]
Site preparation	May 21–June 7, 2001	8
Phase I drilling/rig mobilization	June 8–June 14, 2001	6
Phase II drilling	June 17–June 23, 2001	10
Geophysics/well design	June 23–June 27, 2001	8
Borehole abandonment/demobilization	June 27–June 29 2001	4
Total shifts	May 21–June 29, 2001	36

[a] Shifts are defined as 12 hr in duration. Work performed for any portion of a shift is recorded as one shift in this table.

The sites were initially cleared of trees, stumps, and large boulders. The access road was then graded and improved, followed by construction to level the drill pad and lay down base-course gravel at both sites. For MCOBT-8.5, a 20- by 50- by 4-ft-deep pit with a 3-ft-high berm was excavated and lined with polyethylene sheeting at the south boundary of the drill pad for storage of drilling fluids and cuttings. A cuttings pit of similar capacity was constructed along the north boundary of the drill pad at MCOBT-4.4. No jack cellars were used at either location for either phase of drilling.

A small stream crossing was designed and constructed on the access road to MCOBT-8.5. The structural components of the crossing consisted of steel grating treads and wood cribbing supports. Three sections of galvanized steel channel conduit were installed beneath the crossing to capture and direct surface water flow through the pipe and mitigate the potential for erosion beneath the bridge.

Site preparation continued with the placement and final grading of base-course gravel to complete drill pad construction, installation of 6-mil plastic sheeting to line the cuttings pit, placement of security barriers and signs, and demobilizing of construction equipment by June 8, 2002. Office and supply trailers, generators, and safety lighting equipment were moved to the site during Phase II drilling mobilization for each site.

3.2 MCOBT-4.4 Drilling Activities

3.2.1 MCOBT-4.4 Phase I Drilling

Phase I drilling activities at MCOBT-4.4 occurred between June 1 and June 8, 2001 (Table 3.1-1). SBDC provided a CME-750 HSA drill rig equipped with a small (i.e., 9-in. O.D.) Moss™ wireline core retrieval system. The core barrel was 5 ft long with a 3-in.-I.D. yielding core of the same dimensions. The primary goal of Phase I was to collect continuous core samples from the surface to the base of the Bandelier Tuff, which was predicted to occur at 484 ft below ground surface (bgs). Core samples were collected to determine moisture content and anion, stable isotope, and tritium distributions in a vertical profile through the upper part of the vadose zone.

On June 1, 2001, SBDC mobilized the drill rig and equipment to the MCOBT-4.4 site. Drilling began on the same day. Drilling was conducted daily for one 12-hr shift per day for the duration of Phase I. The borehole was advanced by HSA collecting continuous core samples through alluvium, the Cerro Toledo interval, and the Otowi Member of the Bandelier Tuff to a TD of 310 ft bgs. Selected drill intervals were cored continuously using a 5-ft-long split core barrel from surface to 310 ft bgs advanced in 2.5-ft core runs to optimize recovery. Phase I drilling operations were terminated because of a combination of auger refusal and loss of the lower 35 ft of the HSA. Bentonite was periodically added to the core hole to stabilize flowing sands from perched water zones in the alluvium, as described below. Water from the municipal supply was

obtained from a Los Alamos County fire-protection hydrant and added to the borehole periodically to assist in removing cuttings from the borehole. The lithologic log presented in Appendix C provides specific information with respect to recovered core, unrecovered core, and intervals where core samples were not attempted.

On June 1, 2001, continuous core was collected to a depth of 50 ft bgs when flowing sands caused the core barrel to bind in the augers. Saturated alluvium was first encountered at approximately 34 ft bgs. Flowing sands were observed at 45 ft bgs. The extent of this shallow perched zone is thought to be from approximately 34 to 50 ft bgs. Three bags of Baroid Benseal were added through the augers to seal off this interval and stabilize the flowing sands. The remedy was successful, and coring continued to 115 ft bgs by the shift's end.

On June 2, 2001, coring continued to 160 ft bgs. The augers had to be reamed twice during the day to enable the core barrel to deploy and retract freely. Later in the day, the auger stem was tripped out entirely for cleaning after having difficulty latching onto the core barrel. Augers were tripped in to 35 ft bgs at day's end.

On the morning of June 3, 2001, the augers were used to ream through slough from between approximately 40 to 80 ft bgs. The slough was subsequently tagged at 47 ft bgs, 33 ft inside the augers. The augers were removed and cleaned. Six bags of 3/8-in. bentonite chips were poured into the borehole in an attempt to stabilize the borehole in the upper saturated zone before tripping in to 47 ft and subsequently reaming through slough to 160 ft. Coring continued from 170 ft bgs to 230 ft bgs with three intervals where auger and borehole cleaning took precedence over core sample collection.

On June 4, 2001, coring continued from 230 to 310 ft bgs while periodic borehole cleaning with potable water was conducted to help loosen cuttings. Near the end of the day, the drillers lost auger rotation. Attempts were made to clean the hole with the center bit, and the augers were pulled back to 215 ft bgs. The augers loosened up; however, cuttings return was not established by the shift's end.

On the morning of June 5, 2001, while attempting to ream back to 310 ft bgs, an impenetrable obstruction was encountered at 280 ft bgs. The augers were subsequently tripped out of the hole, and it was observed that 35 ft of auger (i.e., seven flights plus the bit) were left in the borehole from 245 to 280 ft bgs. SBDC made the decision to attempt to retrieve the augers with a fishing tool.

On June 6, 2001, four unsuccessful attempts were made to fish out the lost portion of the auger stem. The decision to plug and abandon the borehole was made jointly by SBDC, WGII, and LANL project personnel. On June 7, 2001, the borehole was backfilled via the tremie method with cement-bentonite grout. Eight and one half 125-gal. batches of Portland cement with 3% bentonite grout were pumped from 245 to 36 ft bgs. The saturated zone in the vicinity of 37 ft bgs took approximately three batches of grout with negligible gain in elevation. Therefore, the decision was made to fill the borehole from 36 ft to 19 ft bgs with 19 bags of 3/8-in. bentonite chips and top off the hole with the cement/bentonite grout mix.

On the morning of June 8, 2001, the drill rig and drilling equipment were decontaminated and moved to the MCOBT-8.5 site.

3.2.2 MCOBT-4.4 Phase II Drilling

Phase II drilling was performed by Dynatec using a fluid-assisted, air-rotary RC system capable of penetrating poorly welded volcanic tuff, basalt, and clastic sedimentary rocks to the required depths planned for MCOBT-4.4. The goals of Phase II drilling were to produce samples of the geologic formations, collect water samples, and provide a deep borehole for well installation. Throughout drilling, cuttings samples for

geologic characterization were collected at 5-ft intervals using a sieve placed directly below the cyclone discharge point.

For deep drilling at MCOBT-4.4, Dynatec furnished a Foremost™ dual-rotation (DR)-24 drill rig equipped with a dust suppression system. In completing Phase II, open-hole and advanced-casing drilling methods were used with various bit sizes and types as appropriate for existing formation conditions. Air-rotary drilling was augmented with drilling fluids consisting of municipal water obtained from a Los Alamos County fire-protection hydrant with or without nominal additives (i.e., EZ-MUD® and foam polymer) to improve lubrication and assist in removing cuttings from the borehole.

Phase II drilling at MCOBT-4.4 began at a location adjacent to the abandoned Phase I borehole on June 9, 2001, and was completed on June 14, 2001. Dynatec mobilized the DR-24 rig and equipment, including drill casing, 7-in. RC rods, and bit assembly components to the site on June 9 and 10, 2001. Drilling operations began on June 10, 2001. Drilling commenced using a 14 1/2-in. under-reaming down-the-hole-hammer bit (UR-DTH) to advance 13 3/8-in. retractable drill casing to 8 ft bgs. Drilling operations were conducted in two 12-hr shifts per day for the duration of Phase II.

On June 11, 2001, Dynatec resumed drilling using the 13 3/8-in. retractable casing and 14 1/2-in. UR-DTH bit to advance the borehole from 8 ft to 130 ft bgs where the casing string was landed in the Otowi Member of the Bandelier Tuff. The 14 1/2-in. UR-DTH was tripped out and replaced with a 12 1/4-in. tricone bit, and the hole was advanced open hole to 442 ft bgs on the morning of June 12, 2001. That day Dynatec continued to advance the borehole open hole to 523 ft bgs, approximately one ft into the Cerros del Rio Basalt where operations were stopped to monitor water. Water levels stabilized for five readings collected over a one-hr period at 477.48 ft bgs. Three carboy sample containers were filled from the cyclone discharge before drilling resumed. After slow hard drilling from 523 to 535 ft bgs, Dynatec tripped out the 12 1/4-in. tricone bit and tripped in a 12 1/4-in. DTH to make more rapid progress through the basalt. By the end of the night shift, on the morning of June 13, 2001, the borehole was advanced to 587 ft bgs.

Dynatec continued to advance the borehole within the Cerros del Rio basalt from 587 to 717 ft bgs by the morning of June 14, 2001. During the day, drilling operations were delayed for more than three hr as a result of access road repairs that prevented service vehicles and the water truck from entering the site.

On June 14, 2001, Dynatec continued to advance the borehole from 717 to 727 ft where drilling was stopped again to monitor water levels. At this time it was uncertain whether the water in the borehole represented accumulated drilling fluids or native groundwater. Water levels over a four-hr period started at 722.15 ft bgs and ended at 704.75 ft bgs. Three carboy sample containers were filled from the cyclone discharge, and field parameters were collected after water level monitoring was completed and before drilling resumed. The borehole was advanced into the Puye Formation, encountered at 735 ft to 767 ft bgs. Water levels were monitored for 45 min during which time the water level dropped from 741.7 ft bgs to 747.35 ft bgs. Dynatec tripped out the 12 1/4-in. DTH, marking the end of drilling at MCOBT-4.4 with a TD of 767 ft bgs.

3.3 MCOBT-8.5 Drilling Activities

3.3.1 MCOBT-8.5 Phase I Drilling

Phase I drilling activities at MCOBT-8.5 occurred between June 8 and June 15, 2001 (Table 3.1-1). Coring at MCOBT-8.5 was performed with the same equipment as described in Section 3.2.1. The primary goal of Phase I drilling at MCOBT-8.5 was to collect continuous core samples from the surface to the base of the Bandelier Tuff, predicted to occur at 342 ft bgs. As with MCOBT-4.4, core samples were collected to determine the moisture content and anion, stable isotope, and tritium distributions in the vadose zone.

The MCOBT-8.5 borehole was advanced by HSA collecting continuous core samples through alluvium, the Cerro Toledo interval, and Otowi Member of the Bandelier Tuff to a TD of 350 ft bgs. Selected drill intervals were cored continuously using a 2.5-ft-long split core barrel from surface to 140 ft bgs. Below 140 ft bgs it became necessary to clear cuttings from the borehole by adding water. After cuttings were cleared from the borehole, the borehole was advanced several ft without coring to clear the water from the hole to avoid compromising the integrity of the subsequent core samples. Starting at 150 ft bgs, core samples were collected at 20-ft intervals to the TD of the borehole. The lithologic log presented in Appendix C provides specific information with respect to recovered core, unrecovered core, and intervals where core samples were not attempted.

Potable water from the municipal supply was obtained from a Los Alamos County fire-protection hydrant and periodically added to the borehole to assist in cleaning the augers and removing cuttings. No flowing sand zones were observed; therefore, no bentonite was added to the borehole during Phase I drilling at MCOBT-8.5.

On June 8, 2001, SBDC mobilized the drill rig and equipment to the site and commenced drilling using 4 1/4-in.-I.D., 9-in.-O.D. Truspin™ HSA with a Moss™ wireline core retrieval system. Continuous coring was conducted to a depth of 25 ft bgs by the end of the shift.

On June 11, 2001, continuous coring resumed from 25 ft bgs to 152.2 ft bgs when the decision was made to collect core samples at 20-ft intervals from this depth to the TD of the borehole. The first zone of saturation was encountered at 94.4 ft bgs. Thin zones of saturation appeared intermittently to 112.5 ft bgs. A water-level measurement was attempted with the TD of the borehole at 110.7 ft bgs, but the probe did not detect standing water in the borehole. Coring finished at 125.0 ft bgs at day's end. No saturated water-bearing zones beyond those mentioned above were encountered. Potable water was added after each set of coring runs to assist with cuttings removal.

On June 12, 2001, continuous coring resumed from 125 ft bgs to 152.2 ft bgs when the decision was made to collect core samples at 20-ft intervals below this depth. Five ft of core (two core runs) were collected at 20-ft intervals to a depth of 212.5 ft bgs by the end of the shift. No saturated zones were encountered. Potable water was added after each set of coring runs to assist with cuttings removal.

On June 13, 2001, core drilling was interrupted when the center bit hoist cable broke. All augers had to be tripped out of the borehole, the cable was temporarily repaired, and coring resumed by mid-afternoon. Coring finished for the day at 270 ft bgs.

The defective hoist cable was replaced early on the morning of June 14, 2001. Thirty gal. of bentonite slurry were added to the borehole prior to the resumption of drilling to assist with cuttings removal. Coring continued in 20-ft increments to the TD of the borehole at 350 ft bgs where auger refusal occurred. An additional 35 gal. of bentonite slurry were periodically added to assist with cuttings removal. After the TD was reached, the augers were tripped out and the borehole was left open for Phase II drilling.

On the morning of June 15, 2001, the HSA drill rig and all drilling equipment were decontaminated and demobilized from the site.

3.3.2 MCOBT-8.5 Phase II Drilling

Phase II drilling was performed by Dynatec using the same equipment and methods, materials, and potable water supply as at MCOBT-4.4 (Section 3.2.2). The goals of Phase II drilling were to produce samples of the geologic formations, collect water samples, and provide a deep borehole for well

installation. Throughout drilling, cuttings samples for geologic characterization were collected at 5-ft intervals using a sieve placed directly below the cyclone discharge point.

Phase II drilling at MCOBT-8.5 began on June 17, 2001, and was completed on June 23, 2001. Dynatec mobilized the DR-24 rig and equipment, including drill casing, 7-in. RC rods, bit assembly components, water storage tanks, and light plants to the site on June 17, 2001. All Phase II drilling operations at MCOBT-8.5 were conducted in two 12-hr shifts per day.

Drilling commenced near midnight on June 17, 2001, by reaming the Phase I borehole with 13 3/8-in. retractable drill casing and casing shoe. Refusal of the casing was encountered at 77 ft bgs. Dynatec continued advancing the 13 3/8-in. casing utilizing a 14 1/2-in. UR-DTH bit to a depth of 130 ft bgs where the casing string was landed in the Otowi Member of the Bandelier Tuff on the morning of June 18, 2001.

On June 18, 2001, Dynatec tripped out the 14 1/2-in. UR-DTH and replaced it with a 12 1/4-in. tricone bit that was used to ream the remaining 9-in. borehole from 130 ft to 347 ft bgs. At 347 ft, Dynatec replaced the 12 1/4-in. tricone bit with the 12 1/4-in. DTH bit in anticipation of encountering the Cerros del Rio basalt in the vicinity of 447 ft bgs. After the drill bits were exchanged and the 12 1/4-in. DTH bit was tripped back into the borehole, the borehole was advanced to 445 ft bgs. Drilling was halted to monitor for groundwater after entering the Cerros del Rio basalt at 429 ft bgs. Because no groundwater accumulated in the borehole, the borehole was then advanced open hole to 510 ft bgs by the end of the night shift.

On June 19, 2001, Dynatec advanced the borehole from 510 to 645 ft bgs where drilling was stopped to monitor water levels. At this time, it was uncertain whether water in the borehole represented accumulating drilling fluid or native groundwater. Water levels measured over a 45-min period started at 621.5 ft bgs and rose to 617.35 ft bgs. After water-level monitoring was completed, and before drilling resumed, three carboy sample containers were filled from the cyclone discharge and field parameters were measured. Drilling continued in the basalt to 690 ft bgs when the drillers had to replace packing in the top-drive head on June 19, 2001. Parts were required for the repair, and drilling was shut down until the parts were delivered and the top-drive head repaired early on Saturday morning, June 23, 2001. The water level was measured at 671 ft bgs before drilling resumed. The borehole was advanced from 690 to 740 ft bgs, 30 ft below the top of the Puye Formation. No significant water production was observed near the base of the Cerros del Rio basalt or within the Puye Formation. The TD of the borehole was called at 740 ft bgs. Dynatec tripped out the 12 1/2-in. DTH, marking the end of drilling activities at MCOBT-8.5.

3.3.3 MCOBT-8.5 Borehole Plugging and Abandonment

The MCOBT-8.5 borehole was plugged and abandoned in two phases, starting on June 25, 2001, and ending on June 29, 2002. The bottom of the borehole was sloughed in to a level of 729 ft bgs. Initially, the borehole was backfilled from 729 ft to 670 ft bgs with 3/8-in. bentonite chips approximately 30 ft above the contact between the Cerros del Rio basalt and the Puye Formation. This first phase of backfill was performed to see if perched water would accumulate in the Cerros del Rio basalt. Water-level trends were then measured with a pressure transducer for approximately 15 hr with inconsistent results. The borehole was then filled to 648 ft bgs with 3/8-in. bentonite chips and capped with 2 ft of 6/9 silica sand. Water in the borehole was bailed to the extent practicable, and depth-to-water-level measurements were collected for approximately four hr to determine if the borehole was recharging with groundwater. Water-level measurements in the open borehole during that time indicated the absence of perched water accumulating in the Cerros del Rio basalt. Because no perched water could be found, the Laboratory decided to plug and abandon MCOBT-8.5. On June 29, 2001, the remainder of the borehole was backfilled from 646 to 54.3 ft bgs with 3/8-in. bentonite chips and to ground surface with a Portland cement/3% bentonite grout.

4.0 WELL DESIGN, CONSTRUCTION, AND DEVELOPMENT

The following sections describe the well design and construction for MCOBT-4.4. The MCOBT-8.5 borehole was abandoned on June 27, 2001, by backfilling with bentonite chips and cement. No well was installed because no groundwater was found during drilling.

4.1 MCOBT-4.4 Well Design

Geophysical logs, video logs, borehole core and cuttings, water-quality data, water-level data, and drillers' observations were reviewed by the Groundwater Integration Team to design the MCOBT-4.4 well. The design for MCOBT-4.4 specified a single screen to establish the monitoring point for contaminants in the perched water zone. The planned and actual screen location is given in Table 4.1-1.

Table 4.1-1
Summary of Well Screen Information for MCOBT-4.4

Screen #	Planned Depth (ft)	Actual Depth (ft)	Geologic/Hydrologic Setting
1	485.7–527.5	482.1–524	Perched water zone in Puye Formation

4.2 MCOBT-4.4 Well Construction

The blank casing and pipe-based screen were constructed of 304 stainless steel fabricated to American Society for Testing of Materials (ASTM) A554 standards. External couplings were also type 304 stainless steel. The couplings used were a mix of ASTM standards A312 and A511, both of which exceed the tensile strength of the threaded casing ends. The combination of coupling standards was necessary for the vendor to provide the casing materials in a timely manner and does not compromise the integrity of the well.

The pipe-based screens were constructed of the same diameter tubing as the blank casing risers (4.5-in.-I.D./5.0-in.-O.D. stainless steel). These screens were constructed by drilling 0.375-in.-diameter holes in 10-ft sections of well casing and welding a wire-wrap (0.010-in. gap) over the perforated interval. The final O.D. of the screens was 5.56 in.

The borehole was progressively backfilled with bentonite pellets and chips from 767 ft to 545 ft bgs, and then the single-screen well was installed, as shown in Figure 4.21. The stainless steel well components were cleaned at the well site using a hot water cleaner and scrub brushes. Stainless steel centralizers were installed above and below the screen and at approximately 39.5 ft bgs (Figure 4.2-1). All backfill materials were emplaced through a tremie pipe (Section 4.2.2).

4.2.1 Steel Installation

Well MCOBT-4.4 was constructed by installing stainless steel well tubing and screen in the open borehole. Dynatec installed the well tubing in one shift on June 30, 2001 (Table 3.1-1). Figure 4.2-1 is an illustration of the final well tubing configuration showing depths below the ground surface.

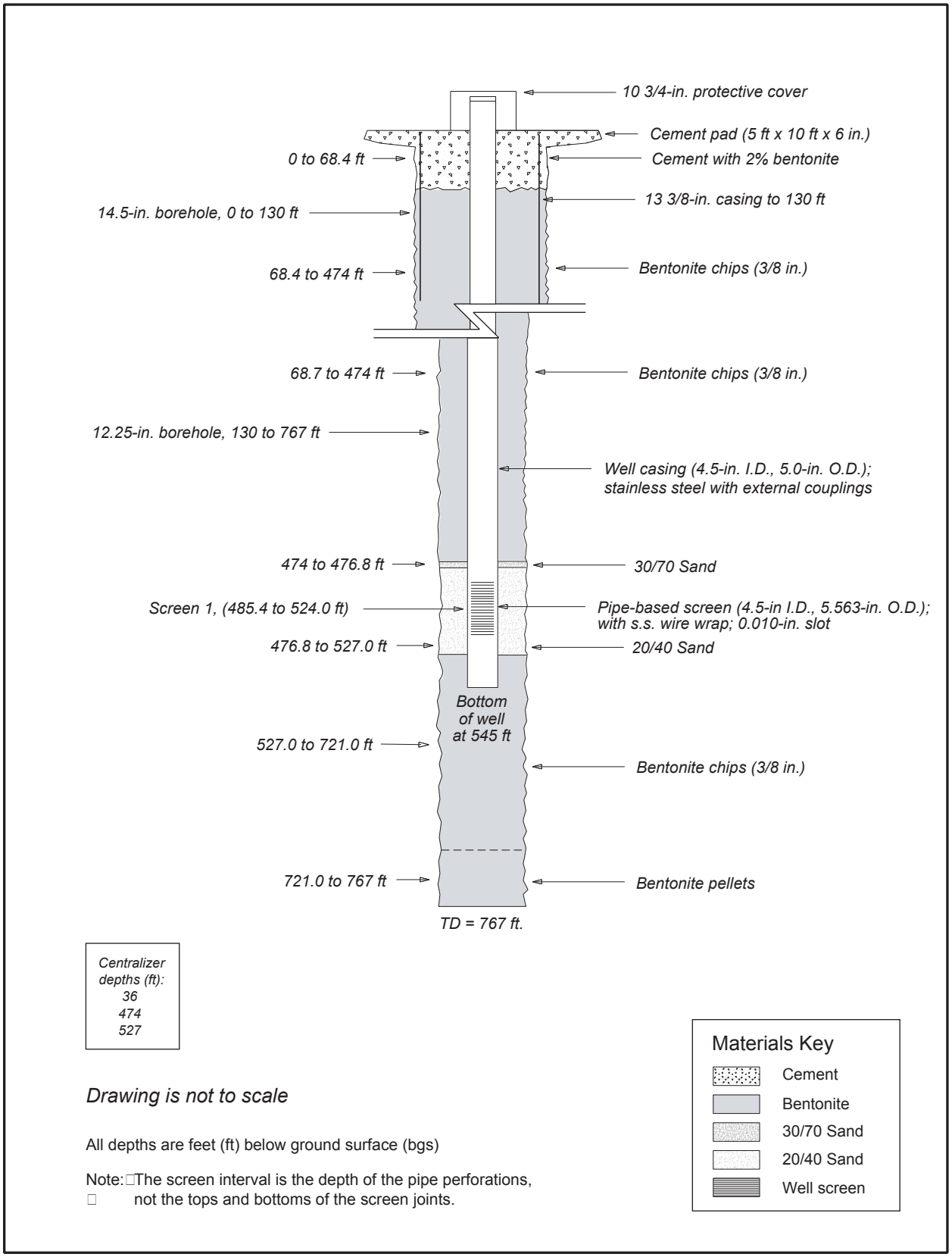

Figure 4.2-1 As-built well configuration diagram, Well MCOBT-4.4

4.2.2 Annular Fill Placement

Dynatec conducted backfill activities from June 14 through July 1, 2001 (Table 3.1-1). Placement of annular fill materials was accomplished using BQ-size (1 13/16-in.-I.D.) steel tremie pipe to deliver annular materials to the specified design depths (Figure 4.2.1). Silica sands were emplaced across the screen interval using municipal water as a fluid slurry. Bentonite materials were emplaced above and below the screened interval to seal the annular space and isolate the perched groundwater zone. The bentonite was delivered using EZ-MUD® (polyacrylamide-polyacrylate copolymer) mixed with municipal water as a fluid slurry. Portland cement (mixed at a ratio of 5 gal. of water for each bag of cement) was used to provide wellhead protection of the annular space in the upper 68 ft of the borehole. Approximately 7080 gal. of municipal water were used to introduce annular-fill materials during the construction of well MCOBT-4.4.

Table 4.2-1 lists the annular fill materials installed during MCOBT-4.4 well construction. The final configuration of the annular materials is also illustrated in Figure 4.2-1.

Table 4.2-1
Annular Fill Materials, Characterization Well MCOBT-4.4

Material	Amount	Unit
20/40 silica sand[a]	79	bags
30/70 silica sand[b]	4	bags
Benseal® bentonite[c]	1.66	bags
Holeplug® bentonite chips[d]	637.37	bags
Pelplug® bentonite pellets[e]	62	buckets
Portland® cement[f]	44	bags

[a] 20/40 sand is medium grained and used to pack screened intervals.
[b] 30/70 sand is fine grained and used to separate screen packs from bentonite or cement from bentonite.
[c] Benseal® is granular bentonite that produces a slurry when mixed with water.
[d] Holeplug® bentonite is 3/8-in. angular and unrefined bentonite chips.
[e] Pelplug® bentonite is 1/4-in. by 3/8-in. refined elliptical pellets.
[f] Portland® cement was mixed with municipal water at a ratio of 5 gal. water to each bag of cement.

4.2.3 Well Development

Well development activities at MCOBT-4.4 were performed in two phases. Preliminary development involved wirebrushing, bailing, and surging. Final development was by pumping. The progress of development was determined by monitoring several water-quality parameters in the field: pH, temperature, specific conductance, and turbidity. Parameters were measured in a water sample from the first bail for comparison with later samples. Additional field-parameter measurements were taken periodically during bailing and at regular intervals during pumping. The goal was to obtain a turbidity of less than 5 nephelometric turbidity units (NTU). Development was halted when field parameters leveled off and turbidity reached this level or could not be improved. A summary of values obtained is given in Table 4.2-2.

The formation adjacent to the screen was not very productive, and it was possible to bail the well dry during development. After bailing, the well was further developed using a surge block deployed by means of a wireline for quick up and down strokes and rapid retrieval for switching to a bailer. The well was bailed between episodes of surging to remove particulates produced, but surging and bailing did not achieve the desired level of development. Specifically, turbidity never got below 50 NTU and sometimes exceeded 200 NTU. Thus, surging and bailing were halted, and further development was delayed until a dedicated pump was installed (Section 7.0).

Table 4.2-2
Development of MCOBT-4.4

			Range of Parameters[a]		
Method	Water Produced (gal.)	pH	Temperature (°C)	Specific Conductance (uS/cm)	Turbidity (NTU)
Bailing[b]	1820	12.4–8.5	15.3–14.8	8330–341	>1000–298
Pumping[c]	75	6.9–7.2	8.3–10	330–323	4.45–0.84

[a] Presented as value at beginning and end of development; values greater or less than those shown may have been obtained during the course of development.

[b] Includes periodic surging with block on wireline.

[c] Using dedicated pump installed in MCOBT-4.4 for monitoring water quality.

Final development to acceptable turbidity levels was readily achieved by pumping (Table 4.2-2). The pump was turned off when pumping yielded a sample whose turbidity was less than 5 NTU. After the well had rested for a brief period (at least 15 min), pumping was resumed and a sample taken to see if an acceptable turbidity value (less than 5 NTU) could be reproduced. This process (pump off/on) was repeated a number of times. Values of less than 5 NTU were obtained for water samples from the outset of pumping. The first sample during pumping was characterized by a turbidity value of 4.45 NTU. Turbidity of 15 consecutive samples, taken at approximately 15-min intervals thereafter, declined to a value of 0.84 NTU. Results of development are shown graphically in Figure 4.2-3.

Some cement was inadvertently introduced into the upper part of the well casing during well construction. Fortunately, this cement never reached the screen. Video logging showed that wirebrushing had removed virtually all of the cement. However, a thin layer remained on the wall of the production casing in places above the water table. The final pH value measured during pumping development indicates that the cement had no further impact on the quality of water in the well.

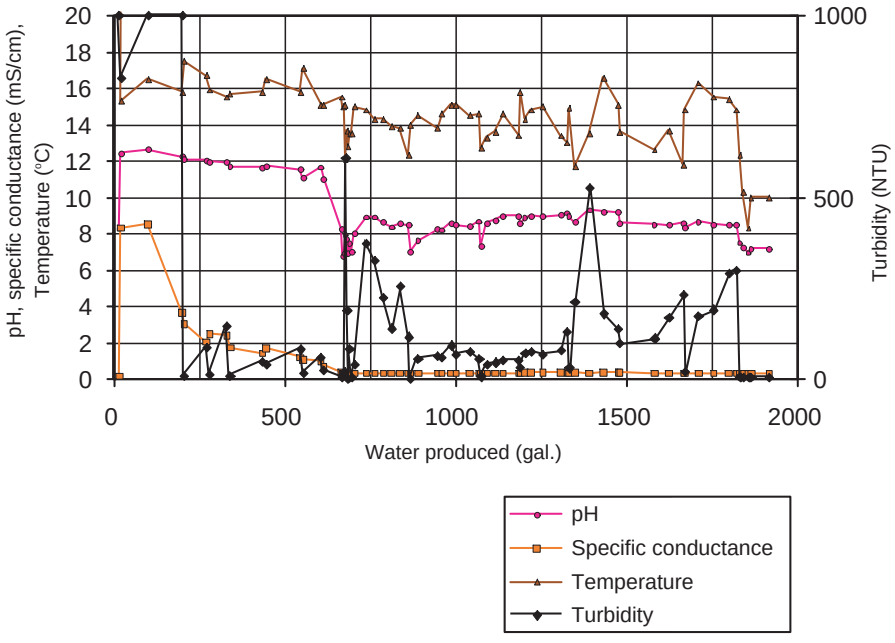

Figure 4.2-3. Results of developing MCOBT-4.4 by all methods

5.0 GEODETIC SURVEY FOR WELL MCOBT-4.4 AND BOREHOLE MCOBT-8.5

The locations for MCOBT-4.4 and MCOBT-8.5 were determined by geodetic survey on December 21, 2001, using a Topcon GTS B-3, 3 Second Theodolite total station. Control for the survey were points from well MCO-7.2 and BC WB-74A and traversed to DS-2 TS. The distance from DS-2 TS to BC WB 74A is 436.23 ft. Field measurements were reduced using Terra Model software.

The survey located the brass cap monument in the northwest corner of the concrete pad at both MCOBT-4.4 and MCOBT-8.5 and measured elevations to the top of the exterior well casing at MCOBT-4.4 (Table 5.0-1). Horizontal well coordinates are New Mexico State Plane Grid Coordinates, Central Zone (North American Datum, 1983 [NAD 83]) and are expressed in ft. Elevation is expressed in ft above mean sea level relative to the National Geodetic Vertical Datum of 1929.

The Facility for Information Management, Analysis, and Display (FIMAD) location identification number for borehole MCOBT-8.5 is MO-10025 and for well MCOBT-4.4 is MO-10026.

Table 5.0-1
Geodetic Data for Well MCOBT-4.4 and Borehole MCOBT-8.5

Description	East	North	Elevation
Brass cap in MCOBT-4.4 pad	1634189.80	1768514.67	6836.18
MCOBT-4.4 top of casing (north edge)	1634196.33	1768512.96	6838.58
Brass cap in MCOBT-8.5 pad	1636710.21	1768725.67	6780.53

6.0 HYDROLOGIC TESTING

The screen installed in MCOBT-4.4 straddles the top of the perched system; therefore, in situ field testing of hydraulic properties was not appropriate.

7.0 DEDICATED PUMP INSTALLATION

Following well development, a dedicated pump for groundwater sampling was installed in the steel-cased well. The pump is a 3-in. Grunfos™ Model SQE submersible one-horsepower pump, rated at 5 gal. per minute (gpm). The dedicated pump assembly, riser pipe, and other components were installed with a Smeal work-over rig, provided and operated by Rio Grande Well Supply.

On February 5, 2002, the pump was assembled. During assembly, the components were laid down on plastic to prevent contamination of the pump and wires. A 1/16-in.-diameter weep hole was drilled into the check valve to allow the riser pipe to drain.

The riser pipe consisted of 1-in. Schedule 40S, type 304 stainless steel connected with 3000-lb F304/F304l stainless steel couplers. The thread compound used was Loctite 567. A 1-in. Schedule 40 PVC flush-thread transducer access pipe was set at the top of the pump to allow unobstructed access for water-level measurements in the future. The pump control leads and the PVC transducer pipe were secured to the riser pipe above the pump, and every 60 ft thereafter, with stainless steel bands. In addition, the leads and the PVC pipe were secured to the riser pipe every 10 ft with cold-weather vinyl cable and pipe tape that are both water and corrosion resistant. The lengths of the pump assembly, the riser joints, and the couplers were measured and constructed to ensure installation of the pump intake at 524 ft bgs.

Pump installation was completed on February 6, 2002. On February 7, 2002, the control box was programmed and wired to the pump leads. The pump control unit is a Grunfos™ CU 300 with an R100 infrared remote control. The pump assembly, tested on February 8, 2002, yielded a discharge rate of 0.21 gpm over a 20-min period at a maximum pump speed of 10,700 rpm.

8.0 WELLHEAD PROTECTION AND SITE RESTORATION

Wellhead protection for well MCOBT-4.4 was completed on September 26, 2001. To ensure long-term structural integrity of the wellhead, a 5000-psi, steel-reinforced concrete pad, 10-ft-long by 5-ft-wide by 1-ft-thick, was poured around the well casing. A 3-in. galvanized-steel conduit was embedded vertically through the pad for the purpose of installing a solar power supply at the wellhead in the future. A 10 3/4-in. steel protective casing with a locking lid protects the well riser. Four 4-in.-diameter steel bollards were placed at each side of the pad boundary. The bollard on the south side is removable to facilitate access to the well for sampling and maintenance activities. Two concrete Jersey traffic barriers were placed in a "V" configuration, pointing upstream to protect the wellhead from floods in Mortandad Canyon.

The MCOBT-4.4 and MCOBT-8.5 site areas were regraded and restored to match the surrounding topography. Prior to regrading, the cuttings pits at both sites were excavated, the plastic lining removed, and the pit refilled with the drill cuttings. All base-course materials used to construct the drill pad were removed from both sites. The straw wattles that are part of the MCOBT-4.4 and MCOBT-8.5 site's best management practices installations remained in place after the post-operational reclamation process. Both sites have been physically reworked and were reseeded with a Laboratory-provided blend of native grasses mixed with straw mulch to facilitate regrowth of groundcover.

PART II: ANALYSES AND INTERPRETATIONS

9.0 GEOLOGY

Both MCOBT-4.4 and MCOBT-8.5 were completed to depths that penetrated through Cerros del Rio lavas and into underlying Puye Formation fanglomerates. One of the primary goals of drilling these holes was to investigate the presence or absence of perched groundwater horizons and to determine the relation of these horizons to stratigraphy. A secondary goal was to collect data on saturation and contaminant distribution through the alluvium or colluvium and into deeper strata of the vadose zone. Accordingly, the geologic data discussed in this section cover information on stratigraphy but also extend to the analysis of colloids associated with vadose-zone waters.

9.1 Stratigraphy of Drill Hole MCOBT-4.4

Geologic units encountered in MCOBT-4.4 consist of the following, in descending order: canyon-bottom alluvium; deposits of the Cerro Toledo interval; the Otowi Member of the Bandelier Tuff, including the basal Guaje Pumice Bed; an upper sequence of fanglomerate and sand deposits of the Puye Formation; lavas, interflow units, and subflow deposits of the Cerros del Rio volcanic field; and a lower sequence of fanglomerate deposits of the Puye Formation. Depths and elevations of the contacts between these units are shown in Figure 9.1-1, with a comparison to the predicted stratigraphy based on the geologic model available at the time drilling began. A summary of unit characteristics is given in the following sections, and a lithologic log is provided in Appendix C.

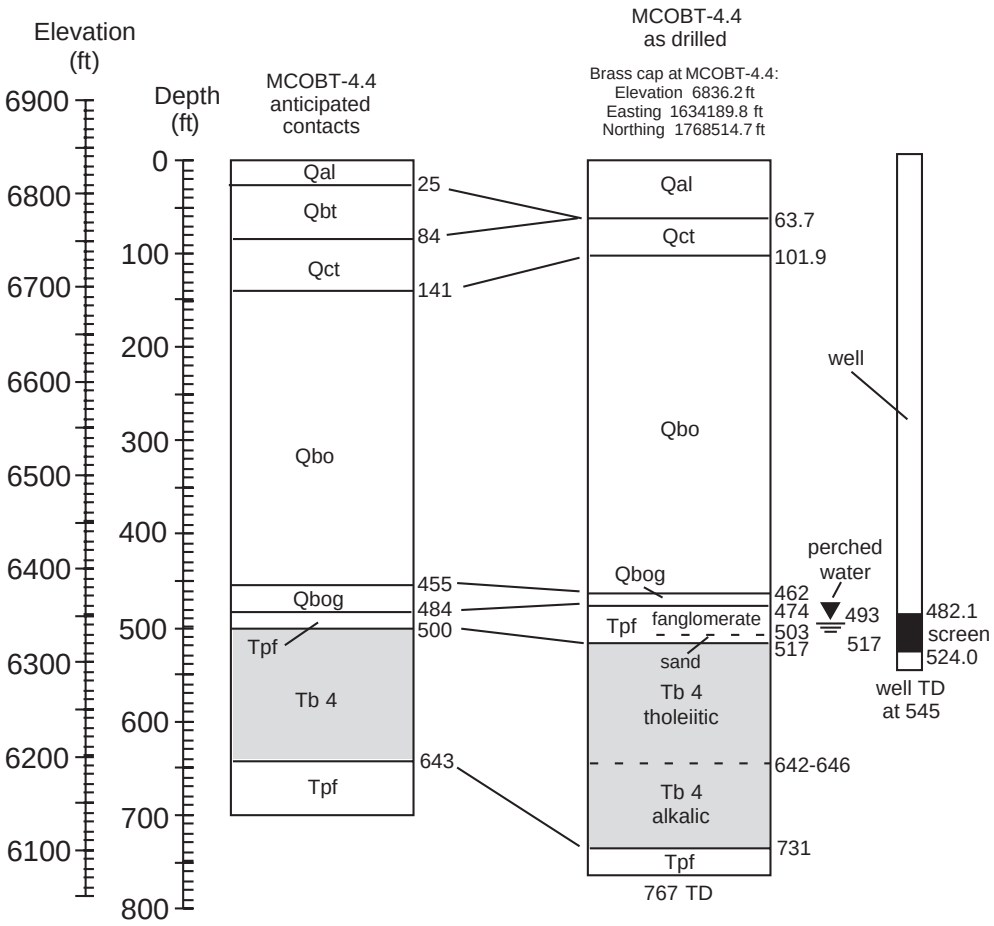

Figure 9.1-1. Anticipated and as-drilled stratigraphy at MCOBT-4.4

Descriptions of geologic units are based on examination of cuttings, geophysical logs, and laboratory analyses of borehole materials. Core was collected from ground surface to 310 ft depth at MCOBT- 4.4; descriptions are based on core samples to this depth. From 310 ft depth to TD (767 ft depth), descriptions are based on cuttings collected by reverse air circulation, thus minimizing admixture of materials from upper portions of the borehole.

Locations of lava flow interiors and breccia zones for the Cerros del Rio were determined by examining the borehole video, as well as the density and conductivity logs (Appendix G). Petrographic data were obtained both by binocular microscope examination of cuttings at the site and by petrographic microscope using thin sections prepared from representative cuttings samples (Appendix D). Mineralogic data were obtained by quantitative X-ray diffraction (QXRD) of 2- to 4-mm size separates or of clay separates. Geochemical data were collected from core and cuttings samples by X-ray fluorescence (XRF). All these data must be considered for stratigraphic correlation. The mineralogic and geochemical data provide information of hydrogeologic importance (*e.g.*, content of relatively soluble glass, clay occurrences, and mineralogy that controls or is affected by changes in Eh and pH).

Figure 9.1-1 shows the location of the screened interval in the completed well at MCOBT-4.4 in relation to drill hole stratigraphy. Geologic samples at the screen location are particularly important for relating geochemistry, petrology, mineralogy, and sedimentology to the interpretation of water occurrences and compositions. Preliminary data for evaluating these and other representative samples are provided in this report; further analyses may be appropriate in the future.

9.1.1 Canyon-bottom Alluvium (Qal, 0 to 63.7 ft depth)

Canyon-bottom alluvium (Qal) was cored from 0 to 63.7 ft depth at MCOBT-4.4. The alluvium consists predominantly of moderately weathered detritus of the Tshirege Member of the Bandelier Tuff. This detritus is unconsolidated and generally sand-sized; coarser detritus derived from the nonwelded lower Tshirege units (Qbt 1g and Qbt 1v) may have been present but is unlikely to survive coring operations intact. Coarse blocks of tuff several centimeters in size are presen, but generally represent the more welded upper units (Qbt 2 and Qbt 3) of the Tshirege. Towards the bottom of the alluvium (~61 ft depth) there is a moderate increase in clay alteration of Tshirege detritus.

9.1.2 Sediments and ash of the Cerro Toledo Interval (Qct, 63.7 to 101.9 ft depth)

Deposits of the Cerro Toledo interval (Qct) were cored from 63.7 to 101.9 ft depth in MCOBT-4.4. These deposits are marked by the first appearance of aphyric pumice, contrasting with the quartz- and sanidine-porphyritic pumice and ash of the Tshirege Member of the Bandelier Tuff. Upper deposits of the Cerro Toledo are mostly air-fall or reworked ash with sandy detritus; below 75 ft depth the abundances of dacitic and related lithic clasts, along with sands rich in quartz and sanidine crystals, indicate extensive sedimentary reworking with inclusion of detritus from Tschicoma Formation volcanic sources as well as from the underlying Otowi Member of the Bandelier Tuff.

An exceptionally well-preserved pumice deposit at 67.5 to 68.2 ft was sampled for petrographic, mineralogic, and chemical analysis to verify that the Cerro Toledo interval is present. This pumice contains fresh glass and is essentially unaltered. The chemical analysis of this sample is listed in column 1 of Table 9.1-1. The major-element composition of this sample is consistent with the range of Cerro Toledo rhyolite compositions described in Heiken et al. (1986, 48638), but this composition is also typical of pumice from both the Otowi Member and the lower Tshirege Member of the Bandelier Tuff. More distinctive are the high Zn content (110 ppm) and low Rb content (189 ppm); they are respectively higher and lower in the most similar vitric materials from the Bandelier Tuff, which have <35 ppm Zn and >300 ppm Rb. Pumice from the Bandelier Tuff would also have a high abundance (5 to 10%) of quartz and sanidine phenocrysts; the pumice from this interval in MCOBT-4.4 is poorly porphyritic, with minor feldspar and trace quartz phenocrysts (Appendix D), consistent with derivation from Cerro Toledo volcanic sources.

In drill holes where the Cerro Toledo interval occurs between intact sequences of the Otowi and Tshirege Members of the Bandelier Tuff, the low natural gamma signal of the Cerro Toledo is distinctive and often sufficient to refine stratigraphic definition of the contacts between these units (for example, drill hole R-15, Longmire et al., 2001, 70103). This is not the case at MCOBT-4.4, where the natural gamma signal of the Cerro Toledo interval is variable and is not lower than either the overlying alluvium or the underlying Otowi ash flows (Figure 9.1-2). A low gamma signal that is typically observed in the Cerro Toledo is principally a consequence of the presence of rhyolitic tephra with less than half the U and Th content of the Bandelier Tuff (Heiken et al. 1986, 48638). Intermixture of detritus from Otowi ash flows can be sufficient to mask this difference, as appears to be the case below 75 to 80 ft depth in MCOBT-4.4. However, the cause of the relatively high natural gamma signal in the Cerro Toledo from 63.7 to 75 ft depth in MCOBT-4.4 is not known at this time.

Table 9.1-1
XRF Analyses of Cerro Toledo Pumice (Qct), Puye Formation Sediments (Tpf), and Cerros del Rio Lavas (Tb4) from MCOBT-4.4

	1	2	3	4	5	6	7	8	9	10	11	12
Sample Number[a]	MCOBT-4.4 68.0–68.2	MCOBT-4.4 502–507	MCOBT-4.4 522–527	MCOBT-4.4 542–547	MCOBT-4.4 562–567	MCOBT-4.4 592–597	MCOBT-4.4 632–637	MCOBT-4.4 657–662	MCOBT-4.4 672–677	MCOBT-4.4 712–717	MCOBT-4.4 737–742	MCOBT-4.4 762–767
Unit[b]	Qct	Tpf	Tb4	Tb4	Tb4	Tb4	Tb4	Tb4	Tb4	Tb4	Tpf	Tpf
XRF Data (major elements)												
SiO_2 %	71.66	69.23	50.05	50.38	50.63	50.14	50.28	50.12	49.29	49.10	66.60	67.12
TiO_2 %	0.09	0.46	1.44	1.44	1.43	1.46	1.46	1.66	1.62	1.73	0.52	0.52
Al_2O_3 %	13.32	14.85	16.45	16.08	16.18	16.00	16.15	15.96	15.78	15.89	14.79	14.69
FeO %[c]	0.48	0.37	4.95	6.23	5.80	5.91	7.61	7.14	5.23	6.25	1.43	1.28
Fe_2O_3 %[c]	0.87	2.77	5.42	4.55	5.02	4.99	3.02	2.99	5.20	4.14	2.29	2.54
MnO %	0.09	0.04	0.13	0.17	0.17	0.17	0.17	0.17	0.17	0.17	0.06	0.06
MgO %	0.08	0.87	6.24	6.37	6.29	6.50	6.54	6.47	7.00	7.39	1.70	1.63
CaO %	0.29	2.21	9.33	8.90	8.98	8.90	8.97	9.06	8.97	9.03	3.37	3.28
Na_2O %	3.35	3.75	2.97	3.29	3.34	3.29	3.32	3.54	3.39	3.53	3.78	3.93
K_2O %	4.66	3.81	0.66	1.08	1.04	1.08	1.09	1.47	1.40	1.50	3.22	3.22
P_2O_5 %	<0.01	0.13	0.35	0.36	0.36	0.37	0.37	0.54	0.55	0.58	0.21	0.22
LOI %[d]	4.24	0.86	1.32	–0.17	–0.05	–0.13	–0.60	–0.64	–0.23	–0.52	0.39	0.27
Total %	94.88	98.48	98.00	98.84	99.24	98.80	98.97	99.12	98.60	99.32	97.97	98.50
XRF Data (trace elements)												
V ppm	<10	40	180	175	191	203	185	202	195	205	52	57
Cr ppm	<8	40	170	173	183	185	167	192	205	208	24	21
Ni ppm	<12	17	70	73	72	75	78	83	115	112	13	13
Zn ppm	110	42	98	100	94	94	93	101	91	92	53	58
Rb ppm	189	116	<9	17	24	21	21	25	24	30	62	63
Sr ppm	<7	326	472	465	489	516	491	676	665	715	478	478
Y ppm	72	20	31	29	41	27	23	32	46	34	21	24
Zr ppm	182	181	152	149	152	156	150	198	188	196	167	172
Nb ppm	104	34	19	19	20	25	18	25	25	29	<8	11
Ba ppm	67	905	495	464	488	585	518	671	734	762	1286	1232

Note: Values reported in percent or parts per million by weight. Analytical errors (2σ) are SiO_2, 0.7; TiO_2, 0.01, Al_2O_3, 0.2; Fe_2O_3, 0.06; MnO, 0.01; MgO, 0.08; CaO, 0.1; Na_2O, 0.1; K_2O, 0.05; P_2O_5, 0.01; V, 10; Cr, 8; Ni, 10; Zn, 12; Rb, 5; Sr, 25; Y, 6; Zr, 30; Nb, 7; and Ba, 50.

[a] Number ranges indicate depth ranges of core (column 1) or cuttings (columns 2–12) in ft.

[b] Unit designations are "Qct" for Cerro Toledo, "Tpf" for Puye Formation fanglomerates, and "Tb4" for Cerros del Rio volcanic rocks.

[c] Ferrous/ferric ratio determined by digestion/titration.

[d] LOI = loss on ignition; negative numbers indicate oxidation of ferrous iron during ignition.

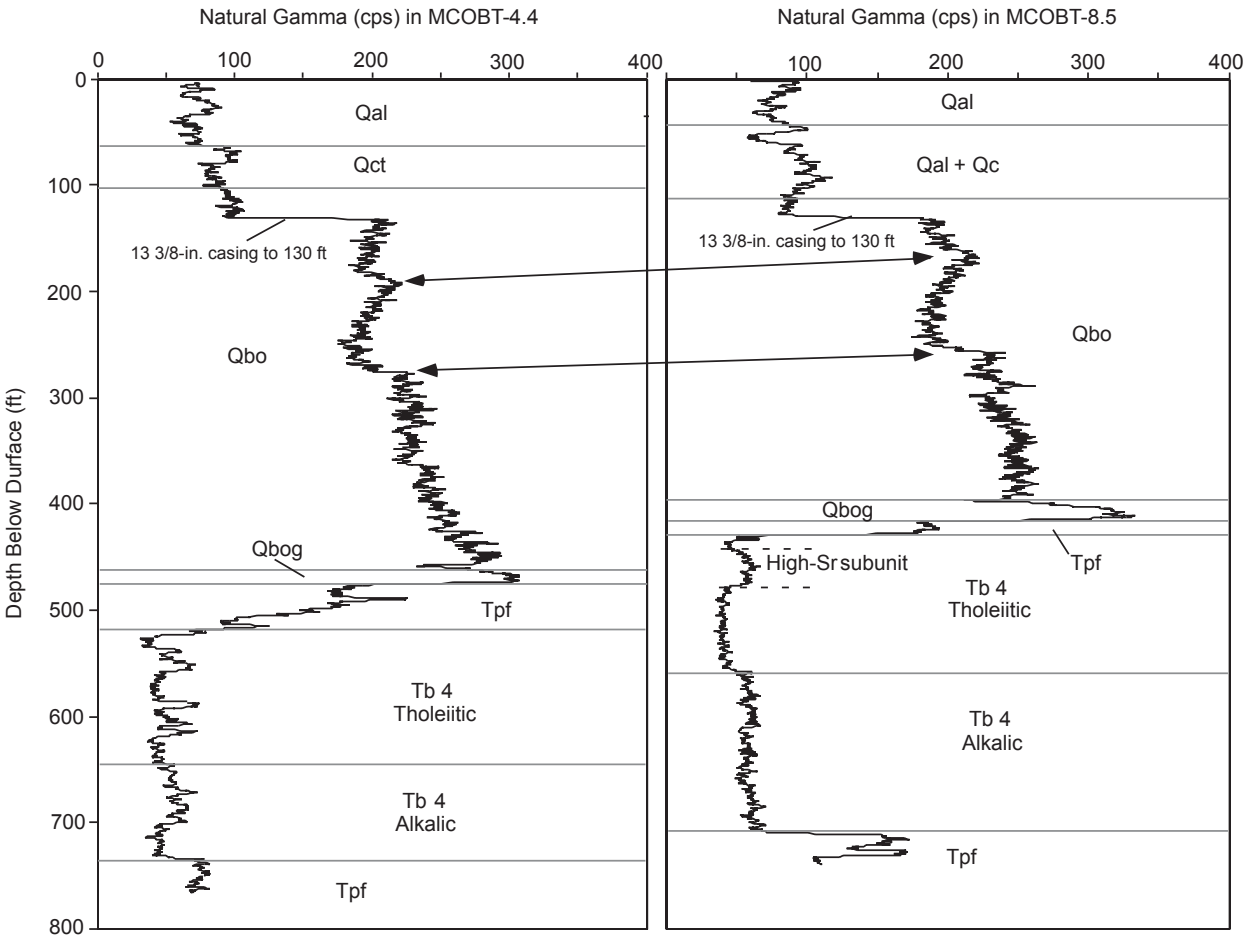

Figure 9.1-2. Comparison of natural gamma signals in MCOBT-4.4 and MCOBT-8.5

9.1.3 Ash Flows and Guaje Pumice Bed of the Otowi Member of the Bandelier Tuff (Qbo, 101.9 to 462 ft depth and Qbog 462 to 474 ft depth)

Otowi ash flows (Qbo) are 360 ft thick at MCOBT-4.4. Core was collected through the upper 208 ft of Otowi ash; coring ceased at 310 ft depth and cuttings were collected from that point downward. The Otowi ash flows have a natural gamma signal that characteristically increases with depth. This rise in the natural gamma signal is not smooth but diminishes and then rises sharply in notable discontinuities at 180 ft depth and 277 ft depth, marked by arrows in Figure 9.1-2. This figure also shows the very similar pattern in the natural gamma signal through the Otowi ash flows in drill hole MCOBT-8.5; natural gamma data from drill hole R-15 repeat the same pattern (Figure 3.3-1 of Longmire et al. 2001, 70103). Repetition of this pattern shows that the natural gamma data can be used to delineate subunits of the Otowi ash flows beneath the central portion of Mortandad Canyon. The natural gamma profile provides stratigraphic reference points within the Otowi ash flows against which saturation, anion, or contaminant concentration profiles can be registered.

The Otowi ash flows in MCOBT-4.4 are nonwelded, vitric, and little altered. The ash flows are porphyritic, with ~10 to 20% phenocrysts of quartz and sanidine. The abundance of lithic clasts rises to ~20% in some intervals but is typically about half that amount. Lithic clasts consist of dacitic to andesitic (?) lavas that are

extensively silicified. Pumice sizes are variable, generally up to ~1 to 5 cm in core; where cuttings are collected, the pumice is seldom recovered intact. Although alteration is limited, orange-to-earthen and spottier black discoloration is common, suggesting the presence of some clay plus Fe or Mn oxyhydroxide minerals or amorphous materials.

The Guaje Pumice Bed (Qbog) at MCOBT-4.4 is marked by a discontinuity with modest rise in the natural gamma signal (Figure 9.1-2). Data from the combined magnetic resonance (CMR) geophysical log (Appendix G) indicate a rise in water content within the Guaje Pumice Bed (although perched water was not detected at this location during drilling). This increase in water content is not associated with any evidence of clay alteration, indicating increased moisture within the more abundant and more porous pumice of the Guaje Pumice Bed, relative to the overlying ash flows.

9.1.4 Upper Sequence of Puye Formation Fanglomerates and Sand (Tpf, 474 to 517 ft depth)

Fanglomerates and a possible sandy soil of the Puye Formation (Tpf) were sampled as cuttings from 474 to 517 ft depth in MCOBT-4.4. Cuttings from 474 to 502 ft depth are dominated by gravels, generally 1 to 2 cm in size, of intermediate-composition lavas. Below 502 ft, the Puye sediments consist of silty sand with more variable volcanic sources, including some fragments of basalt. The basaltic fragments are vesicular, altered, and probably derived from the underlying Cerros del Rio lavas. Column 2 of Table 9.1-1 lists a chemical analysis of 2- to 4-mm fine gravels from 502 to 507 ft depth in this interval (to be compared with deeper Puye sediments in Section 9.1.6). The two subdivisions of the upper Puye Formation at MCOBT-4.4, an upper fanglomerate of 28 ft thickness and the lower 15 ft of sand with dacitic and basaltic clasts, may correspond to the two similar subdivisions in the Puye Formation above Cerros del Rio lavas at R-15 (Longmire et al. 2001, 70103).

Clay alteration is evident throughout the upper Puye Formation at MCOBT-4.4 but not in amounts sufficient to produce balls of clay in the cuttings. Some clay-bound sandy detritus does occur in the cuttings, and clay fills the vesicles of basalt detritus below 502 ft depth.

9.1.5 Lavas, Interflow Units, and Subflow Deposits of the Cerros del Rio Volcanic Field (Tb4, 517 to 731 ft depth)

Lavas, interflow rubble or scoria zones, and subflow deposits of the Cerros del Rio volcanic field (Tb4) were encountered in the interval from 517 to 731 ft depth in MCOBT-4.4. The Cerros del Rio volcanic series is of particular interest in Mortandad Canyon because of the evidence of perched water at the base of this series in drill hole R-15 that contained 3770 pCi/L tritium, 12 ppb perchlorate, and detectable americium (Longmire et al. 2001, 70103).

Cuttings from the Cerros del Rio volcanic series in MCOBT-4.4 contain variable amounts of pale flesh-colored to green-brown clay. These clay occurrences are greatest at the top of the volcanic series (60% of the >35 mesh cuttings); clay accumulations occur in diminishing concentration from breccia zones at greater depth. The depth distribution of these clay zones and the clay abundance in the >35 mesh cuttings is illustrated in Figure 9.1-3. The presence of scoria and the oxidation of basalt cuttings associated with the highest clay abundances suggest that the clays have accumulated in breccia zones (with some scoria) between lava flows.

Petrographic and chemical data from the Cerros del Rio lavas at wells R-9, R-12, and R-15 show consistent variation from more primitive alkalic basalts at depth to more evolved tholeiitic basalts in the later lavas. This same sequence occurs in drill holes of Los Alamos Canyon and Sandia Canyon as well as Mortandad Canyon (see Section 9.3). The rise in the magnesium number (Mg#, representing the cation ratio Mg/[Mg+Fe]) from bottom to top is clearly seen in MCOBT-4.4, based on the geochemical sequence

in columns 3 to 10 of Table 9.1-1 and plotted in Figure 9.1-3. This figure also plots Sr content, a measure of alkalinity in Cerros del Rio lavas. These geochemical data show the pattern characteristic of this sequence of flows, with Mg# and Sr content diminishing upward through the alkalic basalts and a relatively abrupt transition to tholeiitic basalts with lower Mg# and Sr content. The demarcation between alkalic and tholeiitic basalts in MCOBT-4.4 is shown in Figure 9.1-3 as occurring in a zone of vesicular scoria with modest clay abundance (5%) at 6189 to 6194 ft elevation (642 to 646 ft depth).

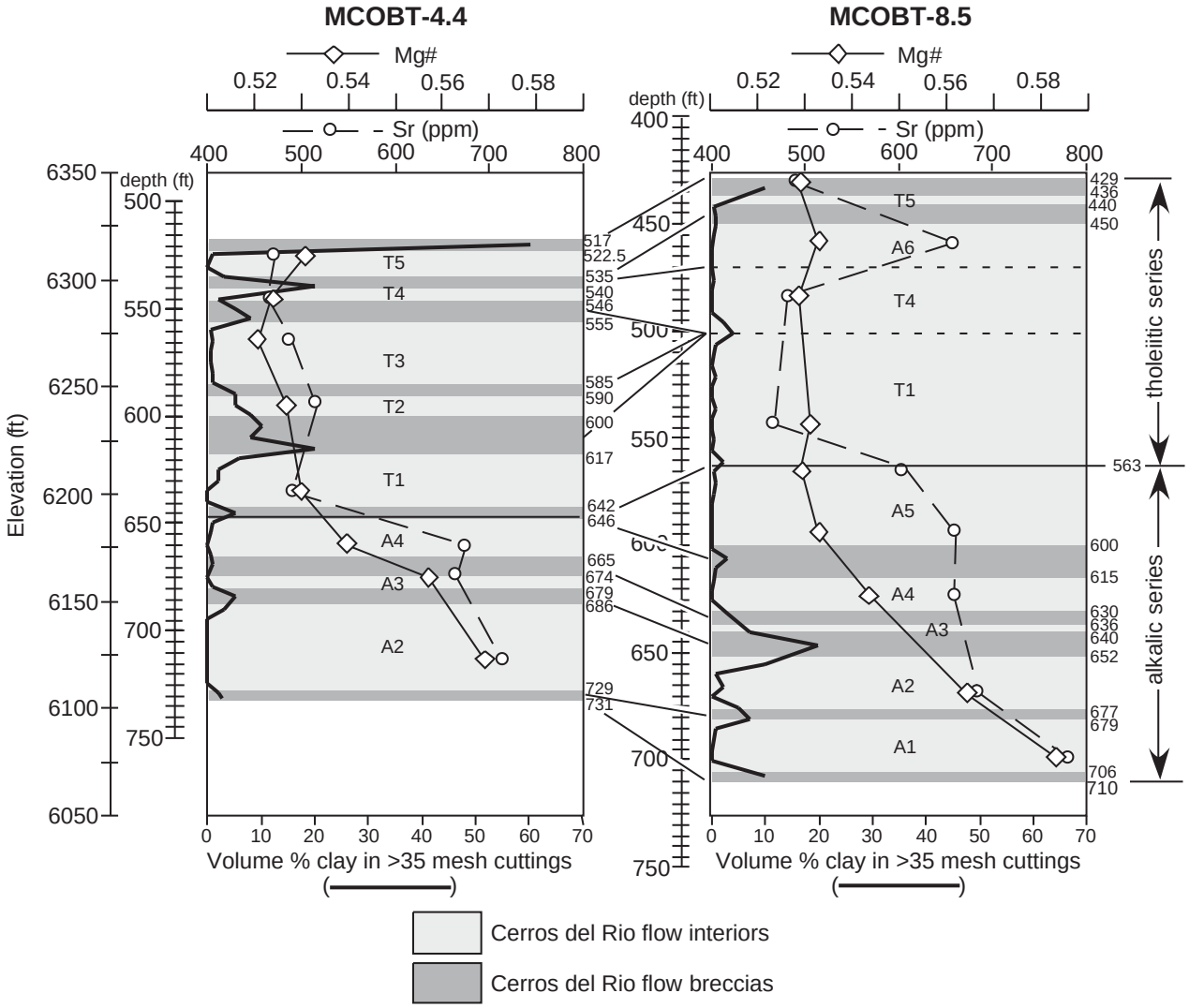

Figure 9.1-3. Breccia zones, clay abundance (% vol. in >35 mesh), Sr concentration, and Mg# [cation ratio Mg/(Mg+Fe)] in the Cerros del Rio volcanic series in MCOBT-4.4 and MCOBT-8.5. Numbers at right of each column are depths in ft to contacts between breccias and more competent lavas, determined from borehole video and borehole density and conductivity logs. Correlation of individual alkalic (A) and tholeiitic (T) flows shown by numbers, as determined from chemical and petrographic character.

The natural gamma signal in the Cerros del Rio at MCOBT-4.4 is noisy and shows no significant difference between the alkalic and tholeiitic lavas (Figure 9.1-2). High gamma spikes in the tholeiitic series at MCOBT-4.4 correlate with clay accumulations in breccia zones; spectral gamma logging (Appendix G) indicates that the relatively high Th and K in these zones probably correlate with breccia clays. Other

borehole logs, summarized in Appendix G, provide additional information. The density log for MCOBT-4.4 rises from ~2 g/cm^3 at the top of the Cerros del Rio lavas (517 ft depth) to a maximum value of ~2.5 g/cm^3 at 526 ft depth, associated with the transition from flow-top rubble to a denser flow interior. This rise in density is associated with the lower limit of a zone of high small-pore (clay) water content that extends from the Puye sediments at 495 ft depth into the Cerros del Rio at 524 ft depth (interpretation based on the CMR log in Appendix G). In general, the Cerros del Rio volcanic series in MCOBT-4.4 varies in density between breccia zones of ~2 g/cm^3 and flow interiors 10 to 40 ft thick (Figure 9.1-3) with densities as high as 2.8 g/cm^3. Occurrences of elevated large-pore water content (CMR log, Appendix G) as well as clay-bound water both occur in the low-density zones.

Clay fractions of 0.25 to 0.1 μm were separated from the rubble zone at the top of the Cerros del Rio volcanic series and from three deeper breccia zones for analysis by X-ray diffraction (XRD). The clay separated from the upper rubble zone (517 to 522.5 ft depth) consists of 96% smectite with no associated glass. In contrast, clays from the deeper breccia zones consist of smectite with significant associated basaltic glass (60% smectite with 36% glass at 600 to 617 ft, 63% smectite with 30% glass at 642 to 646 ft, and 85% smectite with 11% glass at 679 to 686 ft). The retention of glass in the deeper breccia zones indicates incomplete alteration and supports an interpretation of clay formation from basaltic glass in situ. The lack of remnant glass and the high clay abundance in the rubble zone from 517 to 522.5 ft depth indicate thorough alteration.

Based on the details of flow interiors and flow breccias illustrated in Figure 9.1-3, the Cerros del Rio lava series at MCOBT-4.4 and MCOBT-8.5 consists of at least six alkalic flows (A1 to A6) and five tholeiitic flows (T1 to T5). Eight of these flows are present in MCOBT-4.4. Individual flows are distinguished by both chemical (Tables 9.1-1 and 9.2-1) and petrographic (Appendix D) properties. Correlations between flows in MCOBT-4.4, MCOBT-8.5, and other drill holes are discussed below in Section 9.3.

9.1.6 Lower Sequence of Puye Formation Fanglomerates (Tpf, 731 ft depth to TD at 767 ft depth)

A lower sequence of Puye Formation fanglomerates (Tpf) extends from 731 ft depth to the TD of MCOBT-4.4 at 767 ft. These fanglomerates bear some similarities to the upper Puye fanglomerates, but there are several significant differences. Table 9.1-1 shows that the 2- to 4-mm size fraction from the upper Puye is more silica-rich and less calcic than comparable size fractions from Puye sediments below the Cerros del Rio series. There are also differences in trace-element composition, most notably a higher Rb/Sr ratio in the upper Puye (0.36) than in the lower Puye (0.13). These differences correspond to a greater abundance of rhyodacitic detritus in the upper Puye fanglomerates, in contrast to the preponderance of more mafic dacitic sources for the lower Puye Formation. This difference in chemical composition is supported by petrographic observations of more mafic dacitic lithologies from Pajarito and Caballo Mountains in the lower Puye Formation (Appendix D). The lower Puye Formation at MCOBT-4.4 is compositionally similar to Puye sediments underlying the Cerros del Rio lavas at well R-15 (Longmire et al. 2001, 70103).

Table 9.1-2 summarizes mineralogical data obtained by QXRD that further differentiate the upper Puye Formation (row 2, Table 9.1-2) and lower Puye Formation (rows 4 and 5, Table 9.1-2), along with mineralogical information relevant to hydrogeologic properties within these two different sedimentary series. The greater abundance of quartz in the upper Puye Formation correlates with more siliceous volcanic sources. The presence of clay (smectite) and the complete absence of glass in the upper Puye Formation indicate the long-term presence of pore water and extensive alteration in this zone, perhaps associated with the perched zone discussed below in Section 9.1.7. In contrast, the lower Puye Formation is characterized by the lack of clay and an abundance of volcanic glass, indicating less extensive alteration in this zone.

Table 9.1-2
QXRD Analyses of Samples from MCOBT-4.4 and MCOBT-8.5

Sample[a]	Smectite	Kaolinite[b]	Tridymite	Cristobalite	Quartz	Alkali Feldspar	Plagioclase	Glass	Hematite	Biotite	Total
Cerro Toledo Formation Pumice											
(1) MCOBT-4.4 68.0–68.2	—	1.1	—	—	0.3	1.0	1.0	95.1	—	—	98.5
Upper Puye Formation											
(2) MCOBT-4.4 502–507	8.1	—	11.5	9.8	2.8	22.3	37.7	—	0.8	3.0	96.0
(3) MCOBT-8.5 422–427	5.1	—	11.5	10.8	3.8	22.8	33.7	6.7	0.8	2.1	97.2
Lower Puye Formation											
(4) MCOBT-4.4 734–742	—	—	8.6	7.6	0.3	12.9	43.1	21.9	0.7	1.6	96.7
(5) MCOBT-4.4 762–767	—	—	10.3	9.1	0.5	15.3	43.3	15.7	0.8	1.0	96.0
(6) MCOBT-8.5 730–735	3.4	—	10.3	11.2	1.1	21.8	36.0	12.6	0.8	1.2	98.4

Note: Values reported are in weight percent. Analytical errors (2σ) are ~5% of the amount reported for abundances >10% and ~10% of the amount reported for abundances <10%. Dashes indicate that the phase was not detected (detection limits are ~0.1%).

[a] Number ranges indicate depth ranges of core (row 1) or cuttings (rows 2–6) in ft.

[b] Kaolinite and/or halloysite.

9.1.7 Geologic Relationships of the Perched Water Zone in MCOBT-4.4

A perched groundwater zone was encountered during drilling of the MCOBT-4.4 borehole. Section 10.1 of this report describes the discovery of this zone and the efforts taken to determine its vertical extent. Sections 9.1.4 and 9.1.5 provide descriptions of the geologic units making up the perched zone. This section summarizes the geologic interpretations of the perched zone and the perching horizon that led to the design of the well. Figure 9.1-4 highlights key geologic features of this zone in relation to the installed well.

The top of the perched groundwater zone occurs at a depth of about 493 ft, within pebble gravel made up of dacitic volcanic detritus of the Puye Formation. The base of the pebble gravel, at a depth of 503 ft, is underlain by finer-grained clastic sediments made up of silty sand and gravel. These silty sands and gravel, which form the lower part the upper Puye sequence (see Section 9.1.4), extend to a depth of 517 ft, where they overlie Cerros del Rio basalt. Geophysical logs indicate that both the pebble gravel and the silty sand and gravel are zones of moderate porosity and low density (Figure 9.1-4), although porosity and density are more variable in the pebble gravel.

The top of the Cerros del Rio basalt, from 517 to 522.5 ft, consists of flow-top rubble made up of angular blocks of vesicular basalt. Geophysical logs indicate that the rubble zone has high porosity and low density (Figure 9.1-4). Drill cuttings from this zone contain abundant clay minerals (Figure 9.1-4). The rubble zone overlies the interior of a lava flow that extends from 522.5 to 535 ft. This lava is vesicular at the top of the flow and becomes massive downward, an observation consistent with the density log (Figure 9.1-4). A hole in the lava flow intersects one side of the borehole from 528.7 to 529.7 ft (Figure 9.1-4). A borehole video log (obtained while the perched zone was drained of water) showed fogging of the camera lens from 528.7 to 529.7 ft, indicating the flow of warm moist air through a laterally connected zone. Geophysical logs show that the interior of the lava flow is generally an interval of high density and low porosity, except for the depth range from 528.7 to 529.7 ft.

The lava flow described above overlies zones of interflow scoria and breccia that are interbedded with other lava flows (Figure 9.1-4). In general, the clay content of these interflow zones decreases downsection.

The perched water horizon at MCOBT-4.4 spans a depth of 493 ft to an uncertain maximum depth. The top of the perched zone was defined by static water level readings of 493 ft above a packer placed in the interval from 524.5 ft to 531.5 ft in the open borehole; similar water levels were measured in the completed well during development (see Section 10.1). The perching layer may include (1) the silty sand and gravel interval in the lower part the upper Puye sequence (503 to 517 ft), (2) clay-rich brecciated rubble above the lava interior (517 to 522.5 ft), or (3) the massive lava flow interior (approximately 522.5 ft to 535 ft). The silty sand and gravel interval in the lower part the upper Puye sequence and the clay-rich brecciated rubble are zones of moderate porosity and low density (Figure 9.1-4). The massive lava flow interior is characterized by low porosity and high density.

The well design assumed that achievement of a static water level in the open borehole was a strong indication that the packer was placed within a portion of the perching layer. With the top of the packer set at 524.5 ft, the perching layer includes, at least in part, the massive lava flow interior from 522.5 ft to 535 ft. Although the base of the perching layer may coincide with the base of the lava flow interior (535 ft depth), the hole at 528.7 to 529.7 ft was considered a possible lateral pathway within this lava flow. Thus, the bottom of the filter pack for the well was placed at 527 ft, near the upper of two density maxima for the lava flow (Figure 9.1-4). As discussed above, the location of the top of the perching layer is uncertain.

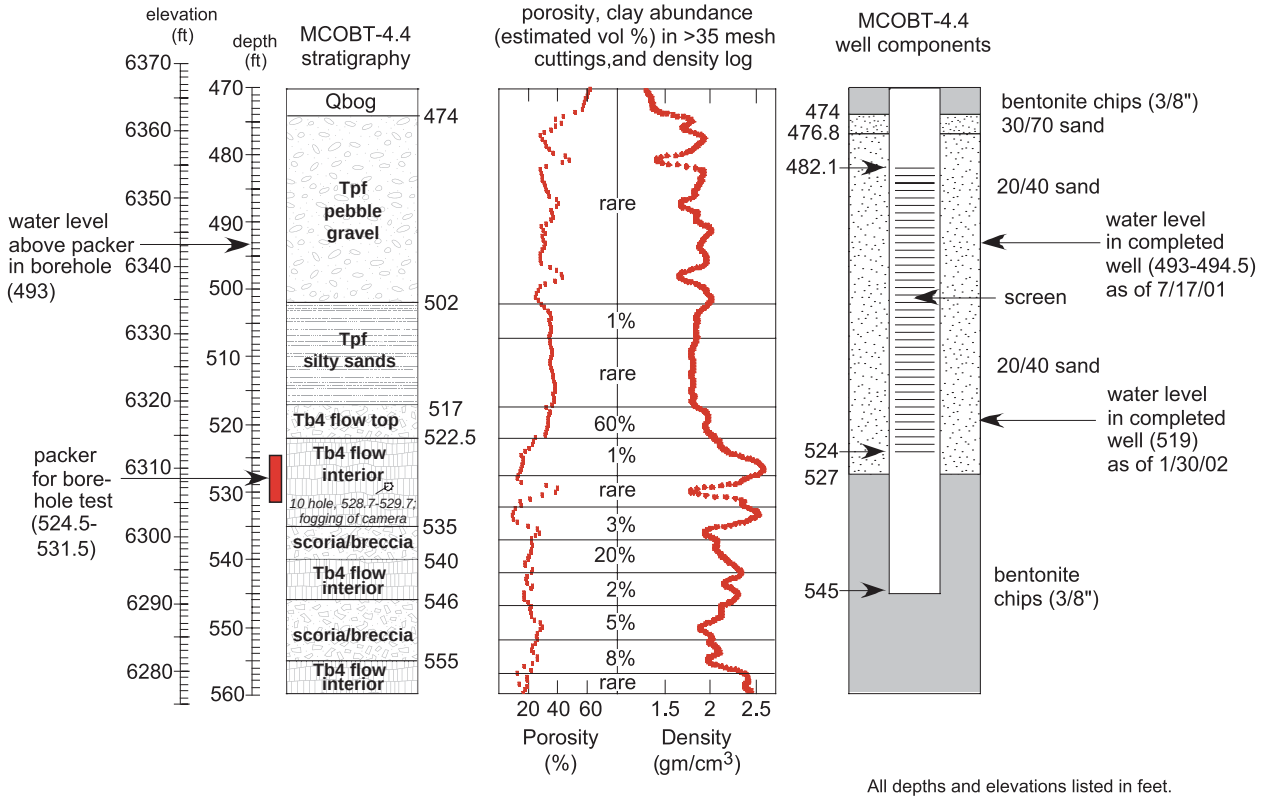

Figure 9.1-4. Geologic relationships of the perched groundwater zone in MCOBT-4.4

9.2 Stratigraphy of Drill Hole MCOBT-8.5

Geologic units encountered in MCOBT-8.5 consist of the following, in descending order: canyon-bottom alluvium; an interval of canyon-bottom alluvium plus colluvium; the Otowi Member of the Bandelier Tuff including the basal Guaje Pumice Bed; an upper sequence of Puye Formation fanglomerates; lavas, interflow units, and subflow deposits of the Cerros del Rio volcanic field; and a lower sequence of fanglomerate deposits of the Puye Formation. Depths and elevations of the contacts between these units are shown in Figure 9.2-1, with a comparison to the predicted stratigraphy based on the 3-D geologic model available at the time drilling began. A summary of unit characteristics is given in the following sections, and a lithologic log is provided in Appendix C. No screened intervals are shown in Figure 9.2-1; the borehole was plugged and abandoned because there was no evidence of perched water.

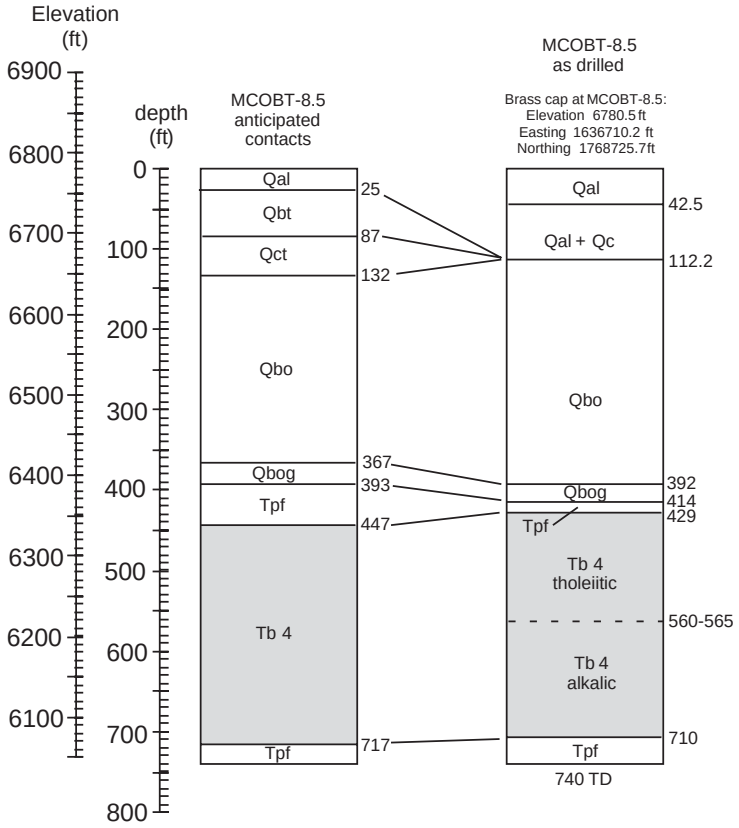

Figure 9.2-1. Anticipated and as-drilled stratigraphy at MCOBT-8.5

As with MCOBT-4.4 (Section 9.1), descriptions of geologic units are based on examination of cuttings, geophysical logs, and laboratory analyses of borehole materials. Core was collected from ground surface to 347 ft depth at MCOBT-8.5; descriptions are based on core samples to this depth. From 347 ft depth to TD (740 ft depth), descriptions are based on cuttings. Cuttings were collected by reverse circulation methods, minimizing admixture of materials from upper portions of the borehole. Cuttings were used to gather petrographic, mineralogic, and geochemical data from units beneath the Bandelier Tuff. Locations of lava flow interiors and breccia zones for the Cerros del Rio volcanic series were determined by examining the borehole video as well as the density and conductivity logs (Appendix H). Petrographic data were obtained both by binocular microscope examination of cuttings at the site and by petrographic microscope using thin sections prepared from representative cuttings samples (Appendix D). Mineralogic data were obtained by QXRD (Table 9.1-2). Geochemical data were collected from cuttings samples by XRF (Table 9.2-1).

Table 9.2-1
XRF Analyses of Sediments and Lavas from MCOBT-8.5

	1	2	3	4	5	6	7	8	9	10	11
Sample Number[a]	MCOBT-8.5 422–427	MCOBT-8.5 432–437	MCOBT-8.5 460–465	MCOBT-8.5 485–490	MCOBT-8.5 545–550	MCOBT-8.5 565–570	MCOBT-8.5 595–600	MCOBT-8.5 625–630	MCOBT-8.5 670–675	MCOBT-8.5 700–705	MCOBT-8.5 730–735
Unit[b]	Tpf	Tb4	Tb4	Tb4	Tb4	Tb4	Tb4	Tb4	Tb4	Tb4	Tpf
XRF Data (major elements)											
SiO_2 %	69.86	50.37	50.39	51.08	50.48	50.24	50.38	49.79	49.26	48.32	69.13
TiO_2 %	0.47	1.46	1.57	1.44	1.45	1.54	1.58	1.64	1.71	1.78	0.41
Al_2O_3 %	14.67	16.15	16.69	15.89	15.92	16.03	16.05	16.02	15.78	15.40	14.58
FeO %[c]	0.54	7.06	5.86	5.67	6.67	5.90	6.06	6.58	7.49	4.83	0.54
Fe_2O_3 %[c]	2.73	3.71	4.47	5.42	3.88	4.31	4.18	3.65	2.83	5.89	2.46
MnO %	0.05	0.17	0.17	0.17	0.16	0.16	0.16	0.17	0.17	0.17	0.05
MgO %	1.07	6.54	6.33	6.64	6.46	6.17	6.29	6.61	7.31	7.98	1.30
CaO %	2.32	8.96	8.90	8.95	9.01	8.97	8.89	9.10	8.91	8.85	2.39
Na_2O %	3.75	3.22	3.54	3.31	3.31	3.50	3.55	3.58	3.54	3.48	3.88
K_2O %	3.78	0.96	1.33	1.02	1.03	1.31	1.39	1.44	1.48	1.54	3.87
P_2O_5 %	0.12	0.34	0.50	0.33	0.36	0.52	0.54	0.55	0.57	0.63	0.11
LOI %[d]	0.61	–0.21	–0.38	–0.28	0.07	0.22	–0.06	–0.54	–0.67	–0.37	0.48
Total %	99.36	98.95	99.75	99.92	98.74	98.65	99.08	99.11	99.06	98.88	98.72
XRF Data (trace elements)											
V ppm	43	194	208	180	195	199	205	206	195	213	42
Cr ppm	44	191	176	201	183	177	173	203	233	240	42
Ni ppm	21	84	77	89	86	79	73	97	131	155	28
Zn ppm	44	102	94	96	98	96	92	83	89	79	39
Rb ppm	99	15	28	19	18	31	29	24	29	31	110
Sr ppm	353	491	661	484	470	607	664	661	688	783	334
Y ppm	28	34	37	28	31	40	45	38	34	34	22
Zr ppm	180	160	194	166	154	181	200	185	204	199	161
Nb ppm	30	24	30	19	23	25	33	23	29	28	34
Ba ppm	862	488	642	503	434	661	743	661	704	770	821

Note: Values reported in percent or parts per million by weight. Analytical errors (2σ) are SiO_2, 0.7; TiO_2, 0.01, Al_2O_3, 0.2; Fe_2O_3, 0.06; MnO, 0.01; MgO, 0.08; CaO, 0.1; Na_2O, 0.1; K_2O, 0.05; P_2O_5, 0.01; V, 10; Cr, 8; Ni, 10; Zn, 12; Rb, 5; Sr, 25; Y, 6; Zr, 30; Nb, 7; and Ba, 50.

[a] Number ranges indicate depth ranges of cuttings in ft.

[b] Unit designations are "Qct" for Cerro Toledo, "Tpf" for Puye Formation fanglomerates, and "Tb4" for Cerros del Rio volcanic rocks.

[c] Ferrous/ferric ratio determined by digestion/titration.

[d] LOI = loss on ignition; negative numbers indicate oxidation of ferrous iron during ignition.

9.2.1 Canyon-bottom Alluvium (Qal, 0 to 42.5 ft depth)

Canyon-bottom alluvium (Qal) was cored from 0 to 42.5 ft depth at MCOBT-8.5. As in MCOBT-4.4, the alluvium consists of predominantly sand-sized, moderately weathered detritus of the Tshirege Member of the Bandelier Tuff. The upper seven ft consist of a dark loamy sand, grading into lighter brown sands and gravels with fragments of calcrete occurring to a depth of 17 ft. Sandy gravels occur to a depth of 42.5 ft, the depth of first occurrence of a large colluvial block (2.5-ft diameter, drilled from 42.5 to 45 ft depth) of moderately welded devitrified tuff derived from nearby cliff-forming units of the Tshirege Member of the Bandelier Tuff.

9.2.2 Canyon-bottom Alluvium plus Colluvium (Qct, 42.5 to 112.2 ft depth)

Deposits of alluvium (Qal) intermixed with canyon-wall colluvium (Qc) were cored from 42.5 to 112.2 ft depth in MCOBT-8.5. The presence of colluvium in this interval is indicated by at least six blocks of colluvium derived from moderately welded Bandelier Tuff (Qbt 2 and Qbt 3) and one block of vitric tuff (Qbt 1g); these blocks range in size from 0.5 to 10 ft, with most in the size range of 1 to 2 ft. In percentage of footage drilled through this interval, 30% consists of such coarse colluvial blocks. The remainder of the material consists of sands and gravels derived from the Tshirege Member, including some dacites that probably represent lithic clasts weathered from the tuff.

9.2.3 Ash Flows and Guaje Pumice Bed of the Otowi Member of the Bandelier Tuff (Qbo, 112.2 to 392 ft depth and Qbog, 392 to 414 ft depth)

Otowi ash flows (Qbo) are 279.8 ft thick at MCOBT-8.5. Core was collected through the upper 235 ft of Otowi ash; coring ceased at 347 ft depth, and cuttings were collected from that point downward. As noted above (Section 9.1.3), the vitric Otowi ash flows have a natural gamma signal that generally increases with depth but has a series of slopes and discontinuities that can be correlated between drill holes MCOBT-4.4 and MCOBT-8.5 (Figure 9.1-2).

The Otowi ash flows in MCOBT-8.5 are very similar to those in MCOBT-4.4: nonwelded, vitric, and little altered. The abundance of lithic clasts rises to ~20% in some intervals, but is more typically about half that amount. Lithic clasts consist of dacitic to andesitic (?) lavas that are highly silicified. Pumice sizes are variable, generally up to ~1 to 3 cm in core; where cuttings are collected the pumice is seldom recovered intact. Alteration is limited, with orange-to-earthen discoloration most common in the larger pumice size range but not in the smaller (<1 cm) pumice.

The Guaje Pumice Bed (Qbog) at 392 to 414 ft depth is marked by a discontinuity with rise in the natural gamma signal (Figure 9.1-2). Similar to the results from MCOBT-4.4, data from the CMR geophysical log in MCOBT-8.5 (Appendix H) indicate a rise in water content within the Guaje Pumice Bed (although perched water was not detected during drilling through this interval in either borehole). This increase in water content is not associated with any evidence of significant clay alteration, indicating increased moisture within the porous pumice beds.

9.2.4 Upper Sequence of Puye Formation Fanglomerates (Tpf, 414 to 429 ft depth)

Fanglomerates of the Puye Formation (Tpf) were sampled as cuttings from 414 to 429 ft depth in MCOBT-8.5. Unlike MCOBT-4.4, this horizon was not associated with any perched water. The two-part distinction between an upper, coarser fanglomerate and a lower sand sequence was not observed in MCOBT-8.5 as it was in MCOBT-4.4 (Section 9.1.4) and well R-15 (Longmire et al. 2001, 70103). Instead, the upper Puye Formation at MCOBT-8.5 consists of sands and rounded (alluvial?) rhyodacitic gravels, with angular clasts of vesicular basalt increasing in abundance toward the bottom. A chemical analysis of 2- to 4-mm clasts from the upper Puye Formation in MCOBT-8.5 is listed in column 1 of Table 9.2-1; this analysis is compared with a similar analysis from the lower Puye Formation in Section 9.2.6. The high silica content

and relatively high Rb/Sr ratio (0.28) make the upper Puye Formation at MCOBT-8.5 more similar to the upper Puye at MCOBT-4.4 than to the lower Puye Formation at that site. This similarity is reinforced by the relatively high quartz abundance in the upper Puye Formation of both drill holes (Table 9.1-2, rows 2 and 3) and the presence of similar proportions of specific dacititic lithologies, although a unique pre-Bandelier rhyolitic pumice is also present in MCOBT-8.5 (Appendix D). The upper Puye Formation at MCOBT-8.5 has less clay and retains a significant amount of glass, in contrast with the upper Puye Formation at MCOBT-4.4.

9.2.5 Lavas, Interflow Units, and Subflow Deposits of the Cerros del Rio Volcanic Field (Tb4, 429 to 710 ft depth)

Lavas, interflow rubble or scoria zones, and subflow deposits of the Cerros del Rio volcanic field (Tb4) were encountered in the interval from 429 to 710 ft depth in MCOBT-8.5. As at MCOBT-4.4, cuttings from the Cerros del Rio volcanic series in MCOBT-8.5 contained variable amounts of pale flesh-colored to green-brown clay. However, the clay abundances at MCOBT-8.5 are less at the top of the Cerros del Rio and increase at greater depth (Figure 9.1-3). As at MCOBT-4.4, the presence of scoria and the oxidation of basalt cuttings associated with the highest clay abundances suggest that the clays have accumulated in scoria or breccia zones between lava flows.

The sequence of lower alkalic to upper tholeiitic lavas is clearly seen in MCOBT-8.5 as it is in MCOBT-4.4, based on Sr content and Mg# (Figure 9.1-3). However, in MCOBT-4.4 the geochemical data show a consistent pattern of diminished Sr content in the tholeiitic basalts relative to the alkalic basalts. This pattern does not occur in MCOBT-8.5, where a high Sr composition marks an alkalic flow among otherwise low-Sr tholeiites (compare column 3 with columns 2, 4, and 5 of Table 9.2-1). This sample nevertheless has an Mg# typical of the adjacent tholeiites and a borderline alkalic ratio of silica to alkalis. Therefore, the principal demarcation between alkalic and tholeiitic basalts in MCOBT-8.5 is shown in Figure 9.1-3 as occurring at the transition from high to low Mg#, in a thin silty interflow zone with low clay abundance (2% volume in the >35 mesh cuttings) at 6218 ft elevation (563 ft depth).

The natural gamma signal through the Cerros del Rio lavas at MCOBT-8.5 is higher in the alkalic lavas and lower in the tholeiites (Figure 9.1-2). The high-Sr subunit near the top of the tholeiites also has an elevated gamma signal. As at MCOBT-4.4, other borehole logs provide additional stratigraphic and hydrogeologic information (Appendix H). The information from these logs yields an image of a lava series considerably different from that at MCOBT-4.4. The density log for MCOBT-8.5 is low (~2 g/cm^3) from the top of the Cerros del Rio lavas, at 429 ft depth, to ~451 ft depth. At 451 ft depth (6330 ft elevation) the density rises abruptly to a value of ~2.75 g/cm^3 and remains near this value to a depth of 600 ft depth (6181 ft elevation). This constant high-density zone corresponds to a massive set of flows, 149 ft thick from the top of A6 down to the base of A5 in Figure 9.1-3, with no significant breccia intervals. It is noteworthy that this set of flows is not chemically homogeneous, for it includes the high-Sr lava within the tholeiites as well as the alkalic lava A5 that underlies the tholeiites (Figure 9.1-3). Below 600 ft depth zones of such high density are only 10 to 20 ft thick and are separated by low-density breccia zones of comparable thickness. Limitations on the possible correlation of individual lava flows between MCOBT-4.4 and MCOBT-8.5 are discussed below in Section 9.3.

The CMR log for MCOBT-8.5 shows no abundance of large-pore saturation at any depth in the Cerros del Rio sequence. However, an abundance of clay-bound water appears at 630 to 650 ft depth (6131 to 6151 ft elevation), corresponding with the uppermost breccias that contain abundant clays in MCOBT-8.5 (Figure 9.1-3). A 0.25- to 0.1-μm clay fraction separated from this interval for XRD analysis contains 77% smectite and 18% glass, consistent with clay formation by incomplete alteration of vitric basalt scoria. Breccia-associated clays are largely restricted to the lower third of the Cerros del Rio volcanic series in MCOBT-8.5.

9.2.6 Lower Sequence of Puye Formation Fanglomerates (Tpf, 710 ft depth to TD at 740 ft depth)

A lower sequence of Puye Formation fanglomerates (Tpf) extends from 710 ft depth to the TD of MCOBT-8.5 at 740 ft. These fanglomerates bear some similarities to the upper Puye fanglomerates, both mineralogically (Table 9.1-2) and chemically (Table 9.2-1). The presence of quartz and a relatively high Rb/Sr ratio indicate that the lower Puye Formation at MCOBT-8.5 had volcanic sources somewhat more siliceous than those that provided detritus to the lower Puye Formation of MCOBT-4.4. These differences in chemistry and mineralogy are supported by the petrographic observation that clasts of rhyodacite lava from upper Rendija Canyon predominate in the lower Puye Formation at MCOBT-8.5, whereas sources are mixed at MCOBT-4.4 (Appendix D). The differences suggest heterogeneity within the Puye fanglomerates at depth in Mortandad Canyon. Also, unlike the lower Puye Formation at MCOBT-4.4, there is a modest amount of clay alteration in the 2- to 4-mm sediment fraction below the Cerros del Rio volcanic series in MCOBT-8.5. In the absence of any evidence for enhanced saturation of rock-altering fluid at this depth, this clay occurrence may reflect early alteration, possibly before or related to emplacement of the Cerros del Rio volcanic series.

9.3 Stratigraphic Correlations Between MCOBT-4.4, MCOBT-8.5, and Other Drill Holes

Stratigraphic correlations between MCOBT-4.4 and MCOBT-8.5 and beyond are relatively straightforward at the scale of major depositional units: Alluvium, Cerro Toledo deposits, Otowi ash flows, the Guaje Pumice Bed, upper Puye Formation deposits, volcanic rocks of the Cerros del Rio volcanic fields, and the lower Puye Formation. Correlations between these strata are shown in Figure 9.3-1, extending from Test Well (TW)-8 to drill hole R-9 (including a preliminary stratigraphy for drill hole R-13). For some regional hydrogeologic studies, this scale of stratigraphic correlation is sufficient. However, finer-scale correlations within some key rock units are desirable to understand movement of groundwater through the vadose zone in Mortandad Canyon.

Figure 9.1-2 shows that natural gamma can be used, at least within central Mortandad Canyon, to define mappable horizons within the Otowi Member of the Bandelier Tuff. This capability is somewhat limited by a lack of understanding of the cause for variation in the gamma signal, but the ability to determine relative stratigraphic position within the otherwise featureless Otowi ash flows provides markers against which variations in saturation or contaminant accumulation can be examined. Preliminary comparison with gamma signals in other drill holes suggests that this gamma-related stratigraphy within the Otowi ash flows may be useful in a regional context, beyond Mortandad Canyon. In modeling exercises the hydrogeologic properties of the Otowi ash flows are typically assumed to be homogeneous throughout, dominated by porous rather than fracture flow and with no hydrogeologic effects at subunit interfaces. Thus, the ability to determine stratigraphic subunits in the Otowi ash flows is probably not critical.

It is more important to subdivide the Cerros del Rio volcanic series into mappable hydrogeologic subunits, where open breccias can be highly transmissive but clay-filled breccias serve as perching horizons, as demonstrated by hydrologic testing in drill hole R-9i (Broxton et al. 2001, 71251). The record obtained from cuttings and from geophysical logs through the Cerros del Rio volcanic series at MCOBT-4.4 and MCOBT-8.5 provides a test of the ability to trace lava geochemical units, breccia horizons, and clay abundances between drill holes at a separation range of ~1 km.

Figure 9.3-1 illustrates the great lateral extent of the two major geochemical subunits, alkalic and tholeiitic, of the Cerros del Rio volcanic series beneath Los Alamos, Sandia, and Mortandad Canyons. This relatively widespread series of related flows extends over a range of at least 5 km (Figure 9.0-1) and perhaps farther. However, geochemical transitions do not necessarily correlate with breccia zones between flows, for individual lava flows can have extensive internal chemical variability, as documented in similar rift-related basaltic lavas of the Taos Volcanic Field (Haskin and Lindstrom 1978, 73643). Chemical and petrographic data are necessary to determine whether the same flow series occurs in different drill holes; vertical variation in chemistry alone is not always sufficient to determine where flow boundaries occur.

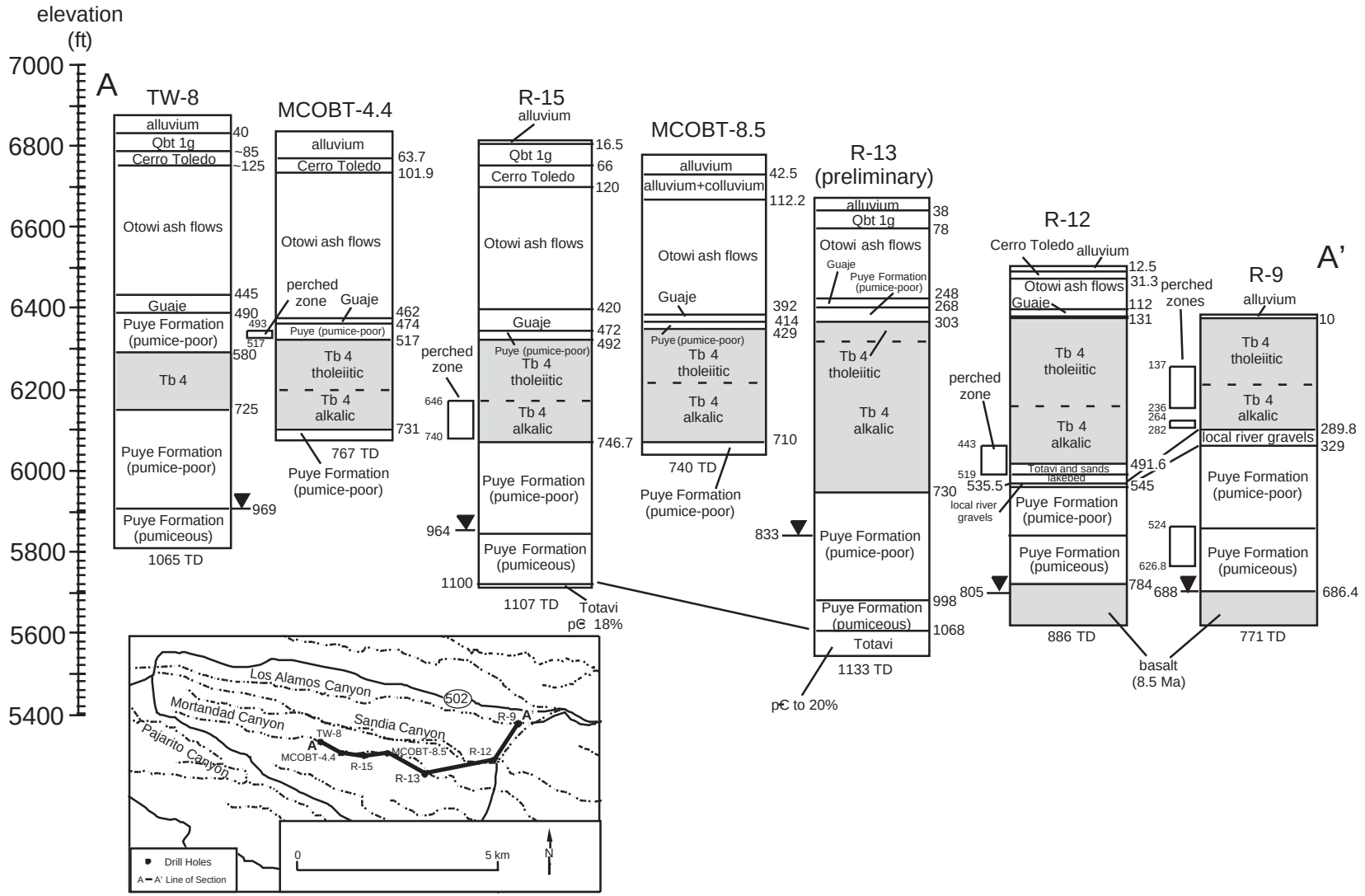

Figure 9.3-1. Correlation of stratigraphy between drill holes in Mortandad, Sandia, and Los Alamos Canyons.

Figure 9.1-3 shows that the demarcation between alkalic and tholeiitic lavas in MCOBT-4.4 is coincident with a breccia zone, but the same contact in MCOBT-8.5 is not. Moreover, the thickness of breccia zones relative to flow interiors in MCOBT-4.4 is much greater than in MCOBT-8.5, and individual breccia horizons do not appear to be traceable over the 1 km distance separating these two drill holes. At the finer scale of individual flows, identified by chemical and petrographic features, Figure 9.1-3 shows a relative loss of alkalic flows from east to west versus a loss of tholeiitic flows from west to east. These results place some limits on the lateral traceability of Cerros del Rio hydrogeologic subunits, but at least two factors make this conclusion less discouraging. First, the westward thinning of the Cerros del Rio rocks through MCOBT-8.5 to MCOBT-4.4 and TW-8 marks the feathering out of multiple flows, a situation where the thicknesses of breccia zones increase at the expense of thinned-out flow interiors and may be modeled as a laterally variable property. Second, observations of clay abundance relative to volcanic stratigraphy provide a guide to hydrogeologic variations that would not be obtained by the more difficult mapping of individual breccia horizons. Patterns of clay accumulation may allow a stratigraphy of relatively transmissive breccias (clay-poor) and sealed breccias (clay-rich) to be developed within the Cerros del Rio lavas on the scale of specific drainages, such as Mortandad Canyon.

Clay distributions in the Cerros del Rio can provide information on vadose-zone flow and transport over time. The high abundance of clay and the lack of glass at the top of Tb4 in MCOBT-4.4 differ from the clay-glass associations in the deeper basaltic breccia zones. This finding opens the possibility that clay versus glass abundances in the Cerros del Rio might be developed as an aid in distinguishing those breccia zones where flow is enhanced from those where extensive clay development impedes flow.

9.4 Mineralogic Analysis of Particulates from Leached Core Samples of the Vadose Zone in MCOBT-4.4 and MCOBT-8.5

Section 11.1.1 of this report describes the extraction and analysis of leachate samples from vadose-zone core collected at MCOBT-4.4 and MCOBT-8.5. For friable samples such as these, leachate extractions are prepared by oven-drying approximately 50 g of core material for 12 hr at 100°C, rotary agitation of the dried sample for 25 hr in an Erlenmeyer flask with approximately 75 g deionized water, settling, and filtration (0.2 μm). This process has been used previously on other core samples (e.g., Broxton et al. 2001, 71250; Broxton et al. 2001, 71252), including drill holes R-15 and MCO-7.2 in Mortandad Canyon (Longmire et al. 2001, 70103). In preparing leachates from the MCOBT-4.4 and MCOBT-8.5 samples, it was found that even after filtration the extracted solutions were unusually clouded by suspended particles, unlike previous samples from cores in Mortandad and other canyons. Suspension of the finest fraction persisted for nine months; based on Stokes' law of settling properties, the suspended particulates are colloids of <50 nm. Colloid presence and colloid-mediated transport processes have been the subject of past studies at Mortandad Canyon with conflicting conclusions (Penrose et al. 1990, 0174; Marty et al. 1997, 73695). The gentle agitation used to collect these particulates may have dislodged colloids but is unlikely to have produced them. These samples provided an opportunity to analyze and identify colloidal material from Mortandad Canyon.

Selected samples of leachates were analyzed by XRD to determine the mineralogy of both the settled and suspended particulates. Results of the analyses are summarized in Table 9.4-1. Based on the initial filtration and the long settling times for materials in the leachate tubes, it was determined that the sediment fraction was composed of 50- to 200-nm particles and the suspended fraction was <50 nm. The major phases most commonly present in both the sediment and the suspension are clay minerals (smectite and halloysite).

Table 9.4-1
Semi-Quantitative XRD Analyses of Particulates in Vadose Zone Leachates of MCOBT-4.4 and MCOBT-8.5

Sample	Size Fraction	Smectite	Halloysite	Illite	Cristobalite	Quartz	Feldspar	Amorphous	Mica	Hematite	Halite	Calcite	Gypsum	Scapolite	Dolomite
MCOBT-4.4															
47.3 – 47.5 alluvium	50–200nm	**M**	m	–	m	m	m	—	—	m	–	–	–	–	–
	<50 nm	**M**	t	m	t	–	–	–	–	–	–	–	–	–	–
49.8 – 50.0 alluvium	50–200nm	**M**	m	m	t	t	m	–	–	m	–	–	–	–	–
	<50 nm	**M**	p	m	–	–	–	–	–	–	–	–	–	–	–
64.8 – 65.0 Cerro Toledo	50–200nm	–	**M**	–	–	t	–	–	–	–	–	–	–	–	–
	<50 nm	–	**M**	–	–	–	–	–	–	–	t	–	–	–	–
89.8 – 90.0 Cerro Toledo	50–200nm	**M**	–	p	–	t	t	p	–	–	–	–	–	–	–
	<50 nm	**M**	–	–	–	–	–	–	–	–	–	p	–	–	–
144.8 – 145.0 Otowi ash flows	50–200nm	**M**	p	p	m	–	m	–	–	m	–	–	–	–	–
	<50 nm	**M**	–	–	–	–	–	–	–	–	–	–	–	–	–
224.8 – 225.0 Otowi ash flows	50–200nm	**M**	–	–	–	t	m	**M**	t	–	–	–	–	–	–
	<50 nm	**M**	–	–	–	–	–	–	–	–	t	–	–	–	–
MCOBT-8.5															
27.2 – 27.4 alluvium	50–200nm	**M**	m	m	m	m	m	p	–	t	–	–	–	–	–
	<50 nm	**M**	–	m	–	–	–	–	–	–	–	–	–	–	–
57.2 – 57.4 alluvium/colluvium	50–200nm	**M**	m	m	m	–	t	–	–	–	–	–	–	–	–
	<50 nm	**M**	–	m	t	–	–	–	–	–	–	–	–	–	–
77.2 – 77.4 alluvium/colluvium	50–200nm	–	m	m	**M**	m	**M**	–	–	t	–	–	–	t	–
	<50 nm	–	**M**	**M**	–	–	–	–	–	–	**M**	**M**	p	–	–
97.2 – 97.4 alluvium/colluvium	50–200nm	–	**M**	**M**	m	–	m	–	–	t	–	–	–	–	–
	<50 nm	–	**M**	**M**	–	–	–	–	–	–	t	–	–	–	–
107.2 – 107.4 alluvium/colluvium	50–200nm	–	**M**	–	m	–	**M**	–	–	–	–	–	–	–	–
	<50 nm	–	**M**	–	–	–	–	–	–	–	m	–	–	–	p
137.2 – 137.4 Otowi ash flows	50–200nm	m	–	–	t	t	m	**M**	–	–	–	–	–	–	–
	<50 nm	**M**	–	–	–	–	–	–	–	–	–	–	–	–	–
232.2 – 232.4 Otowi ash flows	50–200nm	**M**	–	t	m	t	m	**M**	–	–	t	–	–	–	–
	<50 nm	**M**	–	–	–	–	–	–	–	–	–	t	–	–	–

Note: **M** = major component, m = minor component, t = trace component, p = possibly present.

This analysis shows that colloidal clays are common constituents in the alluvium, colluvium, and Cerro Toledo interval at MCOBT-4.4 and MCOBT-8.5. In addition, the colloidal clays in these two drill holes are of two types, either smectite-dominant or halloysite-dominant. Figure 9.4-1 summarizes these differences within both drill holes by plotting the mineralogy of the finer colloidal (<50 nm) particulates (solid circles labeled in italics) against stratigraphy and gravimetric moisture content (dashed line showing percentage by weight of water/dry mass). The colloidal materials in MCOBT-4.4 are predominantly smectite, with the exception of one sample of halloysite within the Cerro Toledo interval where gravimetric moisture content is greatest. The distribution of colloidal materials in MCOBT-8.5 is similar, with smectite both above and below zones of higher gravimetric moisture content where halloysite is present. The data indicate that the two colloidal mineral systems have little correlation with stratigraphy but that halloysite may be favored in wetter horizons.

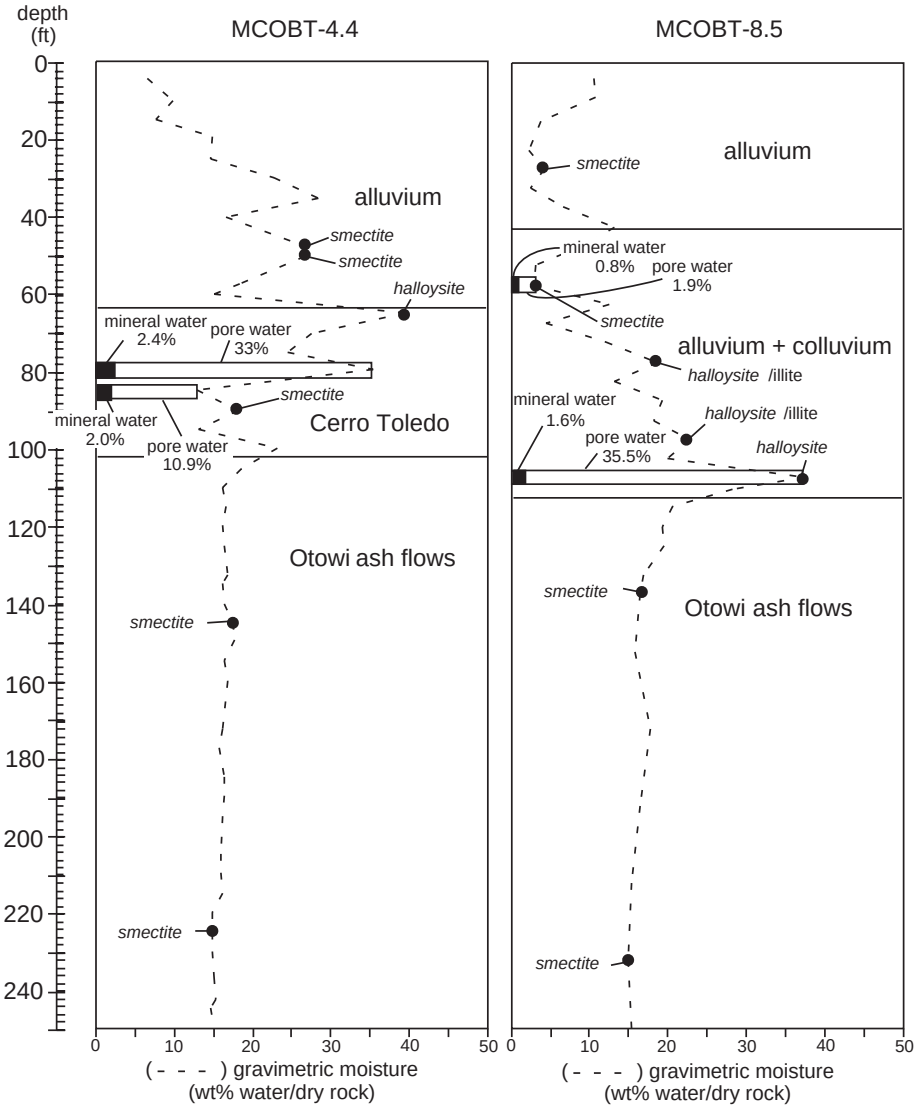

Figure 9.4-1. Colloid mineralogy and gravimetric moisture content in MCOBT-4.4 and MCOBT-8.5. Mineralogy of colloidal material (<50 nm) in selected leachate samples is indicated by solid circles labeled in italics. The hydrous-mineral water content (including water in both clays and volcanic glasses) in paired high- and low-gravimetric moisture samples from both drill holes is also indicated by dark bars, compared to gravimetric pore water content in the paired samples (open bars) (see Section 9.5).

This analysis is sufficient to address the mineralogy of the colloids present but not to determine whether colloid movement occurs at depth. The distinction of smectite- and halloysite-dominated colloid systems shows either that colloid formation is nonuniform or that colloid species are segregated by some yet undetermined process in the subsurface of Mortandad Canyon. It is important to point out that amorphous colloids might also be present, but these would not be detected by XRD.

9.5 Determination of Pore Water versus Hydrous Phases in High-Conductivity Portions of the Vadose Zone in Mortandad Canyon

A surface-based electrical survey was conducted in Mortandad Canyon during June 2002 to assist in determining the location and extent of alluvial groundwater. This survey produced results indicating high conductivity within certain horizons of the vadose zone, either associated with portions of the Cerro Toledo interval or the base of the alluvium or colluvium. The conductivity results leave open the question of whether the high conductivity is caused by pore water or by other factors. Among the other factors that can affect conductivity, such as porosity or the presence of hydrous phases (including hydrous minerals and hydrous glasses), it is possible to determine the abundance of hydrous phases by QXRD. To address the possibility that hydrous phases might account for the high conductivity, paired samples of low and high moisture content were chosen for QXRD analysis from the Cerro Toledo interval in MCOBT-4.4 and from the alluvium/colluvium sequence in MCOBT-8.5.

Most of the water present in the core samples consists of water in pore spaces and cannot be accounted for by clays or hydrous glasses. The hydrous phases present include clay (smectite, ~20% of total weight as water if fully saturated) and volcanic glass (~3% of total weight as water in typical rhyolitic pyroclasts). Table 9.5-1 compares the mineralogy determined, the gravimetric moisture content, and the calculated moisture content attributable to hydrous phases in each sample. These results are also plotted in Figure 9.4-1 as “mineral water” (solid bars showing gravimetric moisture in clays plus glasses) and pore water (open bars showing gravimetric moisture in pore spaces). When the hydrous phases of glass plus clay are accounted for in each sample, the gravimetric water content attributable to them is minimal, ranging from 0.8 wt% to 2.4 wt%.

Table 9.5-1
Moisture Content and Mineralogy in Samples from the Vadose Zone, MCOBT-4.4 and MCOBT-8.5

Sample[a]	Gravimetric moisture (wt%water/dry rock)	Moisture in hydrous phases (wt%; calculated)[b]	Smectite	Tridymite	Cristobalite	Quartz	Alkali Feldspar	Plagioclase	Glass	Hematite	Biotite	Amphibole	Total
Cerro Toledo Interval, MCOBT-4.4													
(1) MCOBT-4.4 79.3–79.5	26.2	2.4	0.1	0.7	0.8	5.3	4.4	8.8	77.8	—	—	0.3	98.2
(2) MCOBT-4.4 84.8–85.0	11.4	2.0	1.7	1.6	1.1	9.2	9.8	17.8	57.3	0.1	—	0.3	98.9
Alluvium/Colluvium, MCOBT-8.5													
(3) MCOBT-8.5 57.2–57.4	2.6	0.8	2.7	8.1	—	33.5	20.0	26.6	4.9	0.5	0.1	—	96.4
(4) MCOBT-4.4 107.2–107.4	27.0	1.6	–-	2.0	0.9	13.5	8.8	20.1	54.3	0.5	—	0.1	100.2

Note: Values reported are in weight percent. Analytical errors (2σ) are ~5% of the amount reported for abundances >10% and ~10% of the amount reported for abundances <10%. Dashes indicate that the phase was not detected (detection limits are ~0.1%).

[a] Number ranges indicate depth ranges of core in ft.

[b] Moisture in hydrous phases is calculated in a manner equivalent to gravimetric rock moisture, using weight ratios of water/dry mass of 20/80 for smectite and 3/97 for volcanic glass. Biotite and amphibole were not included because of their minor abundance.

9.6 Borehole Geophysics

Borehole geophysical data were obtained from two sources: (1) Schlumberger, Inc., personnel obtained a suite of borehole geophysical logs, and (2) Laboratory and drilling support subcontractor personnel obtained borehole video and natural gamma ray surveys using Laboratory geophysical logging equipment.

9.6.1 Schlumberger Borehole Geophysics

Schlumberger performed geophysical logging services at MCOBT-4.4 on June 15, 2001, and at MCOBT-8.5 on June 23, 2001. Both boreholes were logged in 13 3/8-in. drill casing from the surface to 130 ft depth and in 12 1/4-in.-diameter open borehole to total depth below 130 ft.

The primary purpose of the Schlumberger logging was to characterize the hydrogeologic characteristics of the rock units intersected by the boreholes with emphasis on determining moisture distributions, identifying perched groundwater zones, measuring capacity for flow (porosity, moisture, pore-size distribution), and obtaining lithologic/stratigraphic information. Secondary goals included evaluating borehole conditions such as washouts and degree of drilling-fluid invasion. These goals were accomplished by measuring nearly continuously along the length of the boreholes the following parameters: (1) total and effective water-filled porosity and pore size distribution, from which an estimate of hydraulic conductivity was made; (2) bulk density and photoelectric effect; (3) bulk electrical resistivity at multiple depths of investigation; (4) spectra of natural gamma rays, including potassium, thorium, and uranium concentrations; and (5) borehole diameter.

9.6.1.1 Schlumberger Methods

Schlumberger logged the two boreholes using the following tools:

- The Compensated Neutron Tool, model G (CNTG^{TM}) to measure volumetric water content (volume moisture/volume rock mass) in open and cased hole for evaluating moisture content and porosity.
- The combined magnetic resonance (CMR^{TM}) tool to measure the nuclear magnetic resonance response of the formation in open hole for evaluating total and effective water-filled porosity of the formation near the borehole wall and for estimating pore size distribution and hydraulic conductivity;
- The Triple Detector Litho-Density (TLD^{TM}) tool with a single-arm caliper to measure formation bulk density in open and cased hole and photoelectric effect and borehole diameter in open hole for estimating total porosity and to characterize lithology;
- The Array Induction Tool, version H, (AITH^{TM}) to measure formation electrical resistivity (at five depths) and borehole fluid resistivity in open hole for evaluating drilling-fluid invasion into the formation, the presence of moist zones far from the borehole wall, and the presence of clay-rich zones;
- The Micro Cylindrically Focused Log (MCFL^{TM}) to measure high-resolution electrical resistivity in water-filled portions of the open hole, for evaluating drilling-fluid invasion into the formation and to characterize geologic heterogeneity;
- The Natural Gamma Spectroscopy (NGS^{TM}) tool to measure gross natural gamma and spectral natural gamma ray activity, including potassium, thorium, and uranium concentrations, in open and cased hole for evaluating geology and lithology, particularly the amount of clay; and
- In addition, to record calibrated gross gamma ray with every service except the Natural Gamma Spectroscopy tool for the purpose of depth matching the logging runs to each other.

A more thorough description of logging tools, data acquisition, quality control and assessment, and data processing are presented in the Schlumberger logging report in Appendix F.

9.6.1.2 Schlumberger Results

The Schlumberger logging report for both boreholes is presented in Appendix F. The geophysical logs for the MCOBT-4.4 and MCOBT-8.5 boreholes are compiled as montages in Appendices G and H, respectively. Appendices F, G, and H are stored on the CD attached to the inside back cover of this report.

Preliminary results of Schlumberger measurements were generated in the logging truck at the time that geophysical services were performed and were documented in field logs. The field results were subsequently reprocessed by Schlumberger (1) to correct the measurements for borehole environmental conditions, (2) to perform an integrated analysis of the log measurements so that they were coherent, and (3) to combine the logs into a single presentation to integrate interpretation.

Most of the geophysical log measurements from MCOBT-4.4 and MCOBT-8.5 provided good quality results consistent with each other. There were few significant washouts to affect the porosity and density logs. The most significant log quality issue is associated with the CMR logs in the Cerros del Rio basalts. The magnetic resonance signal strength is significantly subdued in this section because considerable magnetic minerals were present, resulting in a low measured signal-to-noise ratio. Despite this problem, the CMR porosity measurements are generally consistent with the other porosity measurements across this interval, and they were successfully integrated with the other logs. However, specific values of individual CMR logs should be used with caution in quantitative analysis. It is recommended that the optimized porosity results from the integrated log analysis (ELAN) be used instead (see Appendix F).

Moisture-sensitive log measurements may be significantly affected by invasion of drilling fluids into the borehole wall and the shallow depth of investigation for geophysical logs (e.g., compensated neutron tool, 7 in.; CMR tool, 1.5 in.).

Important results from the processed geophysical logs in MCOBT-4.4 and MCOBT-8.5 are described below.

(1) The lower Puye Formation has the following log characteristics:

- In MCOBT-4.4 the volumetric moisture content (volume moisture/volume rock mass) for the lower Puye Foundation at the bottom of the well is high (25%) and, correspondingly, the estimated degree of water saturation is relatively high. Uphole, the first presence of significant quantities of air in the pore space occurs above 695 ft.
- In MCOBT-8.5 the volumetric moisture content is low and air space high through most of the lower Puye Formation. However, at the very bottom of the logged interval there is a significant increase in the water-filled porosity.

(2) The Cerros del Rio basalt has “massive” zones with less than 10% porosity (including rock pores, vesicles, and joints), most of which are water filled, and “altered” zones with higher porosity (25 to 35%), higher volumetric moisture content (15%), and different mineralogy (more clay). The “altered” zones comprise a significant portion of the basalt sequence in MCOBT-4.4, while the “massive” zones dominate in MCOBT-8.5.

(3) The Bandelier Tuff sequence in the upper half of the logged interval is clearly distinguished by the logs and is characterized by

- very high porosity (60 to 65%) but only 15 to 25% water content in the Guaje Pumice Bed, and
- lower porosity (45 to 58%) and similar water content (15 to 20%), with only small amounts of moveable water throughout the remainder of the tuff sequence up to the casing depth (130 ft).

(4) A “transitional” zone largely consisting of the upper Puye Formation is characterized by relatively high porosity (25 to 40%), high clay and alkali feldspar mineral content, and possibly the presence of augite or similar minerals. This zone is much more substantial in MCOBT-4.4 (465 to 517 ft.) than MCOBT-8.5 (414 to 428 ft).

(5) The processed geophysical logs and integrated log analysis results can be depth correlated easily between the two wells, although significant differences in the geology and hydrogeology of the two wells are readily apparent from the two sets of logs.

(6) The data quality of the MCOBT-4.4 and MCOBT-8.5 geophysical logs is generally excellent, largely because of the good condition of the two boreholes, making the results conducive to further quantitative analysis aimed at better understanding the geologic and hydrogeologic setting and associated physical processes.

A more thorough discussion of Schlumberger logging results is presented in Appendix F. It should be noted that some of the interpretations based on the Schlumberger geophysical logs are inconsistent with observations made during drilling of MCOBT-4.4 and after installation of the well. For example, a perched zone with a static water level of 493 ft was identified during drilling of MCOBT-4.4 based on the drillers’ observations, borehole video logs, and water-level measurements above a packer set in the borehole. Subsequent measurements in the completed well confirmed the water level. The geophysical logs, however, suggest that the top of saturation occurs at about 500 ft depth and the main zone of saturation extends from 516 ft to 524 ft. Also, the geophysical logs suggest that saturated conditions may be present throughout a significant portion of the Cerros del Rio basalt as well as in the underlying Puye Formation. Packer tests conducted in the open borehole indicated that this is unlikely (see Section 10.1). Additional study is needed to resolve the differences in interpretations between the observational data collected during drilling and the geophysical logs.

9.6.2 Logging with the LANL Geophysical Trailer

Natural gamma logs and borehole videos were made at MCOBT-4.4 and MCOBT-8.5 using the LANL geophysical trailer. Logging and videotaping were performed by drilling subcontractor personnel using LANL-owned equipment.

The LANL gamma tool was run because it provides excellent discrimination of geologic units that contain varying amounts of U, Th, and K. In many cases, key subunits such as the Guaje Pumice Bed in the Otowi Member, clay-rich breccias in the Cerros del Rio basalt, and lithologic subdivisions of the Puye Formation can be differentiated by their natural gamma signature. The borehole video was run to identify geologic and lithologic contacts; to examine possible perched groundwater zones identified by core logging, drillers’ observations, other geophysical logs; and to evaluate borehole conditions such as washouts and borehole wall stability.

9.6.2.1 LANL Methods

A natural gamma survey was performed in MCOBT-4.4 on June 16, 2001, and in MCOBT-8.5 on June 23, 2001. The gamma logs for both boreholes were obtained through 13 3/8-in. heavy-walled drill casing from the surface to 130 ft depth; logging took place in 12 1/4-in.-diameter open borehole from 130 ft to 767 ft in MCOBT-4.4 and from 130 ft to 740 ft in MCOBT-8.5. Measurements were obtained every 0.1 ft while moving the tool uphole at a rate of 15 ft/min.

A borehole videotape was made of MCOBT-4.4 on June 14, 2001, and of MCOBT-8.5 on June 23, 2001. The video logs were obtained for the nominal 12 1/4-in.-diameter open boreholes from 130 ft to 767 ft in MCOBT- 4.4 and from 130 ft to 729 ft in MCOBT-8.5. The videotapes were obtained using a Laval™ 1 3/4-in.-diameter slim-hole borehole video camera.

9.6.2.2 LANL Results

Results of the natural gamma logs for both boreholes are presented graphically in Figure 9.1-2. Borehole videos for MCOBT-4.4 and MCOBT-8.5 are presented as QuickTime™ movies in MPEG format in Appendices I and J, respectively, which are stored on a CD attached to the inside back cover of this report. Interpretation of LANL natural gamma logs and borehole videotapes is incorporated into the discussion of stratigraphy (Sections 9.1 and 9.2) and groundwater occurrence (Section 10.1).

10.0 HYDROLOGY

Both MCOBT-4.4 and MCOBT-8.5 targeted intermediate-depth perched water beneath Mortandad Canyon. Based on observations from well R-15 (Longmire et al. 2001, 70103), it was expected that perched saturation would be encountered near the base of the Cerros del Rio basalt. Perched water was encountered in alluvium and at the top of the Cerros del Rio in MCOBT-4.4, but no perched water was found in MCOBT-8.5. Consequently, this section discusses only the results from MCOBT-4.4.

10.1 Groundwater Occurrence

MCOBT-4.4. Groundwater was first encountered at MCOBT-4.4 in the alluvium. Shallow perched saturation occurred in unconsolidated fine-to-coarse tuffaceous sand and clayey sand between the depths of 34.8 and 50 ft bgs. These sediments were particularly clay rich from 45.5 to 48 ft bgs. The nature of the perching zone could not be determined because core from the interval from 50 to 55 ft bgs was not recovered.

The occurrence of intermediate-depth perched water was not as readily apparent. The driller first noted that borehole might be producing water while drilling at a depth of 523 ft bgs within the Cerros del Rio basalt. Drilling was halted and the water level was measured with drill casing extending from the surface to a depth of 130 ft bgs. The water level was allowed to recover for 2.5 hr, and then the depth was measured with an electric probe to be 477.5 ft bgs. A screening groundwater sample was collected from the borehole to determine if the water was groundwater or accumulated drilling fluid. Based on low concentrations of nitrate (0.03 ppm nitrate as N) and perchlorate (0.0021 ppm, at detection J value), it was concluded that the water probably represented drilling fluid, and no effort was made to isolate this portion of the borehole with drill casing before drilling ahead with open-hole methods.

No increase in water production was observed as the borehole was advanced to a depth of 727 ft bgs (in the lower part of the basalt). However, drilling was halted at that depth to evaluate water level before leaving the basalt. After letting the fluid in the borehole recover for five hr, the water level rose from 716.4 ft bgs to 704.7 ft bgs (in the lower part of the basalt). Because of the slow rate of water rise in the borehole (2.3 ft/hr), drilling resumed before a static water level was achieved.

Neither an increase in water production nor a significant clay horizon was observed as drilling continued open-hole into the underlying Puye Formation (top at 731 ft bgs) to a depth of 767 ft bgs. Video logging was conducted at this point (June 14, 2001) and showed the borehole walls to be moist beginning at 473 ft bgs (in the Guaje Pumice Bed). The amount of moisture on the borehole wall increased at a depth of 495 ft bgs (in the upper interval of the Puye Formation), and water was seen to be flowing on the borehole wall at a depth of 525 ft bgs (in the basalt). Fractures, possibly clay-filled, were observed in the interval 550 to 552 ft bgs. The downhole camera entered standing water in the borehole at a depth of 753 ft bgs (in the lower interval of Puye).

Geophysical logging by Schlumberger, Inc., suggested abundant free pore water occurred at a much shallower depth: between 500 and 526 ft bgs. Schlumberger's analysis of the log suite indicated that the interval from 516 to 524 ft bgs was the likely water-producing zone.

The source of the water in the borehole was then investigated in two ways. First, the bottom of the borehole was filled with bentonite to a depth of 725.4 ft bgs (about 3 ft up into the base of a massive, fracture-free basalt flow) to determine whether the lower Puye interval was actually saturated or merely collecting water drained from the overlying basalt. It was also deemed possible that water in the bottom of the borehole was accumulating from the zone between 516 to 524 ft bgs, identified as the likely water-producing zone by the Schlumberger geophysical logs. Water-level measurements made at regular intervals over a ten-day period fluctuated, suggesting that the basalt was not completely isolated from the lower Puye interval. Second, an inflatable packer was set in the upper part of the basalt with the base of the packer at 531.5 ft bgs and the top at 524.5 ft bgs. Then, as much water as possible was evacuated from the hole below the packer by airlifting, and the water level was monitored. Water depth below the packer, 4.75 hr after airlifting, was 671.8 ft bgs but slowly declined to a value of 675.1 ft bgs after 33.17 hr. Water-level depth above the packer was consistently within 0.01 ft of 493.4 ft bgs (in the upper Puye interval). The water level above the packer was constant, but the level below the packer declined. Thus, it was concluded that the water originally detected in the lower part of the Cerros del Rio basalt and underlying the lower Puye interval originated from a perched zone above the inflatable packer. Section 9.1.7 describes the geologic setting of the perched zone.

The MCOBT-4.4 well was constructed with a screened interval of 482.1 to 524 ft bgs and a sand pack interval of 474.0 to 527 ft bgs. The well design was based on the following information: (1) a static water level was measured at 493 ft bgs above the inflatable packer (524.5 to 531.5 ft bgs) in the open borehole; (2) a likely water-producing zone from 516 to 524 ft bgs was identified by the geophysical logs; and (3) the massive basalt from 522.5 to 535 ft bgs was considered a possible perching layer. Water levels measured inside the newly completed well seemed to validate the well design. Nine hr after backfilling the annulus, the water level inside the well was 495.3 ft bgs. A week later, at the beginning of well development (bailing), the depth-to-water was 493.2 ft. The well was then bailed for two days and allowed to recover. After 98.7 hr of recovery, on July 17, 2001, depth-to-water was measured at 494.5 ft bgs.

Following well development, there was an unexplained decline in the static water level in MCOBT-4.4. A borehole video was run in the well casing on January 30, 2002, prior to installation of the submersible pump. The borehole video camera showed that the static water level had dropped from 493 ft to 519 ft bgs and that water was entering the screen at a depth of 497 ft bgs. Water levels are being monitored to establish a longer baseline for water-level fluctuations.

MCOBT-8.5. Evidence of groundwater was observed at two depths in the alluvium during coring operations at MCOBT 8.5. On June 11, 2001, the core run from 97.5 to 100.0 ft bgs provided evidence of a saturated zone of silty sand from 97.9 ft bgs to 98.5 ft bgs. This uppermost zone of saturation appeared to be located above a zone of consolidated tuff (probably a block of tuff in colluvium at 98.5 to 100.4 ft bgs) in the alluvium. A second saturated zone was observed within the alluvium at a depth of 109.0 to 110.6 ft bgs. Drilling was stopped and the drill hole with a TD of 110.7 ft bgs was checked for water. No measurable water was observed in the hole. This second zone is located approximately 1.6 ft above the Otowi Member of the Bandelier Tuff. Coring continued to a depth of 350 ft bgs, and no additional saturated zones were observed. Drilling operations continued with the emplacement of 13 3/8 in. steel casing to a depth of 130 ft to seal off alluvial water. Drilling with fluids was conducted from 350 ft bgs to 465 ft bgs. On June 19, 2001, the drillers reported the possible presence of groundwater in the borehole with a TD of 465 ft bgs. Fourteen gal. of water were collected for sample analysis before the hole went dry. The borehole was then allowed to recover for 1 hr and 30 min with water levels monitored every 15 to 30 min. No water was observed. The water sample collected before the hole went dry showed low concentrations

of nitrate (0.57 ppm nitrate as N) and perchlorate (<0.004 ppm, U value), and it was concluded that the water probably represented drilling fluid.

Open hole drilling with fluids continued down from 465 to 645 ft bgs without any observable increase in formation water production. At 645 ft bgs, the drillers reported that the formation had loosened up. Drilling was stopped to monitor water levels after evacuating as much drilling fluid as possible from the borehole. Thirty min after evacuating the borehole, water levels were measured but accuracy was suspect because of possible interference from residual drilling foam. Defoamer was added to the hole and readings continued for the next 33 min, with the last reading at 617.35 ft bgs. Seven gal. of water were obtained for sample analysis prior to the hole going dry. The water sample showed low concentrations of nitrate (0.26 ppm nitrate as N) and perchlorate (<0.002 ppm, U value), and it was concluded that the water probably represented drilling fluid.

Drilling continued to a depth of 690 ft in the Cerros del Rio basalt when the drill rig broke down. Water levels could not be measured during the downtime because the drill head was connected to the RC rods. On June 23, 2001, approximately 79 hr after drilling had ceased, a water measurement was obtained at 671 ft bgs. Water production was monitored as drilling continued from 690 to 740 ft bgs. No increase in water discharge was observed as drilling went from basalt into the Puye Formation at approximately 708 ft bgs. Drilling was stopped with the hole at a TD of 740 ft bgs. Schlumberger ran a comprehensive suite of borehole geophysical logs on June 23, 2001. According to Schlumberger personnel, the water level was at approximately 730 ft bgs. Geophysical logs indicate low water content in the lower Puye Formation with an increase in water-filled porosity at the very bottom of the logged interval.

On June 24, 2001, a pressure transducer was set in the hole. Data from the pressure transducer indicated a 1.6 ft drop in water level in a 5-hr and 10-min interval. The pressure transducer was removed after 12 hr and 30 min with a total drop in water level of 2.7 ft. A manual water-level measurement indicated a depth-to-water of 733.97 ft bgs.

Schlumberger returned to obtain sidewall core samples in the borehole. Water was added to the hole to assist in the core sampling. A water level of 641.2 ft bgs was taken 23 min after core sampling was completed. The pressure transducer was lowered back into the well on June 26, 2001. The water level was measured at 675 ft bgs, and in the next 6 hr and 14 min the water level was observed to drop from 675 to 679.7 ft bgs.

The video camera was run using the side-view camera on June 25, 2001. The camera showed the depth-to-water at 684 ft bgs with no visible water moving downhole. To isolate possible zones of perched water, the borehole was then backfilled with bentonite up to 670 ft bgs into the Cerros del Rio basalt and the water levels monitored. The water level appeared to be stable with measurements ranging from 644.95 ft bgs to 645.2 ft bgs over the next 21 hr and 30 min.

To continue to isolate possible water-bearing zones, the well was backfilled with bentonite to 646.1 ft bgs in the Cerros del Rio basalt. The bentonite was allowed to hydrate for 3 hr, after which the water level was measured at 634.72 ft bgs. Approximately 20 to 30 gal. of water were bailed from the well to monitor any inflow of water from perched zones. Water levels were monitored for 4 hr. The water level fluctuated slightly from 639.21 ft bgs to 639.16 ft bgs and appeared to stabilize at 639.17 ft bgs in the last 1.5 hr, indicating that no water was entering the hole from perched zones.

To summarize, although some indication of excess water appeared at 465 ft bgs and again at 740 ft bgs, only 10 ft of water were observed in the bottom of the borehole. The water level proceeded to drop 2.7 ft within the next 12 hr and 30 min. Sidewall core samples were obtained in conjunction with geophysical logging, which required adding water to the borehole. Following sidewall coring, the water level was initially measured at 641.2 ft bgs, but it declined to 684 ft bgs over the next 19 hr, indicating that the water was going out into the formation. To isolate and identify any perched-water zones, the bottom of the borehole

was incrementally sealed off. After sealing the borehole back to 670 ft bgs and then to 646.2 ft bgs, no water was observed to be recharging the borehole. Consequently, MCOBT-8.5 was plugged and abandoned on June 27, 2001, following a determination that no intermediate saturated zones had been encountered.

10.2 Soil-Water Occurrence in Cores

10.2.1 Methods

Moisture content was determined for core samples collected from the uppermost 310 ft of MCOBT-4.4 and 350 ft of MCOBT-8.5. A total of 50 samples were collected for moisture analysis in MCOBT-4.4, and 38 samples were collected in MCOBT-8.5. After core or cuttings were screened for radioactivity, samples were immediately placed in pre-weighed and pre-labeled jars with tightly fitting lids. The moisture content was determined gravimetrically by drying the samples in an oven according to ASTM method D2216-90. Samples collected for moisture content are listed with the analytical results in Appendix E. Moisture contents are given as the ratio of the weight of water to the weight of the dry sample (ASTM standard for reporting moisture content).

10.2.2 Results

In MCOBT-4.4, the moisture content in the alluvium is about 2% to 10% gravimetric near the surface and generally increases, with substantial fluctuation, to a maximum of about 25% to 28% gravimetric in the zone of perched alluvial groundwater from about 35 ft to 50 ft depth (Figure 10.2-1). Moisture content decreases to 15% to 18% at the base of the alluvium. The Cerro Toledo interval has the highest moisture content measured in the cored interval of MCOBT-4.4, but no saturation was detected in this unit during coring operations. Moisture content ranges from 25% to 40% in the upper half of the Cerro Toledo interval with maxima at 64 ft and 79 ft depths (Figure 10.2-1). Moisture content decreases to 13% to 24% in the lower half of the Cerro Toledo. This pattern of moisture distribution for the Cerro Toledo interval was also seen in core from borehole R-15 (Longmire et al. 2002, 70103). The Otowi Member contains between 15% and 18% moisture (Figure 10.2-1).

In MCOBT-8.5, moisture content in alluvium and colluvium is about 2% to 10% gravimetric near the surface and generally increases, with substantial fluctuation, to a maximum of about 37% gravimetric near the base of the unit (Figure 10.2-1). The zone of high moisture at the base of the alluvium corresponds with occurrence of two separate zones of saturation between 94.4 to 112.5 ft depth (Figure 10.2-1) that were observed during coring operations. Moisture content in the Otowi Member ranges from 19% to 20% at the contact with overlying alluvium and decreases slightly to 15% to 18% in the remainder of the member.

In both MCOBT-4.4 and MCOBT-8.5, the moisture profiles for the Otowi Member show much less variability than those for alluvium or Cerro Toledo interval (Figure 10.2-1). The low variability of moisture in the Otowi Member probably reflects the relative homogeneity of the ash-flow tuffs that comprise this unit compared to the stratified sedimentary deposits that make up the alluvium and Cerro Toledo interval. Also, the mean moisture for the Otowi Member in MCOBT-4.4 (16.1% ± 0.9% [1 σ]) is statistically indistinguishable from that in MCOBT-8.5 (16.8% ± 1.6% [1 σ]). Moisture contents to depths 300 ft for the Otowi Member in R-15 are similar (17.0% ± 1.2% [1 σ]) to those for MCOBT-4.4 and MCOBT-8.5. In contrast, the alluvium and Cerro Toledo interval are made up of more diverse lithologies, and their variable moisture contents reflect this heterogeneity.

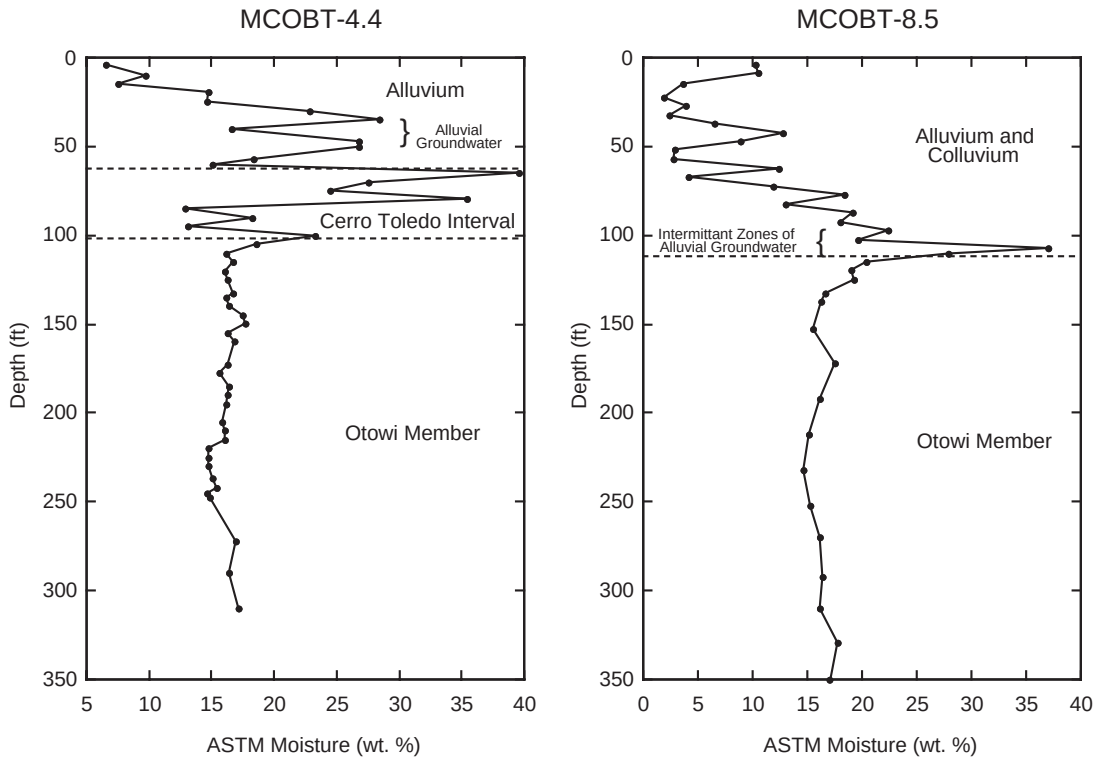

Figure 10.2-1. Gravimetric moisture contents for boreholes MCOBT-4.4 and MCOBT-8.5

11.0 GEOCHEMISTRY OF SAMPLED CORE AND WATERS

Sampled waters at MCOBT-4.4 and MCOBT-8.5 include pore water leachates from core or cuttings collected in the vadose zone and groundwater samples collected from the upper Puye Formation and the Cerros del Rio basalt at MCOBT-4.4. Groundwater was not encountered in MCOBT-8.5; thus, groundwater samples were not collected from this borehole. Groundwater samples were collected from MCOBT-4.4 after well development (pre-characterization sampling) using a submersible pump. This section focuses on the geochemical data obtained from vadose zone pore waters and from perched groundwater.

11.1 Geochemistry of Vadose Zone Pore Waters

Anion (acetate, bromide, chloride, fluoride, formate, nitrate, nitrite, perchlorate, phosphate, oxalate, and sulfate) and stable isotope ($\delta^{18}O$ and δD) profiles were determined from MCOBT-4.4 and MCOBT-8.5 core and cuttings. The anion samples were colocated with the moisture content samples described in Section 10.2. The sampling and analytical methods used were previously described in Broxton et al. (2001, 71250). Weighing errors are ±2% or less. The analytical precision of the ion chromatograph used to determine leachate concentrations is ±5% or less. Total errors are probably <10%.

11.1.1 Pore Water Methods

Anion leaching methods. HSA and sidewall core collected from MCOBT-4.4 and MCOBT-8.5 were analyzed for anion concentrations using a leaching process previously described by Broxton et al. (2001, 71250). The analytical suite included acetate, bromide, chloride, fluoride, formate, nitrate, nitrite, perchlorate, phosphate, oxalate, and sulfate. Nitrate is reported as nitrate (as opposed to N) unless otherwise noted.

Pore water anion concentrations were calculated using leachate concentrations, gravimetric moisture contents, and estimated bulk densities. Moisture content data are reported in Section 10.2. The bulk density estimates increase the uncertainty in the pore water concentrations; however, a bulk density error of 10% changes a pore water anion concentration by only <0.1 mg/L.

In the MCOBT-4.4 borehole, HSA core was collected between 4 and 310 ft from Alluvium (Qal), the Cerro Toledo interval (Qct), and the Otowi Member of the Bandelier Tuff (Qbo). In the MCOBT-8.5 borehole, HSA core was collected from 4 to 350 ft from Qal and Qbo.

During drilling of the two boreholes, an alternative technique for sample collection was evaluated. This technique involved using a sidewall-coring tool to collect samples in situations where not enough water was available to use standard water sampling methods (e.g., bailers or pumps) or where conventional coring was not feasible. The sidewall tool uses a 3/4-in.-diameter water-cooled cutter to collect approximately 2-in.-long core samples from the side of the borehole. Eighteen sidewall core samples were taken from depths between 272 to 735 ft in the MCOBT-4.4 borehole, and nine sidewall samples were collected between 405 and 709 ft in the MCOBT-8.5 borehole. Sidewall samples were collected from Qbo, the base of the Guaje Pumice Bed (Qbog), interflow zones in the Cerros del Rio basalt (Tb4), and upper portions of the Puye Formation (Tpf). Sidewall lithologies included sand, clay, basalt, and scoriaceous breccia. Two sets of duplicate sidewall samples were collected at MCOBT-8.5 to examine variation in sidewall sample results.

Moisture contents of sidewall core were preserved by wrapping samples in foil and placing them in sealed glass containers. Sample orientations in relation to the outer wall of the borehole were indicated either on the wrapping or on the jar. A 5-mm section of the sample nearest the borehole wall was removed to avoid potential contamination from drilling fluids. In most cases, the entire remaining “clean” sample was used in the leaching process. The amounts of rock and water used were greatly reduced compared to a typical core leaching. Several leachate samples were clouded by suspended particulates; the nature of these particulates is discussed in Section 9.4.

Pore water anion concentrations were calculated for dried samples of the HSA and sidewall core using leachate concentrations, gravimetric moisture contents, and bulk densities. Moisture content data are reported in Tables 11.1-1 and 11.1-2. Bulk density was not measured on the samples; therefore, estimates that are representative of rock units encountered on the Pajarito Plateau were used. The bulk density estimates increase the uncertainty in the pore water concentrations; however, they are not expected to introduce significant error.

Stable isotope methods. Stable isotope extractions ($\delta^{18}O$, δD, and $\delta^{15}N_{AIR}$–NO_3) were performed on moisture-protected core samples from both boreholes. When they arrived from the field, the moisture-protected core samples for $\delta^{15}N_{AIR}$–NO_3 analyses were placed in a freezer to prevent biological fractionation of the nitrogen isotopes. The $\delta^{15}N_{AIR}$–NO_3 cores were kept frozen until the start of the leach procedure. Sample preparation for determining the $\delta^{15}N_{AIR}$–NO_3 ratios was similar to the anion leaching procedure. Two changes to the procedure included (1) performing the leaching on moisture-protected core that was not dried (because it was not known if drying would fractionate the nitrogen isotopes, as discussed below), and (2) using larger volumes of rock and water to obtain a solution with a minimum concentration of 4 ppm nitrate (N) in 1 L of leachate (an analytical requirement of the $\delta^{15}N_{AIR}$–NO_3 analysis). The amounts of rock and water used were between 0.7 and 1.5 kg of rock leached in 1.3 to 1.5 kg of water. In most cases, the moisture-protected core was removed from the freezer immediately before weighing. Most samples were easily disaggregated using a mortar and pestle. However, four samples from MCOBT-4.4 were saturated and required partial thawing before they could be prepared for leaching. Defrosting was accomplished with the rock enclosed in the sealed sample bag for intervals up to one hr before weighing. Once the sample could be manipulated, it was broken into smaller pieces, and sample preparation proceeded as for the rest of the samples.

Table 11.1-1
Anion concentrations from the MCOBT-4.4 core

Sample ID	Depth (ft)	Unit	θg (%)	Br (mg/L)	Cl (mg/L)	ClO_4 (mg/L)	F (mg/L)	NO_3 as NO_3 (mg/L)	PO_4 as PO_4 (mg/L)	SO_4 as SO_4 (mg/L)	Ox (mg/L)	Acetate (mg/L)	Formate (mg/L)	NO_2 as NO_2 (mg/L)
Hollow-stem augered core														
GWM4-01-0031	4.1	Qal	6.48	3.44	6.61	<0.002	5.25	66.90	37.49	70.07	0	—	—	0.0
GWM4-01-0032	9.8	Qal	9.74	1.83	4.58	<0.002	7.70	1.07	19.16	41.35	<0.02	—	—	0.5
GWM4-01-0033	14.45	Qal	7.53	3.18	4.52	<0.002	9.63	13.42	34.99	32.72	<0.02	—	—	<0.01
GWM4-01-0034	19.15	Qal	14.71	1.94	8.94	<0.002	5.36	12.66	11.13	32.46	3.6	—	—	<0.01
GWM4-01-0035	24.9	Qal	14.64	0.51	4.20	<0.002	5.63	13.86	8.07	29.59	2.7	—	—	<0.01
GWM4-01-0036	29.7	Qal	22.83	0.71	8.08	<0.002	4.49	13.89	4.69	30.84	2.9	—	—	0.4
GWM4-01-0037	34.9	Qal	28.44	0.34	11.31	0.09	14.88	79.17	7.02	16.40	<0.02	—	—	<0.01
GWM4-01-0038	39.9	Qal	16.56	0.76	12.68	0.09	28.50	21.51	10.04	31.02	<0.02	—	—	<0.01
GWM4-01-0039	47.4	Qal	26.76	0.23	13.23	0.12	13.06	31.06	3.28	46.75	<0.02	—	—	<0.01
GWM4-01-0040	49.9	Qal	26.72	0.24	13.91	0.18	13.43	24.46	2.11	54.66	<0.02	—	—	0.5
GWM4-01-0041	57.4	Qal	18.32	1.53	26.83	0.18	6.24	129.48	<0.02	73.25	<0.02	—	—	0.7
GWM4-01-0042	59.9	Qal	15.07	1.14	17.67	0.15	10.38	85.97	4.41	33.43	<0.02	—	—	<0.01
GWM4-01-0043	64.9	Qct	39.60	0.51	23.88	0.20	4.76	111.01	2.33	42.47	<0.02	—	—	<0.01
GWM4-01-0044	69.9	Qct	27.57	0.48	21.47	0.21	7.05	105.49	2.51	38.82	<0.02	—	—	<0.01
GWM4-01-0045	74.9	Qct	24.48	0.22	16.70	0.13	6.81	113.45	0.54	17.02	<0.02	—	—	<0.01
GWM4-01-0046	79.4	Qct	35.43	<0.02	23.88	0.10	3.41	92.22	<0.02	27.16	<0.02	—	—	<0.01
GWM4-01-0047	84.9	Qct	12.87	0.35	26.24	0.17	7.29	160.93	<0.02	28.95	<0.02	—	—	<0.01
GWM4-01-0048	89.9	Qct	18.21	0.47	30.48	0.19	6.37	177.83	1.33	33.56	<0.02	—	—	<0.01
GWM4-01-0049	94.9	Qct	13.06	0.40	27.91	0.18	6.91	172.40	0.74	30.03	<0.02	—	—	<0.01
GWM4-01-0050	99.9	Qct	23.24	0.49	32.62	0.20	4.19	191.66	0.52	35.94	<0.02	—	—	<0.01
GWM4-01-0051	104.9	Qbo	18.60	0.62	25.93	0.20	7.80	156.89	<0.02	28.94	<0.02	—	—	<0.01
GWM4-01-0052	109.9	Qbo	16.16	<0.01	25.48	0.18	7.70	149.70	<0.02	26.82	<0.02	—	—	<0.01
GWM4-01-0053	114.9	Qbo	16.68	0.31	31.11	0.22	5.34	181.10	0.86	33.14	<0.02	—	—	<0.01

Table 11.1-1 (continued)

Sample ID	Depth (ft)	Unit	θg (%)	Br (mg/L)	Cl (mg/L)	ClO_4 (mg/L)	F (mg/L)	NO_3 as NO_3 (mg/L)	PO_4 as PO_4 (mg/L)	SO_4 as SO_4 (mg/L)	Ox (mg/L)	Acetate (mg/L)	Formate (mg/L)	NO_2 as NO_2 (mg/L)
Hollow-stem augered core (continued)														
GWM4-01-0054	119.9	Qbo	16.03	0.41	28.58	0.21	5.81	158.31	<0.02	30.27	<0.02	—	—	<0.01
GWM4-01-0055	124.9	Qbo	16.31	0.39	24.32	0.20	3.95	167.01	<0.02	26.65	<0.02	—	—	<0.01
GWM4-01-0056	132.4	Qbo	16.76	0.31	22.66	0.20	8.10	132.48	<0.02	20.70	<0.02	—	—	<0.01
GWM4-01-0057	134.9	Qbo	16.19	0.68	20.24	0.18	7.77	105.74	<0.02	16.83	<0.02	—	—	<0.01
GWM4-01-0058	139.9	Qbo	16.33	<0.01	17.85	0.19	10.24	87.67	<0.02	12.11	<0.02	—	—	<0.01
GWM4-01-0059	144.9	Qbo	17.52	0.57	21.74	0.25	12.29	94.46	0.73	10.06	1	—	—	<0.01
GWM4-01-0060	149.4	Qbo	17.68	0.31	14.77	0.21	13.62	17.60	<0.02	4.84	2	—	—	6.30
GWM4-01-0062	159.9	Qbo	16.77	0.98	12.80	0.22	14.58	55.28	<0.02	3.56	<0.02	+	+	<0.01
GWM4-01-0063	172.4	Qbo	16.22	0.64	7.38	0.11	13.93	19.58	0.27	2.19	<0.02	+	+	<0.01
GWM4-01-0065	184.9	Qbo	16.39	0.90	5.11	0.06	15.42	4.21	<0.02	1.97	<0.02	+	+	<0.01
GWM4-01-0067	194.9	Qbo	16.20	<0.01	3.68	0.04	14.82	0.55	0.28	3.77	<0.02	—	—	<0.01
GWM4-01-0068	204.9	Qbo	15.88	<0.01	5.00	0.03	17.69	0.74	<0.02	3.52	<0.02	+	+	<0.01
GWM4-01-0070	214.9	Qbo	16.08	<0.01	3.40	<0.002	13.61	1.16	<0.02	2.87	<0.02	—	—	<0.01
GWM4-01-0072	224.9	Qbo	14.73	<0.01	3.90	<0.002	12.37	1.17	<0.02	3.22	<0.02	+	+	<0.01
GWM4-01-0074	236.9	Qbo	15.10	<0.01	1.49	<0.002	9.82	<0.01	<0.02	2.28	<0.02	—	—	<0.01
GWM4-01-0077	247.4	Qbo	14.79	0.10	1.86	<0.002	10.02	0.31	0.41	2.69	<0.02	—	—	<0.01
GWM4-01-0078	272.4	Qbo	16.96	0.36	2.58	<0.002	8.35	0.18	<0.02	3.29	<0.02	—	—	<0.01
GWM4-01-0079	289.9	Qbo	16.39	0.63	2.70	<0.002	10.52	0.81	<0.02	3.60	<0.02	+	+	<0.01
GWM4-01-0080	309.9	Qbo	17.15	0.58	2.91	<0.002	9.74	1.50	0.67	2.83	<0.02	+	+	<0.01
MCOBT-4.4 sidewall core														
GWM4-01-0141	272	Qbo	42.89	0.87	16.0	<0.002	2.9	0.73	0.28	35.7	<0.02	+	+	0.10
GWM4-01-0142	289	Qbo	42.95	0.98	23.0	<0.002	4.0	1.17	0.43	17.8	<0.02	+	+	0.27
GWM4-01-0143	309	Qbo	37.98	0.99	13.5	<0.002	3.4	1.03	0.37	44.4	<0.02	+	+	<0.01
GWM4-01-0144	350	Qbo	35.75	0.11	11.4	<0.002	8.0	0.57	0.34	30.9	<0.02	+	+	<0.01

Table 11.1-1 (continued)

Sample ID	Depth (ft)	Unit	θg (%)	Br (mg/L)	Cl (mg/L)	ClO_4 (mg/L)	F (mg/L)	NO_3 as NO_3 (mg/L)	PO_4 as PO_4 (mg/L)	SO_4 as SO_4 (mg/L)	Ox (mg/L)	Acetate (mg/L)	Formate (mg/L)	NO_2 as NO_2 (mg/L)
MCOBT-4.4 sidewall core (continued)														
GWM4-01-0145	390	Qbo	37.46	1.15	13.3	<0.002	5.3	0.82	<0.02	18.4	<0.02	+	+	0.49
GWM4-01-0146	430	Qbo	55.59	0.73	11.7	<0.002	3.8	0.09	<0.02	24.1	<0.02	—	—	0.48
GWM4-01-0147	470	Qbog	46.18	0.82	10.6	<0.002	2.8	<0.01	0.08	13.7	3.41	—	—	<0.01
GWM4-01-0140	480	Tpf	11.08	<0.01	36.81	<0.002	13.97	1.34	2.96	43.92	11.33	472	345	1.3
GWM4-01-0139	512	Tpf	34.20	0.13	10.57	<0.002	0.93	3.35	<0.02	10.48	1.0	261	116	0.0
GWM4-01-0138	549	Tb4	45.09	<0.01	9.50	<0.002	1.07	0.17	<0.02	6.61	0.8	<1	37	0.3
GWM4-01-0137	588	Tb4	14.68	<0.01	12.53	<0.002	11.11	1.02	4.89	18.44	1.5	<1	36	<0.01
GWM4-01-0136	607	Tb4	7.73	<0.01	29.97	<0.002	9.36	1.53	12.03	27.30	4.6	<1	40	<0.01
GWM4-01-0135	615	Tb4	4.78	<0.01	15.50	<0.002	4.34	5.58	9.30	24.18	3.1	65	38	<0.01
GWM4-01-0134	645	Tb4	4.71	<0.01	27.42	<0.002	5.74	5.42	31.57	24.23	3.6	40	23	<0.01
GWM4-01-0133	670	Tb4	4.26	<0.01	21.46	<0.002	8.80	2.11	33.07	31.31	4.4	<1	31	<0.01
GWM4-01-0132	684	Tb4	9.38	<0.01	27.52	<0.002	14.24	0.48	11.04	36.32	4.3	<1	43	<0.01
GWM4-01-0131	730	Tb4	22.60	<0.01	16.28	0.02	4.47	5.67	<0.02	35.96	2.3	<1	10	<0.01
GWM4-01-0130	735	Tpf	16.01	<0.01	28.13	<0.002	10.88	10.50	<0.02	41.07	1.7	<1	24	<0.01
MAX	NA	NA	55.59	3.44	36.81	0.25	28.50	191.66	37.49	73.25	11.33	472	345	6.30
MIN	NA	NA	4.26	<0.01	1.49	<0.002	0.93	<0.01	<0.02	1.97	<0.02	<1	10	<0.01

Bulk density value used for Qbog is same as Qbo
Bulk density values for Qbo and Qal from Rogers and Gallaher (1995, 49824.1).
Bulk density values for Tb4 from D. Broxton, best estimate (personal communication).
Bulk density estimates for Qct assuming pure dacite.
Bulk density for Tp is for a sand.
NA = Not applicable.
+ = Detected acetate or formate, but not quantifiable.
— = No detection of acetate or formate.

Table 11.1-2
Anion concentrations from the MCOBT-8.5 core

Sample ID	Depth (ft)	Unit	θg (%)	Br (mg/L)	Cl (mg/L)	ClO_4 (mg/L)	F (mg/L)	NO_3 as NO_3 (mg/L)	PO_4 as PO_4 (mg/L)	SO_4 as SO_4 (mg/L)	Ox (mg/L)	Acetate (mg/L)	Formate (mg/L)	NO_2 as NO_2 (mg/L)
Hollow-stem augered core														
GWM8-01-0046	4.0	Qal	10.19	1.32	5.4	<0.002	14.3	1.2	6.6	31.2	<0.02	+	+	<0.01
GWM8-01-0048	14.8	Qal	3.62	<0.01	486.5	<0.002	33.8	17.3	46.6	263.9	<0.02	+	+	<0.01
GWM8-01-0050	27.3	Qal	3.94	4.14	15.8	<0.002	49.3	42.1	60.6	32.3	<0.02	+	+	<0.01
GWM8-01-0052	37.3	Qal	6.44	2.96	9.1	<0.002	36.5	42.2	26.9	25.1	<0.02	+	+	<0.01
GWM8-01-0054	47.3	Qal	8.86	1.33	7.6	<0.002	30.4	48.3	18.1	13.9	<0.02	—	—	<0.01
GWM8-01-0056	57.3	Qal	2.69	0.00	31.0	<0.002	99.5	43.0	75.6	13.1	<0.02	+	+	<0.01
GWM8-01-0058	67.3	Qal	4.16	0.00	22.6	<0.002	27.3	8.0	37.5	8.0	<0.02	+	+	<0.01
GWM8-01-0060	77.3	Qal	18.34	0.73	29.0	0.35	9.1	235.0	6.6	56.5	<0.02	—	—	<0.01
GWM8-01-0062	87.3	Qal	19.13	<0.01	28.3	0.40	5.0	243.8	4.1	45.3	<0.02	+	+	<0.01
GWM8-01-0064	97.3	Qal	22.42	0.40	16.7	0.61	9.7	34.7	3.3	45.6	<0.02	+	+	<0.01
GWM8-01-0066	107.3	Qbo	37.05	0.97	26.6	0.84	7.1	54.1	1.4	56.1	<0.02	—	—	<0.01
GWM8-01-0068	114.8	Qbo	20.39	0.58	31.7	0.37	14.1	176.6	5.0	66.0	<0.02	+	+	<0.01
GWM8-01-0070	124.8	Qbo	19.21	<0.01	22.3	0.31	9.5	196.9	2.6	29.7	<0.02	+	+	<0.01
GWM8-01-0072	137.3	Qbo	16.23	0.63	21.9	0.33	16.4	135.3	2.7	42.6	<0.02	+	+	<0.01
GWM8-01-0074	152.3	Qbo	15.56	<0.01	26.9	0.42	18.2	174.0	1.8	65.4	<0.02	+	+	<0.01
GWM8-01-0075	172.3	Qbo	17.49	<0.01	24.4	0.37	19.1	165.4	2.1	57.7	<0.02	—	—	<0.01
GWM8-01-0076	192.3	Qbo	16.14	<0.01	22.8	0.30	17.0	134.4	3.1	51.0	<0.02	—	—	<0.01
GWM8-01-0077	212.3	Qbo	15.17	<0.01	25.4	0.39	12.0	155.2	1.3	60.8	<0.02	—	—	<0.01
GWM8-01-0078	232.3	Qbo	14.64	<0.01	20.3	0.32	12.3	110.8	2.2	41.4	<0.02	—	—	<0.01
GWM8-01-0079	252.3	Qbo	15.20	0.10	18.5	0.29	12.0	87.4	1.7	40.3	<0.02	+	+	<0.01
GWM8-01-0080	269.8	Qbo	16.15	<0.01	13.9	0.26	12.6	47.5	1.6	40.8	<0.02	—	—	<0.01
GWM8-01-0082	292.3	Qbo	16.34	0.18	10.4	0.27	15.5	26.3	1.5	35.1	<0.02	—	—	<0.01
GWM8-01-0083	309.8	Qbo	16.16	0.19	10.0	0.31	16.0	11.1	1.4	38.2	<0.02	—	—	<0.01
GWM8-01-0084	329.2	Qbo	17.73	0.16	11.6	0.31	14.3	11.6	1.1	41.5	<0.02	+	+	<0.01
GWM8-01-0085	349.8	Qbo	17.04	0.26	12.6	0.34	19.8	12.4	1.4	41.1	<0.02	—	—	<0.01

Table 11.1-2 (continued)

Sample ID	Depth (ft)	Unit	θg (%)	Br (mg/L)	Cl (mg/L)	ClO_4 (mg/L)	F (mg/L)	NO_3 as NO_3 (mg/L)	PO_4 as PO_4 (mg/L)	SO_4 as SO_4 (mg/L)	Ox (mg/L)	Acetate (mg/L)	Formate (mg/L)	NO_2 as NO_2 (mg/L)
MCOBT-8.5 sidewall core														
GWM8-01-0091	405	Qbo	39.21	0.13	11.97	<0.002	5.94	0.52	0.95	20.04	<0.02	+	+	0.39
GWM8-01-0092	425	Tpf	5.48	1.63	50.58	<0.002	21.21	3.81	44.33	23.93	3.81	+	+	<0.01
GWM8-01-0093	447	Tb4	5.60	1.93	153.96	<0.002	21.90	4.19	46.70	44.13	<0.02	+	+	<0.01
GWM8-01-0094	604	Tb4	6.09	2.47	67.48	<0.002	22.63	5.35	47.73	37.85	<0.02	+	+	<0.01
GWM8-01-0095	651 "a"	Tb4	21.22	1.89	33.54	<0.002	5.60	0.45	1.51	150.66	<0.02	+	+	<0.01
GWM8-01-0096	651 "b"	Tb4	29.66	0.56	14.73	<0.002	5.73	0.28	3.17	48.36	<0.02	+	+	<0.01
GWM8-01-0097	681	Tb4	8.00	2.49	31.02	<0.002	23.78	4.30	51.17	17.44	<0.02	+	+	<0.01
GWM8-01-0098	709 "a"	Tb4	13.50	5.79	161.75	<0.002	16.13	1.51	10.33	114.89	<0.02	+	+	<0.01
GWM8-01-0099	709 "b"	Tb4	20.11	1.05	29.75	<0.002	12.13	0.82	1.40	55.76	5.60	+	+	<0.01
MAX	NA	NA	39.21	5.79	486.5	0.84	99.5	243.8	75.6	263.9	3.81	NA	NA	0.39
MIN	NA	NA	2.69	<0.01	5.4	<0.002	5.0	1.2	1.1	8.0	<0.2	NA	NA	<0.1

Bulk density value used for Qbo-g is same as Qbo

Bulk density values for Qbo and Qal from Rogers and Gallaher (1995, 49824.1)

Bulk density values for Tb4 from D. Broxton, best estimate (personal communication)

Bulk density for Tp is for a sand.

NA = Not applicable

+ = Detected acetate or formate, but not quantifiable.

— = No detection of acetate or formate.

The disaggregated rock was weighed, placed in a 4-L jar with deionized water, agitated for a minimum of 48 hr, and then allowed to settle overnight. Five mL of the supernatant were removed to determine nitrate concentrations. The remaining leachate was transferred into a 1-L plastic bottle and acidified to a pH less than 2.0 using concentrated sulfuric acid. Samples were refrigerated until they were shipped for analysis. Analyses for $\delta^{15}N$ were performed at Coastal Laboratories using a method modified from Velinsky et al. (1989). The analytical precision for the $\delta^{15}N$ analyses by isotope ratio mass spectrometry (IRMS) is reported as ±1‰.

There was uncertainty about the effect of drying on $\delta^{15}N_{AIR}$–NO_3 ratios. Using dried samples for $\delta^{15}N_{AIR}$-NO_3 analyses is desirable because the method allows direct calculation of anion pore water concentrations from the same leaching solution and because samples from other sites analyzed in the future may not be moisture protected. To examine if drying caused appreciable fractionation, leachate analyses were performed on colocated sample splits from different sections of core from MCOBT-4.4 and MCOBT-8.5. One set of the samples was prepared as described above (i.e., not dried). The other sample splits were prepared by removing the core from the moisture-protected sleeves and drying them overnight in a 110°C oven. All samples were then leached as described above. A total of four pairs of samples were analyzed to examine drying effects.

Analyses for $\delta^{18}O$ and δD of core pore waters were performed at the New Mexico Tech Stable Isotope Laboratory. The sample preparation for $\delta^{18}O$ and δD analyses was previously described by Broxton et al. (2000, 71251) and used the vacuum distillation method of Shurbaji and Campbell (1997, 64063) and the $\delta^{18}O$ and δD extraction methods of Socki et al. (1992, 64064) and Kendall and Coplen (1985, 64061). The analytical precision for the $\delta^{18}O$ and δD analyses by IRMS was better than ±0.2‰ and ±4‰, respectively.

11.1.2 Pore Water Results

Anion results from HSA core. The vertical distributions of bromide, chloride, fluoride, nitrate, oxalate, perchlorate, phosphate, and sulfate from the HSA core samples collected from the MCOBT-4.4 and-8.5 boreholes are shown in Figures 11.1-1 to 11.1-8, and the results are listed in Tables 11.1-1 and 11.1-2. Vertical distributions of anions from sidewall core samples are also shown by different symbols in Figures 11.1-1 to 11.1-8. Results from the sidewall samples are very different from the HSA samples, and their interpretation is hampered by issues of sample collection and data quality (see “Discussion of sidewall core use” below).

Acetate and formate results are not included in the anion profiles because their concentrations were usually lower than the analytical detection limit. The results are listed in Tables 11.1-1 and 11.1-2, and in most cases are denoted as detects (+) or nondetects (–). Nitrite concentrations for most samples are also below detection limits and are not depicted in the figures. Except for acetate and formate, the anions whose concentrations fall below the detection limit are reported as less than values in Tables 11.1-1 and 11.1-2. A value of 0 is used in place of less than values to construct the figures presented in this report. The leaching process results in substantial dilution, and thus anions with low concentrations can be reduced to levels below the detection limit.

Bromide concentrations from the MCOBT-4.4 core are highest in upper Qal and fluctuate around 0.5 and 1 mg/L throughout Qct, Qbo, and Qbog. (Figure 11.1-1a). Bromide concentrations decline in Tpf and are below detection limits throughout Tb4. The pattern of bromide concentrations in the MCOBT-8.5 core is similar to that in MCOBT-4.4, with concentrations generally greatest in the upper part of the core. The concentrations, however, are low throughout Qbo and increase in upper Tpf and Tb4 (Figure 11.1-1b). It is possible that increasing concentrations of bromide found in Tb4 at MCOBT-8.5 may be related to aspects of basalt interflow hydrogeology (*e.g.*, precipitates in "drier" interflow zones) or to greater flushing of salts in the vicinity of MCOBT-4.4 than at MCOBT-8.5.

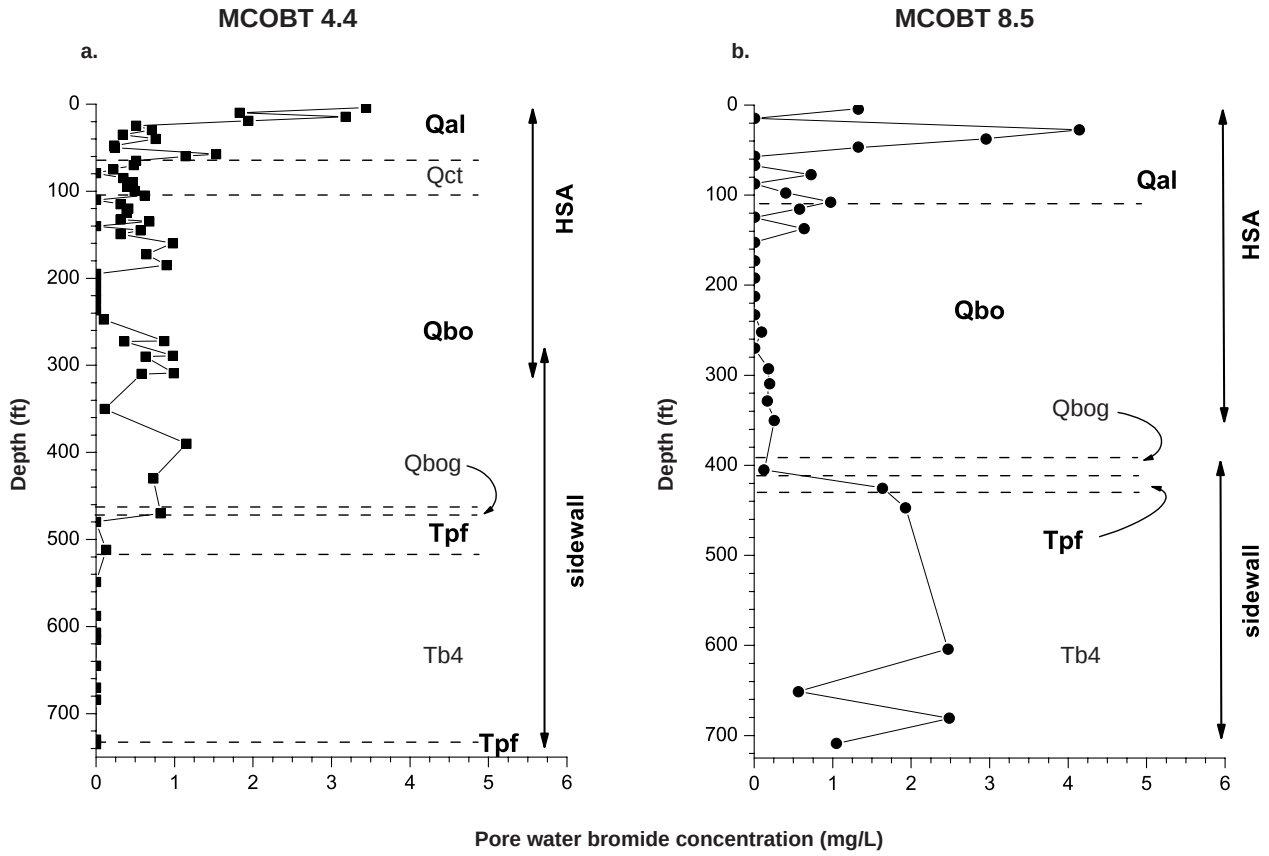

Figure 11.1-1. Pore water bromide concentrations for boreholes MCOBT-4.4 and MCOBT-8.5. Because sidewall estimates have much greater uncertainty than HSA samples, sidewall anion results should be treated with caution.

The chloride profile from the MCOBT-4.4 core has a bulge across Qal, Qct and upper Qbo, with the maximum concentrations around 32 mg/L at the Qct/Qbo contact (Figure 11.1-2a). Below 310 ft, concentrations are lower but are largely constant, averaging around 20 mg/L. Maximum chloride concentrations in the MCOBT-8.5 core are much greater than in MCOBT-4.4 (Figure 11.1-2b). Peaks in chloride concentrations of 489 and 162 mg/L are found in the upper Qal and upper Tb4, respectively. Chloride concentrations between these peaks are fairly constant, averaging 20 mg/L.

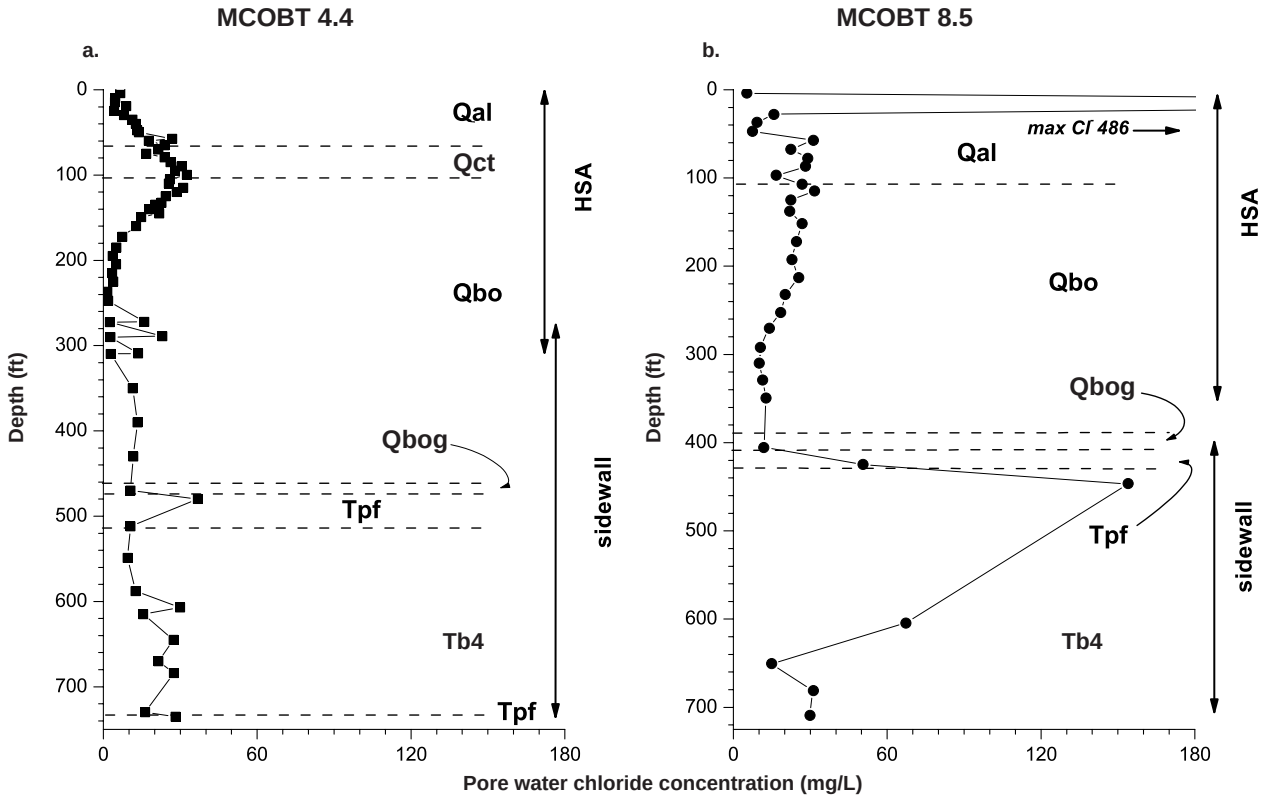

Figure 11.1-2. Pore water chloride concentrations for boreholes MCOBT-4.4 and MCOBT-8.5. Because sidewall estimates have much greater uncertainty than HSA samples, sidewall anion results should be treated with caution.

In MCOBT-4.4 and MCOBT-8.5 the highest fluoride concentrations are observed in Qal (Figures 11.1-3a and 3b). Fluoride concentrations are slightly higher in MCOBT-8.5 core, but the profiles are similar for both cores, with a small bulge in the upper Qbo and fairly constant concentrations in the mid- to lower profile.

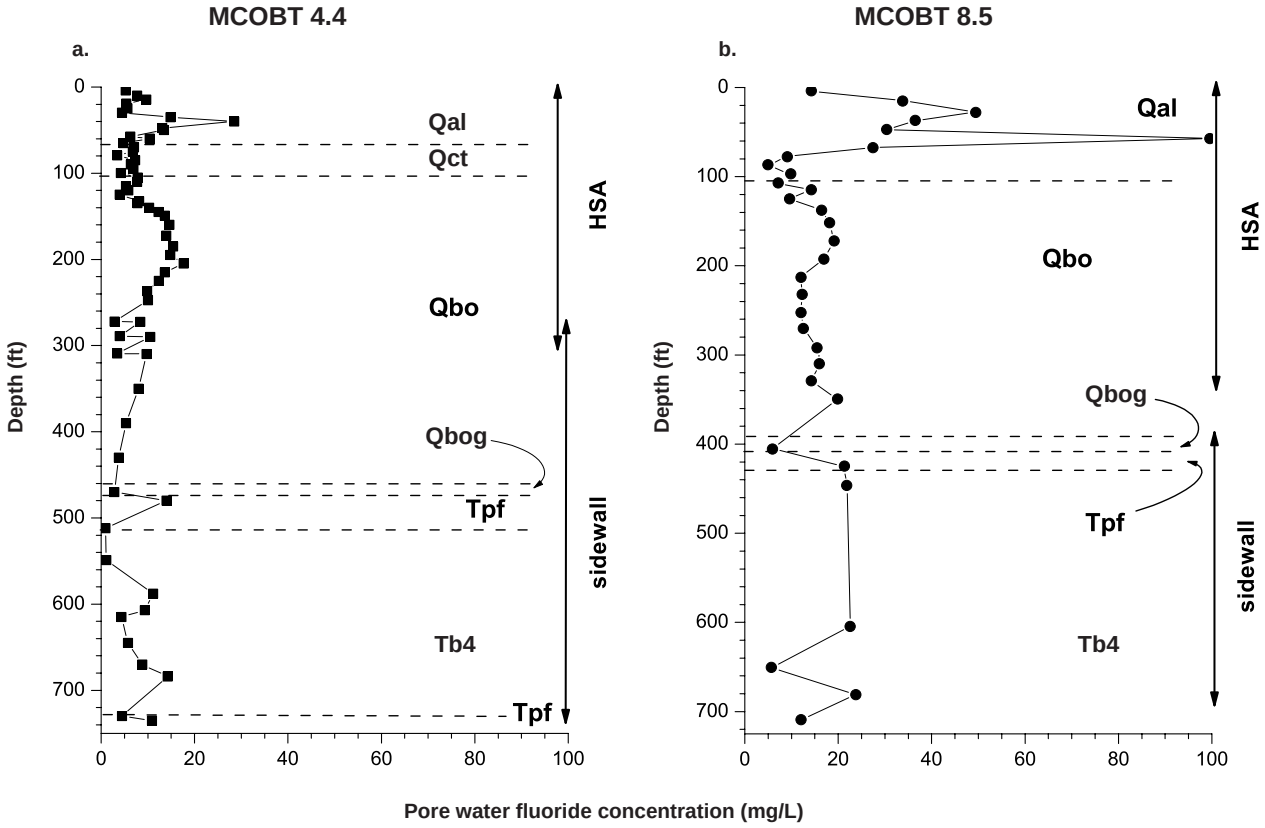

Figure 11.1-3. Pore water fluoride concentrations for boreholes MCOBT-4.4 and MCOBT-8.5. Because sidewall estimates have much greater uncertainty than HSA samples, sidewall anion results should be treated with caution.

The nitrate (as nitrate) profile in the MCOBT-4.4 core is similar to the chloride profile in that it has a bulge across the Qal, Qct, and upper Qbo with a maximum at the Qct/Qbo contact (Figure 11.1-4a). Below the bulge, nitrate concentrations in MCOBT-4.4 decrease to near or below detection limits. The bulge probably represents the vertical extent of nitrate contamination from percolation in the vicinity of the MCOBT-4.4 borehole. An asymmetric nitrate bulge is observed in the MCOBT-8.5 profile. The bulge has an irregular upper portion, and the maximum occurs near the Qal/Qbo contact (Figure 11.1-4b). Nitrate concentrations remain high throughout the lower Qbo and then drop off to near detection limits below the Qbo/Qbog contact. As with MCOBT-4.4, the nitrate bulge in MCOBT-8.5 probably represents the vertical extent of nitrate contamination from percolation in the vicinity of the borehole.

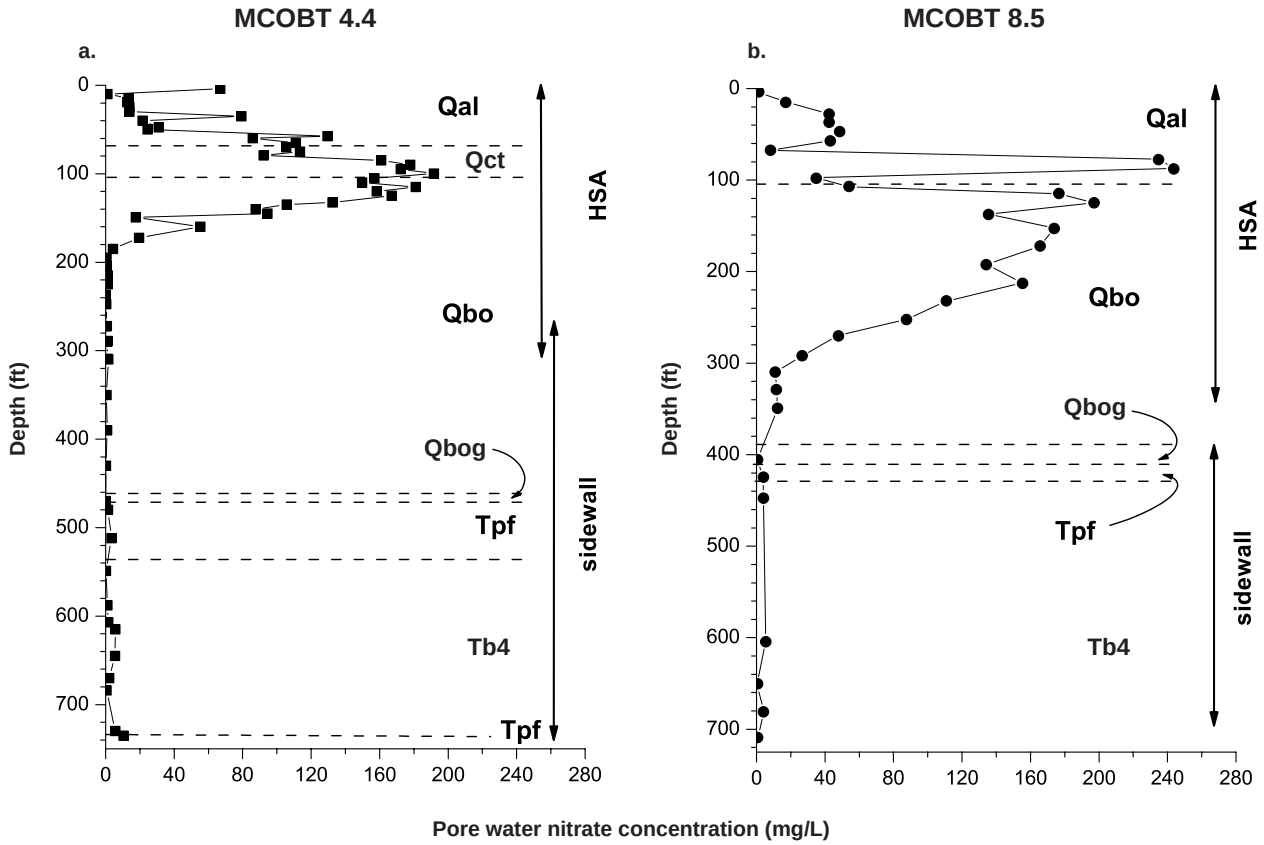

Figure 11.1-4. Pore water nitrate (as nitrate) concentrations for boreholes MCOBT-4.4 and MCOBT-8.5. Because sidewall estimates have much greater uncertainty than HSA samples, sidewall anion results should be treated with caution.

The MCOBT-4.4 core shows the presence of oxalate across portions of all of the rock units except Qct (Figure 11.1-5a). In contrast, oxalate in the MCOBT-8.5 core can be observed in only two sidewall core samples from the Qbog/Tpf contact and near the base of Tb4 (Figure 11.1-5b). The oxalate concentrations in the Qbog, Tb4, and Tpf in both holes may be related to buried soils in these units.

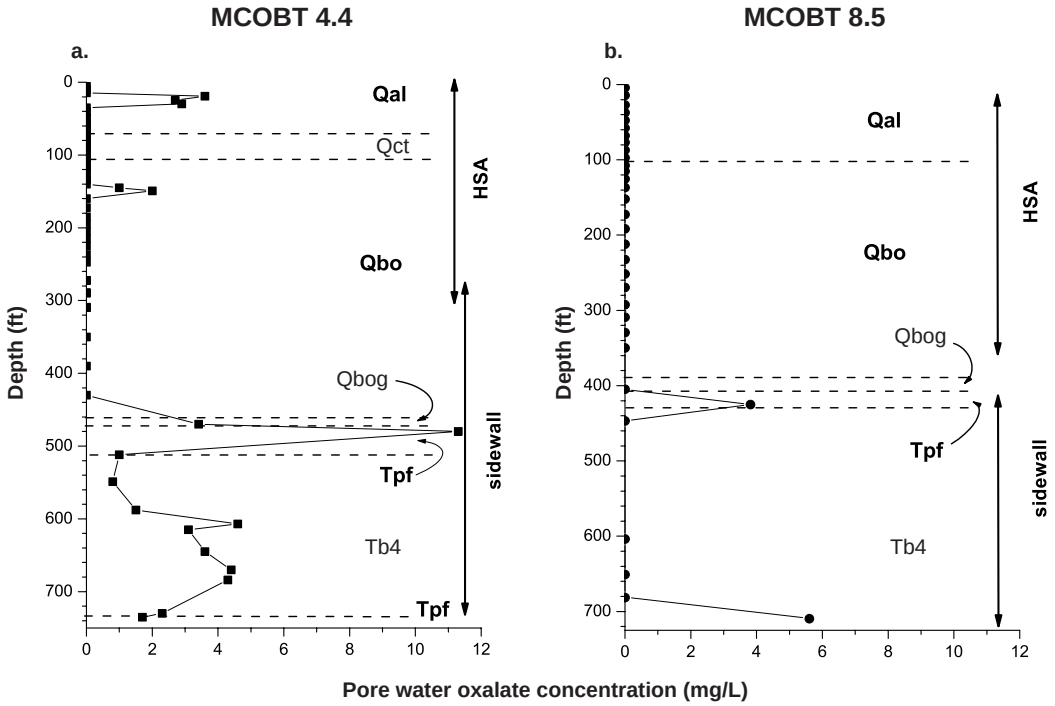

Figure 11.1-5. Pore water oxalate concentrations for boreholes MCOBT-4.4 and MCOBT-8.5. Because sidewall estimates have much greater uncertainty than HSA samples, sidewall anion results should be treated with caution.

Average measurable concentrations of perchlorate and nitrate (as N) in leachates analyzed from core samples collected from 4.1 to 309.9 ft were 0.16 and 15.99 (70.35 nitrate as nitrate) mg/L, respectively. Average dissolved concentrations of perchlorate and nitrate plus nitrite (as N) observed in the alluvial monitoring wells are 0.235 (235 μg/L) and 8.40 mg/L, respectively, during 2000 (ESP 2001, 71301). Contaminant distributions for these two anions in the alluvium, Cerro Toledo interval, and Bandelier Tuff observed in 2000 suggest that significant concentrations of nitrate and perchlorate have migrated in the subsurface of Mortandad Canyon. Higher concentrations of perchlorate, however, were measured within the alluvium during 2000 (ESP 2001, 71301) than in the perched zone at MCOBT-4.4 (Table 11.2-2a).

The perchlorate profile from MCOBT-4.4 core shows a bulge across Qal, Qct and upper Qbo (Figure 11.1-6a). Below 205 ft, only one sample (sidewall core at 730 ft) has detectable concentrations of perchlorate. By contrast, the MCOBT-8.5 anion profile shows the presence of perchlorate throughout the upper half of the core (Figure 11.1-6b). The concentrations are greatest at the Qal/Qbo contact. Below the contact, perchlorate concentrations decline and remain constant throughout Qbo. No perchlorate is observed below 350 ft in the MCOBT-8.5 sidewall core.

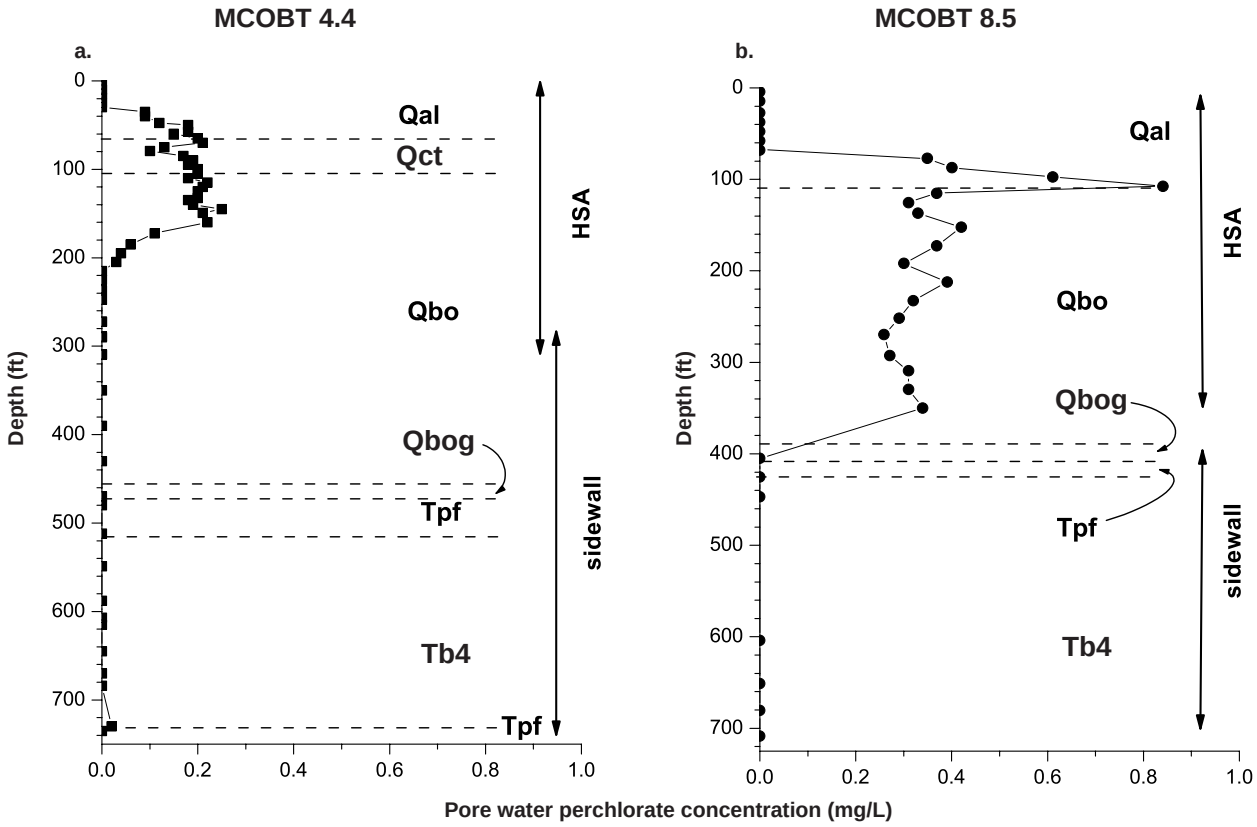

Figure 11.1-6. Pore water perchlorate concentrations for boreholes MCOBT-4.4 and MCOBT-8.5. Because sidewall estimates have much greater uncertainty than HSA samples, sidewall anion results should be treated with caution.

Phosphate profiles from both boreholes are similar with high concentrations in Qal, low to below detection limits in Qct and Qbo, and high concentrations at depths below Qbog (Figures 11.1-7a and 11.1-7b). As with some of the other anions, phosphate concentrations in the MCOBT-8.5 core are generally greater than in the MCOBT-4.4 core. It should be noted that phosphate is a constituent of drilling fluids, which were present in the sidewall cores.

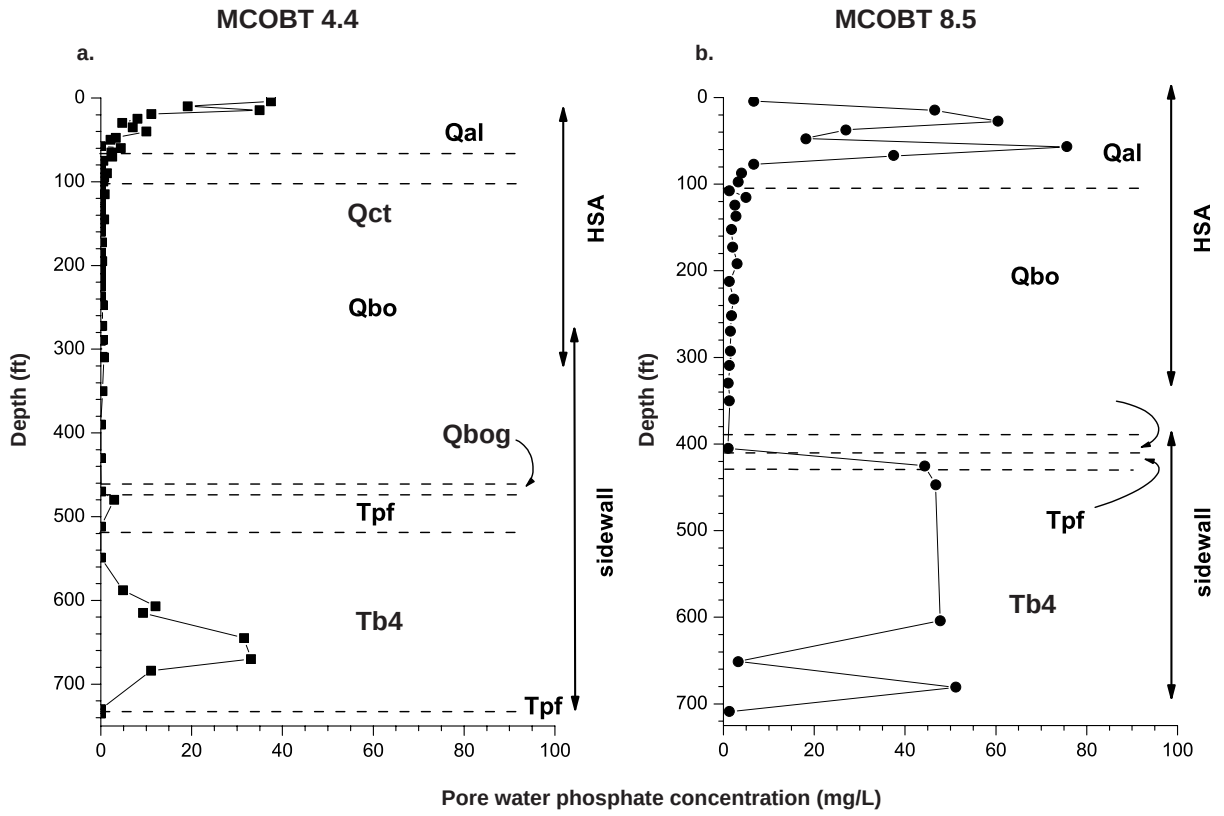

Figure 11.1-7. Pore water phosphate concentrations for boreholes MCOBT-4.4 and MCOBT-8.5. Because sidewall estimates have much greater uncertainty than HSA samples, sidewall anion results should be treated with caution.

The sulfate profile for the MCOBT-4.4 core shows high, sporadic concentrations in Qal, declining concentrations from depths in Qct to upper Qbo, and sporadic concentrations in lower Qbo and Tpf (Figure 11.1-8a). Sulfate concentrations in the lower MCOBT-4.4 core in Tb4 increase with depth. The MCOBT-8.5 sulfate profile shows generally higher concentrations than observed in the MCOBT-4.4 core (Figure 11.1-8b). A large sulfate peak occurs in Qal and concentrations remain fairly constant, around 40 mg/L, to the bottom of the core.

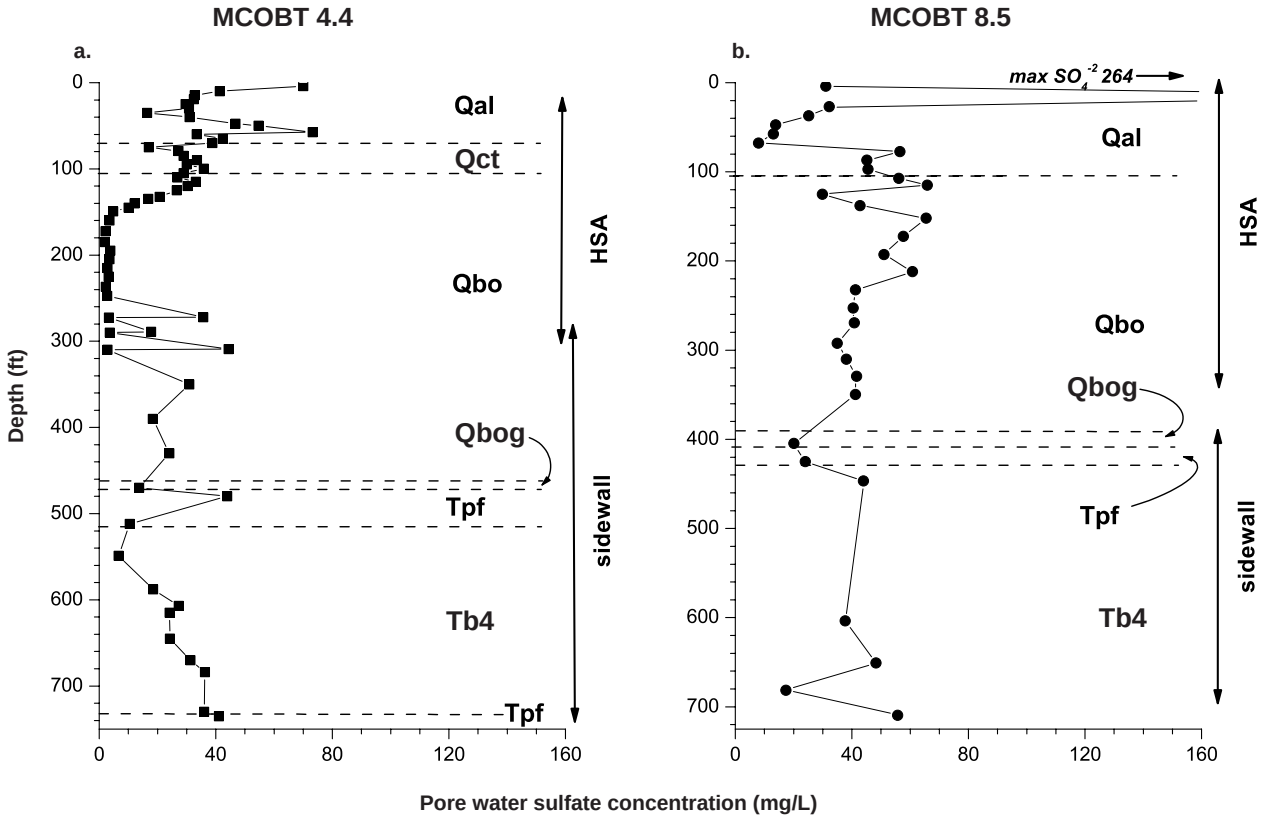

Figure 11.1-8. Pore water sulfate concentrations for boreholes MCOBT-4.4 and MCOBT-8.5. Because sidewall estimates have much greater uncertainty than HSA samples, sidewall anion results should be treated with caution.

Anion results from sidewall core. Visual observations of seven sidewall samples between 272 and 470 ft depths from Qbo in MCOBT-4.4 indicated that the samples consisted of loose moist, gray, pumiceous tuff. These shallow sidewall cores were notably wet, and in many cases free water was observed in the jar or inside the foil wrapping. Except for a few samples, bromide, perchlorate, chloride, fluoride, sulfate, phosphate, and nitrate concentrations in pore waters from the sidewall cores fall within the range of values from the HSA core (Figures 11.1-1 to 11.1-8 and Tables 11.1-1 and 11.1-2). Because of issues of sample and data quality, as discussed in the following section, the chemical data from sidewall core samples should only be used to indicate the *possibility* of contamination and not to derive a quantitative estimate of concentration.

Oxalate concentrations from sidewall core are considerably elevated over concentrations measured from the HSA core. However, this result may be related to buried soils in the deeper stratigraphic units where most of the sidewall samples were collected (Table 11.1-1). Oxalate was found to be associated with soil horizons in boreholes R-9 and R-12 but is not a known breakdown product of drilling fluid. Acetate and

formate are detected in 89% of sidewall core, while only 17% of HSA core shows the presence of acetate and formate. The increase in detection of acetate and formate in the sidewall cores suggests that breakdown products from drilling additives (e.g., EZ-MUD®) had affected the samples.

A 38-ft interval occurs near the bottom of the HSA portion of the MCOBT-4.4 borehole where sidewall and HSA samples overlapped. Comparison of the two core types shows that bromide, chloride, and sulfate are greater in the sidewall core (Figures 11.1-9a to 11.1-9c). By contrast, fluoride is greater in the HSA core (Figure 11.1-9d), and nitrate and phosphate results are mixed (Figure 11.1-9a).

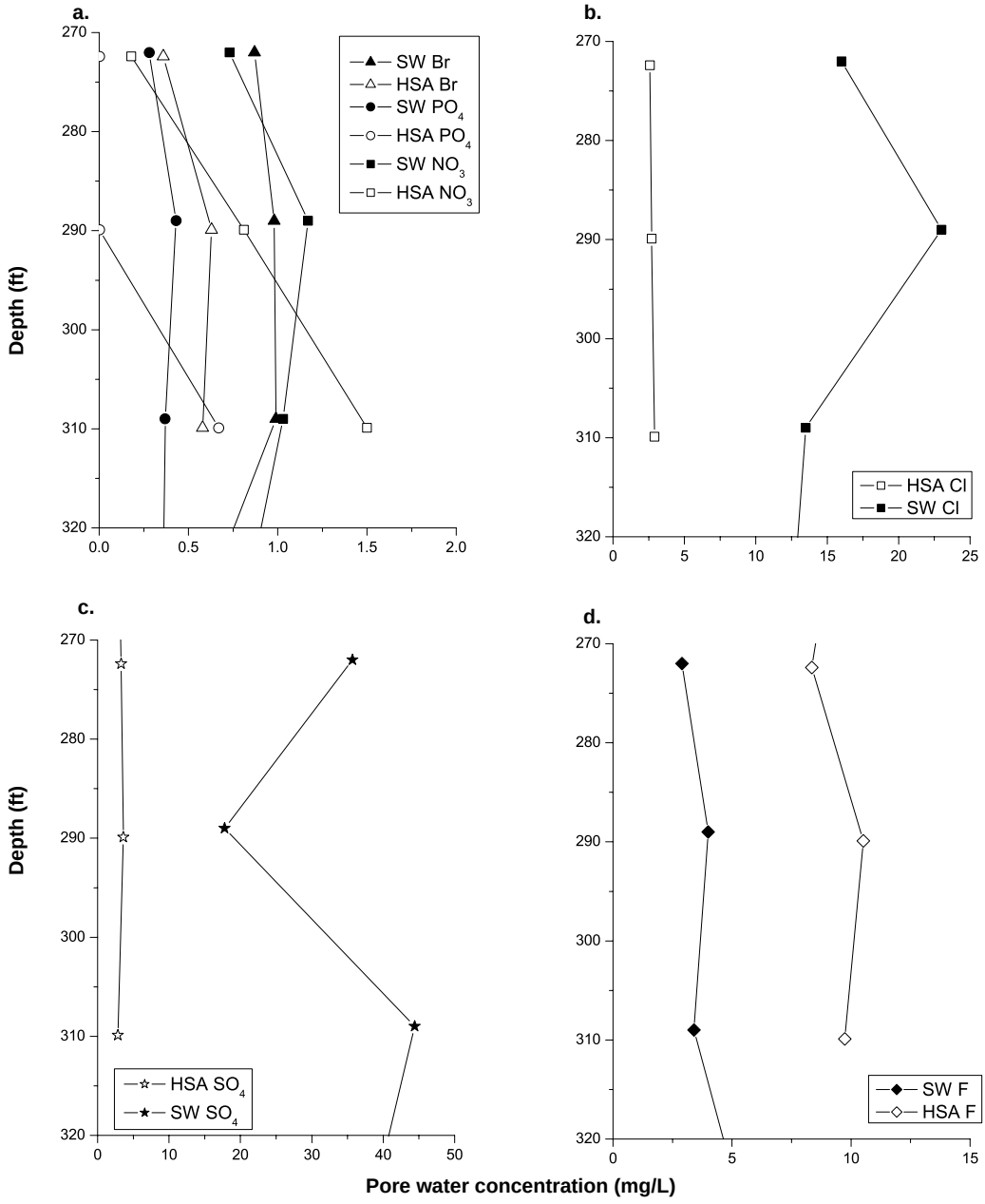

Figure 11.1-9. Comparison of pore water anion concentrations for HSA core samples and sidewall (SW) core samples collected from MCOBT-4.4

In the MCOBT-8.5 borehole, bromide, chloride, fluoride, sulfate and phosphate concentrations in sidewall samples generally do not exceed the range of values from the HSA core (Figures 11.1-1 to 11.1-8). In addition, although concentrations of acetate and formate are not high enough to measure quantitatively, all the sidewall samples show the presence of these analytes (probably the effect of drilling fluid breakdown products), while only 56% of the HSA core shows the presence of acetate or formate.

Two sets of "duplicate" sidewall samples were collected from the MCOBT-8.5 core at 651 ft and 709 ft in basalt interbed zones. Although it would appear that these sample sets are replicates, small variations occurred in the coring depths, and the "A" and "B" duplicates differ in lithology. Therefore, these samples are not true replicates and instead express some of the heterogeneity present in the interbed zones. The sidewall sample pairs from 651 and 709 ft in MCOBT-8.5 provide the opportunity to examine this heterogeneity. Sidewall cores A and B collected at 651 ft have clay and scoriaceous breccia lithologies, respectively. Sidewall cores A and B collected at 709 ft are both basaltic sands. However, the B sample is more indurated than the A sample. In general, the concentrations of fluoride, phosphate, and nitrate are similar in both pairs of samples, while bromide sulfate and chloride concentrations are higher in the A samples (Table 11.1-2).

Discussion of sidewall core use. Sidewall coring provides a method for obtaining samples when other methods are not feasible. However, it is expensive and its future use as part of the LANL drilling/characterization program needs to be examined relative to the quality of the data produced. This initial study reveals three problems related to sidewall coring. First, the cores can be contaminated by introduced water, mud, and/or drilling additives (as shown by the formate and acetate results), and these contamination effects are difficult to eliminate during sample preparation. Second, it is possible that introduced water could dilute concentrations of other analytes. Third, the small amount of sample produced by sidewall coring is difficult to work with and requires a modified leaching procedure. The small sample size also may not be representative of a larger volume of rock and may provide misleading estimates (high or low) of contaminant concentrations.

The issue of sample size also relates to collection of duplicate samples. The results show that "duplicate" samples (i.e., two sidewall cores collected next to each other) do not always produce similar results. In MCOBT-4.4 and MCOBT-8.5, results show that small adjustments in the location of the sidewall sampler produced samples of different lithologies and with different pore water concentrations. This disparity is particularly apparent in the heterogenous interbeds between basalt flows and flow-base sediments. For example, the clay-rich matrix of a basalt interbed may be sampled by one core, while the adjacent "duplicate" sample may be core from a basalt clast. However, the approach of taking two samples, while of dubious use as true analytical duplicates, improves the chances of obtaining an adequate sample from small scale features such as interbeds. This testing verifies that the sidewall method can be used to sample interbed or flow-base material.

This initial test of sidewall coring leads to the following conclusions: (1) the sidewall approach can be used to target features such as interbeds to gather lithologic and mineralogic information and to possibly detect contaminants such as nitrate and perchlorate; and (2) drilling fluids impact the chemical results and small sample sizes reduce the overall quality of the data compared to standard sampling approaches (e.g., sampling from vertical core).

Sidewall sampling may be adequate when standard coring or water sampling cannot be performed. However, sidewall coring should be used only as a contingency in situations where stratigraphic or lithologic targets are well defined or where contaminants are expected or suspected. Though useful for geologic study and for initial contaminant characterization or screening, sidewall core data should not be viewed with the same level of confidence as data from standard coring or water sampling. At best, the

chemical data should be used to indicate possible contamination and not to derive a quantitative estimate of concentration.

Nitrogen-isotope results. Values for $\delta^{15}N_{AIR}$–NO_3 and their associated leachable nitrate concentrations are given for MCOBT-4.4 and MCOBT-8.5 in Table 11.1-3. Figure 11.1-10 shows the distribution of $\delta^{15}N_{AIR}$–NO_3 as a function of stratigraphic position in the two boreholes.

During a three-year period from October 1986 to September 1989, nitrate derived from nitric acid left over from the production of a pure ^{15}N tracer was released through the TA-50 outfall into Mortandad Canyon at LANL. From 1986 through 1989, the volume of isotopically light nitrate released from TA-50 was 70,000 gal. (Moss 2002, 73690). During this same period , the volume of effluent discharged from TA-50 was 11.2 million gal. The released nitrate had very negative $\delta^{15}N_{AIR}$–NO_3 ratios because it was strongly enriched in ^{14}N. The $\delta^{15}N_{AIR}$–NO_3 ratio of the isotopically light nitric acid (nitrate) is not known; however, if it was 100% pure nitrogen-14, the isotopic ratio could be –1000‰. The most negative $\delta^{15}N_{AIR}$–NO_3 ratio measured in pore water from core samples was –115.3‰ (Table 11.1-3).

Table 11.1-3
MCOBT-4.4 and 8.5 Nitrate and $\delta^{15}N_{AIR}$–NO_3

Mid depth (ft)	Unit	NO_3 as NO_3 (ppm)*	NO_3 as N (ppm)*	$\delta^{15}N_{AIR}$–NO_3	Note	Standard deviation
MCOBT-4.4						
3.4	Qal	13.7	3.09	–1.3	—	—
34.3	Qal	13.3	3.00	–92.4	dry rep	7.4
34.3	Qal	8.14	1.84	–102.9	wet rep	—
46.8	Qal	4.92	1.11	–1.3	—	—
49.3	Qal	3.81	0.86	–1.9	—	—
69.3	Qct	10.9	2.46	–52.1	—	—
89.3	Qct	14.1	3.18	–115.3	—	—
109.3	Qbo	12.8	2.89	–82.3	wet rep	0.7
109.3	Qbo	13.5	3.05	–81.3	wet rep	1.1
109.3	Qbo	16.3	3.68	–79.7	dry rep	—
131.8	Qbo	8.99	2.03	–27.0	—	—
MCOBT-8.5						
72.3	Qal	4.93	1.11	–59.8	wet rep	0.0
72.3	Qal	6.64	1.50	–59.8	dry rep	—
92.3	Qal	8.38	1.89	–2.1	—	—
114.2	Qbo	11.9	2.69	–77.6	wet rep	1.2
114.2	Qbo	11.8	2.66	–75.9	wet rep	—
151.7	Qbo	8.50	1.92	–5.7	—	—
171.7	Qbo	8.27	1.87	+6.4	—	
211.7	Qbo	7.20	1.63	+6.5	wet rep	2.0
211.7	Qbo	12.4	2.80	+3.7	dry rep	—
231.7	Qbo	5.36	1.21	+6.7	—	—
291.7	Qbo	4.48	1.01	+2.4	—	—

wet rep = sample splits prepared from moisture protected core.
dry rep = sample splits that were oven dried before leaching.
* Nitrate and N concentrations are leachate concentrations, not pore water concentrations, as shown in Tables 11.1-1 and 11.1-2.

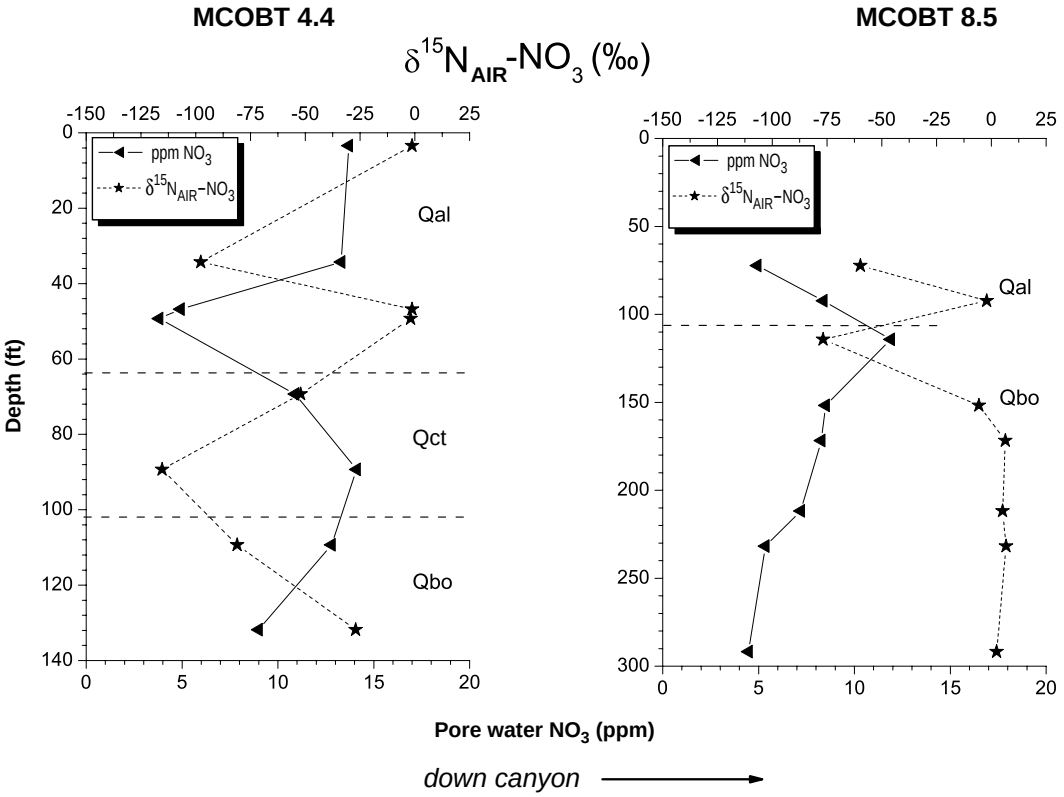

Figure 11.1-10. Pore water nitrate and $\delta^{15}N_{AIR}$–NO_3 for boreholes MCOBT-4.4 and MCOBT-8.5

The narrow timeframe of disposal and the negative $\delta^{15}N_{AIR}$–NO_3 ratios of the discarded solutions provide an ideal tracer to monitor subsurface nitrate transport downgradient of the outfall. Samples from the near-surface alluvium (>20 ft depth) from the MCOBT-4.4 core have $\delta^{15}N_{AIR}$–NO_3 values around 0‰, typical of atmospherically derived N and nitrate derived from dissociated nitric acid (Longmire 2002, 72800) (Table 11.1-3 and Figure 11.1-10). Below the near surface the very negative ratios from the 1986 to 1989 effluent releases can be seen. A general inverse relationship occurs between nitrate concentrations and $\delta^{15}N_{AIR}$–NO_3. The $\delta^{15}N_{AIR}$–NO_3 ratios for leachate with nitrate concentrations greater than 10 ppm are less than – 50‰ and are as low –115‰. These negative $\delta^{15}N_{AIR}$–NO_3 ratios are indicative of nitrate released during the 1986 to 1989 period.

Since 1986, isotopically light nitrate has migrated to a depth of 132 ft at MCOBT-4.4 and 152 ft at MCOBT-8.5 (see Figure 11.1-10). Vertical transport rates for these isotopically light nitrate fluids are calculated to be 8.2 ft/yr at MCOBT-4.4 and 9.5 ft/yr at MCOBT-8.5. The slightly higher infiltration rate calculated for MCOBT-8.5 is consistent with the distribution of nitrate at greater depths than at MCOBT-4.4. These calculated rates represent estimates for nitrate transport in the vadose zone based on core samples. Isotopically light nitrate is also found at a depth of 493 ft in the perched groundwater zone at MCOBT-4.4 (see Section 11.2.2). Since 1986, the vertical rate of migration of isotopically light nitrate to the perched zone is 30.8 ft/yr.

Overall, the nitrate concentrations in the MCOBT-8.5 core are lower than those observed in the MCOBT- 4.4 core. A few low $\delta^{15}N_{AIR}$–NO_3 ratios are observed in the lower Qal and upper Qbo, but for the most part $\delta^{15}N_{AIR}$–NO_3 ratios throughout the MCOBT-8.5 core are close to 0‰. These data suggest that much of the tracer-derived (isotopically light) nitrate has not migrated below 152 ft in the MCOBT-8.5 borehole.

Results from replicate and dried samples show good agreement for most replicates (Table 11.1-3). The variation for the replicate samples is less than 2‰. Results for the dry samples deviate as much as 7‰ for one pair, but most pairs agree within 2‰. Thus, drying does not appear to induce significant fractionation of the nitrogen isotopes.

Oxygen-hydrogen isotope results. The stable isotope profile from the MCOBT-4.4 core shows a large shift in the isotopic composition of pore fluids from high ratios (enrichment of δD and δ^{18}O) at the surface to lower ratios in the upper 30 ft of core (Figure 11.1-11a and Table 11.1-4). At depths below 30 ft, δD and δ^{18}O ratios increase to near those of the surface pore fluids. At about 40 to 50 ft, the stable isotope ratios decrease steadily with depth.

Table 11.1-4
MCOBT-4.4 and 8.5 δ^{18}O and δD Results

MCOBT-4.4

Mid depth (ft)	δ^{18}O (‰)	δD (‰)	Unit
3.4	–7.2	–68	Qal
9.0	–11.9	–93	Qal
13.7	–12.9	–96	Qal
18.4	–12.8	–96	Qal
24.1	–13.4	–91	Qal
28.9	–14.8	–108	Qal
34.1	–11.8	–82	Qal
39.1	–9.7	–64	Qal
46.6	–9.2	–64	Qal
49.1	–9.5	–67	Qal
89.1	–10.0	–74	Qct
109.1	–9.9	–74	Qbo
131.6	–9.7	–75	Qbo
149.1	–10.1	–79	Qbo
171.6	–12.7	–89	Qbo
189.1	–11.0	–84	Qbo
209.1	–11.5	–84	Qbo
229.1	–11.4	–81	Qbo
246.6	–11.6	–82	Qbo
271.6	–11.3	–83	Qbo
289.1	–11.5	–82	Qbo
309.1	–11.6	–86	Qbo

MCOBT-8.5

Mid depth (ft)	δ^{18}O (‰)	δD (‰)	Unit
3.4	–11.6	–89	Qal
8.3	–12.4	–95	Qal
14.1	–11.5	–100	Qal
21.6	–8.2	–82	Qal
26.6	–8.3	–86	Qal
31.6	–8.2	–80	Qal
36.1	–8.4	–85	Qal
41.6	–7.7	–79	Qal
46.6	–8.4	–80	Qal
51.3	–8.8	–80	Qal
56.6	–9.5	–87	Qal
71.6	–10.4	–82	Qal
91.6	–9.7	–77	Qal
131.6	–10.2	–73	Qbo
151.1	–10.1	–72	Qbo
171.6	–10.3	–73	Qbo
191.6	–10.5	–73	Qbo
211.6	–10.2	–71	Qbo
231.7	–12.1	–86	Qbo
251.6	–10.2	–70	Qbo
270.0	–10.2	–71	Qbo
291.5	–9.4	–69	Qbo
308.7	–10.1	–71	Qbo
328.6	–9.8	–73	Qbo
349.0	–9.8	–74	Qbo

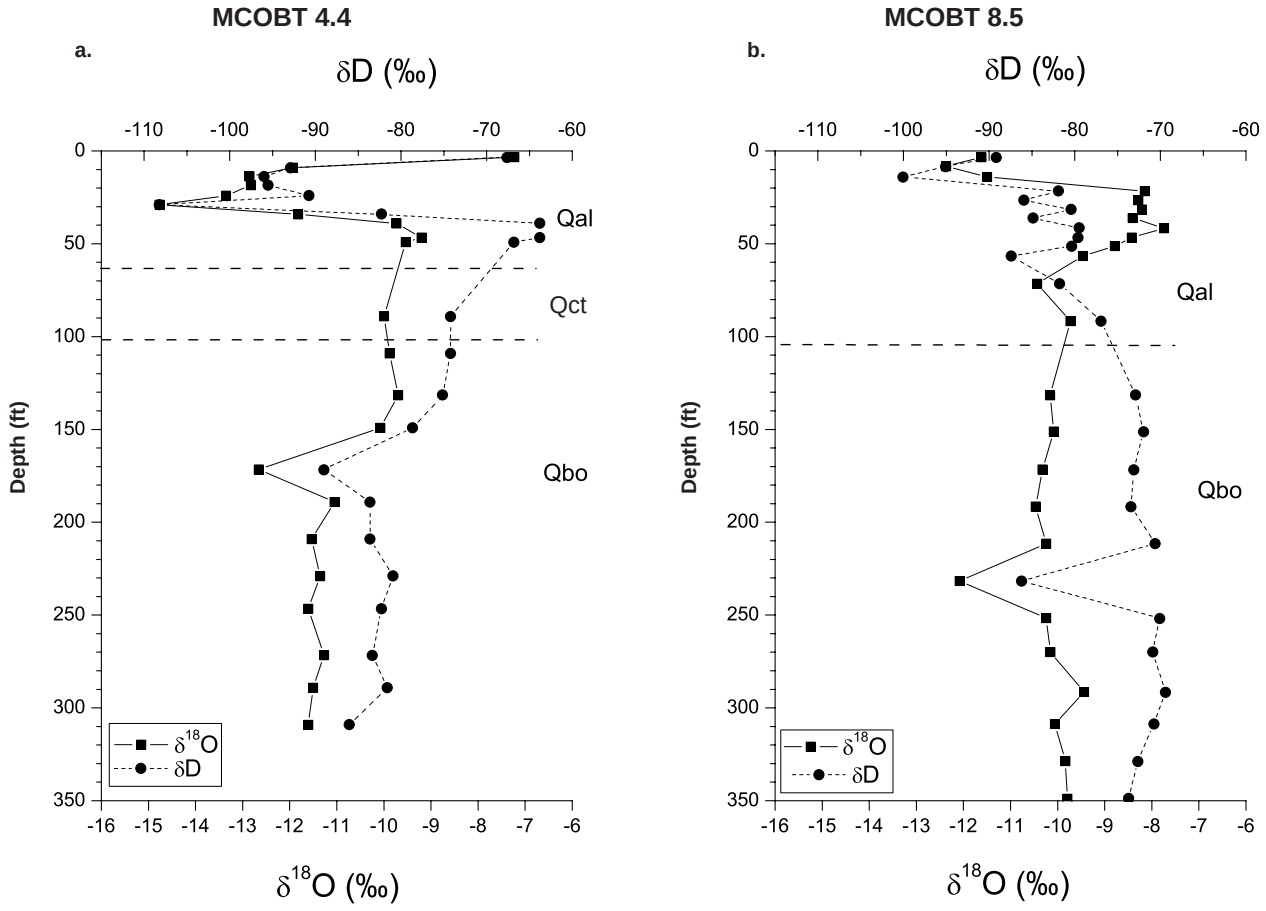

Figure 11.1-11. Stable oxygen and hydrogen isotopes for boreholes MCOBT-4.4 and MCOBT-8.5

The isotopic composition and depth relations for pore waters from the MCOBT-8.5 core are quite different than those observed for the MCOBT-4.4 core. The surface pore fluids have lighter $\delta^{18}O$ and δD ratios, and the isotopic compositions of the pore waters increase in the upper 30 ft of Qal (Figure 11b and Table 11.1-4). Ratios of $\delta^{18}O$ and δD fluctuate from 30 to 50 ft. With a few exceptions, δD ratios generally increase below 50 ft, reaching an approximate ratio of at –73‰ at depths below 130 ft. Below 50 ft, $\delta^{18}O$ ratios decline, and below 130 ft they stabilize at –10.2‰. Variations in the isotopic composition of pore waters at each borehole and differences between the boreholes probably reflect variations in the isotopic composition of the infiltrating surface waters in Mortandad Canyon.

A plot of pore water $\delta^{18}O$ versus δD shows that while some samples plot along or near the local meteoric water line, many samples fall to the right of the line (Figure 11.1-12). Most notable are the samples from the surface in both cores and from depths between 10 and 60 ft in the MCOBT-8.5 core. The relatively heavier $\delta^{18}O$ ratios from the MCOBT-8.5 core probably reflect infiltration of evaporated surface water. Waters present in Mortandad Canyon are derived from runoff, treated Laboratory effluent (consisting largely of municipal water), and native groundwater, all of which have different isotopic signatures.

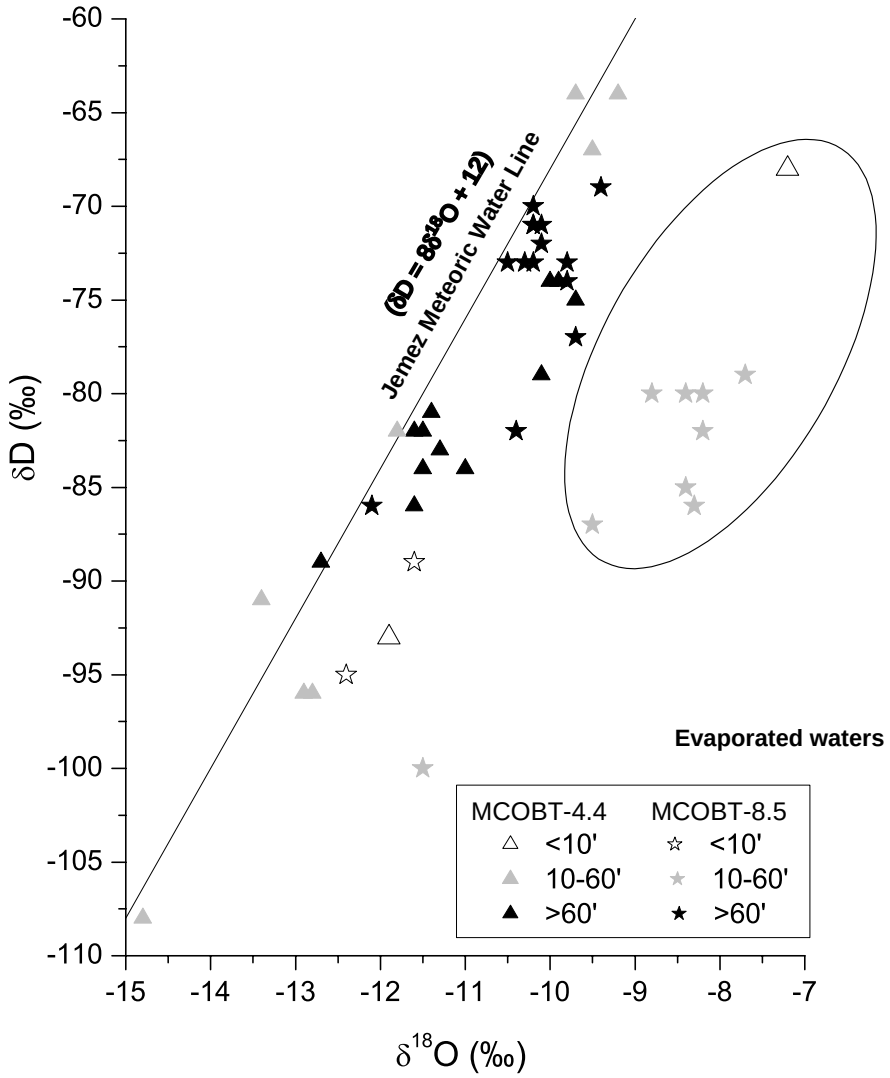

Figure 11.1-12. Stable oxygen and hydrogen isotopes for boreholes MCOBT-4.4 and MCOBT-8.5

11.2 Geochemistry of Perched Groundwater

At MCOBT-4.4, a suite of groundwater samples was collected on April 22, 2002, from the completed well approximately two months after well-development activities were completed. These samples were analyzed for radionuclides, anions including perchlorate, metals and trace elements, volatile organic compounds, and stable isotopes of hydrogen, nitrogen, and oxygen. The samples were collected primarily to determine if potential contaminants were present in the perched groundwater in Mortandad Canyon. Potential contaminants of concern include tritium, nitrate, fluoride, TDS, perchlorate, strontium-90, cesium-137, americium-241, and uranium and plutonium isotopes. The groundwater samples collected did not contain significant amounts of drilling fluids based on the low total organic carbon (TOC) concentrations (<1.0 mgC/L), and they were representative of native or pre-drilling groundwater. Analytical results for the suite of samples collected on April 22, 2002, indicate that groundwater in the perched zone at MCOBT-4.4 exceeds the US Environmental Protection Agency (EPA) primary standard for nitrate (10 mg/L) and the draft provisional risk-based level for perchlorate (0.001 mg/L, 1μg/L).

11.2.1 Methods

Groundwater samples were collected from well MCOBT-4.4 following development using a submersible pump (Grunfos™ Redi-Flo 3 SQE-NE, model number 5SQE10C-38ONE) with the pump intake set at 524 ft bgs. Temperature, dissolved oxygen, alkalinity, turbidity, pH, and specific conductance were determined on-site. Temperature, specific conductance, and pH were measured with an Orion meter (model 1230); turbidity was measured with a HACH® meter (model 53600-00). Both meters were calibrated daily using buffer solutions (pH 4.0 and 7.0) and known standards for turbidity. Dissolved oxygen was measured with a spectrophotometer (HACH® meter, model DR/2010) during pre-characterization sampling. Both filtered (radionuclides [excluding tritium], metals, trace elements, dissolved organic carbon [DOC], and major cations and anions) and nonfiltered (tritium, metals, trace elements, major cations, TOC, stable isotopes of hydrogen, nitrogen, and oxygen) samples were collected for chemical and radiochemical analyses. Aliquots of the samples were filtered through 0.45-µm Gelman filters. Samples were acidified with analytical-grade HNO_3 to a pH of 2.0 or less for radionuclide, metal, and major cation analyses. The samples collected in the field were stored at 4°C prior to analyses. Alkalinity was also determined in the laboratory using standard titration techniques. The reported alkalinity made in laboratory deviates from field alkalinity because of sample degassing.

Groundwater samples were analyzed using techniques specified in the EPA SW-846 manual. These include ion chromatography (IC) for bromide, chloride, fluoride, nitrate plus nitrite (as N), perchlorate, phosphate, and sulfate; ion selective electrode (ISE) for ammonium; total Kjeldahl nitrogen (TKN) by distillation; and cold vapor atomic absorption (CVAA) for mercury. Inductively coupled (argon) plasma optical emission spectroscopy (ICPOES) was the analytical method used for aluminum, arsenic, barium, boron, calcium, chromium, cobalt, copper, iron, magnesium, nickel, potassium, selenium, silver, sodium, strontium, vanadium, and zinc. Inductively coupled (argon) plasma mass spectrometry (ICPMS) was the analytical method used for antimony, beryllium, cadmium, lead, manganese, molybdenum, thallium, and uranium (nonisotopic). A contract laboratory, General Engineering Laboratories (GEL), performed this work.

Radionuclide activity in groundwater was determined by liquid scintillation for tritium; alpha spectrometry for americium-241, plutonium-238, plutonium-239,240, uranium-234, uranium-235, and uranium-238; gas proportional counting for strontium-90; and gamma spectrometry for cesium-137 and other gamma-emitting isotopes. Contract laboratories performing this work were GEL (radionuclides) and the University of Miami (tritium).

Stable isotopes of oxygen (oxygen-18 and oxygen-16, $\delta^{18}O$), and hydrogen (hydrogen and deuterium, δD), were analyzed by Geochron Laboratories (Cambridge, Massachusetts). Stable isotopes of nitrogen (nitrogen-15 and nitrogen-14, $\delta^{15}N_{AIR}$–NO_3) were analyzed by Coastal Science Laboratories, Inc. (Austin, Texas) using IRMS.

Laboratory blanks were collected and analyzed in accordance with EPA and LANL procedures. The precision limits (analytical error) for major ions and trace elements were generally ±10%.

11.2.2 Results of Geochemical Analysis of Perched Groundwater Samples at MCOBT-4.4

Field parameters, including pH, temperature, dissolved oxygen, turbidity, alkalinity, and specific conductance, measured at MCOBT-4.4 are provided in Table 11.2-1. Analytical results for the groundwater samples collected from MCOBT-4.4 are provided in Tables 11.2-2a and 11.2-2b. Perched groundwater is oxidizing based on measurable dissolved oxygen (9.2 mg/L). Turbidity is less than 5 NTU, which suggests that the well was satisfactorily developed after drilling. Carbonate alkalinity was measured in the field, and pH was buffered by bicarbonate and partial pressure of carbon dioxide gas in the perched zone. Groundwater samples were clear and no odors of sulfide and petroleum were detected during sampling.

Table 11.2-1
Field Parameters Measured for Perched Groundwater Sample Collected at MCOBT-4.4

Depth (ft)	**524**
Geologic Unit	**Puye Formation/Cerros del Rio Basalt**
Date Sampled	**04/20/02**
pH	7.52
Temperature (°C)	19.2
Specific Conductance (μS/cm) [a]	327
Turbidity (NTU)	0.34
Dissolved Oxygen (mg/L)	9.2
Field Alkalinity (mg $CaCO_3$/L)	41.0

[a] μS/cm means microsiemens per centimeter

Table 11.2-2a
Hydrochemistry of Perched Groundwater Samples at MCOBT-4.4
(Filtered and Nonfiltered Samples)

Depth (ft)	**524**	**524**
Preparation	**Filtered**	**Nonfiltered**
Geologic Unit	**Puye Formation/ Cerros del Rio Basalt**	**Puye Formation/ Cerros del Rio Basalt**
Date Sampled	**04/22/02**	**04/22/02**
Alkalinity (Lab) (mg $CaCO_3$/L)	41.2	Not analyzed
Al (mg/L)	[0.034], U	[0.034], U
NH_4 (as N) (mg/L)	[0.02], U	Not analyzed
Sb (mg/L)	0.00014	0.00017
As (mg/L)	[0.0046], U	[0.0046], U
Ba (mg/L)	0.013	0.013
Be (mg/L)	[0.000034], U	[0.000034], U
B (mg/L)	0.017	0.018
Br (mg/L)	[0.02], U	Not analyzed
Cd (mg/L)	[0.00005], U	[0.00005], U
Ca (mg/L)	31.9	32.0
ClO_4 (mg/L)	0.142	Not analyzed
Cl (mg/L)	17.3	Not analyzed
Cr (mg/L)	0.053	0.054
Co (mg/L)	[0.00029], U	[0.00029], U
Cu (mg/L)	[0.0027], U	[0.0027], U
F (mg/L)	0.42	Not analyzed
Fe (mg/L)	[0.021], U	[0.021], U
Pb (mg/L)	0.00008	0.00009
Mg(mg/L)	5.40	5.42

Table 11.2-2a (continued)

Depth (ft)	524	524
Preparation	**Filtered**	**Nonfiltered**
Geologic Unit	**Puye Formation/ Cerros del Rio Basalt**	**Puye Formation/ Cerros del Rio Basalt**
Date Sampled	**04/22/02**	**04/22/02**
Mn (mg/L)	0.0026	0.0025
Hg (mg/L)	[0.000073], U	[0.000073], U
Ni (mg/L)	0.0032	0.0028
NO_3 + NO_2 (as N) (mg/L)	13.2	Not analyzed
P total (mg/L)	0.03	Not analyzed
K (mg/L)	0.63	0.64
Se (mg/L)	[0.0031], U	[0.0031], U
Ag (mg/L)	[0.00020], U	[0.00020], U
Na (mg/L)	20.5	20.6
Sr (mg/L)	0.153	0.154
SO_4 (mg/L)	27.5	Not analyzed
TKN (mg/L)	0.24	Not analyzed
Tl (mg/L)	0.00002	0.00003
U (mg/L)	0.000281	0.000285
DOC (mgC/L)	0.68	Not applicable
V (mg/L)	[0.0011], U	[0.0011], U
Zn (mg/L)	[0.0032], U	[0.0028], U
TDS (mg/L)	167.6	Not applicable
MEQ cations	2.945	Not applicable
MEQ anions	2.843	Not applicable
Charge balance	+1.77	Not applicable

Note: U = not detected. Total dissolved solids (TDS) were calculated. MEQ means milliequivalents.

Table 11.2-2b
Hydrochemistry of Perched Groundwater Samples at MCOBT-4.4

Depth (ft)	524
Geologic Unit	**Puye Formation/Cerros del Rio Basalt**
Date Sampled	**04/22/02**
Tritium (pCi/L), NF	12,797±1,368 (3σ)
Am-241 (pCi/L), F	[0.0255±0.0258 (3σ)]; U, RL, 0.020; DL, 0.00767
Cs-137 (pCi/L), F	[–0.13], U
Co-60 (pCi/L), F	[–0.38], U
Eu-152 (pCi/L), F	[0.77], U
Gross α (pCi/L), F	[–0.96], U
Gross β (pCi/L), F	[1.91], U
Gross γ (pCi/L), F	42.7

Table 11.2-2b (continued)

Pu-238 (pCi/L), F	[–0.006], U
Pu-239,240 (pCi/L), F	[0.005], U
Sr-90 (pCi/L), F	[0.032], U
U-234 (pCi/L), F	0.253±0.087 (3σ); RL, 0.089; DL, 0.020
U-235 (pCi/L), F	[0.0697±0.0702 (3σ)], U; RL, 0.0466; DL, 0.005
U-238 (pCi/L), F	0.158±0.108 (3σ); RL, 0.0586; DL, 0.020
TOC (mgC/L), NF	0.80
δD (‰), NF	–75
$\delta^{15}N_{AIR}$–NO_3 (‰), NF	–3.1, –2.7
$\delta^{18}O$ (‰), NF	–10.8

Note: F = filtered. NF = nonfiltered. U = not detected. ‰ means permil. RL = reporting limit. DL = detection limit.

The filtered groundwater samples collected from within the perched zone at MCOBT-4.4 are characterized by a mixed (calcium-sodium-nitrate-sulfate-bicarbonate) ionic composition (Table 11.2-2a and Figure 11.2-1). Concentrations of major ions are less in MCOBT-4.4 than in alluvial wells MCO-3, MCO-5, MCO-6, and MCO-7 (Figure 11.2-1). Solutes migrating through the vadose zone are probably being diluted in the perched zone by native groundwater.

Concentrations of nitrate plus nitrite (as N), perchlorate, sulfate, fluoride, and chloride in the perched zone at MCOBT-4.4 were 13.2, 0.142 (142 μg/L), 27.5, 0.42, and 17.3 mg/L, respectively. Concentrations of nitrate exceed the EPA primary standard for nitrate (10 mg/L), and perchlorate exceeds the draft provisional risk-based level for perchlorate (0.001 mg/L, 1μg/L). Sulfate, fluoride, and chloride do not exceed New Mexico Water Quality Control Commission (NMWQCC) and EPA standards.

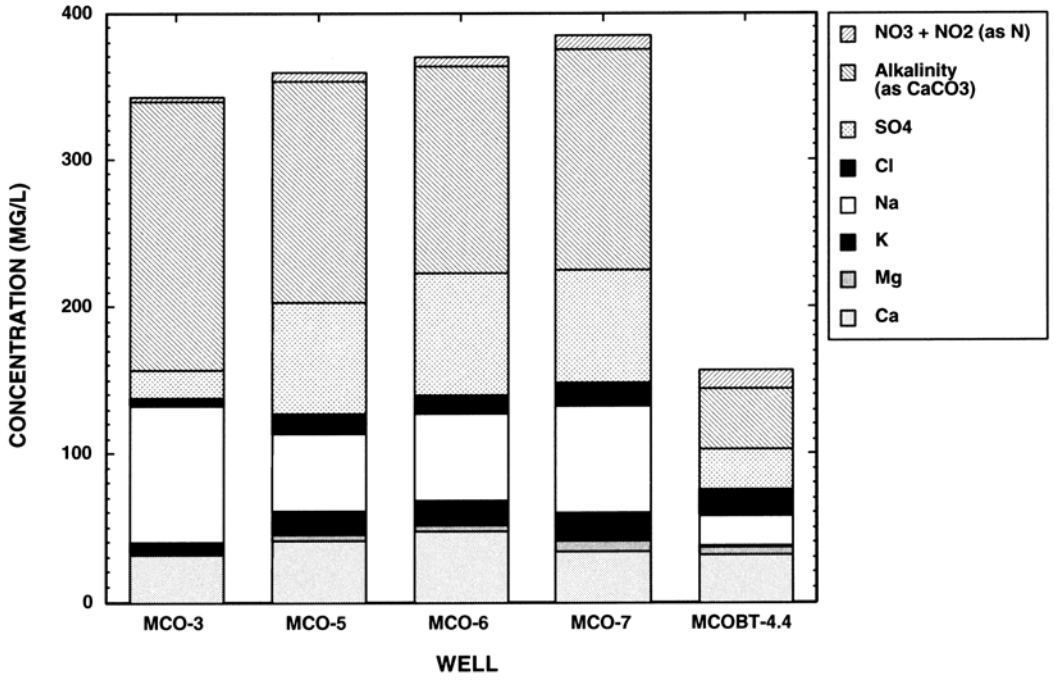

Figure 11.2-1. Distribution of major ions in alluvial wells MCO-3, MCO-5, MCO-6, and MCO-7 and intermediate-depth well MCOBT-4.4 in Mortandad Canyon

Elevated occurrences of nitrate plus nitrite (as N), perchlorate, chloride, fluoride, and sulfate in MCOBT-4.4 suggest that recharge from alluvial groundwater has impacted groundwater in the perched zone. For example, average dissolved concentrations of perchlorate and nitrate plus nitrite (as N) observed in alluvial monitoring wells (MCO-3, MCO-5, MCO-6, MCO-7, MCO-7.5) are 0.235 (235 μg/L) and 8.40 mg/L, respectively, during 2000 (ESP 2001, 71301). Most likely though, concentrations of contaminants measured in the perched zone reflect past releases from TA-50 that generally had higher concentrations of solutes. For example, from 1964 to 1995 the average concentration of nitrate (as N) was 37.2 mg/L (32 values) for MCO-7 and was 41.7 mg/L (31 values) for MCO-7.5. Although the chemistry and radiochemistry of the TA-50 discharge has varied since 1963 (LANL 1997, 56835), the alluvial groundwater is probably well mixed along the groundwater flow path with respect to conservative or nonadsorbing solutes.

The average residence time of alluvial groundwater in Mortandad Canyon is probably on the order of several years (Purtymun 1974, 5476; Purtymun et al.1977, 11846; and Purtymun et al. 1983, 6407). More recent data show that nitrate and perchlorate continue to occur in alluvial groundwaters, even though concentrations of these two solutes have greatly decreased in the past several years. However, Purtymun showed that most of the mass of the nonsorbing solutes is not accumulating in the alluvial groundwater, thus implying that these solutes infiltrated the vadose zone and deeper perched groundwater.

Nitrate, nitrite, and perchlorate are likely to persist in the subsurface of Mortandad Canyon. Nitrate, nitrite, and perchlorate are stable as anions under oxidizing conditions, and they are mobile in groundwater with minimal adsorption occurring on aquifer material (Longmire 2002, 72614). Reduction of nitrate to nitrogen gas and perchlorate to chloride occurs under anaerobic conditions in the presence of anaerobic bacteria and electron donors, including reactive organic carbon (for example, acetate) and dissolved sulfide. Such electron donors are probably absent in Mortandad Canyon because alluvial and perched groundwater is oxidizing based on measurable dissolved oxygen (>1 mg/L), nitrate plus nitrite, and sulfate and absence of dissolved sulfide, methane, and elevated concentrations of iron and manganese.

A number of geochemical parameters suggest that the perched zone is characterized by aerobic conditions. Measured concentrations of dissolved oxygen were 9.2 mg/L, although this measurement is possibly influenced by well construction and sampling conditions (see Section 10.1). If atmospheric oxygen is present in the groundwater sample, true in situ readings of dissolved oxygen would be difficult to obtain. Under relatively oxidizing conditions, iron and manganese precipitate from solution, forming moderately insoluble (oxy)hydroxide phases. Concentrations of iron and manganese in the perched zone are less than the detection limit (0.02 mg/L and 0.003 mg/L, respectively, Table 11.2-2a). Absence of both ammonium and elevated TOC also suggest that the perched groundwater is oxidizing.

Based on the distribution of perchlorate (and nitrate) in pore waters extracted from core samples (see Section 11.1.2), it is unlikely that the contaminants found in the perched zone at MCOBT-4.4 were the result of vertical recharge. The perched groundwater has higher concentrations of perchlorate (0.142 mg/L) and nitrate plus nitrite (13.2 as N) (see Table 11.2-2a) than pore water in core samples between 205 and 493 ft (Figures 11.1-4 and 11.1-6). A decreasing hydraulic gradient to the east in the alluvial groundwater system would mean that the major source of recharge to the perched zone encountered at MCOBT-4.4 probably occurs from the west.

Concentrations of aluminum, arsenic, beryllium, cadmium, cobalt, copper, mercury, selenium, silver, vanadium, and zinc are less than method detection limits ([MDL] ICPMS and ICPOES) in the groundwater samples collected from the perched zone at MCOBT-4.4 (Table 11.2-2a). Total and dissolved concentrations of strontium are 0.154 and 0.153 mg/L, respectively, suggesting that strontium occurs as a solute (Sr^{2+}) rather than as a trace element associated with suspended material. Concentrations of total and dissolved uranium are 0.000285 (0.285 μg/L) and 0.000281 mg/L (0.281 μg/L), respectively, within the

perched zone (Table 12.2-2a). This finding suggests that most of the uranium occurs in the dissolved fraction in MCOBT-4.4.

Activities of tritium observed in MCOBT-4.4 are 12,797±1,368 pCi/L (3σ error) (Table 11.2-2b). The probable source of tritium is Laboratory discharges at TA-50. Tritium activities for TA-50 effluent discharges have decreased over time; these changes in the source term are reflected in lower activities for tritium in more recent Mortandad Canyon alluvial groundwater. Between 1972 and 1995, average tritium activities in alluvial groundwater were 224,000 pCi/L (Rogers 1998, 59169). Activities of tritium observed in MCO-3, MCO-5, MCO-6, MCO-7, and MCO-7.5 during 2000 ranged from 6686 to 76,300 pCi/L, with the highest activity occurring at MCO-3 (ESP 2001, 71301).

Activities of americium-241, cesium-137, plutonium-238, plutonium-239,240, strontium-90, and uranium-235 were less than detection in groundwater samples collected from MCOBT-4.4 (Table 11.2-2b). The nondetected activity reported for americium-241 was 0.0255±0.0258 (3σ error) pCi/L with a detection limit (DL) and reporting limit (RL) of 0.00767 and 0.020 pCi/L, respectively (Table 12.2-2b). Additional characterization sampling for americium-241 has been planned for well MCOBT-4.4.

Activities of uranium-234, uranium-235 (nondetect), and uranium-238 in groundwater samples collected from MCOBT-4.4 were 0.253, 0.0697±0.0702 (3σ), and 0.158 pCi/L, respectively (Table 11.2-2b), using alpha spectrometry. Additional analyses of uranium are recommended during characterization sampling of MCOBT-4.4 to further evaluate the isotopic nature of uranium observed at this well. Activities of uranium-238 and uranium-234 at MCOBT-4.4 were within the distribution of uranium observed in supply well PM-5 (≤ 0.3 pCi/L) during 2000 (ESP 2001, 71301).

Activities of gross alpha and beta were less than detection, whereas gross gamma activity was 42.7 pCi/L (Table 11.2-2b). Measurable gross gamma activity results from the presence of gamma-emitting isotopes within the U-238 and U-235 decay chains. These include Pa-234, Rn-222, Po-218, Bi-214, Po-214, Bi-210, and Po-210 for the U-238 decay series and U-235, Pa-231, Th-227, Ra-223, Rn-219, Po-215, Tl-207, Po-214, and Pb-207 for the U-235 decay series.

Concentrations of DOC and TOC were 0.68 and 0.80 mgC/L (Table 11.2-2a), respectively, suggesting the general absence of residual drilling fluids during the time of sampling. Acetone is detected, however, at a concentration of 5.3 μg/L. The laboratory blank associated with this sample did not contain any volatile organic compounds. The presence of acetone is probably a false positive from isopropyl alcohol present in residual amounts of QUIKFOAM® that was used during drilling (Longmire 2002, 73282). No other volatile organic compounds have been detected at MCOBT-4.4.

Ratios of δD and $\delta^{18}O$ measured in groundwater samples collected from MCOBT-4.4 were –75 and –10.8‰, respectively, suggesting that the perched groundwater is derived from a meteoric (atmospheric) source and evaporation has not taken place to a significant extent. The equation for the Jemez Mountains meteoric line (JMML) (Blake et al. 1995, 49931) is given by the following expression:

$$\delta D = 8\delta^{18}O + 12.$$

Measured ratios for δD and $\delta^{18}O$ plot slightly above the JMML with analytical errors for δD and $\delta^{18}O$ of ± 4 and 0.2‰, respectively. Isotopic ratios for δD and $\delta^{18}O$ measured at MCOBT-4.4 are similar to those measured in regional aquifer at well R-15 (Longmire 2002, 72614).

Nitrogen isotopes provide a useful tool for distinguishing different sources of nitrate and other nitrogen species found in the unsaturated zone and groundwater at the Laboratory. The dominant source of nitrate discharged from TA-50 is from dissociated nitric acid. Nitric acid is produced by first reacting nitrogen gas

with hydrogen gas to produce ammonia gas and then reacting ammonia gas with oxygen gas. Ammonia is oxidized to nitrate through a series of reactions involving nitrous oxide, nitric oxide, and nitric dioxide, which eventually form nitric acid. Ammonia gas has a $\delta^{15}N_{AIR}$–NO_3 ratio of 0‰ because the nitrogen is derived from the atmosphere. The standard for $\delta^{15}N_{AIR}$–NO_3 also is 0‰ based on atmospheric nitrogen (Clark and Fritz 1997, 59168). Nitrate derived from nonfractionated nitric acid has a $\delta^{15}N_{AIR}$–NO_3 ratio of 0‰ or slightly higher (<+3‰).

During 1997, the treated effluent from TA-50 was characterized by an average $\delta^{15}N_{AIR}$–NO_3 ratio of +2.1‰ (n = 2) and nitrate (5.7 mg/L as N) derived from a diluted nitric acid standard had a $\delta^{15}N_{AIR}$–NO_3 ratio of +1.0‰ (n = 4) (Broxton et al. 2001, 71252). The nitrogen isotope signature of the TA-50 effluent is not generally expected to deviate, except during the period from 1986 through 1989, because nitrate is dominantly derived from dissociated nitric acid with a low $\delta^{15}N_{AIR}$–NO_3 ratio (0 ≤ +3‰). Isotopically light nitrate (nitrogen-14 enriched), however, was discharged to Mortandad Canyon from 1986 to 1989 (Moss 2002, 73690) and the residual footprint of this very unique nitrate was recently observed in alluvial groundwater (Kendrick 1999, 66141). (For additional for information about light nitrogen releases from 1986 to 1989, see Section 11.1.2, “Nitrogen-isotope results.”)

Isotopically light nitrate provides a useful tracer for quantifying water movement in the subsurface beneath Mortandad Canyon. Duplicate analyses of $\delta^{15}N_{AIR}$–NO_3 were performed on a groundwater sample collected from MCOBT-4.4, and the results were –3.1 and –2.7‰ (average of –2.9‰). Dissolved concentrations of nitrate plus nitrite (as N) observed in perched groundwater at MCOBT-4.4 were 13.2 mg/L. All eleven $\delta^{15}N_{AIR}$–NO_3 ratios from core samples were negative, ranging from –115.3 to –1.3‰ (Table 11.1-3). The majority of the nitrate consisting of isotopically light $\delta^{15}N_{AIR}$-NO_3 occurs within the unsaturated zone above the perched groundwater at MCOBT-4.4 (Table 11.1-3). These light isotopic ratios suggest that nitrate plus nitrite (as N) was derived from an abiotic source that includes a component of nitrogen-14-enriched nitrate. Mixing of isotopically light nitrate with isotopically heavier nitrate (nitrogen-15 enriched) derived from dissociated nitric acid has probably occurred in the subsurface of Mortandad Canyon. This mixing has resulted in heavier $\delta^{15}N_{AIR}$–NO_3 ratios observed in the perched zone as compared to the overlying vadose zone (Table 11.1-3).

Mixing of nitrate plumes characterized by different $\delta^{15}N_{AIR}$–NO_3 ratios has taken place within the surface water, shallow groundwater, perched groundwater, and vadose zone beneath Mortandad Canyon. This observation is based on significant variation in $\delta^{15}N_{AIR}$–NO_3 ratios presented in Tables 11.1-3 and 11.2-2b. The following discussion focuses on quantifying the TA-50 isotopic signature that has resulted from the mixing of two isotopically distinct forms of nitrate derived from nitric acid. The mixing equation modified from Clark and Fritz (1997, 59168) is

$$\delta^{15}N_{TA\text{-}50} = X\delta^{15}N_A + (1–X)\delta^{15}N_B,$$

where

$X\delta^{15}N_A$ is the isotopic ratio of nitrogen in water A multiplied by fraction “X,”

$(1\text{-}X)\delta^{15}N_B$ is the isotopic ratio of nitrogen in water B multiplied by fraction “1–X,” and

$\delta^{15}N_{TA\text{-}50}$ is the isotopic ratio of the nitrogen in the composite TA-50 effluent produced by mixing of fractions “X” and “1–X.”

Two calculations are presented below estimating the $\delta^{15}N_{TA-50}$ ratio. These consider the following:

- Two types of concentrations of nitric acid with two distinct concentrations and isotopic ratios were discharged from TA-50 from 1986 through 1989; and
- different concentrations of nitric acid with two distinct isotopic ratios were discharged from TA-50 from 1964 through 2001, including the unique isotopically light nitrate discharged from 1986 through 1989.

Calculation 1:

From October 1986 through November 1989, the volume of isotopically light nitrate was 70,000 gal. (Moss 2002, 73690), and the total volume of TA-50 effluent was 28,736,842 gal. (LANL 1997, 56835). The $\delta^{15}N_{AIR}$–NO_3 ratio of the isotopically light nitrate is not known. The mass of isotopically light nitrate is calculated to be 28,116 kg based on 70,000 gal. of 7.5 normal (N) nitric acid (Moss 2002, 73690). During this period, the isotopically light nitrate represents the fraction denoted by "X" and has a value of 0.59137. The first assumption is that the total volume of TA-50 effluent from 1986 through 1989 has a $\delta^{15}N_B$ ratio of +1‰. Ratios of $\delta^{15}N$ between 1 and 3‰ were measured from TA-50 effluent and nitrate from nitric acid (Broxton et al. 2001, 71252). This fraction is denoted by "1–X," having a value of 0.40863 and consisting of 47,544 kg nitrate. The second assumption is that the isotopically light nitrate was characterized by a $\delta^{15}N_{AIR}$–NO_3 ratio of –1000‰ ($\delta^{15}N_A$), which is 100% pure nitrogen-14. This limiting value is a bounding case, representing the limit of depleted (negative) nitrogen isotope ratio that might have entered Mortandad Canyon from 1986 to 1989. The TA-50 effluent is the dominant source of nitrate entering Mortandad Canyon, although other sources of water, including runoff and cooling water, probably contribute a small amount of nitrate and other solutes in the canyon. The nitrogen contribution of these other sources is negligible and does not significantly affect the calculated nitrogen isotope ratio for the TA-50 effluent.

Solving for $\delta^{15}N_{TA-50}$,

$$\delta^{15}N_{TA-50} = (0.59137)(-1000‰) + (1-0.59137)(+1‰),$$

$$\delta^{15}N_{TA-50} = -591‰.$$

This calculated $\delta^{15}N_{AIR}$–NO_3 ratio possibly represents a lower extreme for the lightest nitrate associated with TA-50 effluent discharged between 1986 and 1989.

Calculation 2:

From the previous calculation, the mass of isotopically light nitrate released to Mortandad Canyon during the period from October 1986 through November 1989 was 28,116 kg. The contribution of this isotopically light nitrate to the total nitrate released from TA-50 for the period from 1964 through 2001 represents the fraction (0.14241) denoted by "X." The first assumption is that 7.5 N nitric acid consists of a $\delta^{15}N_B$ ratio of +1‰ that is denoted by "1–X" (0.85759). From 1964 through 2001, the total mass of nitrate discharged from TA-50 was 197,431 kg. The second assumption is that the isotopically light nitrate was characterized by a $\delta^{15}N_{AIR}$–O_3 ratio of –1000‰ ($\delta^{15}N_A$), which is 100% pure nitrogen-14. The TA-50 effluent is the dominant source of nitrate entering Mortandad Canyon, although other sources of water, including runoff and cooling water, may also contribute a small amount of nitrate and other solutes to the canyon.

Solving for $\delta^{15}N_{TA-50}$,

$\delta^{15}N_{TA-50} = (0.14241)(-1000‰) + (1-0.14241)(+1‰)$,

$\delta^{15}N_{TA-50} = -142‰$.

The calculated $\delta^{15}N_{AIR}$–NO_3 ratio for the mixture is lighter than those values measured in the unsaturated zone at MCOBT-4.4 and MCOBT-8.5 (Table 11.1-3). Mixing of isotopically heavier nitrate with lighter nitrate at various concentrations will produce less negative $\delta^{15}N_{AIR}$–NO_3 ratios, similar to those observed in the unsaturated zone (Table 11.1-3) and the perched zone (Table11.2-2b).

These two calculations provide lower bound-end members for estimating the isotopic ratio of mixed nitrate sources if the unknown $\delta^{15}N_{AIR}$–NO_3 ratio of the isotopically light nitrate was –1000‰, and both assume complete mixing of the source waters. These calculations would result in heavier $\delta^{15}N_{AIR}$–NO_3 ratios if the (unknown) isotopically light nitrate were assumed to be heavier. Variations of $\delta^{15}N_{AIR}$–NO_3 ratios observed for core samples collected from the vadose zone could be produced by mixing different volumes and concentrations of isotopically distinct nitrate and from incomplete mixing of the effluent water. These calculations also assume that evaporation and denitrification have not affected the $\delta^{15}N_{AIR}$–NO_3 ratios.

Finally, these calculations provide a basis for evaluating the range of observed nitrogen isotope ratios in vadose zone samples, including those as light as –115‰ up to values of –3‰ or +1‰. Nonuniform mixing of nitrogen over time in the groundwater and vadose zone likely led to a range of values for the nitrogen isotope ratio in groundwater.

The presence of isotopically light nitrate in the perched zone at MCOBT-4.4 suggests that surface water has migrated to a depth of 493 ft since 1986, the time of initial discharge of isotopically light nitrate from TA-50. Based on the nitrogen isotopic ratio values found in the perched zone in 2002, an estimated transport velocity for nitrate is 30.8 ft/yr, assuming no dispersion. A transport velocity for tritium (without dispersion) is 12.6 ft/yr, assuming that tritium was initially discharged to Mortandad Canyon in 1963. Additional investigations of the unsaturated zone in Mortandad Canyon should refine these estimates of water movement.

Vertical migration of isotopically light nitrate is expected to continue in Mortandad Canyon. Elevated concentrations of nitrate plus nitrite (as N), ranging from 2.20 to 2.40 mg/L, with $\delta^{15}N_{AIR}$–NO_3 ratios ranging from –0.8 to +1.3‰, have been observed at the regional water table at well R-15 (Longmire 2002, 72614). The isotopically heavier nitrate observed at well R-15 probably represents older nitrate discharged in Mortandad Canyon prior to 1986. Typical concentrations of nitrate plus nitrite (as N) observed in supply wells during 2000 ranged from 0.35 to 0.59 mg/L (ESP 2001, 71301).

Based on observed negative $\delta^{15}N_{AIR}$–NO_3 ratios, it would appear that denitrification is not occurring to a significant extent in either the vadose zone above the perched zone or within the perched zone at MCOBT-4.4. Denitrification produces positive $\delta^{15}N_{AIR}$–NO_3 ratios (+3 to > +30 ‰) because nitrogen-14 is consumed by catabolic organisms resulting in enriched nitrogen-15 in solid waste (manure) (Clark and Fritz 1997, 59168).

11.3 Groundwater Geochemical Calculations

11.3.1 Computer Program Selection

Geochemical calculations of groundwater samples collected from well MCOBT-4.4 were conducted to evaluate speciation of solutes (dissolved species) and to quantify the state of saturation of solid phases

that control groundwater composition under equilibrium conditions. These calculations provide insight into processes that control water/rock interactions, including mineral precipitation and adsorption occurring in both natural and contaminated water. Geochemical calculations of water were conducted to evaluate geochemical processes influencing natural water composition and contaminant chemistry and transport.

Calculations of solute speciation, PCO_2 gas, and solid-phase saturation indices were made using the computer program MINTEQA2 (Allison et al. 1991, 49930), with single-ion activity coefficients calculated using the Davies equation. MINTEQA2 was developed by Battelle Northwest for the EPA for use at Resource Conservation and Recovery Act (RCRA) and Superfund sites. The model is constrained by solute concentrations and involves silicate, glass, and clay minerals at well MCOBT-4.4. MINTEQA2 quantifies possible rock/water and water/atmosphere reactions, but modeling results should be interpreted with caution and are limited by the scope of our understanding of hydrologic flow conditions (saturated and unsaturated), possible reaction mechanisms, and kinetic constraints in a disequilibrium-dominated system. One source of error in using the computer program is the accuracy of the chemical thermodynamic data contained in the database. Errors are greater for trace solutes for which experimental data are inaccurate and/or incomplete, including thallium, beryllium, and cadmium. The uranium database contained in MINTEQA2 has been critically evaluated by Grenthe et al. (1992, 71511). Fewer errors are associated with the major ions and with solid phases consisting of carbonate, silicate, and ferric oxyhydroxide minerals (Langmuir 1997, 56037).

11.3.2 Speciation Calculations

Speciation calculations using the computer program MINTEQA2 (Allison et al. 1991, 49930) were performed to evaluate stable forms of dissolved solutes, which influence mineral precipitation and adsorption reactions occurring in natural and contaminated waters. Fate and transport of uranium, chromium, and strontium observed at well MCOBT-4.4 are controlled by both aqueous speciation and adsorption/desorption processes. The input file for the calculations is provided in Appendix K.

Solutes of importance at well MCOBT-4.4 included major ions, nitrate, perchlorate, fluoride, uranium, and tritium. Results of the speciation calculations are provided in Table 11.3-1. Dissolved calcium, sodium, magnesium, and potassium are calculated to be dominantly stable as free or noncomplexed solutes (not provided in Table 11.3-1). Dissolved nitrate, chloride, and fluoride are calculated to be stable as noncomplexed anions. Sulfate is calculated to be dominantly stable as the noncomplexed anion with minor amounts of $MgSO_4^0$ (1.9%) and $CaSO_4^0$ (7.7%). Chromium(VI) is calculated to be stable as CrO_4^{2-} and $HCrO_4^-$ and Cr(III) is stable as $Cr(OH)_2^+$ and $Cr(OH)_3^0$ with a total dissolved chromium concentration of 0.053 mg/L (53 μg/L) (Table 11.2-2a). The dissolved concentration of uranium was 0.00028 mg/L (0.28 μg/L) (Table 11.2-2a). Dissolved uranium [(U(VI)] is calculated to be stable as uranyl carbonato, uranyl phosphato, and uranyl hydroxo complexes ($UO_2CO_3^0$, $UO_2(CO_3)_2^{2-}$, $UO_2(CO_3)_3^{4-}$, $UO_2(OH)_2^0$, $UO_2(OH)_3^-$, and $UO_2PO_4^-$) under oxidizing conditions that are characteristic of the perched zone. Oxidizing conditions are indicated by low concentrations of DOC, iron, and manganese, the presence of nitrate and sulfate, and measurable dissolved oxygen. Uranyl carbonato complexes are poorly to semisorbing onto hydrous ferric oxide between a pH range of 5.0 and 7.0, depending upon carbonate concentration (Langmuir 1997, 56037).

Results of speciation calculations showed that chromium(VI) species were stable as chromate and bichromate and nitrate, fluoride, and chloride were stable as non complexed solutes.

Table 11.3-1
Results of Speciation Calculations Using MINTEQA2 for Well MCOBT-4.4 (493 ft), Mortandad Canyon

Solute	Dominant Speciation	Percentage
Cr(VI)	CrO_4^{2-}	92.6
Cr(VI)	$HCrO_4^-$	7.1
Cr(III)	$Cr(OH)_2^+$	30.2
Cr(III)	$Cr(OH)_3^0$	69.2
U(VI)	$UO_2CO_3^0$	6.6
U(VI)	$UO_2(CO_3)_2^{2-}$	65.5
U(VI)	$UO_2(CO_3)_3^{4-}$	9.2
U(VI)	$UO_2(OH)_2^0$	14.9
U(VI)	$UO_2(OH)_3^-$	1.2
U(VI)	$UO_2PO_4^-$	2.2
Sr(II)	Sr^{2+}	96.6
Sr(II)	$SrSO_4^0$	2.9

11.3.3 Saturation Index Calculations

Solid-solution phase calculations were performed with MINTEQA2 (Allison et al. 1991, 49930) using analytical results obtained from filtered (less than 0.45 µm membrane) groundwater samples collected from MCOBT-4.4. The saturation index (SI) is a measure of the degree of saturation, undersaturation, or oversaturation of a solid phase in water (SI = $\log_{10}$ {activity product/solubility product}; at equilibrium SI = 0 ± 0.05) (Langmuir 1997, 56037). These calculations were used to assess the importance of precipitation reactions for controlling the transport of chromium, uranium, and other solutes at well MCOBT-4.4.

Table 11.3-2 shows SI values for several key phases for well MCOBT-4.4. Groundwater samples collected from the well were calculated to be undersaturated with respect to $BaSO_4$ (barite), $BaCrO_4$, $CaCO_3$ (calcite), CaF_2 (fluorite), $Cr(OH)_3$ (amorphous), $MnCO_3$ (rhodochrosite), silica gel, silica precipitate, $(UO_2)_2SiO_4 \cdot 2H_2O$ (soddyite), and $SrCO_3$ (strontianite). Migration of fluoride, strontium, barium, and manganese is predicted to be controlled by adsorption processes because groundwater is calculated to be undersaturated with solid phases containing these elements. Fluoride is expected to be mobile under circumneutral pH conditions because adsorbents including silica glass and smectite are characterized by net-negative surface charges (Langmuir 1997, 56037). Groundwater was calculated to be oversaturated with respect to $Cr(OH)_3$ (crystalline), $Mg_2Cr_2O_4$, and $Ca(UO_2)_2(Si_2O_5)_3 \cdot 5H_2O$ (haiweeite) (Table 11.3-2). Migration of chromium(III, VI) and uranium(VI), however, is expected to be controlled by precipitation and/or adsorption processes because groundwater is calculated to be both over- and undersaturated with solid phases containing these elements.

Table 11.3-2
Results of Saturation Index (SI) Calculations Using MINTEQA2 for Well MCOBT-4.4 (493 ft), Mortandad Canyon

Solid Phase or Gas	Saturation Index
$BaSO_4$	-0.78
$BaCrO_4$	-3.53
$CaCO_3$	-0.78
CaF_2	-1.60
$Cr(OH)_3$(am)	-0.82
$MnCO_3$	-3.06
SiO_2(gel)	-0.17
SiO_2(ppt)	-0.49
$(UO_2)_2SiO_4 \cdot 2H_2O$	-2.10
$SrCO_3$	-1.21
$Cr(OH)_3$(c)	1.73
$Mg_2Cr_2O_4$	0.55
$Ca(UO_2)_2(Si_2O_5)_3 \cdot 5H_2O$	0.27
CO_2 gas (log atmosphere)	-2.86

Note: am means amorphous and c means crystalline.

12.0 SUMMARY OF SIGNIFICANT RESULTS AT MCOBT-4.4 AND MCOBT-8.5

12.1 Stratigraphy

MCOBT-4.4 and MCOBT-8.5 provide new geologic control for stratigraphic units in Mortandad Canyon. In descending order, geologic units penetrated include alluvium or colluvium, tephras and volcaniclastic sediments of the Cerro Toledo interval (MCOBT-4.4 only), Otowi Member of the Bandelier Tuff, upper Puye Formation, Cerros del Rio basalt, and lower Puye Formation.

The Cerro Toledo interval thickens eastward beneath Mortandad Canyon from TW-8 to R-15, probably because of deposition in paleovalleys cut into the underlying Otowi Member. East of R-15, the distribution of Cerro Toledo deposits is less certain. It is absent at MCOBT-8.5, where alluvium directly overlies the Otowi Member, and is absent between the Tshirege and Otowi Members at R-13 (Figure 1.0-1).

A thin wedge of Puye fanglomerate overlies Cerros del Rio basalt in Mortandad Canyon. These upper Puye deposits are saturated and contain Laboratory contaminants in the vicinity of MCOBT-4.4. Similar deposits at R-15 and MCOBT-8.5 are unsaturated.

Cerros del Rio basalts thicken eastward from TW-8 to R-13. These basalts consist of at least eight lava flows separated by rubble or scoria zones. Throughout the Mortandad Canyon area and into Sandia and Los Alamos Canyons, the lavas can be subdivided into an upper tholeiitic series and a lower alkalic series. The percentage of interflow rubble or scoria making up the Cerros del Rio basalt appears to increase westward towards the distal part of the unit.

The lower Puye Formation in MCOBT-4.4 is generally similar to that found in well R-15. However, the detritus making up lower Puye deposits in MCOBT-8.5 is more siliceous than that for MCOBT-4.4 or R-15.

12.2 Hydrogeology

At MCOBT-4.4, an intermediate-depth perched zone was encountered at a depth of 493 ft. This perched system occurs in the upper Puye Formation and may extend into the top of the underlying Cerros del Rio basalt. The location of this perched system is higher than expected based on the occurrence of perched water in the lower Cerros del Rio basalt at R-15. Perched water was also considered possible at MCOBT-8.5, but no saturation was detected when the borehole was drilled. Observations from R-15, MCOBT-4.4, and MCOBT-8.5 suggest that perched water zones beneath Mortandad Canyon are likely to be of local extent and can occur above a variety of perching layers because of stratigraphic variation. From the data available it cannot be determined whether these deep perched zones in Mortandad Canyon (e.g., MCOBT-4.4 and R-15) are hydrologically connected.

Moisture profiles have been determined for the upper 310 ft of MCOBT-4.4 and the upper 350 ft of MCOBT-8.5. In both boreholes, the moisture profiles for the Otowi Member show much less variability than those for alluvium or Cerro Toledo interval. The low variability of moisture in the Otowi Member probably reflects the relative homogeneity of the ash-flow tuffs that comprise this unit compared to the stratified sedimentary deposits that make up the alluvium, colluvium, and Cerro Toledo interval.

12.3 Geochemistry

Based on analytical results for the MCOBT-4.4 and MCOBT-8.5 core samples and for groundwater samples collected from MCOBT-4.4, contamination from Laboratory discharges is present in both unsaturated rocks of the vadose zone and in perched groundwater. Tritium, fluoride, nitrate plus nitrite (as N), and perchlorate are mobile solutes that migrate through the vadose and saturated zones at depths greater than 500 ft beneath Mortandad Canyon. Concentrations of nitrate and perchlorate exceed the EPA primary standard for nitrate (10 mg/L) and the draft provisional risk-based level for perchlorate (0.001 mg/L, 1μg/L). Rates of transport in Mortandad Canyon (MCOBT-4.4) were calculated to range between 8.2 and 30.8 ft/yr based on the subsurface distribution of unique isotopically light nitrate effluent released to the canyon from 1986 to 1989. Additional characterization sampling is being conducted at MCOBT-4.4 to evaluate contaminant concentrations in the perched zone.

13.0 ACKNOWLEDGEMENTS

Deba Daymon and John McCann supported all phases of this investigation as the ER focus area leaders responsible for execution of the drilling program.

Charlie Nylander of ESH-18 is Program Manager for the Institutional Groundwater Issues Program and chairman for the Groundwater Integration Team. He participated in planning and decisions regarding drilling methods, well design, and evaluation of data collection.

David Rogers, Armand Groffman, and Robert Enz provided critical reviews of the document and offered many useful suggests for its improvement.

Ted Ball provided contract oversight for drilling activities, and Steve Pearson provided field oversight of drilling activities.

Dynatec Drilling Company provided the rotary drilling services under the direction of John Eddy. Steward Brothers Drilling Company provided hollow-stem auger drilling services under the direction of Stanley Johnson.

James Jordan, Rick Lawrence, Clarence Pigman, Paula Schuh, and Eric Tow provided support for well-site geology and sample collection.

Ken Gillespie of WGII was the site safety officer for drilling activities. Eloy Trujillo of ESH-5 provided Laboratory oversight for health and safety.

Roy Bohn provided oversight for waste management, and Renee Evans provided support for waste management.

Gene Turner of the Department of Energy (DOE), Los Alamos Area Office, provided DOE oversight.

John Young of the NMED Hazardous and Radioactive Materials Bureau provided regulatory oversight during drilling operations. Michael Dale of the New Mexico Environment Department DOE Oversight Bureau collected sample splits from groundwater zones and acted as liaison with the regulators.

Meena Sachdeva was editor for this document, and Randi Moore was compositor.

Tanya Herrera provided administrative support.

14.0 REFERENCES

Allison, J.D., D.S. Brown, and K.J. Novo-Gradac, March 1991. "MINTEQA2/PRODEFA2, A Geochemical Assessment Model for Environmental Systems: Version 3.0 User's Manual," EPA/600/3-91/021, Office of Research and Development, Athens, Georgia. (Allison et al. 1991, 49930)

Blake, W.D., F. Goff, A.I. Adams, and D. Counce, May 1995. "Environmental Geochemistry for Surface and Subsurface Waters in the Pajarito Plateau and Outlying Areas, New Mexico," Los Alamos National Laboratory report LA-12912-MS, Los Alamos, New Mexico. (Blake et al. 1995, 49931)

Broxton, D., R. Gilkeson, P. Longmire, J. Marin, R. Warren, D. Vaniman, A. Crowder, B. Lowry, D. Rogers, W. Stone, S. McLin, G. WoldeGabriel, D. Daymon, and D. Wycoff, May 2001. "Characterization Well R-9 Completion Report," Los Alamos National Laboratory report LA-13742-MS, Los Alamos, New Mexico. (Broxton et al. 2001, 71250)

Broxton D., D. Vaniman, W. Stone, S. McLin, M. Everett, and A. Crowder, May 2001. "Characterization Well R-9i Completion Report," Los Alamos National Laboratory report LA-13821-MS, Los Alamos, New Mexico. (Broxton et al. 2001, 71251)

Broxton D., R. Warren, D. Vaniman, B. Newman, A. Crowder, M. Everett, R. Gilkeson, P. Longmire, J. Marin, W. Stone, S. McLin, and D. Rogers, "Characterization Well R-12 Completion Report." Los Alamos National Laboratory report LA-13822-MS, Los Alamos, New Mexico. (Broxton et al. 2001, 71252)

Clark, I.D., and P. Fritz, 1997. *Environmental Isotopes in Hydrogeology*, Lewis Publishers, New York, New York. (Clark and Fritz 1997, 59168).

ESP (Environmental Surveillance Program), October 2001. "Environmental Surveillance at Los Alamos during 2000," Los Alamos National Laboratory report LA-13861-ENV, Los Alamos, New Mexico. (ESP 2001, 71301)

Haskin, L.A. and M.M. Lindstrom, 1978. "Trace-Element Fractionation During Crystallization of Thin Tholeiitic Lava Flows," *Lunar and Planet. Sci.*, IX, pp. 468 to 470. (Haskin and Lindstrom 1978, 73643).

Heiken G., F. Goff, J. Stix, S. Tamanyu, M. Shafiqullah, S. Garcia, and R. Hagan, 1986. "Intracaldera Volcanic Activity, Toledo Caldera and Embayment, Jemez Mountains, New Mexico," *J. Geophys. Res*., 91, pp. 1799 to 1815 (Heiken et al. 1986, 48638).

Kendall, C., and T.B. Coplen, 1985. "Multisample Conversion of Water to Hydrogen by Zinc for Stable Isotope Determination," *Anal. Chem*., 57, pp. 1437 to 1446. (Kendall and Coplen 1985, 64061)

Kendrick, B., January, 1999. "Revised Summary Table," Memorandum from B. Kendick, TechLaw Inc., to P. Longmire, Los Alamos National Laboratory, Los Alamos, New Mexico. (Kendrick 1999, 66141)

Langmuir, D. 1997. *Aqueous Environmental Geochemistry*, Prentice-Hall, Inc. Upper Saddle River, New Jersey. (Langmuir 1997, 56037)

LANL (Los Alamos National Laboratory), January 1996. "Groundwater Protection Management Program Plan," Rev. 2.0, Los Alamos, New Mexico. (LANL 1996, 70215)

LANL (Los Alamos National Laboratory), May 22, 1988. "Hydrologeological Workplan," Los Alamos, New Mexico. (LANL 1988, 59599)

LANL (Los Alamos National Laboratory), September 1997. "Work Plan for Mortandad Canyon," Los Alamos National Laboratory document LA-UR-97-3291, Los Alamos New Mexico. (LANL 1997, 56835)

LANL (Los Alamos National Laboratory), May 2001. "Field Implementation Plan for the Drilling and Testing of LANL Intermediate Zone Characterization Wells MCOBT-4.4 and MCOBT-8.5," Los Alamos National Laboratory document LA-UR-01-3385, Los Alamos, New Mexico. (LANL 2001, 70928)

Longmire, P., March 2002. "Characterization Well R-15 Geochemistry Report," Los Alamos National Laboratory report LA-13927-MS, Los Alamos, New Mexico. (Longmire 2002, 72614)

Longmire, P., April 2002. "Characterization Wells R-9 and R-9i Geochemistry Report," Los Alamos National Laboratory report LA-13927-MS, Los Alamos, New Mexico. (Longmire 2002, 72713)

Longmire, P., June 2002. "Characterization Well R-12 Geochemistry Report," Los Alamos National Laboratory report LA-13952-MS, Los Alamos, New Mexico. (Longmire 2002, 72800)

Longmire, P., D. Broxton, W. Stone, B. Newman, R. Gilkeson, J. Marin, D. Vaniman, D. Counce, D. Rogers, R. Hull, Steve McLin, and R. Warren, May 2001. "Characterization Well R-15 Completion Report," Los Alamos National Laboratory report LA-13749-MS, Los Alamos New Mexico. (Longmire et al. 2001, 70103)

Longmire, P., June 2002. "Characterization Well R-19 Geochemistry Report," Los Alamos National Laboratory report LA-13964-MS, Los Alamos, New Mexico. (Longmire 2002, 73282)

Marty, R.C., D. Bennett, and P. Thullen, 1997. "Mechanism of Plutonium Transport in a Shallow Aquifer in Mortandad Canyon, Los Alamos National Laboratory, New Mexico," *Environ. Sci. Technol*., 31, pp. 2020-2027. (Marty et al. 1997, 73695).

Moss, D., December 02, 2002. Personal Communication with P. Longmire, Los Alamos National Laboratory, Los Alamos, New Mexico. (Moss 2002, 73690)

Penrose, W.R., W.L. Polzer, E.H. Essington, D.M. Nelson, and K.A. Orlandini, 1990. "Mobility of Plutonium and Americium through a Shallow Aquifer in a Semiarid Region," *Environ. Sci. Technol*., 24, pp. 228 to 234 (Penrose et al. 1990, 0174)

Purtymun, W.D., September 1974. "Dispersion and Movement of Tritium in a Shallow Aquifer in Mortandad Canyon at the Los Alamos Scientific Laboratory," Los Alamos Scientific Laboratory report LA-5716-MS, Los Alamos, New Mexico. (Purtymun 1974, 5476)

Purtymun, W.D., J.R. Buchholz, and T.E. Hakonson, 1977, "Chemical Quality of Effluents and Their Influence on Water Quality in a Shallow Aquifer," *J. Environ. Qual.*, 6, pp. 29 to 32. (Purtymun et al. 1977, 11846)

Purtymun, W.D., W.R. Hansen, and R.J. Peters, March 1983. "Radiochemical Quality of Water in the Shallow Aquifer in Mortandad Canyon 1967 to 1978," Los Alamos National Laboratory report LA-9675-MS, Los Alamos, New Mexico. (Purtymun et al. 1983, 6407)

Rogers, D.B., July 1998. "Impact of Tritium Disposal on Surface Water and Groundwater at Los Alamos National Laboratory through 1997," Los Alamos National Laboratory report LA-13465-SR. (Rogers 1998, 59169)

Rogers, D.B., and B.M. Gallaher, September 1995. "The Unsaturated Hydraulic Characteristics of the Bandelier Tuff," Los Alamos National Laboratory report LA-12968-MS. (Rogers and Gallaher 1995, 49824.1)

Shurbaji, A.R.M. and A. R. Campbell, 1997. "A Study of Evaporation and Recharge in Desert Soils Using Environmental Tracers, New Mexico, USA," *Environ. Geol*., 29, pp. 147 to 151. (Shurrbaji and Campbell 1997, 64063)

Socki, R. A., H.R. Karlsson, and E.K. Gibson, 1992. "Extraction Technique for Determination of Oxygen-18 in Water Using Pre-Evacuated Glass Vials," *Anal. Chem*., 64, pp. 829 to 831. (Socki et al. 1992, 64064)

Velinsky, D.J., J.R. Pennock, J.H. Sharp, L.A. Cifuentes, and M.L. Fogel, 1989. "Determination of the Isotopic Composition of Ammonium-Nitrogen at the Natural Abundance Level from Estuarine Waters," *Marine Chem*., 26, pp. 351 to 361. (Velinsky et al. 1989)

Appendix A

Activities Planned for MCOBT-4.4 and MCOBT 8.5
Compared with Work Performed

APPENDIX A. ACTIVITIES PLANNED FOR MCOBT-4.4 AND MCOBT 8.5 COMPARED WITH WORK PERFORMED

Activity	Work Plan for Mortandad Canyon	MCOBT-4.4 and MCOBT-8.5 Field Implementation Plan	MCOBT-4.4 and MCOBT-8.5 Actual Work
Planned Depth	MCOBT-4.4 proposed depth of 510 ft MCOBT-8.5 proposed depth of 420 ft	The expected total depth (TD) for MCOBT-4.4 is approximately 700 ft, and the expected depth for MCOBT-8.5 is approximately 740 ft.	Total drill depth for MCOBT-4.4=767 ft Total drill depth for MCOBT-8.5=740 ft
Drilling Method	Methods may include, but are not limited to, hollow-stem auger (HAS), air-rotary/Odex/Stratex, air-rotary/Barber rig, and mud-rotary drilling	Method planned: hollow-stem auger and casing advance/open hole, fluid-assisted, air-rotary methods	Method used: hollow-stem auger and casing advance/open hole, fluid-assisted, air-rotary methods
Amount of Core	Core will be collected along the total depth of the borehole.	Core to approximately 484 ft in MCOBT-4.4 and 342 ft in MCOBT-8.5	Cored to 310 ft in MCOBT-4.4 and to 350 ft in MCOBT-8.5
Lithologic Log	Log to be prepared from core, cuttings, and drilling performance data	Log to be prepared from core, cuttings, geophysical logs, and drilling performance data	Log was prepared from core, cuttings, and geophysical logs
Number of Water Samples Collected for Contaminant Analysis	Up to 3 water samples in the perched water	Up to 3 borehole groundwater screening samples will be collected for geochemical and contaminant characterization during drilling. When water is encountered, the geochemistry task leader will be notified to determine if 1 of the 3 samples should be collected.	One water sample was obtained from completed well from a perched zone. No water samples were collected from MCOBT-8.5; no deep perched zones were intersected.
Water Sample Analysis	Major and minor ions, trace elements, organic compounds, dissolved organic carbon, total suspended solids, total dissolved solids, neutral species (SiO_2), hardness, cyanide, stable and radiogenic isotopes, and radionuclides	Metals (dissolved), anions (dissolved), gamma spectrometry, ^{241}Am, ^{137}Cs, ^{238}Pu, $^{239,240}Pu$, ^{234}U, ^{235}U, ^{238}U, ^{90}Sr (total) Stable isotopes: $^{18}O/^{16}O$, D/H, $^{15}N/^{14}N$, tritium, tritium (low level or direct counting) RVGross-alpha, beta plus RVGross-gamma, TUICPMS, TKN, CLO_4^-	MCOBT-4.4: trace elements/metals anions: Br, Cl, F, PO_4, SO_4, NO_3, NO_2, NH_4 Stable and radiogenic isotopes: $^{18}O/^{16}O$, D/H, $^{15}N/^{14}N$ Radionuclides: ^{3}H, ^{90}Sr, ^{241}Am, ^{137}Cs, ^{238}Pu, $^{239,240}Pu$, ^{234}U, ^{235}U, ^{238}U, gamma spectrometry, gross alpha, gross beta, gross gamma, TUICPMS,TKN, CLO_4^-
Water Sample Field Measurements	Alkalinity, pH, specific conductance, dissolved oxygen, temperature, turbidity	pH, specific conductance, temperature, turbidity	pH, specific conductance, temperature, turbidity

Activity	Work Plan for Mortandad Canyon	MCOBT-4.4 and MCOBT-8.5 Field Implementation Plan	MCOBT-4.4 and MCOBT-8.5 Actual Work
Number of Core/Cuttings Samples Collected for Contaminant Analysis	MCOBT-4.4: 36 core samples proposed, 3 from 0–25ft, 4 from 25–70 ft, 1 from 70–73ft, 7 from 73–140 ft, 15 from 140–450 ft, 4 from 450–490 ft, and 2 from 490–510 ft MCOBT-8.5: 33 core samples proposed, 7 from 0–65 ft, 7 from 65–125 ft, 13 from 125–360 ft, 4 from 360–400 ft, 2 from 400–420 ft Sample locations are based on predicted formation depths.	Core to be collected during auger drilling: one sample every 5 ft for the first 50 ft, and one sample every 20 ft thereafter (moisture-protected) Sidewall core samples from Puye Formation and Cerros del Rio lava: approximately one sample every 10 ft; locations determined after running suite of geophysical logs after hole reaches TD. Within water-bearing zones: up to 5 samples for the entire borehole, sample location and frequency to be determined by the geochemistry task leader. Planned totals: MCOBT-4.4: Approximately 46 core samples MCOBT-8.5: Approximately 57 core samples	Core collected during auger drilling: MCOBT-4.4: 42 core samples obtained approximately every 5 ft to 150 ft bgs and approximately every 10 ft from 150 to 310 ft bgs MCOBT-8.5: 25 core samples obtained approximately every 10 ft to 125 ft bgs and approximately every 20 ft from 125 to 350 ft bgs Sidewall core samples collected: MCOBT-4.4: 11 sidewall core samples at depths of 480, 512, 549, 588, 607, 615, 645, 670, 684, 730 and 735 ft bgs MCOBT-8.5: 7 sidewall core samples at depths of 405, 425, 447, 604, 651, 681, and 709 ft bgs Totals: Fifty-three core samples were submitted for anion analysis from MCOBT-4.4. Thirty-two core samples were submitted for anion analysis from MCOBT-8.5.
Core/Cuttings Sample Analytes	Analytical suite for borehole core samples includes anions, trace elements, organic compounds, total organic carbon, cyanide, and radionuclides.	Auger drilling: anions and stable isotope profiles through the Bandelier Tuff Sidewall core: boron, bromide, chloride, fluoride, nitrate, nitrite, oxalate, perchlorate, phosphate, and sulfate Within water-bearing zones: radiological, metals and anions/stable isotopes/^{3}H profiles	Auger drilling: anions Sidewall core: boron, bromide, chloride, fluoride, nitrate, nitrite, oxalate, perchlorate, phosphate, and sulfate Within water-bearing zones: anions
Laboratory Hydraulic-Property Tests	Physical properties analyses will be conducted on core samples and will typically include moisture content, moisture potential, and saturated hydraulic conductivity.	A moisture profile through the Bandelier Tuff will be obtained by collecting core samples at intervals of approximately 5 ft during hollow-stem auger drilling.	Totals: Fifty-three core samples were submitted for moisture analysis from MCOBT-4.4. Thirty-two core samples were submitted for moisture analysis from MCOBT-8.5.

Activity	Work Plan for Mortandad Canyon	MCOBT-4.4 and MCOBT-8.5 Field Implementation Plan	MCOBT-4.4 and MCOBT-8.5 Actual Work
Geology	Selected samples of core or cuttings will be collected for petrographic, X-ray fluorescence (XRF), X-ray diffraction (XRD) and K/Ar or $^{39}Ar/^{40}Ar$ isotopic dating analyses.	The geology task leader will determine the number of samples for characterization of mineralogy, petrography, and rock chemistry based on geologic and hydrologic conditions encountered during drilling.	Eighteen samples from MCOBT-4.4 and sixteen samples from MCOBT-8.5 were submitted for mineralogy, petrography, and rock chemistry analysis
Geophysics	Natural gamma, neutron moisture, and density logs may be run in shallower portions of the boreholes. Natural gamma, neutron moisture, and density logs may be run if the drilling method and borehole stability permit. Other geophysical logs may be considered if, in the opinion of the technical team, they will satisfy a technical need. In general, open-hole geophysics includes caliper, electromagnetic induction, magnetic susceptibility, borehole color videotape (axial and sidescan), fluid temperature (saturated), single-point resistivity (saturated), and spontaneous potential (saturated). In general, cased-hole geophysics includes gamma-gamma density, natural gamma, and thermal neutron.	Typical wire-line logging service as planned: Open-hole geophysics includes array induction imager, triple litho density, combinable magnetic resonance, natural gamma, natural gamma spectrometry, epithermal compensated neutron log, caliper, fullbore formation micro-imager, elemental capture spectrometer, and borehole videotape In general, cased-hole geophysics includes triple litho density, natural gamma, natural gamma spectrometry, epithermal compensated neutron log and elemental capture spectrometer	Downhole geophysical log surveys conducted: MCOBT-4.4: Video (LANL tool): 130–767 ft, natural gamma (LANL tool): cased 0–130 ft, open hole 130–767 ft, Schlumberger geophysics (0–130 ft cased, 130–767 ft open hole): compensated neutron, lithodensity combinable magnetic resonance, spectral gamma, array induction, natural gamma, and elemental capture sonde MCOBT-8.5: Video (LANL tool): 130–740 ft, natural gamma (LANL tool): cased 0–130 ft, open hole 130–740 ft, Schlumberger geophysics (0–130 ft cased, 130–-740 ft open hole): compensated neutron, spectral gamma, array induction, combinable magnetic resonance and litho density
Water-Level Measurements	Not specified in work plan	When a saturated zone of perched water is first encountered, a static water level shall be measured by the field technical leader using a dedicated water-level meter and/or a pressure transducer system.	MCOBT-4.4: Water levels in the perched water zone indicated a stable water level of approximately 493 ft bgs. MCOBT-8.5: Perched groundwater was not detected in the borehole.
Field Hydraulic-Property Tests	Not specified in work plan	Hydraulic properties of materials in perched zones and, if applicable, the regional water table shall be investigated by in-situ methods, as far as possible. The hydrology task leader shall design and conduct slug or pumping tests once the well is completed.	Borehole and well conditions were not appropriate for in situ testing of hydraulic properties.

Activity	Work Plan for Mortandad Canyon	MCOBT-4.4 and MCOBT-8.5 Field Implementation Plan	MCOBT-4.4 and MCOBT-8.5 Actual Work
Surface Casing	Approximately 20-in. O.D., extends from land surface to 10-ft depth in underlying competent layer and grouted in place.	18-in. O.D. schedule 40, low carbon steel casing will be installed as deep as possible below ground level (nominally 35–40 ft) and will extend approximately 3 ft above the ground surface and cemented in place.	MCOBT-4.4 and MCOBT-8.5 were drilled without surface casing.
Minimum Well Casing Size	6 5/8-in. O.D.	5-in. O.D. x 4.5-in. I.D.	5.5-in O.D. (4.5-in. I.D.) stainless steel casing w/ external couplings was utilized in MCOBT-4.4. MCOBT-8.5: No well was completed in borehole.
Well Screen	Machine-slotted (0.01-in.) stainless steel screens with flush-jointed threads; number and length of screens to be determined on a site-specific basis and proposed to NMED	Well screen shall be constructed with multiple sections of 5.56-in. O.D., pipe based stainless steel screen with a 0.01 in. slot size.	The screened interval for well MCOBT-4.4 was constructed of 5.5-in. O.D. (4.5-in. I.D.) pipe-based, stainless steel, wire wrapped, 0.010-in. slotted screen. MCOBT-8.5: No well was completed in borehole.
Filter Material	>90% silica sand, properly sized for the 0.010-in. slot size of the well screen; extends 2 ft above and below the well screen.	Primary filter pack shall consist of round, clean, washed and reseived silica sand with a uniformity coefficient of 2.0 or less. The primary filter pack shall extend a minimum distance 10 ft above and 5 ft below the well screen. The size of the filter pack shall be selected based on the characteristics of the formation to be screened. Either 20/40, 8/12, or other appropriate size may be used. Secondary filter pack is finer (30/70) silica sand placed a minimum of 2 ft below and above the primary filter pack.	MCOBT-4.4: Primary filter pack constructed of 20/40 silica sand placed 3 ft below and 8.6 ft above the screen. Secondary filter pack of 30/70 silica sand was constructed in a nominal 2.8-ft-thick layer above the primary filter pack. MCOBT-8.5: No well was completed in borehole.
Backfill Material (exclusive of filter materials)	Uncontaminated drill cuttings below sump and bentonite above sump.	The interval from TD to approximately 10 ft below the bottom well screen may be filled with gravel, silica sand, bentonite, and/or cement. The annular space in the blank zones between filter packs associated with screens (for a multiscreen well) and above the top-most secondary filter pack of a single-completion well shall be sealed with a mixture of approximately 50% bentonite (chips or pellets) and 50% gravel or sand. As necessary, 5- to 10-ft cement plugs may be placed within the bentonite and gravel/sand intervals to provide stable floors for the placement of annular fill. The annular space from a depth of approximately 75 ft to land surface shall be sealed with cement grout.	MCOBT-4.4: Bentonite chips were poured into the borehole below the well casing and were placed below and above filter pack. Cement-bentonite grout was slurried from 68.4 ft bgs to ground surface. MCOBT-8.5: No well was completed in borehole.

Activity	Work Plan for Mortandad Canyon	MCOBT-4.4 and MCOBT-8.5 Field Implementation Plan	MCOBT-4.4 and MCOBT-8.5 Actual Work
Sump	Stainless steel casing with an end cap	5.56-in. diameter stainless steel casing 30 ft long	MCOBT-4.4: 5.56-in. diameter stainless steel casing 21 ft long MCOBT-8.5: No well was completed in borehole.
Bottom Seal	Bentonite	Bentonite	MCOBT-4.4: Bentonite chips (3/8 in.) MCOBT-8.5: No well was completed in borehole.

Appendix B

Operations Chronology Graphs for
MCOBT 4.4 and 8.5

APPENDIX B. OPERATIONS CHRONOLOGY GRAPHS FOR MCOBT 4.4 AND 8.5

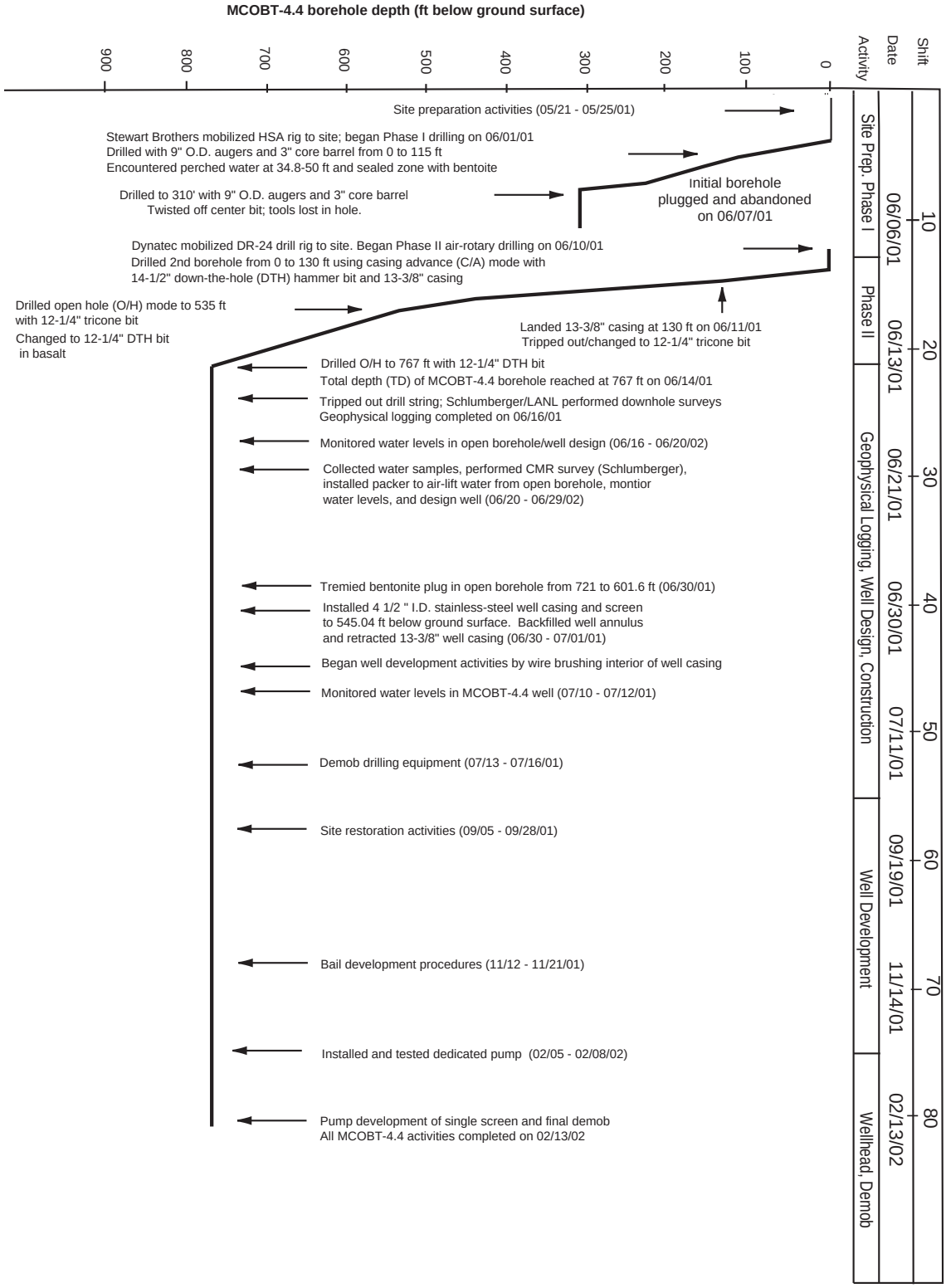

Well MCOBT-4.4 operations chronology graph

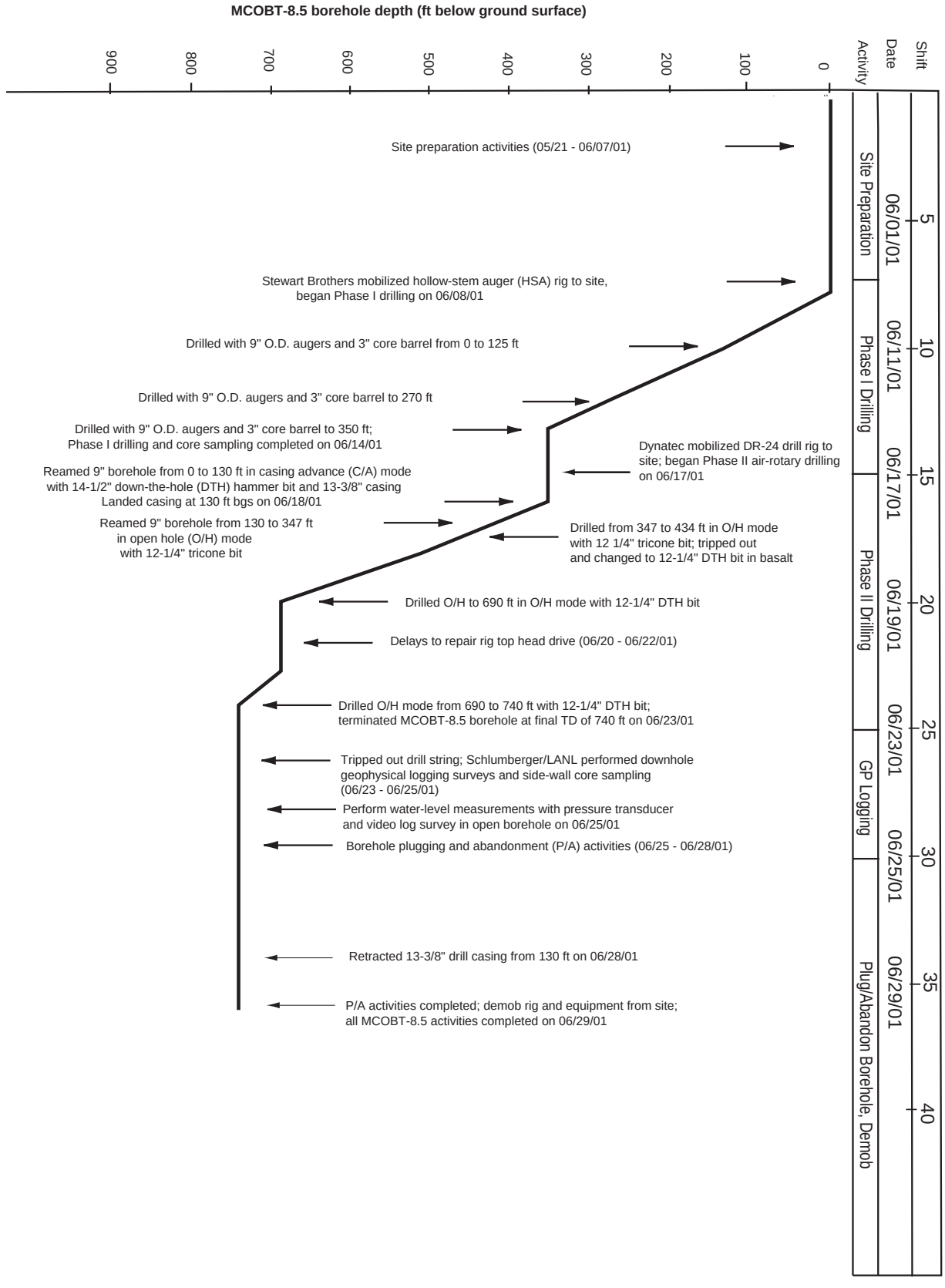

Borehole MCOBT-8.5 operations chronology graph

Appendix C

Lithologic Logs

MCOBT-4.4: C-1 to C-6
MCOBT-8.5: C-7 to C-13

APPENDIX C. LITHOLOGIC LOGS

Lithologic descriptions of core and drill cuttings at borehole MCOBT-4.4

Geologic Unit	Lithologic Description[a]	Sample Interval (ft)	Elevation Range (ft above msl)
Construction fill	Gravelly base-coarse construction fill. Note: rockcore samples collected and described from 0 to 310 ft bgs.	0–1	6836.2–6835.2
Qal, alluvium	Unconsolidated sediments, sand (SW), pale yellowish brown (10YR 6/2), fine to very coarse sand, well graded, moist.	1–7.5	6835.2–6828.7
	Unconsolidated sediments, silty sand (SM), moderate yellowish brown (10YR 5/4), silt to fine sand, well graded, angular to subrounded, moist.	7.5–11	6828.7–6825.2
	Unconsolidated sediments, sand (SW), pale brown (10YR 5/2), fine to coarse sand, well graded, angular to subrounded, some cobbles of weathered tuff, moist.	11–20	6825.2–6816.2
	Unconsolidated sediments, silty sand (SM), dark yellowish brown (5YR 5/6), silt to coarse sand, well graded, angular to subrounded grains, moist.	20–26.8	6816.2–6809.4
	No core recovery.	26.8–27.5	6809.4–6808.7
	Unconsolidated sediments, silty sand (SM), similar to interval 20 to 26.8 ft.	27.5–34	6808.7–6802.2
	Unconsolidated sediments, sand (SW), pale brown (5YR 5/2), fine to coarse tuffaceous sand, well graded, angular to subrounded, wet to saturated at 34.8 ft bgs. Clasts consist mainly of volcanic tuff.	34–45.5	6802.2–6790.7
	Unconsolidated sediments, clayey sand (SC), moderate brown (5YR 4/4), clay to coarse sand, well graded, angular to subrounded, saturated. Sediments very clayey from 45.5–48 ft bgs.	45.5–50	6790.7–6786.2
	No core recovery. No core attempted in interval 52.5–55.0 ft.	50–55	6786.2–6781.2
	Unconsolidated sediments, clayey sand (SC), similar to interval 45–50 ft, becoming gravelly with depth at 61–62 ft bgs.	55–63.7	6781.2–6772.5
Qct, Cerro Toledo Interval	Air-fall tuff/tuffaceous sediments, light brown (5YR 6/4), pumice-rich, non-welded. Composed of 55% white devitrified pumice, 10% quartz-sanidine phenocrysts, 5–15% small black lithic fragments, 20–30% ash matrix.	63.7–66.8	6772.5–6769.4
	Air-fall tuff/tuffaceous sediments, grayish orange pink (5YR 7/2), pumice-rich, non-welded. Subangular pumice with no matrix; pumice-supported, few dark gray lithic fragments.	66.8–69	6769.4–6767.2
	Air-fall tuff/tuffaceous sediments, grayish orange pink (5YR 7/2), pumice-rich, non-welded. Dominantly pumice with few lithic fragments, some ash matrix.	69–72	6767.2–6764.2
	Air-fall tuff/tuffaceous sediments, light brown (5YR 6/4), pumice-rich, non-welded. Dominantly pumice with minor sanidine phenocrysts and lithic fragments.	72–75	6764.2–6761.2
	Air-fall tuff/tuffaceous sediments, sand (SW) pale yellowish brown (10YR 6/2), pumice-rich, fine to coarse sand, well graded, angular to subrounded. Clasts composed of pumice clasts (40–60%), quartz-sanidine crystals (20%), volcanic lithics (5%). Lithic fragments (dacite) increase in abundance and size with depth; interval has a gravelly basal bed with clasts up to 3 cm from 100 to 101.9 ft.	75–101.9	6761.2–6734.3

Geologic Unit	Lithologic Description[a]	Sample Interval (ft)	Elevation Range (ft above msl)
Qbo, Otowi Member of the Bandelier Tuff	Volcanic tuff, moderate reddish orange (10YR 6/6), pumice-rich, poorly welded. Dominantly devitrified pumice fragments (up to 3 cm), quartz-sanidine crystals (5%), and dark lithics fragments (3%).	101.9–137.5	6734.3–6698.7
	Volcanic tuff, light pinkish gray (5YR 7/2), poorly welded, friable. Composed of 5–10% quartz-sanidine phenocrysts (1 mm), 5–10% dark colored lithic fragments, 5–10% white vitric pumice (1 mm), 70–80% fine ash.	137.5–140	6698.7–6696.2
	Volcanic tuff, light pinkish gray (5YR 7/2), vitric, poorly welded, friable. Composed of 5–15% quartz-sanidine phenocrysts (1 mm), 7–10% dark colored lithic fragments (0.5–1 mm) that are locally rimmed by Fe-oxide (limonite), 10–15% flattened white vitric pumice (2 mm), 60–70% vitric ash matrix.	140–147.5	6696.2–6688.7
	Volcanic tuff, light pinkish gray (5YR 7/2), vitric, poorly welded, friable. Composed of 15–20% quartz-sanidine phenocrysts (1 mm), 10–15% dark gray lithic fragments (dacite, 1–2 mm), 20–30% white vitric pumice (1–8 mm), uncompressed, locally limonite-stained; 30–40% vitric ash matrix.	147.5–157.5	6688.7–6678.7
	Volcanic tuff, light pinkish gray (5YR 7/2), vitric, poorly welded, friable. Composed of 10–20% quartz-sanidine phenocrysts (up to 1.5 mm), 5–15% dark gray siliceous lithic fragments (dacite, 1–3 mm), 10–15% vitric pumice (1–30 mm), fiber-textured, locally flattened, larger pumices orange-tan due to Fe-oxide (limonite) staining; 25–35% vitric ash matrix.	157.5–160	6678.7–6676.2
	No core attempted.	160–170	6676.2–6666.2
	Volcanic tuff, light pinkish gray (5YR 7/2), vitric, poorly welded, friable. Similar to interval 157.8–160 ft.	170–179.8	6666.2–6656.4
	Volcanic tuff, light pinkish gray (5YR 7/2), vitric, poorly welded, friable. Composed of 10–20% quartz-sanidine phenocrysts (0.5–1 mm), 10–20% dark gray lithic fragments (dacite-andesite, 1–4 mm), 15–25% frothy vitric pumice, 30–40% vitric ash matrix.	179.8–195	6656.4–6641.2
	No core attempted.	195–200	6641.2–6636.2
	Volcanic tuff, light pinkish gray (5YR 7/2), vitric-crystal tuff, poorly welded, friable. Composed of 20–30% quartz-sanidine phenocrysts (up to 2 mm), 5–15% dark gray siliceous lithic fragments (dacite, 0.5–2 mm), 10–15% white vitric pumice (1–30 mm), locally flattened, 25–35% vitric ash matrix.	200–204.8	6636.2–6631.4
	Volcanic tuff, light pinkish gray (5YR 7/2), vitric, pumice-rich, poorly welded, friable. Composed of 5–15% quartz-sanidine phenocrysts (up to 1 mm), 5–15% dacite lithic fragments (0.5–1 mm), 20–40% vitric pumice (5–60 mm), locally flattened, displaying parallel elongated vesicles, prominent larger pumices are orange-tan colored due to Fe-oxide (limonite) staining; 30–40% vitric ash matrix.	204.8–212.2	6631.4–6624
	No core recovery.	212.2–212.5	6624–6623.7
	Volcanic tuff, light pinkish gray (5YR 7/2), pumice-rich, poorly welded, friable. Composed of 15–20% quartz-sanidine phenocrysts (0.5 to 1 mm), 5–15% dark gray dacite lithic fragments (0.5–3 mm), 20–40% vitric pumice (5–50 mm), prominent larger pumices are pale orange colored due to Fe-oxide (limonite) staining; 25–35% vitric ash matrix.	212.5–225	6623.7–6611.2

Geologic Unit	Lithologic Description[a]	Sample Interval (ft)	Elevation Range (ft above msl)
	No core attempted.	225–227.5	6611.2–6608.7
Qbo, Otowi Member of the Bandelier Tuff (cont.)	Volcanic tuff, light pinkish gray (5YR 7/2), vitric, pumice-rich, poorly welded, friable. Composed of 10–15% quartz-sanidine phenocrysts (0.5 to 1 mm), 5–15% dark gray lithic fragments (dacite, 0.5–1 mm), 30–40% white vitric pumice (1–50 mm), larger pumices are orange-colored limonite-stained; 30–40% vitric ash matrix.	227.5–230	6608.7–6606.2
	No core attempted.	230–235	6606.2–6601.2
	Volcanic tuff, light pinkish gray (5YR 7/2), vitric, poorly welded, friable. Composed of 10–20% quartz-sanidine phenocrysts (0.5 to 1 mm), 10–20% dark gray lithic fragments (dacite, 0.5–0 mm, rarely up to 20mm), 30–40% white vitric pumice (1–2 mm) and orange-colored (limonite-stained, 5–40 mm), fibrous, compressed; 25–35% vitric ash matrix.	235–247.5	6601.2–6588.7
	No core attempted.	247.5–267.5	6588.7–6568.7
	Volcanic tuff, light pinkish gray (5YR 7/2), vitric, poorly welded, friable. Composed of 10–20% quartz-sanidine phenocrysts (0.5 to 1 mm), 5–15% dark gray lithic fragments (dacite, 0.5–1mm), 20–30% white vitric pumice (1–15 mm), 35–40% vitric ash matrix.	267.5–272.5	6568.7–6563.7
	No core attempted.	272.5–287.5	6563.7–6548.7
	Volcanic tuff, light pinkish gray (5YR 7/2), vitric, poorly welded, friable. Composed of 10–20% quartz-sanidine phenocrysts (0.5 to 1 mm), 5–15% dark gray lithic fragments (dacite, 0.5–1mm), 20–30% white vitric pumice (1–10 mm), frothy textured; 35–45% vitric ash matrix.	287.5–290	6548.7–6546.2
	No core attempted.	290–307.5	6546.2–6528.7
	Volcanic tuff, light pinkish gray (5YR 7/2), vitric, poorly welded, friable. Composed of 10–20% quartz-sanidine phenocrysts (0.5 to 1 mm), 5–15% dark gray siliceous lithic fragments (dacite, 0.5–1mm), 25–35% white vitric pumice (1–10 mm), 25–35% vitric ash matrix.	307.5–310	6528.7–6526.2
	Volcanic tuff, light gray (N7), lithic- and crystal-poor. +10F (i.e., plus No. 10 sieve size fraction): 90% white (N9) vitric pumice, vitreous luster, elongated vesicles; 10% dacite lithics and quartz-sanidine crystals. Note: rotary drill cuttings collected and described from 310 to 767 ft bgs.	310–312	6526.2–6524.2
	Volcanic tuff, light gray (N7), lithic- and crystal-rich. +10F: mostly siliceous volcanic (dacite) lithic fragments. +35F: mostly quartz-sanidine crystals.	312–322	6524.2–6514.2
	Volcanic tuff, light gray (N7), pumice-rich vitric-lithic tuff. +10F: 50–80% vitric pumice, 20–50% andesite, dacite rock fragments. Pumice becoming less abundant with depth. +35F(i.e., plus No. 35 sieve size fraction): mostly quartz-sanidine crystals.	322–342	6514.2–6494.2
	Volcanic tuff, mottled to light gray (N7), pumice-rich. +10F: 50–85% pumice fragments with vitreous to earthy luster, lesser amounts of porphyritic volcanic rocks (andesite to dacite composition).	342–352	6494.2–6484.2
	Volcanic tuff, mottled to light gray (N7), lithic- and crystal-rich. +10F: dominantly porphyritic intermediate rock fragments, minor pumice. +35F: dominantly quartz-feldspar crystals, rare pumice.	352–362	6484.2–6474.2
	Volcanic tuff, white (N9), pumice-rich. +10F: 100% vitric pumice fragments, typically with distinct vitreous luster. Phenocrysts are	362–367	6474.2–6469.2

Geologic Unit	Lithologic Description[a]	Sample Interval (ft)	Elevation Range (ft above msl)
	apparently absent. WR (i.e., unseived whole rock) sample contains pumice with orange-brown alteration coatings.		
Qbo, Otowi Member of the Bandelier Tuff (cont.)	Volcanic tuff, mottled to light gray (N7), lithic- and crystal-rich. +10F: abundant porphyritic andesite and dacite rock fragments, locally up to 50% pumice. +35F: contains abundant quartz-sanidine crystals.	367–382	6469.2–6454.2
	Volcanic tuff, white (N9), pumice-rich. +10F: 95% vitric pumice, 3–5% quartz-sanidine crystals.	382–387	6454.2–6449.2
	Volcanic tuff, mottled to light gray (N7), lithic- and crystal-rich. +10F: abundant porphyritic andesite and dacite rock fragments, lesser amounts of pumice. +35F: contains abundant quartz-sanidine crystals, minor lithics and pumice.	387–402	6449.2–6434.2
	Volcanic tuff, white (N9), pumice-rich. +10F: 98% frothy, vitric pumice fragments and quartz-sanidine crystals, minor andesite lithic fragments.	402–417	6434.2–6419.2
	Volcanic tuff, light gray (N7), lithic- and pumice-rich. +10F: 70–85% porphyritic andesite and dacite rock fragments, pumice locally up to 20%. +35F: contains abundant quartz-sanidine crystals.	417–422	6419.2–6414.2
	Volcanic tuff, white (N9), pumice-rich. +10F: 90–95% vitric pumice, locally minor volcanic (dacite) lithics. +35F: uniquely pumice fragments.	422–437	6414.2–6399.2
	Volcanic tuff, mottled to light gray (N7), lithic- and crystal-rich. +10F: 95–98% volcanic (dacite) lithics, locally minor quartz-sanidine crystals. +35F: dominantly quartz-sanidine crystals, minor pumice and lithics.	437–447	6399.2–6389.2
	Volcanic tuff, mottled to light gray (N7), lithic-rich. +10F: 70–80% vitric pumice, 20–30% andesite-dacite lithic fragments.	447–457	6389.2–6379.2
	Volcanic tuff, light gray (N7), lithic- and crystal-rich. +10F: 95% silicic volcanic (dacite, rhyodacite) lithics, locally minor quartz-sanidine crystals. +35F: dominantly quartz-sanidine crystals, minor pumice and lithics.	457–462	6379.2–6374.2
Qbog, Guaje Pumice Bed	Volcanic tuff, light gray (N7), pumice-rich. +10F: 90–95% vitric pumice, 5–10% dacite, rhyodacite lithics.	462–472	6374.2–6364.2
Qbog/Tpf	Transitional interval marking contact between Qbo and Tpf. Contact suggested at 474 ft bgs. WR/+10F: mixed pumice (i.e., tuff component) and dacite volcanic clasts that are partly rounded..	472–477	6364.2–6359.2
Tpf Puye Formation	Clastic sediments. Gravel (GP), light gray (N7), pebble gravel, subrounded clasts (4–15 mm). WR/+10F: 100% volcanic lithics (dacite, rhyodacite porphyry).	477–487	6359.2–6349.2
Tpf	Clastic sediments. Gravel with sand (GW), light gray (N7), pebble gravel, subangular to subrounded and broken clasts (4–15 mm). WR/+10F: 80% volcanic (siliceous quartz porphyry, rhyodacite, dacite) rocks, 20–30% tuffaceous quartz-sanidine crystals.	487–502	6349.2–6334.2
	Clastic sediments. Silty sand with gravel (SM), pinkish pale brown (5YR 5/2), pebbles (4–12 mm) are subangular to subrounded. WR/+10F: 98% lithic clasts made up of a wide variety of volcanic (felsic tuff, rhyodacite, dacite, minor vesicular basalt, rare vitrophyre) rocks, locally abundant tan (tuffaceous?) siltstone particles.	502–517	6334.2–6319.2

Geologic Unit	Lithologic Description[a]	Sample Interval (ft)	Elevation Range (ft above msl)
Tb, Cerros del Rio Basalt	Transitional interval marking contact between Tpf and Tb. Contact estimated at 519 ft bgs. WR/+10F: 75% vesicular basalt fragments, broken, angular; 25% tan (tuffaceous?) sillstone particles.	517–522	6319.2–6314.2
	Basalt, dark gray (N3), weakly porphyritic with aphanitic groundmass (GM), strongly vesicular to scoriaceous. WR/+10F: minor olivine phenocrysts, fracture surfaces and vesicles commonly coated/lined with Fe-oxide (limonite). Strongly oxidized interval.	522–532	6314.2–6304.2
	Basalt, dark gray (N3), aphyric, aphanitic, vesicular becoming massive downward. Groundmass appears weakly to moderately hydrothermally altered, minor white clay and orange-brown limonite lining vesicles.	532–537	6304.2–6299.2
	Basalt, dark gray (N3), aphyric, aphanitic, scoriaceous. Abundant white clay filling vesicles, minor limonite alteration.	537–542	6299.2–6294.2
	Basalt, dark gray (N3), aphyric, aphanitic, vesicular to scoriaceous, local white clay filling vesicles. Rare olivine phenocrysts are replaced by iddingsite.	542–557	6294.2–6279.2
	Basalt, dark gray (N3), aphyric, aphanitic, vesicular to scoriaceous, local white clay filling vesicles. Rare olivine phenocrysts are replaced by iddingsite.	557–572	6279.2–6264.2
	Basalt, medium gray (N5), weakly porphyritic with aphanitic groundmass, massive to weakly vesicular. Groundmass moderately altered, white clay locally filling vesicles and coating fracture surfaces, minor Fe-oxide staining.	572–582	6264.2–6254.2
	Basalt, medium gray (N5), aphyric, aphanitic, vesicular to scoriaceous. Groundmass moderately altered, abundant white clay lining vesicles and coating fractures surfaces, local weak Fe-oxide staining.	582–592	6254.2–6244.2
	Basalt, medium gray (N4), aphyric, aphanitic, vesicular. White clay lining vesicles, locally weak Fe-oxide staining.	592–602	6244.2–6234.2
	Basalt, dark gray (N3), aphyric, aphanitic, vesicular. Groundmass weakly altered, abundant white clay and local Fe-oxide lining vesicles.	602–627	6234.2–6209.2
	Basalt, medium gray (N5), weakly porphyritic with aphanitic GM, massive to locally vesicular. Olivine phenocrysts (1mm) appear fresh, pale green, groundmass weakly altered.	627–642	6209.2–6194.2
	Basalt, medium dark gray (N4), porphyritic with aphanitic GM, vesicular. Pale green olivine phenocrysts (1 mm) are fresh, groundmass weakly altered, moderate white clay lining vesicles.	642–652	6194.2–6184.2
	Basalt, light gray (N7), weakly porphyritic with aphanitic GM, massive to weakly vesicular. Olivine phenocrysts appear fresh, pale green, groundmass weakly altered.	652–662	6184.2–6174.2
	Basalt, reddish gray to medium gray (N5), massive. Fractures coated with reddish Fe-oxide (hematite). Note: drillers observed dark reddish brown drilling fluid at 666 ft bgs. Strongly oxidized zone.	662–667	6174.2–6169.2
	Basalt, medium gray (N5), porphyritic with aphanitic GM, massive to weakly vesicular. Phenocrysts altered, reddish brown, indistinct boundaries; white clay filling vesicles and coating fractures. WR sample clayey.	667–682	6169.2–6154.2

Geologic Unit	Lithologic Description[a]	Sample Interval (ft)	Elevation Range (ft above msl)
Tb (cont.)	Basalt, medium gray (N5), porphyritic with aphanitic GM, massive to weakly vesicular. Phenocrysts altered, reddish brown, indistinct boundaries; white clay filling vesicles and coating fractures. WR sample clayey.	682–692	6154.2–6144.2
	Basalt, light gray (N7), porphyritic with aphanitic GM, massive to weakly vesicular. Olivine phenocrysts (up to 2 mm) weakly altered, rare plagioclase; groundmass is pitted with tiny vugs and "spider-webbed" with microscopic veinlets of white clay(?).	692–707	6144.2–6129.2
	Basalt, light gray (N7), porphyritic with aphanitic GM, massive. Olivine phenocrysts mostly oxidized or replaced by dark reddish iddingsite, groundmass moderately to strongly altered and displays pitted texture, groundmass feldspar sericitized; locally microscopic veinlets of white clay(?).	707–727	6129.2–6109.2
	Basalt, dark reddish to orange brown (10YR 4/6), porphyritic with aphanitic GM, massive to partly vesicular. Olivine phenocrysts oxidized, groundmass alteration as in interval above, local Fe-oxide coating fracture surfaces or completely replacing rock matrix, white clay coating fractures or as amygdules. WR sample has distinctive reddish silty to clayey matrix indicating strong zone of oxidation. Note: appearance of subrounded dacite pebbles in lower 5 ft of interval suggests contact with Tpf at approximately 735 ft bgs.	727–737	6109.2–6099.2
Tpf, Puye Formation	Clastic sediments. Sandy gravel (GW), medium gray (N5), pebbles (up to 15 mm) are subangular to subrounded. WR/+10F: 98% lithic clasts made up of various porphyritic volcanic (rhyodacite, dacite) rocks, locally abundant tan (tuffaceous?) siltstone particles.	737–752	6099.2–6084.2
Tpf	Clastic sediments. Gravelly sand (SW), light gray (N7), pebbles (up to 7 mm) are subangular to subrounded. WR/+10F: 100% volcanic lithic clasts including dacite, andesite, rare basalt.	752–757	6084.2–6079.2
	Clastic sediments. Sand with gravel (SW), medium gray (N5), pebbles (4–7 mm) are subangular to broken fragments. WR/+10F: 100% lithic clasts made up of various dacite, andesite, and minor basalt.	757–767	6079.2–6069.2
	Total borehole depth (TD) is at 767 ft bgs.		

Note: American Society for Testing Materials (ASTM) standards were used in describing the texture of drill chip samples for sedimentary rocks such as alluvium and the Puye Fanglomerate. ASTM method D 2488-90 incorporates the Unified Soil Classification System (USCS) as a standard for field examination and description of soils. The following is a glossary of standard USCS symbols used in the MCOBT-4.4 lithlog.

[a] SW = Well graded sand; GW = Well graded gravel; GP = Poorly graded gravel; SW = Silty sand

References

ASTM D 2488-90. Standard Practice and Identification of Soils (Visual-Manual Procedure)

Note: Cuttings were collected at nominal 5-ft intervals and divided into three sample splits: (1) unsieved, or whole rock (WR), sample; (2) +10F sieved fraction (No. 10 sieve equivalent to 2.0 mm); and (3) +35F sieved fraction (No. 35 sieve equivalent to 0.50 mm).

Note: The term "percent," as used in the above descriptions, refers to percent by volume for a given sample component.

Lithologic descriptions of core and drill cuttings at borehole MCOBT-8.5

Geologic Unit	Lithologic Description[a]	Sample Interval (ft)	Elevation Range (ft above msl)
Qal, alluvium	Unconsolidated sediments, sand with silt (SW), grayish brown (5YR 3/2) very fine to coarse sand, well graded, angular to subangular, moist. The interval contains 0–0.7 ft dark loamy sand; local carbonate-cemented clasts (caliche) at 0.7–14 ft. Note: rock core samples collected and described from 0 to 347 ft bgs.	0–14	6780.5–6766.5
	Unconsolidated sediments, silty sand (SM), pale yellowish brown (10YR 6/2), silt to coarse sand, well graded, subangular to subrounded clasts, dry. Local caliche clasts.	14–18	6766.5–6762.5
	Unconsolidated sediments, sand with silt (SW), pale yellowish brown (10YR 6/3), silt to fine sand, some pebbles (up to 2 cm), well graded, angular to subrounded grains, dry.	18–26	6762.5–6754.5
	Unconsolidated sediments, silt with sand (ML), moderate yellowish brown (10YR 5/4), silt to fine sand, weak plasticity, dry.	26–28.3	6754.5–6752.2
	Unconsolidated sediments, sand (SW), pale yellowish brown (10YR 6/2), fine to mostly coarse sand, well graded, angular to rounded grains, dry.	28.3–41.3	6752.2–6739.2
	Unconsolidated sediments, silt with sand (ML), moderate yellowish brown (10YR 5/4), fine to coarse sand, well graded, angular to subangular grains, 10% tuffaceous quartz-sanidine crystals, moist. Block of indurated tuff in interval 42.5–45 ft.	41.3–50	6739.2–6730.5
	Unconsolidated sediments, silty sand (SM), moderate yellowish brown (5YR 5/4), medium to coarse sand, well graded, subangular to subrounded, minor dacite lithic fragments.	50–59	6730.5–6721.5
	Unconsolidated sediments, silt with sand and tuff boulders (ML), moderate yellowish brown (5YR 5/4), silt to fine sand, moist. Angular tuff clasts (0.5–6 cm), pinkish gray (5YR 8/1), occurrence decreasing with depth. Blocks of indurated devitrified tuff in the intervals 59–69 ft, 73.0–73.5 ft, and 75.6–76.5 ft.	59–80	6721.5–6700.5
	Unconsolidated sediments, silt (ML), dark yellowish orange (10R 6/6), moist. Interval made up of indurated weathered tuff, ash, grains of quartz- sanidine crystals, and pumice.	80–83.5	6700.5–6697
	Unconsolidated sediments, silt with sand (ML), dark yellowish orange (10YR 6/6) to pale yellowish brown (10YR 6/2), well-graded, subrounded grains, moist. Grains composed of quartz-sanidine crystals; grayish pink (5YR 7/2) to yellowish orange (10YR 6/6) clasts of tuff (0.5 –6 cm). The intervals 86–87 and 98.5–100.4 composed of consolidated tuff. Saturated zone at 97.9 to 98.5 ft bgs.	83.5–100.4	6697–6680.1
	Unconsolidated sediments, sand (SW), grayish orange 10YR 6/6), fine to medium sand, well graded, moist.	100.4–105.4	6680.1–6675.1
	Unconsolidated sediments, sand with gravel (SW), dark yellowish orange (10YR 6/6), fine to medium sand, well graded, moist. Grains consist of quartz-sanidine, clasts of tuff with blocks as large as 2.3 ft in diameter. Saturated zone from 109.0 to 110.6 ft bgs.	105.4–112.2	6675.1–6668.3

Geologic Unit	Lithologic Description[a]	Sample Interval (ft)	Elevation Range (ft above msl)
Qbo, Otowi Member of the Bandelier Tuff	Volcanic tuff, strongly weathered, light brown (5YR 5/6), very moist. poorly welded, friable. Composed of 5–10% quartz-sanidine phenocrysts (1 mm), 5–10% dark colored lithic fragments, 5–10% white vitric pumice (1 mm), 70–80% fine ash.	112.2–120	6668.3–6660.5
	Volcanic tuff, light pinkish gray (5YR 8/1), weakly to moderately welded, friable. Composed of 20–30% white and yellow-orange (10YR 6/6) vitric pumices (2–40 mm); larger pumices tend to be Fe-oxide stained (limonite); 5–15% quartz-sanidine phenocrysts; 10–20% dark colored dacite volcanic fragments (0.5–5 mm); 30–40% vitric ash matrix.	120–125	6660.5–6655.5
	Volcanic tuff, light pinkish gray (5YR 7/2) to mottled with dark orange (10YR 6/6), weakly to moderately welded, friable. Composed of 30–40% vitric pumice, white (2–10 mm) and larger yellow-orange (10–40 mm); larger pumices exhibit fibrous structure, porphyritic, tend to be limonite-stained (limonite); 10–20% quartz-sanidine phenocrysts; 10–20% dark colored volcanic (dacite) lithics (0.5 –4 mm); 25–35% vitric ash matrix.	125–137.5	6655.5–6643
	Volcanic tuff, light pinkish gray (5YR 7/2) with clots of dark yellow-orange (10YR 6/6), weakly to moderately welded, friable. Composed of 30–40% white vitric pumice fragments (1–5 mm) and locally larger (10–40 mm) yellow-orange pumices that exhibit distinctive fibrous structure with parallel vesicles; 5–15% quartz-sanidine phenocrysts (1–2 mm); 10–20% dark colored intermediate volcanic lithics; 30–40% vitric ash matrix.	137.5–140	6643–6640.5
	No sample recovery. No core attempted.	140–145	6640.5–6635.5
	Volcanic tuff, light pinkish gray (5YR 7/2), weakly to moderately welded, friable. Composed of 20–30% vitric pumice fragments, white (2–10 mm) and locally larger (10–40 mm) yellow-orange; 5–15% quartz-sanidine phenocrysts (1–2 mm); 10–20% dark colored intermediate volcanic lithics (1–4 mm); 40–50% vitric ash matrix.	145–152.5	6635.5–6628
	No sample recovery. No core attempted.	152.5–167.5	6628–6613
	Volcanic tuff, light pinkish gray (5YR 7/2), weakly to moderately welded, friable. Composed of 10–20% vitric pumice fragments, white (1–3 mm); 10–20% quartz-sanidine phenocrysts (1–2 mm); 5–15% dark colored volcanic lithics (dacite, 2–10 mm); 50–60% vitric ash matrix.	167.5–172.5	6613–6608
	No sample recovery. No core attempted.	172.5–187.5	6608–6593
	Volcanic tuff, light pinkish gray (5YR 7/2), weakly welded, friable. Composed of 10–20% vitric pumice fragments, white (2–10 mm) and locally yellow-orange (10–30 mm) that are limonite stained; 10–20% quartz-sanidine phenocrysts (1–2 mm); 5–15% gray volcanic lithics (dacite, 0.5–4 mm); 40–50% vitric ash matrix.	187.5–192.5	6593–6588
	No sample recovery. No core attempted.	192.5–207.5	6588–6573

Geologic Unit	Lithologic Description[a]	Sample Interval (ft)	Elevation Range (ft above msl)
Qbo, Otowi Member of the Bandelier Tuff (cont.)	Volcanic tuff, light pinkish gray (5YR 7/2), weakly welded, friable. Composed of 10–20% vitric pumice fragments, white (2–5 mm) and locally dark yellow-orange (10–30 mm) that are Fe-oxide (limonite) stained; 10–20% quartz-sanidine phenocrysts (1–2 mm); 5–15% gray dacite volcanic lithics (0.5–2 mm); 40–50% vitric ash matrix.	207.5–212.5	6573–6568
	No sample recovery. No core attempted.	212.5–227.5	6568–6553
	Volcanic tuff, light pinkish gray (5YR 7/2), weakly welded, friable. Composed of 10–20% white devitrified pumice (1–4 mm) and locally dark yellow-orange (10 YR 6/6, 10–30 mm) that are Fe-oxide (limonite) stained; 10–20% quartz-sanidine phenocrysts (1 mm); 5–15% dacite lithic fragments (0.5 –2 mm); 40–50% clay-rich, devitrified ash matrix.	227.5–232.5	6553–6548
	No sample recovery. No core attempted.	232.5–247.5	6548–6533
	Volcanic tuff, light pinkish gray (5YR 7/2), weakly welded, friable. Composed of 10–20% vitric pumice fragments, white (1–5 mm) and locally dark yellow-orange, limonite-stained vitric pumice (10–30 mm) ; 10–20% quartz-sanidine phenocrysts (1 mm); 5–15% dark colored dacite lithic fragments (1–15 mm); 40–50% vitric ash matrix.	247.5–252.5	6533–6528
	No sample recovery. No core attempted.	252.5–267.5	6528–6513
	Volcanic tuff, light pinkish gray (5YR 7/2), weakly welded, friable. Composed of 10–20% vitric pumice, white (1–3 mm) and locally dark yellow-orange, limonite-stained vitric pumice (10–20 mm); 10–20% quartz-sanidine phenocrysts (1 mm); 5–15% dark colored dacite lithic fragments (0.5–2 mm); 40–50% vitric ash matrix.	267.5–270	6513–6510.5
	No sample recovery. No core attempted.	270–287.5	6510.5–6493
	Volcanic tuff, light pinkish gray (5YR 7/2), weakly welded, friable. Composed of 10–20% vitric pumice, white to brownish gray (5–40 mm), locally limonite-stained; 10–20% quartz-sanidine phenocrysts (1–2 mm); 5–15% dark colored dacite lithic fragments (1–4 mm); 40–50% vitric ash matrix.	287.5–292.5	6493–6488
	No sample recovery. No core attempted.	292.5–307.5	6488–6473
	Volcanic tuff, light pinkish gray (5YR 7/2), weakly welded, friable. Composed of 15–25% vitric pumice, tan colored (10–30 mm); 10–20% quartz-sanidine phenocrysts (1–2 mm), broken to subhedral; 5–15% dark (dacite) volcanic lithic fragments (1–3 mm); 40–50% vitric ash matrix.	307.5–310	6473–6470.5
	No sample recovery. No core attempted.	310–327.5	6470.5–6453
	Volcanic tuff, light pinkish gray (5YR 7/2), weakly welded, friable. Composed of 20–30% vitric pumice, white to tan colored (2–30 mm); 10–20% quartz-sanidine phenocrysts (1 mm), broken to subhedral; 10–20% dark (dacite) volcanic lithic fragments (0.5–3 mm); 30–40% vitric ash matrix.	327.5–330	6453–6450.5
	No sample recovery. No core attempted.	330–347.5	6450.5–6433

Geologic Unit	Lithologic Description[a]	Sample Interval (ft)	Elevation Range (ft above msl)
Qbo, Otowi Member of the Bandelier Tuff (cont.)	Volcanic tuff, light pinkish gray (5YR 7/2), weakly welded, friable. Composed of 20–30% vitric pumice, white (1–5 mm) to pale tan colored (10–30 mm); 10–20% quartz-sanidine phenocrysts (1 mm), broken to subhedral; 10–20% dark (dacite) volcanic lithic fragments (0.5–4 mm); 30–40% vitric ash matrix.	347.5–350	6433–6430.5
	Volcanic tuff, white (N9), pumice-rich. +10F (i.e., plus No. 10 sieve size fraction): 95–97% vitric pumice (up to 20 mm), vitreous luster, elongated vesicles surrounding quartz, sanidine, minor Mn-oxide; 1–3% dark colored lithic fragments (andesite, dacite) and quartz-sanidine crystals. Note: rotary drill cuttings collected and described from 347 to 740 ft bgs.	350–352	6430.5–6428.5
	Volcanic tuff, varicolored gray (N4) to white (N9), lithic-rich, moderately welded. +10F: 30–40% indurated tuff fragments (up to 15 mm), 20% quartz-sanidine crystals and vitric pumice, 40–50% porhyritic lithic fragments (dacite, rhyodacite and minor vitrophyre, up o 5 mm) that are subrounded to subangular, commonly with Fe-oxide coatings.	352–367	6428.5–6413.5
	Volcanic tuff, white (N9), pumice-rich lapilli tuff. +10F: 80–85% vitric pumice with vitreous luster and quartz-sanidine crystals, 15–20% gray to varicolored volcanic lithics of felsic to intermediate composition, minor vitrophyre; lithics commonly coated with Fe-oxide.	367–377	6413.5–6403.5
	Volcanic tuff, light pinkish gray (5YR 8/1), pumice- and lithic-rich. +10F: 30–50% vitric pumice (vitreous to earthy luster, up to 5 mm), and quartz-sanidine crystals; 50–70% porhyritic volcanic lithic fragments (up to 20 mm) of felsic to intermediate composition, minor black vitrophyre; lithics subrounded and broken, commonly coated with Fe-oxide. WR (i.e., unseived whole rock) sample clay rich at 377–387 ft.	377–392	6403.5–6388.5
Qbog, Guaje Pumice Bed	Air-fall tuff, white (N9), pumice-rich lapilli tuff. +10F: 95–97% vitric pumice fragments (up to 10 mm), vitreous luster, parallel elongated vesicles; 3–5% dacite lithic fragments (up to 5 mm).	392–402	6388.5–6378.5
Qbog	Air-fall tuff, pale tan (5YR 7/2), crystal- and lithic-rich. +10F: 15% white vitric pumice, vitreous luster, elongated vesicles; 10% dacite lithics and quartz-sanidine crystals.	402–407	6378.5–6373.5
	Air-fall tuff, pale pinkish gray (5YR 7/2), pumice-rich. +10F: 99% white (N9) vitric pumice fragments (up to 15 mm), earthy to vitreous luster, elongated vesicles; rare volcanic lithic fragments are strongly oxidized. WR sample at 407–412 ft is clay rich. Apparent Qbog/Tpf contact at 414 ft bgs.	407–417	6373.5–6363.5
Tpf	Clastic sediments, gravel with sand (GW), medium gray brown (5YR 4/1), pebble gravel (4–10 mm), fine to medium sand, clasts rounded to subrounded. WR/+10F: composed dominantly of siliceous porphyritic dacite, rhyodacite. The presence of basalt chips in the interval 427–432 ft suggests Tpf/Tb contact at approximately 429 ft.	417–432	6363.5–6348.5

Geologic Unit	Lithologic Description[a]	Sample Interval (ft)	Elevation Range (ft above msl)
Tb, Cerros del Rio Basalt	Basalt. WR/+10F: 75–85% basalt chips, dark gray (N3), porhyritic with aphanitic groundmass (GM), strongly vesicular, pale green olivine phenocrysts are fresh; replaced by iddingsite; 15–25% composed of a variety of subangular to subrounded volcanic (dacite, rhyodacite, andesite, pumice) clasts (up to 15 mm), Fe-oxide coatings common. +35F (plus No. 35 sieve size): orange brown clay present.	432–437	6348.5–6343.5
	No sample recovered.	437–442	6343.5–6338.5
	Basalt, medium gray (N4), porphyritic with aphanitic groundmass (GM), vesicular to scoriaceous. WR/+10F: olivine phenocrysts (1 mm) moderately fresh to oxidized, local inddingsite rims, Fe-oxide coating vesicles, local white clay filling vesicles and coating fracture surfaces. Rare olivine phenocrysts are replaced by iddingsite.	442–450	6338.5–6330.5
	Basalt, dark gray (N3) to reddish brown (5YR 6/4), strongly vesicular, olivine phenocrysts oxidized, prominent Fe-oxide and white clay coating fracture surfaces and vesicles. Interval of strong oxidation and apparent fracturing.	450–455	6330.5–6325.5
	Basalt, medium light gray (5YR 6/1), porphyritic with aphanitic GM, weakly vesicular to massive. +10F: dark brown olivine(?) phenocrysts appear oxidized (iddingsite alteration). WR sample at 455–465 ft is clay rich.	455–470	6325.5–6310.5
	Basalt, medium gray (N4), porphyritic with aphanitic GM, weakly vesicular. +10F: dark brown oxidized olivine(?) phenocrysts (1–4mm). WR sample clay rich.	470–480	6310.5–6300.5
	Basalt, medium gray (N4), weakly porphyritic, weakly vesicular. WR sample lacks clay content but otherwise this interval is similar to 470–480 ft.	480–495	6300.5–6285.5
	Basalt, medium gray (N4), porphyritic with aphanitic GM, weakly vesicular. +10F: olivine(?) and rare plagioclase phenocrysts somewhat altered, groundmass strongly altered (sericitized) and/or coated with rock flour, strong Fe-oxide coating fracture surfaces at 500-505 ft. WR sample at is very clay rich.	495–515	6285.5–6265.5
	Basalt, medium gray (N4), weakly porphyritic with aphanitic GM, partly aphyric. WR/+10F: rock is moderately to strongly altered, groundmass feldspars sericitized, rare secondary quartz coating fracture surfaces.	515–530	6265.5–6250.5
	Basalt, dark gray (N4), weakly porphyritic to aphyric, aphanitic. +10F: groundmass feldspars mostly altered to sericite. WR sample generally clayey or clay rich.	530–545	6250.5–6235.5
	Basalt, medium dark gray (N4), porphyritic with aphanitic GM. +10F: phenocrysts of olivine, plagioclase, and minor pyroxene; groundmass altered/recrystallized. WR sample is silty.	545–565	6235.5–6215.5
	Basalt, medium dark gray (N4), porphyritic with aphanitic GM. +10F: phenocrysts of olivine and plagioclase; groundmass altered/recrystallized.	565–570	6215.5–6210.5

Geologic Unit	Lithologic Description[a]	Sample Interval (ft)	Elevation Range (ft above msl)
Tb, Cerros del Rio Basalt	Basalt, medium to dark gray (N4 to N5), porphyritic with aphanitic GM. +10F: phenocrysts of olivine and plagioclase, iddingsite rims on some olivines; groundmass altered/recrystallized. WR samples are silty to clay-rich.	570–600	6210.5–6180.5
	Basalt, medium gray (N5), porphyritic with aphanitic GM, strongly vesicular to scoriaceous. +10F: phenocrysts of olivine and plagioclase; scoria locally Fe-oxide stained with calcite rinds.	600–605	6180.5–6175.5
	Basalt, light brownish gray (5YR 6/1), weakly porphyritic with aphanitic GM, vesicular to scoriaceous. +10F: phenocrysts of olivine and plagioclase, white balls of clay (amygdaloidal?) common. WR sample is silty to clay-rich.	605–610	6175.5–6170.5
	Basalt, grayish orange pink (5YR 7/2), aphyric, aphanitic, vesicular to scoriaceous. +10F: rare olivine-plagioclase phenocrysts, rinds and amygdules of clay common. WR sample is clayey. Interval may represent oxidized zone between basalt flows.	610–615	6170.5–6165.5
	Basalt, brownish gray (5YR 4/1), porphyritic with aphanitic GM. +10F: phenocrysts of olivine (up to 2mm) and plagioclase, groundmass altered/recrystallized.	615–630	6165.5–6150.5
	Basalt, medium gray (N5), porphyritic with aphanitic GM, vesicular. +10F: phenocrysts of olivine and plagioclase, amygdaloidal clay or zeolite(?) common. WR sample at 630–635 ft is clayey.	630–640	6150.5–6140.5
	Basalt, pinkish gray (5YR 8/1) aphyric to weakly porphyritic, weakly vesicular. +10F: olivine-pyroxene phenocrysts, numerous balls of (amydaloidal?) clay present. WR sample at is clay rich.	640–645	6140.5–6135.5
	Basalt, medium gray (N5), aphyric to weakly porphyritic, vesicular. +10F: few olivine phenocrysts, amygdaloidal clay or zeolite(?) common, clay coatings on fracture surfaces. WR samples are clayey.	645–660	6135.5–6120.5
	Basalt, dark gray (N4), weakly porphyritic with aphanitic GM, weakly vesicular. +10F: phenocrysts of olivine and pyroxene are corroded, groundmass altered (i.e., GM feldspars sericitized), minor white clay on fracture surfaces. WR sample is clay rich.	660–670	6120.5–6110.5
	Basalt, light gray (N6), weakly porphyritic with aphanitic GM. +10F: groundmass strongly altered, feldspars argillized or removed resulting in a pitted/corroded texture. +35F: free olivine crystals appear fresh.	670–675	6110.5–6105.5
	Basalt, medium gray (N5), porphyritic with aphanitic GM, weakly vesicular. +10F: olivine (up to 2 mm) phenocrysts fresh to locally replaced by iddingsite, vesicles commonly filled with white clay. WR sample is clay rich.	675–685	6105.5–6095.5
	Basalt, dark gray (N3), porphyritic with aphanitic GM, weakly vesicular. +10F: olivine phenocrysts appear corroded and are completely replaced by dark brown to reddish iddingsite, minor white clay filling some vesicles.	685–690	6095.5–6090.5
	Basalt, medium to light gray (N4-N5), porphyritic with aphanitic GM, weakly vesicular. +10F: olivine phenocrysts (up to 5mm) completely replaced by iddingsite, groundmass sericitized to argillized. WR sample is clay rich. Apparent Tb/Tpf contact at 708 ft bgs.	690–710	6090.5–6070.5

Geologic Unit	Lithologic Description[a]	Sample Interval (ft)	Elevation Range (ft above msl)
Tpf Puye Formation	Clastic sediments, clayey gravel (GC), reddish brown (10R 5/4), pebble gravel with silt/clay matrix, angular to subrounded clasts. +10F: 100% volcanic lithic fragments of felsic to intermediate composition.	710–715	6070.5–6065.5
	Clastic sediments, gravel with sand (GW), pale reddish brown (10R 6/2). +10F: 100% dacite to rhyodacite lithic clasts, rounded to subrounded.	715–720	6065.5–6060.5
	Clastic sediments, gravel with sand (GW), pale reddish brown (10R 5/4). +10F: 100% lithic clasts made up of rhyodacite, dacite (up to 10 mm), subangular to subrounded.	720–725	6060.5–6055.5
	Clastic sediments, gravel with sand (GP), light gray (N3). +10F: 100% quartz rhyodacite to rhyolite porphyry lithic clasts (4–20 mm), rounded to subrounded.	725–735	6055.5–6045.5
	Clastic sediments, gravel with sand and clay (GW), light gray (N3). +10F: 100% pebbles (4–10 mm) of quartz porphyry (rhyodacite, rhyolite), subangular to subrounded.	735–740	6045.5–6040.5
	Total borehole depth (TD) is at 740 ft bgs.		

Note: American Society for Testing Materials (ASTM) standards were used in describing the texture of drill chip samples for sedimentary rocks such as alluvium and the Puye Fanglomerate. ASTM method D 2488-90 incorporates the Unified Soil Classification System (USCS) as a standard for field examination and description of soils. The following is a glossary of standard USCS symbols used in the MCOBT-8.5 lithlog.

[a] GW = Well graded gravel; GP = Poorly graded gravel; GC = Clayey gravel

References

ASTM D 2488-90. Standard Practice and Identification of Soils (Visual-Manual Procedure)

Note: Cuttings were collected at nominal 5-ft intervals and divided into three sample splits: (1) unsieved, or whole rock (WR), sample; (2) +10F sieved fraction (No. 10 sieve equivalent to 2.0 mm); and (3) +35F sieved fraction (No. 35 sieve equivalent to 0.50 mm).

Note: The term "percent," as used in the above descriptions, refers to percent by volume for a given sample component.

Appendix D

Descriptions of Geologic Samples

APPENDIX D. DESCRIPTIONS OF GEOLOGIC SAMPLES

MCOBT-4.4 Geologic Samples

Sample Number	Description[a]
MCOBT-4.4-68	This polished thin section represents 21 fragments of vitric pumice from a single unit, sampled from core at 68 ft depth in MCOBT-4.4. All fragments are fine-tube pumice with colorless glass and <10% authigenic smectite coating tube walls. Rare felsic phenocrysts (0.4%) include plagioclase (55% of felsic phenocrysts, median area 0.24 mm^2) and sanidine (45%, 0.17 mm^2), and rare quartz (0.5%). Rare, unaltered magnetite (80 ppmV) and associated zircon (0.6 ppmV) constitute the only other primary minerals present.
MCOBT-4.4-502/507	This polished thin section represents 17 large fragments plus two small fragments separated from cuttings collected between 502 and 507 ft depths from drill hole MCOBT-4.4. Two large fragments (17% of split) are sandy argillite that represents the *in situ* sediment. These fragments contain massive authigenic smectite that fills sparse voids and coats the corner of a large lithic clast. Including phenocrysts within matrix and hydroclastic shards, felsic phenocrysts are 1.8% of the split; 56% of these are plagioclase and the remainder are quartz, all with an apparent volcanic provenance. Plagioclase dominates in matrix whereas quartz dominates in hydroclastic shards. Mafics are rare, with 150 ppmV hornblende, and 50 ppmV each biotite and strongly altered clinopyroxene. Traces of magnetite (50 ppmV) and ilmenite (5 ppmV), and metamorphic minerals muscovite (10 ppmV), epidote and garnet (each 5 ppmV) occur in matrix. Unless otherwise noted, all hydroclastic shards and lithic clasts contain acicular groundmass pyroxene, with orthopyroxene dominant, and all represent lava with substantial groundmass feldspar. One large and one small fragment each represent vitric massive pale brown glass, classified as hydroclastic shards. The small fragment (0.6% of split) contains as the sole phenocrysts 1.6% plagioclase, and is similar to the dacite of drill hole SHB-1. The large fragment (3.8% of split) contains 20% felsic phenocrysts of quartz (73% of felsic phenocrysts) and plagioclase (27%), and 0.3% blackened hornblende, and is assigned as rhyodacite of Rendija Canyon. Including hydroclastic shards and lithic clasts, 2 fragments assigned as dacite of SHB-1 represent 7.9% of the split, and contain phenocrysts of 0.2% plagioclase, 0.04% clinopyroxene, and 0.2% orthopyroxene. Including hydroclastic shards and lithic clasts, 12 large fragments assigned as rhyodacite of Rendija Canyon, frequently with vapor-phase alteration, represent 67% of the split, and contain 8.5% felsic phenocrysts of plagioclase (71% of felsic phenocrysts), quartz (27%), and a trace of sanidine (0.8%). Mafics include 0.55% biotite, 0.14% hornblende, both blackened to pseudomorphic, 0.02% clinopyroxene, and 0.03% mafic pseudomorphs. Fe-Ti oxides are magnetite (0.18%) and generally unaltered ilmenite (0.02%), and unaltered accessories are apatite (110 ppmV), sphene (35 ppmV), and zircon (19 ppmV). The rare sanidine correlates with rhyodacite of Rendija Canyon from the Pueblo Canyon area. Two large and one very small fragment (7.9% of split) represent unidentified units of the Tschicoma Formation that contain phenocrysts of plagioclase (2-5% of such clasts), clinopyroxene (0.3%), and biotite (0.2%).
MCOBT-4.4-522/527	This polished thin section represents 24 fragments separated from cuttings collected between 522 and 527 ft depths from drill hole MCOBT-4.4. All fragments represent argillic medium grained pilotaxitic basalt with common phenocrysts of olivine (2.8% of split, median area 0.51 mm2) and scarce microphenocrysts of plagioclase (3.2%, 0.049 mm^2). The olivine phenocrysts contain 0.35% inclusions of spinel. Smectite (21.8%) fills large vesicles up to 1 mm in diameter and microvesicles, replacing all antecedent glass and most olivine phenocrysts except within two fragments, where olivine phenocrysts are unaltered except for thin iddingsite rims. Although unaltered in most fragments, plagioclase microphenocrysts are partly to mostly replaced by smectite within a few fragments where in close proximity to large voids entirely filled with smectite. Groundmass mafics are unaltered clinopyroxene (9.8%, 0.0005 mm^2) and pseudomorphic olivine (1.3%, 0.0004 mm^2). Groundmass olivine has been replaced by iddingsite within the two least altered fragments, and partly to iddingsite, mostly to smectite within all other fragments; thus its abundance might be underestimated due to the pervasive presence of smectite. Unaltered groundmass Fe-Ti oxides are magnetite (1.9%, 0.00004 mm^2) and acicular ilmenite (50 ppmV).

MCOBT-4.4-542/547	This polished thin section represents 11 large fragments separated from cuttings collected between 542 and 547 ft depths from drill hole MCOBT-4.4, and one tiny fragment. All fragments represent medium grained pilotaxitic basalt with scarce to common microphenocrysts of plagioclase (7.0% of split, median area 0.059 mm^2) and scarce phenocrysts of olivine (1.2%, 0.30 mm^2), which contain 0.64% inclusions of unaltered spinel and generally show thin iddingsite rims. The basalt is slightly vesicular (3.1% voids), with the two largest vesicles, each 2 mm square, free of secondary minerals. Minor smectite (0.9%) fills one large vesicle >1 mm long at the edge of one fragment, and another, elongate vesicle with a long axis of 0.7 mm. Minor cryptocrystalline groundmass constitutes 3.1% of the split. Groundmass mafics are unaltered clinopyroxene (14.4%, 0.0008 mm^2) and olivine (7.6%, 0.0007 mm^2), which often has thin iddingsite rims. Groundmass magnetite (1.8%, 0.00004 mm^2) occurs primarily in skeletal forms, and is moderately to strongly oxidized to maghemite.
MCOBT-4.4-562/567	This polished thin section represents three large fragments, one very large, separated from cuttings collected between 562 and 567 ft depths from drill hole MCOBT-4.4. All fragments represent medium-grained pilotaxitic basalt with common phenocrysts of olivine (3.6% of split, median area 0.36 mm^2), and scarce to common microphenocrysts of plagioclase (5.7%, 0.047 mm^2). Olivine phenocrysts contain 0.39% inclusions of unaltered spinel, generally show thin iddingsite rims, and are often blackened, particularly at rims. The basalt is moderately vesicular (6.8% voids), with generally squarish vesicles to 3 by 1 mm, free of secondary minerals. Minor smectite (3.2%) fills one large vesicle 1.8 mm long, and replaces a single olivine phenocryst. Minor cryptocrystalline groundmass constitutes 2.9% of the split. Groundmass mafics are unaltered clinopyroxene (12.9%, 0.00055 mm^2) and olivine (2.9%, 0.0011 mm^2), which is often blackened, particularly at rims. Groundmass magnetite (4.6%, 0.0001 mm^2) occurs primarily in skeletal forms, and is unaltered to moderately oxidized to maghemite. Unaltered ilmenite (500 ppmV) occurs as tiny groundmass laths.
MCOBT-4.4-592/597	This polished thin section represents four large fragments separated from cuttings collected between 592 and 597 ft depths from drill hole MCOBT-4.4. All fragments represent fine to medium-grained pilotaxitic basalt; three (60.7% of split) have minor cryptocrystalline groundmass (5.9%), which is a major constituent (23%) within the fourth fragment. Except for magnetite, absent within the fourth fragment, mineral abundances are indistinguishable among the fragments and their areas are also indistinguishable, except for groundmass clinopyroxene, more than a order of magnitude smaller with a median area of 0.00002 mm^2 within the fourth fragment versus 0.00033 mm^2 in the others. Minerals analyzed within the fourth fragment are designated within host “devitrified matrix”. Together, the four fragments contain common phenocrysts of olivine (3.0% of split, median area 0.19 mm^2), and scarce to common microphenocrysts of plagioclase (4.4%, 0.049 mm^2). Olivine phenocrysts contain 0.41% inclusions of unaltered spinel, and generally have thin iddingsite rims. The basalt is moderately vesicular (8.0% voids), with generally squarish vesicles to 2 mm, free of secondary minerals. Minor smectite (0.6%) fills one large vesicle. Groundmass mafics are unaltered clinopyroxene (13.3%, 0.0002 mm^2) and olivine (3.0%, 0.0009 mm^2), which generally has thin iddingsite rims. Groundmass magnetite (1.5%, 0.00004 mm^2) occurs primarily in skeletal forms, and is unaltered to moderately oxidized to maghemite.
MCOBT-4.4-632/637	This polished thin section represents three large and four small fragments separated from cuttings collected between 632 and 637 ft depths from drill hole MCOBT-4.4. All fragments represent fine- to medium-grained pilotaxitic basalt with minor cryptocrystalline groundmass (2.4%), common to abundant phenocrysts of olivine (5.5% of split, median area 0.34 mm^2), and scarce to common microphenocrysts of plagioclase (2.8%, 0.061 mm^2). Olivine phenocrysts contain 0.46% inclusions of spinel. All primary phases are unaltered. The basalt is slightly vesicular (2.4% voids). Groundmass mafics are clinopyroxene (11.9%, 0.0004 mm^2) and olivine (8.0%, 0.0005 mm^2). Groundmass magnetite (1.8%, 0.00095 mm^2) is markedly coarser than in samples of overlying basalt, and generally tiny, acicular ilmenite (200 ppmV) sometimes mantles magnetite.
MCOBT-4.4-657/662	This polished thin section represents three large and two small fragments separated from cuttings collected between 657 and 662 ft depths from drill hole MCOBT-4.4. All fragments represent medium-grained pilotaxitic basalt with common to abundant phenocrysts of olivine (5.9% of split, median area 0.29 mm^2), and scarce to common microphenocrysts of plagioclase (3.6%, 0.042 mm^2). Olivine phenocrysts contain 0.26% inclusions of spinel. A single

	clinopyroxene phenocryst (0.04%) occurs as a glomerophyric intergrowth with plagioclase, and may represent minor ophitic crystallization rather than phenocryst agglomeration. All primary phases except for magnetite are unaltered. The basalt is moderately vesicular (6.5% voids), with generally squarish vesicles to 0.7 mm, free of secondary minerals. Groundmass mafics are clinopyroxene (13.0%, 0.0006 mm^2) and olivine (6.2%, 0.0011 mm^2), and relatively coarse groundmass Fe-Ti oxides are slightly to moderately oxidized magnetite (0.3%) and ilmenite laths (0.3%).
MCOBT-4.4-672/677	This polished thin section represents six large fragments and one small fragment separated from cuttings collected between 672 and 677 ft depths from drill hole MCOBT-4.4. All fragments represent fine- to medium-grained pilotaxitic basalt with minor cryptocrystalline groundmass (3.6%), common to abundant phenocrysts of olivine (6.5% of split, median area 0.38 mm^2), and scarce to common microphenocrysts of plagioclase (4.9%, 0.059 mm^2). Olivine phenocrysts contain 0.32% inclusions of spinel and generally have thin iddingsite rims. Rare clinopyroxene phenocrysts (0.03%) are strongly resorbed. The basalt is slightly to moderately vesicular (4.5% voids), with the largest vesicle 0.6 by 0.3 mm, lined by a reaction rim of groundmass clinopyroxene, which probably represents a reaction rim with a xenocryst of quartz that lies outside the thin section plane. One large vesicle is filled with massive smectite, which is otherwise rare (0.6%). Groundmass mafics are unaltered clinopyroxene (13.0%, 0.0005 mm^2) and olivine (6.5%, 0.0012 mm^2), which is strongly altered to iddingsite. Groundmass Fe-Ti oxides are skeletal, moderately oxidized magnetite (3.6%, 0.00004 mm^2), tiny within three fragments with the darkest matrix, but in other fragments considerably coarser and accompanied by acicular ilmenite laths (200 ppmV of split).
Sample Number	Description[a]
MCOBT-4.4-712/717	This polished thin section represents three large, two small, and three tiny fragments separated from cuttings collected between 712 and 717 ft depths from drill hole MCOBT-4.4. All fragments represent medium- to coarse-grained, slightly vesicular pilotaxitic basalt with 1.5% voids, common to abundant phenocrysts of olivine (6.1% of split, median area 0.50 mm^2), and scarce microphenocrysts of plagioclase (1.5%, 0.051 mm^2). Olivine phenocrysts contain 0.50% inclusions of spinel. A single clinopyroxene phenocryst (0.1%), intergrown with olivine, is strongly resorbed. Unaltered groundmass mafics are clinopyroxene (13.0%, 0.0016 mm^2) and olivine (7.8%, 0.0016 mm^2). Coarse, slightly oxidized groundmass Fe-Ti oxides are magnetite (3.0%, 0.0032 mm^2) and ilmenite (2000 ppmV).
MCOBT-4.4-737/742	This polished thin section represents 22 fragments of lithics from a clastic sediment at 737-742 ft depth in drill hole MCOBT-4.4. With only 0.11% adhering matrix, the nature of the finer matrix is unknown. All fragments were derived from lavas; one of these, 5.2% by volume, is classified as a vitric hydroclast with brown glass that constitutes 3.0% of the split. This vitric hydroclast, together with 12 clasts of devitrified, somewhat felty, and often vapor-phase lava, constitute 55% of the split and are assigned as upper dacite of Pajarito Mountain. Phenocrysts in these clasts are plagioclase (13%), mafics of orthopyroxene (3.7%), clinopyroxene (0.57%), and hornblende pseudomorphs (0.056%), Fe-Ti oxides of magnetite (0.47%) and ilmenite (760 ppmV), and apatite (290 ppmV). Five clasts of devitrified, moderately felty, somewhat vapor-phase lava constitute 31% of the split and are assigned as dacite of Caballo Mountain. Phenocrysts in these clasts are plagioclase (4.6%), mafics of orthopyroxene (2.7%), clinopyroxene (1.3%), generally blackened hornblende pseudomorphs (1.2%), and generally blackened and/or pseudomorphic biotite (1.2%), Fe-Ti oxides of magnetite (0.64%) and ilmenite (200 ppmV), and apatite (1100 ppmV), and a trace of zircon (6 ppmV). Two clasts of devitrified, moderately felty, somewhat vapor-phase lava constitute 8.7% of the split and are assigned as rhyodacite of Rendija Canyon. Phenocrysts in these clasts are plagioclase (4.1%) and a single grain of quartz (0.16%), mafics of blackened pseudomorphs of both biotite (0.87%) and hornblende (0.11%), magnetite (0.012%), and apatite (58 ppmV). A single clast of devitrified lava constitutes 3.3% of the split and is assigned as latite of Los Alamos Canyon. Phenocrysts in this clast are plagioclase (12%), mafics of clinopyroxene (8.5%) and orthopyroxene (4.5%), Fe-Ti oxides of magnetite (0.86%) and ilmenite (0.56%), and apatite (310 ppmV). The final remaining clast of devitrified, moderately felty lava constitutes 2.8% of the split and is assigned as dacite of drill hole SHB-1. Phenocrysts in this clast are plagioclase (0.84%), mafics of orthopyroxene (2.2%) and clinopyroxene (0.55%), magnetite (0.63%), and apatite (360 ppmV).

MCOBT-4.4-762/767	This polished thin section represents 21 fragments of lithics from a clastic sediment at 762-767 ft depth in drill hole MCOBT-4.4. With only 0.05% adhering matrix, the nature of the finer matrix is unknown. All fragments were derived from lavas; one of these, 4.4% by volume, is classified as a vitric hydroclast with brown glass that constitutes 3.3% of the split. This vitric hydroclast, together with 15 clasts of devitrified, moderately felty, and often vapor-phase lava, constitute 83% of the split and are assigned as upper dacite of Pajarito Mountain. Phenocrysts in these clasts are plagioclase (13%), mafics of orthopyroxene (3.8%), clinopyroxene (0.53%), and blackened biotite (0.010%), Fe-Ti oxides of magnetite (0.55%) and ilmenite (360 ppmV), and apatite (260 ppmV). Three clasts of devitrified, somewhat felty, moderately vapor-phase lava constitute 7.3% of the split and are assigned as dacite of Caballo Mountain. Phenocrysts in these clasts are plagioclase (9.9%), mafics of orthopyroxene (1.2%), clinopyroxene (0.66%), almost entirely pseudomorphic hornblende (0.61%), and blackened biotite (0.29%), Fe-Ti oxides of magnetite (1.5%) ilmenite (89 ppmV), and apatite (210 ppmV). A single clast of devitrified, moderately felty lava constitutes 7.3% of the split and is assigned as rhyodacite of Rendija Canyon. Phenocrysts in this clast are plagioclase (1.3%) and quartz (0.82%), mafics of blackened biotite (0.54%) and clinopyroxene (0.025%), magnetite (0.086%), and apatite (18 ppmV). The final remaining clast of devitrified, somewhat felty, and moderately vapor-phase lava constitutes 2.3% of the split and is assigned as latite of Los Alamos Canyon. Phenocrysts in this clast are plagioclase (19%), mafics of clinopyroxene (1.9%) and orthopyroxene (0.59%), magnetite (1.1%), and apatite (550 ppmV).

MCOBT-8.5 Geologic Samples

Sample Number	Description[a]
MCOBT-8.5-422/427	This polished thin section represents 11 clasts separated from sedimentary rock, as well as one large and one small pumice fragment, and one fragment of clastic matrix at 422–427 ft depth in drill hole MCOBT-8.5. The fragment of matrix is argillic sandstone with smectite coatings on particles, but vitric pyroclasts that contribute 8.1% glass strongly dominate. Within this matrix, and including all pyroclasts, are felsic phenocrysts (1.65% of split) of quartz (50% of felsic phenocrysts), sanidine (34%), and plagioclase (15%). Other phenocrysts are magnetite (300 ppmV of split), clinopyroxene (280 ppmV), hornblende (81 ppmV), biotite (57 ppmV), sphene (38 ppmV), rutile/anatase (15 ppmV), garnet (9 ppmV), apatite (8 ppmV), and zircon (6 ppmV). Lithics dominate the split (76%), all 10 such clasts derived from lavas. The remaining large clast is classified as a vitric hydroclast with colorless glass; such pyroclasts constitute 8.2% of the split. This vitric hydroclast, together with 8 clasts of devitrified, somewhat felty, and often vapor-phase lava, constitute 82% of the lithics plus hydroclasts, and are assigned as rhyodacite of Rendija Canyon. Felsic phenocrysts (5.8% of such clasts) are plagioclase (59% of felsic phenocrysts), quartz (30%), and sanidine (11%), with feldspar often very strongly resorbed. Other phenocrysts are generally blackened biotite (1.1% of such clasts) that is often reacted with matrix, generally blackened, almost entirely pseudomorphic hornblende (0.28%), clinopyroxene (0.081%), Fe-Ti oxides of magnetite (0.13%) and ilmenite (26 ppmV), sphene (140 ppmV), apatite (130 ppmV), and zircon (4 ppmV). One clast of devitrified, somewhat felty lava constitutes 10% of such clasts and is assigned as dacite of drill hole SHB-1. Phenocrysts in this clast are plagioclase (1.8%), and mafics of clinopyroxene (0.64%) and orthopyroxene (0.15%). The final remaining clast is moderately felty lava. All primary phases within this clast have been destroyed by hydrothermal alteration, yielding a secondary mineral assemblage that includes epidote plus an unrecognized phase thought to be amphibole. The two pumice clasts separated constitute 99% of the colorless pumice that constitutes 8.8% of the split. Phenocrysts in these clasts are sanidine (2.75%), quartz (0.32%), clinopyroxene (26 ppmV), and magnetite (170 ppmV). These pumices are assigned as a presently unrecognized precursor unit of the Bandelier Tuff.

MCOBT-8.5-432/437	This polished thin section represents 9 fragments separated from cuttings collected between 432 and 437 ft depths from drill hole MCOBT-8.5. One partly vitric fragment contains orange-brown glass; all other fragments represent fine-grained pilotaxitic basalt, and all fragments contain cryptocrystalline matrix (9.2% of split). Microphenocrysts of plagioclase (4.1% of split, median area 0.027 mm^2) and phenocrysts of olivine (2.2%, 0.19 mm^2) are both scarce to common; olivine contains 0.72% inclusions of unaltered spinel and generally shows thin iddingsite rims. The basalt is moderately to highly vesicular (16% voids), with vesicles generally free of secondary minerals, although minor smectite (0.3%) fills a few vesicles. Groundmass mafics are micro-ophitic, unaltered clinopyroxene (12.0%, 0.0002 mm^2) and olivine (3.8%, 0.0011 mm^2), which often has iddingsite rims. Groundmass magnetite (0.3%, 0.00004 mm^2) is entirely oxidized to maghemite. Silty particles (0.3% of split) that are mostly colorless glass shards partly fill a large void. The meniscus of these particles forms an angle of 70 degrees to the meniscus of clay partly filling the same void. This discordance suggests that the glass shards represent contaminant added from drilling or less likely from preparation of the thin section.
MCOBT-8.5-460/465	This polished thin section represents 14 fragments, one very small, separated from cuttings collected between 460 and 465 ft depths from drill hole MCOBT-8.5. All fragments represent medium-grained pilotaxitic basalt with a trace of cryptocrystalline matrix (0.3% of split). The basalt is slightly vesicular, with 3.9% voids up to 0.5 by 0.8 mm. Microphenocrysts of plagioclase (3.6% of split, median area 0.061 mm^2) are scarce to common and phenocrysts of olivine (3.2%, 0.35 mm^2) are common. The olivine contains 0.96% inclusions of strongly altered spinel and generally has thin iddingsite rims, except within a single fragment, where it is altered to opaque pseudomorphic forms. Groundmass mafics are unaltered clinopyroxene (12.1%, 0.0005 mm^2) and olivine (6.0%, 0.0009 mm^2), which often has iddingsite rims. Coarse groundmass magnetite (3.9%, 0.0005 mm^2) is strongly oxidized to maghemite. Acicular apatite (7100 ppmV, 0.00006 mm^2) is ubiquitous in the groundmass.
MCOBT-8.5-485/490	This polished thin section represents 8 fragments, two very small, separated from cuttings collected between 485 and 490 ft depths from drill hole MCOBT-8.5. All fragments represent slightly vesicular, fine- to medium-grained pilotaxitic basalt with 3.6% voids and minor cryptocrystalline matrix (2.7% of split). Microphenocrysts of plagioclase (3.3% of split, median area 0.12 mm^2) are scarce to common. Common to abundant moderately altered phenocrysts of olivine (5.5%, 0.36 mm^2) contain 0.77% inclusions of moderately altered spinel. Groundmass mafics are unaltered clinopyroxene (11.2%, 0.0009 mm^2) and moderately altered olivine (5.8%, 0.0014 mm^2). Coarse groundmass magnetite (2.2%, 0.0080 mm^2) is almost entirely oxidized to maghemite and limonite. Two fragments contain microporphyritic and vitric lenses (7.9% of split), lacking phenocrysts of plagioclase and olivine, but with a groundmass mineralogy similar to host basalt, albeit with much coarser groundmass phases, and a ubiquitous presence of acicular apatite. The median area for groundmass plagioclase within such vitric lenses is 0.039 mm^2, at least 5 times larger than within the host, with an abundance of 46.15% from point count. Vesicles associated with these lenses generally are completely filled with clay (0.3% of split). Colorless glass constitutes 23% of these lenses, indicating that they reflect reaction of host basalt with rhyolite, either as magma or as vitric clasts.
MCOBT-8.5-545/550	This polished thin section represents 8 fragments separated from cuttings collected between 545 and 550 ft depths from drill hole MCOBT-8.5. All fragments represent massive medium-grained pilotaxitic basalt. Smectite is pervasive as a partial filling in microvesicles and partly replaces olivine phenocrysts and groundmass. Microphenocrysts of plagioclase (8.1% of split, median area 0.11 mm^2) are common and those of clinopyroxene (122 ppmV) are rare. Common to abundant phenocrysts of olivine (6.8%, 0.34 mm^2) contain 0.69% inclusions of unaltered spinel. Groundmass mafics are unaltered clinopyroxene (13.6%, 0.0015 mm^2) and olivine (6.8%, 0.0034 mm^2). Very coarse groundmass magnetite (1.3%, 0.0120 mm^2) is strongly intergrown with ilmenite (6500 ppmV); both phases are unaltered.

MCOBT-8.5-565/570	This polished thin section represents 10 fragments separated from cuttings collected between 565 and 570 ft depths from drill hole MCOBT-8.5. All fragments represent massive fine-grained pilotaxitic basalt. Smectite fills microvesicles and rare vesicles to 0.7 mm diameter, and to a lesser extent partly replaces olivine phenocrysts and groundmass and plagioclase phenocrysts. Phenocrysts of plagioclase (3.7% of split, median area 0.21 mm^2) are scarce to common. Common phenocrysts of olivine (3.7%, 0.47 mm^2) contain 0.27% inclusions of unaltered spinel. Groundmass mafics are unaltered clinopyroxene (15.1%, 0.0005 mm^2), olivine (4.0%, 0.0008 mm^2), and rare euhedral orthopyroxene (100 ppmV) protruding into vesicles. Coarse groundmass magnetite (3.5%, 0.0015 mm^2) is strongly intergrown with ilmenite (8000 ppmV), encasing much of the ilmenite; both phases are unaltered. Acicular apatite (6200 ppmV, 0.00006 mm^2) is ubiquitous in groundmass.
MCOBT-8.5-595/600	This polished thin section represents 7 fragments, one small, and another very small, separated from cuttings collected between 595 and 600 ft depths from drill hole MCOBT-8.5. All fragments represent massive fine-grained pilotaxitic basalt. Recognizable voids constitute 0.7% of the split; a trace of smectite lines larger vesicles. Phenocrysts of plagioclase (3.4% of split, median area 0.10 mm^2) are scarce to common. Common to abundant phenocrysts of olivine (5.8%, 0.36 mm^2) contain 0.21% inclusions of unaltered spinel and are altered to iddingsite along thin rims and fractures, as is groundmass olivine. Groundmass mafics are unaltered clinopyroxene (11.3%, 0.0002 mm^2) and olivine (5.1%, 0.0007 mm^2). Medium-grained to coarse groundmass magnetite (2.4%, 0.0004 mm^2) is strongly intergrown in coarser grains with ilmenite (1.0%), encasing much of the ilmenite; both phases are unaltered. Acicular apatite (3400 ppmV, 0.00006 mm^2) is ubiquitous in groundmass.
MCOBT-8.5-625/630	This polished thin section represents 7 fragments, three small, separated from cuttings collected between 625 and 630 ft depths from drill hole MCOBT-8.5. All fragments represent moderately microvesicular fine- to medium-grained pilotaxitic basalt with voids 4.5% of the split. Microphenocrysts of plagioclase (3.9% of split, median area 0.079 mm^2) are scarce to common. Common unaltered phenocrysts of olivine (3.9%, 0.63 mm^2) contain 0.34% inclusions of unaltered spinel. Groundmass mafics are unaltered clinopyroxene (9.3%, 0.0009 mm^2) and slightly altered olivine (5.7%, 0.0009 mm^2). Moderately coarse groundmass magnetite (3.6%, 0.0022 mm^2) is moderately altered and ilmenite (6200 ppmV) is unaltered. Acicular apatite (3000 ppmV, 0.00002 mm^2) is ubiquitous in groundmass.
MCOBT-8.5-670/675	This polished thin section represents 11 fragments separated from cuttings collected between 670 and 675 ft depths from drill hole MCOBT-8.5. All fragments represent slightly vesicular medium-grained pilotaxitic basalt with voids 4.7% of the split; rare smectite thinly lines vesicles. Microphenocrysts of plagioclase (1.7% of split, median area 0.044 mm^2) are scarce. Abundant unaltered phenocrysts of olivine (9.1%, 0.74 mm^2) are often zoned and contain 0.36% inclusions of unaltered spinel. Unaltered groundmass mafics are clinopyroxene (9.4%, 0.0014 mm^2) and olivine (6.7%, 0.0022 mm^2). Coarse groundmass magnetite (4.0%, 0.0017 mm^2) and much finer ilmenite laths (3400 ppmV) are both unaltered. Acicular apatite occurs in groundmass.
MCOBT-8.5-700/705	This polished thin section represents 7 fragments separated from cuttings collected between 700 and 705 ft depths from drill hole MCOBT-8.5. All fragments represent slightly vesicular, fine- to medium-grained pilotaxitic basalt with 1.8% voids. Common to abundant phenocrysts of olivine (6.7%, 0.25 mm^2) have thin iddingsite rims and contain 0.30% inclusions of unaltered spinel. Groundmass mafics are unaltered clinopyroxene (15.8%, 0.0008 mm^2) and almost entirely pseudomorphic, blackened olivine (2.5%, 0.0011 mm^2). Coarse groundmass magnetite (4.6%, 0.0016 mm^2) is strongly oxidized to maghemite, and tiny ilmenite laths occur in low abundance. Acicular apatite (3500 ppmV, 0.00006 mm^2) is ubiquitous in groundmass. Two fragments contain microporphyritic lenses (13.3% of split), lacking phenocrysts of plagioclase and olivine, but with a groundmass mineralogy similar to the host basalt, albeit with much coarser groundmass phases and a ubiquitous presence of acicular apatite. The median area for groundmass feldspar within such vitric lenses is at least 5 times larger than within host, with an abundance of 60.53% from point count. Minor microspherulitic groundmass and colorless glass, both rhyolitic, occur within the smaller lens, indicating that these lenses reflect reaction of host basalt with rhyolite, either as magma or as vitric clasts. The highly irregular shape of the larger lens suggests magma mixing.

MCOBT-8.5-730/735	This polished thin section represents 18 clasts separated from sedimentary rock at 730-735 ft depth in drill hole MCOBT-8.5. With only 0.25% adhering matrix, the nature of this sediment is unknown. Lithics dominate the split (91%); all 16 such clasts are derived from devitrified, felty, and often vapor-phase lavas. The two remaining clasts are classified as vitric hydroclasts, one with colorless glass (5.5% of split), and the other with pale brown glass (3.0% of split). These hydroclasts contribute 6.2% glass to the split. All clasts are assigned as rhyodacite of Rendija Canyon. Felsic phenocrysts (4.4% of such clasts) are plagioclase (86.7% of felsic phenocrysts), quartz (13%), and sanidine (0.3%), with feldspar often very strongly resorbed. Mafic phenocrysts are generally blackened biotite (1700 ppmV of such clasts), clinopyroxene (460 ppmV), and single grains of pseudomorphic hornblende (120 ppmV), reacted with matrix, and blackened orthopyroxene (34 ppmV). Fe-Ti oxides are generally strongly oxidized magnetite (750 ppmV) and slightly oxidized ilmenite (71 ppmV), and accessories are apatite (140 ppmV), sphene (39 ppmV), and zircon (5 ppmV). Sphene is slightly blackened and often jacketed by limonite. Acicular pyroxene, mostly somewhat altered orthopyroxene, is abundant within groundmass.

[a] ppmV = parts per million by volume

Appendix E

Moisture Results for Core Samples

APPENDIX E. MOISTURE RESULTS FOR CORE SAMPLES

MCOBT-4.4					
Laboratory Sample ID	Upper Depth (ft)	Lower Depth (ft)	Loss at 110°C wt. % [a]	Water Content wt. % [b]	ER Sample ID
MC0BT4.4-4.3	3.9	4.3	6.09	6.48	GWM4-01-0031
MC0BT4.4-9.9	9.7	9.9	8.88	9.74	GWM4-01-0032
MC0BT4.4-14.6	14.3	14.6	7.01	7.53	GWM4-01-0033
MC0BT4.4-19.3	19.0	19.3	12.83	14.71	GWM4-01-0034
MC0BT4.4-25	24.8	25.0	12.77	14.64	GWM4-01-0035
MC0BT4.4-29.8	29.6	29.8	18.59	22.83	GWM4-01-0036
MC0BT4.4-35	34.8	35.0	22.14	28.44	GWM4-01-0037
MC0BT4.4-40	39.8	40.0	14.20	16.56	GWM4-01-0038
MC0BT4.4-47.5	47.3	47.5	21.11	26.76	GWM4-01-0039
MC0BT4.4-50	49.8	50.0	21.09	26.72	GWM4-01-0040
MC0BT4.4-57.5	57.3	57.5	15.48	18.32	GWM4-01-0041
MC0BT4.4-60	59.8	60.0	13.10	15.07	GWM4-01-0042
MC0BT4.4-65	64.8	65.0	28.37	39.60	GWM4-01-0043
MC0BT4.4-70	69.8	70.0	21.61	27.57	GWM4-01-0044
MC0BT4.4-75	74.8	75.0	19.67	24.48	GWM4-01-0045
MC0BT4.4-79.5	79.3	79.5	26.16	35.43	GWM4-01-0046
MC0BT4.4-85	84.8	85.0	11.40	12.87	GWM4-01-0047
MC0BT4.4-90	89.8	90.0	15.41	18.21	GWM4-01-0048
MC0BT4.4-95	94.8	95.0	11.55	13.06	GWM4-01-0049
MC0BT4.4-100	99.8	100.0	18.86	23.24	GWM4-01-0050
MC0BT4.4-105	104.8	105.0	15.68	18.60	GWM4-01-0051
MC0BT4.4-110	109.8	110.0	13.91	16.16	GWM4-01-0052
MC0BT4.4-115	114.8	115.0	14.30	16.68	GWM4-01-0053
MC0BT4.4-120	119.8	120.0	13.82	16.03	GWM4-01-0054
MC0BT4.4-125	124.8	125.0	14.02	16.31	GWM4-01-0055
MC0BT4.4-132.5	132.3	132.5	14.35	16.76	GWM4-01-0056
MC0BT4.4-135	134.8	135.0	13.93	16.19	GWM4-01-0057
MC0BT4.4-140	139.8	140.0	14.04	16.33	GWM4-01-0058
MC0BT4.4-145	144.8	145.0	14.91	17.52	GWM4-01-0059
MC0BT4.4-150	148.8	150.0	15.02	17.68	GWM4-01-0060
MC0BT4.4-155	154.8	155.0	14.02	16.30	GWM4-01-0061
MC0BT4.4-160	159.8	160.0	14.36	16.77	GWM4-01-0062
MC0BT4.4-172.5	172.3	172.5	13.96	16.22	GWM4-01-0063
MC0BT4.4-177.5	177.3	177.5	13.53	15.64	GWM4-01-0064
MC0BT4.4-185	184.8	185.0	14.08	16.39	GWM4-01-0065

Laboratory Sample ID	Upper Depth (ft)	Lower Depth (ft)	Loss at 110°C wt. % [a]	Water Content wt. % [b]	ER Sample ID
MC0BT4.4-190	189.8	190.0	14.01	16.30	GWM4-01-0066
MC0BT4.4-195	194.8	195.0	13.94	16.20	GWM4-01-0067
MC0BT4.4-205	204.8	205.0	13.70	15.88	GWM4-01-0068
MC0BT4.4-210	209.8	210.0	13.81	16.03	GWM4-01-0069
MC0BT4.4-215	214.8	215.0	13.86	16.08	GWM4-01-0070
MC0BT4.4-220	219.8	220.0	12.87	14.77	GWM4-01-0071
MC0BT4.4-225	224.8	225.0	12.84	14.73	GWM4-01-0072
MC0BT4.4-230	229.8	230.0	12.85	14.74	GWM4-01-0073
MC0BT4.4-237.5	236.3	237.5	13.12	15.10	GWM4-01-0074
MC0BT4.4-242.5	242.3	242.5	13.31	15.35	GWM4-01-0075
MC0BT4.4-245	244.8	245.0	12.72	14.57	GWM4-01-0076
MC0BT4.4-247.5	247.3	247.5	12.88	14.79	GWM4-01-0077
MC0BT4.4-272.5	272.3	272.5	14.50	16.96	GWM4-01-0078
MC0BT4.4-290	289.8	290.0	14.08	16.39	GWM4-01-0079
MC0BT4.4-310	309.8	310.0	14.64	17.15	GWM4-01-0080

[a] Loss at 110 degrees celcius calculated as wt loss/initial sample wt.

[b] Water content measured in accordance with ASTM D2216-90 (wt loss/dried sample wt).

MCOBT-8.5					
Laboratory Sample ID	**Upper Depth (ft)**	**Lower Depth (ft)**	**Loss at 110°C wt. % [a]**	**Water Content wt. % [b]**	**ER Sample ID**
MC0BT8.5-4.1	3.9	4.1	9.25	10.19	GWM8-01-0046
MC0BT8.5-8.9	8.7	8.9	9.46	10.45	GWM8-01-0047
MC0BT8.5-14.9	14.7	14.9	3.49	3.62	GWM8-01-0048
MC0BT8.5-22.4	22.2	22.4	1.86	1.90	GWM8-01-0049
MC0BT8.5-27.4	27.2	27.4	3.79	3.94	GWM8-01-0050
MC0BT8.5-32.4	32.2	32.4	2.27	2.33	GWM8-01-0051
MC0BT8.5-37.4	37.2	37.4	6.05	6.44	GWM8-01-0052
MC0BT8.5-42.4	42.2	42.4	11.35	12.81	GWM8-01-0053
MC0BT8.5-47.4	47.2	47.4	8.14	8.86	GWM8-01-0054
MC0BT8.5-52.1	51.9	52.1	2.76	2.84	GWM8-01-0055
MC0BT8.5-57.4	57.2	57.4	2.62	2.69	GWM8-01-0056
MC0BT8.5-62.4	62.2	62.4	10.99	12.35	GWM8-01-0057
MC0BT8.5-67.4	67.2	67.4	4.00	4.16	GWM8-01-0058
MC0BT8.5-72.4	72.2	72.4	10.65	11.92	GWM8-01-0059
MC0BT8.5-77.4	77.2	77.4	15.50	18.34	GWM8-01-0060
MC0BT8.5-82.4	82.2	82.4	11.46	12.95	GWM8-01-0061
MC0BT8.5-87.4	87.2	87.4	16.06	19.13	GWM8-01-0062

Laboratory Sample ID	Upper Depth (ft)	Lower Depth (ft)	Loss at 110°C wt. % [a]	Water Content wt. % [b]	ER Sample ID
MC0BT8.5-92.4	92.2	92.4	15.24	17.98	GWM8-01-0063
MC0BT8.5-97.4	97.2	97.4	18.32	22.42	GWM8-01-0064
MC0BT8.5-102.4	102.2	102.4	16.41	19.63	GWM8-01-0065
MC0BT8.5-107.4	107.2	107.4	27.03	37.05	GWM8-01-0066
MC0BT8.5-110.2	110.0	110.2	21.84	27.94	GWM8-01-0067
MC0BT8.5-114.9	114.7	114.9	16.93	20.39	GWM8-01-0068
MC0BT8.5-119.9	119.7	119.9	15.98	19.01	GWM8-01-0069
MC0BT8.5-124.9	124.7	124.9	16.11	19.21	GWM8-01-0070
MC0BT8.5-132.4	132.2	132.4	14.26	16.63	GWM8-01-0071
MC0BT8.5-137.4	137.2	137.4	13.97	16.23	GWM8-01-0072
MC0BT8.5-152.4	152.2	152.4	13.46	15.56	GWM8-01-0074
MC0BT8.5-172.4	172.2	172.4	14.89	17.49	GWM8-01-0075
MC0BT8.5-192.4	192.2	192.4	13.90	16.14	GWM8-01-0076
MC0BT8.5-212.4	212.2	212.4	13.17	15.17	GWM8-01-0077
MC0BT8.5-232.4	232.2	232.4	12.77	14.64	GWM8-01-0078
MC0BT8.5-252.4	252.2	252.4	13.20	15.20	GWM8-01-0079
MC0BT8.5-269.9	269.7	269.9	13.91	16.15	GWM8-01-0080
MC0BT8.5-292.4	292.2	292.4	14.05	16.34	GWM8-01-0082
MC0BT8.5-309.9	309.7	309.9	13.91	16.16	GWM8-01-0083
MC0BT8.5-329.2	329.1	329.2	15.06	17.73	GWM8-01-0084
MC0BT8.5-349.9	349.7	349.9	14.56	17.04	GWM8-01-0085

[a] Loss at 110°C calculated as wt loss/initial sample wt.

[b] Water content measured in accordance with ASTM D2216-90 (wt loss/dried sample wt).

Appendix F

Geophysical Logging Report
(on CD, inside back cover)

Appendix G

Montage of Well MCOBT-4.4
(on CD, inside back cover)

Appendix H

Montage of Borehole MCOBT-8.5
(on CD, inside back cover)

Appendix I

Borehole Video of Well MCOBT-4.4
(on CD, inside back cover)

Appendix J

Borehole Video of MCOBT-8.5
(on CD, inside back cover)

Appendix K

Geochemical Calculations (Input File for the Computer Program MINTEQA2)

APPENDIX K. GEOCHEMICAL CALCULATIONS (INPUT FILES FOR THE COMPUTER PROGRAM MINTEQA2)

A description of the input file for the computer program MINTEQA2 (Allison et al. 1991, 49930) is provided below.

Rows one and two (blank) consist of the title for the calculations.

Row three consists of temperature, units of concentration, and calculation of ionic strength.

Row four is blank.

Row five consists of query for charge balance termination (> 30%); alkalinity or inorganic carbon as carbonate; query for oversaturated solids that are not allowed to precipitate excluding infinite and finite phases; maximum number of iterations (40, 100, and 200); selection for calculating activity coefficient (Davies equation); level of output; pH; Eh or pe; and a query for choosing a different file to modify or return to output filename prompt.

Row six is blank.

Row seven contains zeros (not specific to input file).

Row eight is blank.

Rows nine through 28 contains species number, concentration, log base 10 activity, a prompt (y) for refining calculation of activity for each species, and the chemical symbol for each species.

Row 29 is blank.

Row 30 consists of pH input (measured)

Row 31 consists of pH including its species number, pH value, and chemical symbol.

```
GEOCHEMICAL CALCULATIONS FOR MCOBT-4.4.
SAMPLED ON 04/22/02.
19.20 MG/L   0.000  0.00000E-01
1 0 1 0 3 0 0 0 1 1 0 0 0
0   0   0
    330  0.000E-01   -7.52 y                    /H+1
    140  2.470E+01  -20.07 y                    /Total CO3-2 alkali
    100  1.300E-02   -7.02 y                    /Ba+2
    150  3.190E+01   -3.10 y                    /Ca+2
    180  1.730E+01   -3.31 y                    /Cl-1
    211  8.800E-02   -5.99 y                    /Cr(OH)2+
    212  1.180E-01   -5.99 y                    /CrO4-2
    270  4.200E-01   -4.66 y                    /F-1
    600  8.000E-05   -9.41 y                    /Pb+2
    460  5.400E+00   -3.65 y                    /Mg+2
    470  2.600E-03   -7.32 y                    /Mn+2
    540  3.200E-03   -7.26 y                    /Ni+2
    492  5.810E+01   -3.03 y                    /NO3-1
    580  9.000E-02   -6.02 y                    /PO4-3
    410  6.300E-01   -4.79 y                    /K+1
    500  2.050E+01   -3.05 y                    /Na+1
    800  1.530E-01   -5.76 y                    /Sr+2
    732  2.750E+01   -3.54 y                    /SO4-2
    893  3.200E-04   -8.93 y                    /UO2+2
    770  5.340E+01   -3.26                      /H4SiO4

  3   1
    330     7.5200     0.0000                   /H+1
```

Los Alamos NM 87545